The Control of Foxp3^{+} Regulatory T Cell by Interleukin-4 Receptor Alpha-Mediated Signaling

Submitted by

Nada Abdel Aziz Mohamed Abdel Rahman

Thesis Presented for the Degree of

Doctor of Philosophy

Department of Pathology
Division of Immunology (Immuno-Biotechnology)
International Centre for Genetic Engineering and Biotechnology
Institute of Infectious Disease and Molecular Medicine
Faculty of Health Science
University of Cape Town
June 2018

Declaration

I, Nada Abdel Aziz, hereby declare that the work on which this thesis is based, is my original work and that neither the whole work or any part thereof is being, has been, or is to be submitted for another degree in this or any other University.

This thesis/dissertation has been submitted to the Turnitin module (or equivalent similarity and originality checking software) and I hereby confirm that my supervisor has seen my report and any concerns revealed by such have been resolved with my supervisor.

Name: Nada Abdel Aziz Mohamed Abdel Rahman Ahmed

Student number: ABDNAD008

Signature: Signed by candidate

Date: 12th June 2018.

Acknowledgements

First of all, I praise GOD, the Almighty for providing me with this opportunity and granting me the capability to proceed successfully to become who I am.

This thesis appears in its current format due to the support and guidance of many people.

I would like to express my sincere gratitude to my supervisor Professor Frank Brombacher, for giving me the opportunity to be in his team with full authority to access all the state-of-the-art facilities and full support to get all the reagents needed for the present study to be in the current format, for his excellent supervision, guidance, caring, encouragement, and for his continuous support during my PhD study that made the present achievement possible. Joining Brombacher's lab is indeed a turning point in my academic career and a wonderful experience.

I would like to express my deepest gratitude to my co-supervisor Dr. Justin Komguep Nono, for his continuous support in each and every step in my PhD study, for his guidance in innumerable intricate experimental procedures, and for his invaluable help and assistance in the experimental work as well as perfecting the thesis writing. His patience, motivation, encouragement, caring, invaluable advices, and insightful and critical discussions have brought this study to the current stage. Indeed, the present achievement is in majority a result of his investment on me to become a better scientist.

Special thanks to Mr. Thabo Victor Mpotje for being a friend and a supportive labmate. I am indeed indebted for all the late nights work, the discussions, and all the fun we had during my PhD endeavour.

My thanks extend to all the members of Brombacher's lab. In particular, I am grateful to Ms. Lerato Hlaka, Dr. Hlumani Ndlovu, Ms. Munadia Ansarie, Ms. Fadwah Booley, Ms. Wendy Green, Ms. Lizette Fick, and Ms. Zarinah Sonday for their technical and administrative support as well as to Mr. Ronnie Dreyer for his assistance for cell sorting. Thanks for all the fun we had together.

I would like to thank the animal facility staff of the faculty of Health Science of the University of Cape Town for excellent technical assistance, training, and advice.

I am sincerely grateful for the International Centre for Genetic Engineering and Biotechnology for awarding me the highly competitive Arturo Falaschi PhD Fellowship to pursue my PhD study.

I would like to thank my previous supervisors and mentors for their precious help and support throughout.

The last but not the least, I would like to express my deepest gratitude to my family for their unconditional love, care, warm encouragement, and endless support. Indeed, thank you will never be enough to convey my gratitude to my Father (Dr. Abdel Aziz Mohamed), my Mother (Chemist. Howyda Ali), and my Brother (Dr to be Mohamed Abdel Aziz). Your confidence in me, inspiration, and motivation have paved the path for the present achievement and throughout my life. I became who I am simply because of You. Thank you for all what you have done for me.

Finally, may Allah bless you all for me and give you all the best in return as you always bless my life.

List of Publications

1. Part of the thesis work has been submitted for publication:

Abdel Aziz N, Nono JK, Mpotje T, Brombacher F. The Foxp3^{+} regulatory T cell population requires an intact IL-4Rα signaling to control inflammation during helminth infections. Revised manuscript submitted for publication in PLoS Biol.

2. In addition to the work presented in this thesis, I have made significant contributions, during my PhD, in the following publications:

Tallima H, Dovark J, Kareem S, Aboueldahab M, **Abdel Aziz N**, Dalton JP, El Ridi R (2017) Protective immune responses against *Schistosoma mansoni* infection by immunization with functionally active gut-derived cysteine peptidases alone and in combination with glyceraldehyde 3-phosphate dehydrogenase. PloS Negl Trop Dis 11(3): e0005443.

Nono JK, Ndlovu H, **Abdel Aziz N**, Mpotje T, Hlaka L, Brombacher F (2017) Interleukin-4 receptor alpha is still required after Th2 polarization for the maintenance and the recall of protective immunity to nematode infection. PLoS Negl Trop Dis 11:e0005675.

Nono JK, Ndlovu H, **Abdel Aziz N**, Mpotje T, Hlaka L, Brombacher F (2017) Host regulation of liver fibroproliferative pathology during experimental schistosomiasis via interleukin-4 receptor alpha. PLoS Negl Trop Dis 11:e0005861.

Guler R, Mpotje T, Ozturk M, Nono JK, Parihar SP, Chia J, **Abdel Aziz N**, Hlaka L, Kumar S, Penn-Nicholson A, Hanekom WA, Zak DE, Scriba TJ, Suzuki H, Brombacher F. Batf2 differentially regulates tissue immunopathology in type 1 and type 2 diseases. Revised manuscript submitted for publication in Mucosal Immunol.

Ndlovu H, Nono JK, **Abdel Aziz N**, Mpotje T, Brombacher F. Interleukin-4 receptor alpha responsive B cells are essential to down modulate host granulomatous inflammation against trapped *Schistosoma mansoni* eggs. Manuscript submitted for publication in Front Immunol.

Nono JK, Mpotje T, **Abdel Aziz N**, Brombacher F. Batf2 drives host susceptibility to chronic schistosomiasis by altering the intestinal microbiome. Manuscript submitted for publication.

Table of Content

Declaration.....……	2
Acknowledgement…….....	3
List of Publications …...……...	5
List of Abbreviations…….....	13
List of Tables…….	16
List of Flowcharts……...…….	17
List of Figures……...	18
Abstract…….	21
Chapter 1: Background and Problematic……..	22
1.1 The immune system…….….	23
1.2 The regulation of the adaptive immune system…….	23
1.3 T cell-meditated immune regulation…….	24
1.4 Foxp3 is the master regulator of Treg cells development and function….	26
1.5 Mechanisms of Treg-mediated suppression…….….	28
1.5.1 Immune suppression by transmembrane molecules……..	28
1.5.2 Immune suppression by secreted molecules …….	29
1.6 Treg-mediated control of distinct immune responses……	31
1.7 Cytokine-mediated regulation of Foxp3$^+$ Treg cells ….……..….	32
1.8 Interleukin-4 and Interleukin-4 receptor alpha-mediated signaling……..	34
1.8.1 Interleukin-4…….….	34
1.8.2 Interleukin-4 receptor alpha……..….	35
1.8.3 Interleukin-4 receptor alpha-mediated signaling pathway…….	35
1.9 Th2 disease models……..….	37
1.9.1 Schistosomiasis……..…	37
1.9.1.1 Schistosome life cycle……...….	37
1.9.1.2 Immunobiology of schistosomiasis…….……..….	39
1.9.1.3 Foxp3$^+$ Treg cells in schistosomiasis…….	41
1.9.2 *Nippostrongylus brasiliensis*…….	42
1.9.2.1 *Nippostrongylus brasiliensis* life cycle…….….	42
1.9.2.2 Immunobiology of *Nippostrongylus brasiliensis*……..….	43
1.9.2.3 Foxp3$^+$ Treg cells in *N. brasiliensis* infection…….	44

1.10 The controversial effect of IL-4Rα-mediated signaling on Foxp3$^+$ Treg cells……	45
1.11 Objectives……	47
Chapter 2: Materials and Methods……	48
2.1 Mice generation and genotyping……..….	49
2.2 Ethics statement……...….	53
2.3 Mice infection……..….	54
2.3.1 *Schistosoma mansoni*…….	54
2.3.1.1 Life cycle maintenance…….….	54
2.3.1.2 Mice infection and egg count…….	55
2.3.2 *Nippostrongylus brasiliensis*…….	55
2.3.2.1 Life cycle maintenance……..……...….	55
2.3.2.2 Mice infection and worm count…….	55
2.3.2.3 *Nippostrongylus brasiliensis* antigen preparation……...…	56
2.4 Cells isolation……..….	56
2.4.1 Thymus, mesenteric lymph nodes, and hepatic lymph nodes…….	56
2.4.2 Spleen……...….	57
2.4.3 Lung……...…	57
2.4.4 Liver and small intestine……...….	58
2.5 Flow cytometry…….	58
2.5.1 Antibodies……..…	58
2.5.2 Intracellular cytokine staining……..….	59
2.5.3 Intranuclear staining…….….	59
2.6 Real-time polymerase chain reaction……...….	60
2.6.1 Genotypic evaluation of efficiency and specificity of IL-4Rα deletion…….….	60
2.6.2 Transcriptional evaluation of Foxp3 expression by qRT-PCR…….	60
2.6.2.1 RNA extraction…….….	60
2.6.2.2 Complementary DNA synthesis…….	61
2.6.2.3 RT-PCR amplification…….……..….	62
2.7 Cell culture……...…	62
2.7.1 Cytokine stimulation…….…	62
2.7.2 Ex-vivo restimulation of MLN cells…….….	63

2.8 *In vitro* Treg assays…….….	63
2.8.1 $CD4^+$ T cell enrichment……..…	63
2.8.2 Cell sorting……	64
2.8.3 Treg conversion assay. ……..…….	64
2.9 Serum analyses…….	64
2.9.1 Serum collection and measurement of immunological parameters…	64
2.9.2 Liver enzymes……..….	64
2.10 Immunological analyses…….….	65
2.10.1 Cytokine measurement by sandwich ELISA……..….	65
2.10.2 Antibody isotype…….	65
2.11 Histology…….	66
2.11.1 *S. mansoni* infection……...….	66
2.11.2 *N. brasiliensis* infection…….….	66
2.12 Tissue homogenate for cytokine analyses……..….	66
2.13 Hydroxyproline quantifications……..….	67
2.14 Statistics……..….	67
Chapter 3: The Role of IL-4Rα-mediated Signaling on $Foxp3^+$ Treg Cells under Steady-State……..……	68
3.1 Results……..	69
3.1.1 $Foxp3^+$ Treg cells express IL-4Rα under steady-state……	69
3.1.2 Generation and characterization of $Foxp3^{cre}$ IL-4$Rα^{-/lox}$ BALB/c mice……...	70
3.1.2.1 Generation of $Foxp3^{cre}$ IL-4$Rα^{-/lox}$ BALB/c mice……...	70
3.1.2.2 Genotypic evaluation of IL-4Rα deletion on $Foxp3^+$ Treg cells	76
3.1.2.3 Phenotypic evaluation of IL-4Rα deletion on $Foxp3^+$ Treg cells	77
3.1.2.4 Functional evaluation of IL-4Rα deletion on $Foxp3^+$ Treg cells	78
3.1.3 The role of IL-4Rα signaling on $Foxp3^+$ Treg cells under steady-state *in vivo*……	80
3.1.3.1 Deletion of IL-4Rα specifically within $Foxp3^+$ Treg population does neither alter body weight, organs weight, nor tissue cellularities……..	80

3.1.3.2 Deletion of IL-4Rα specifically on Foxp3$^+$ Treg population does not alter Tregs or other lymphocyte-compartments in primary lymphoid organ……..	81
3.1.3.3 Deletion of IL-4Rα specifically on Foxp3$^+$ Treg population does not alter Tregs or other lymphocyte-compartments in secondary lymphoid organs……...……...……...	82
3.1.3.4 Deletion of IL-4Rα specifically on Foxp3$^+$ Treg population does not alter Tregs or other lymphocyte-compartments in peripheral tissues……...……..	83
3.1.3.5 Deletion of IL-4Rα specifically on Foxp3$^+$ Treg population does not lead to spontaneous inflammatory disorder in young mice	84
3.1.4 The role of IL-4Rα signaling on Foxp3$^+$ Treg cells *in vitro*……	86
3.1.4.1 IL-4Rα signaling inhibits Treg conversion *in vitro*…….	86
3.1.4.2 IL-4Rα signaling promotes the survival of CD4$^+$ CD25$^+$ Tregs and enhances their Foxp3 expression……..	87
3.2 Discussion……	89
3.2.1 Foxp3$^+$ Treg cells might need IL-4Rα signaling to potentiate their suppressive function……..	89
3.2.2 IL-4Rα-mediated signaling on Foxp3$^+$ Treg cells is dispensable in young mice to maintain immune homeostasis……..….	91
3.2.3 IL-4Rα-mediated signaling on Treg cells *in vitro*……..…	92
Chapter 4: The Role of IL-4Rα-mediated Signaling on Foxp3$^+$ Treg Cells under Inflammatory Conditions……	94
4.1 Results……..	95
4.1.1 Foxp3$^+$ Treg cells upregulate IL-4Rα expression upon *S. mansoni* infection…….	95
4.1.2 IL-4Rα-mediated signaling on Foxp3$^+$ Treg cells is required to control egg-driven fibrogranulomatous inflammation during schistosomiasis……..	96
4.1.2.1 Evaluation of efficiency and specificity of IL-4Rα deletion…..	96
4.1.2.2 IL-4Rα-mediated signaling on Foxp3$^+$ Treg cells is required for Treg cells accumulation and maintenance/upregulation of	

suppressive markers to suppress overshooting inflammation in the liver during *S. mansoni* infection …… 97
4.1.2.2.1 IL-4Rα-mediated signaling on Foxp3$^+$ Treg cells is crucial for Treg accumulation……... 97
4.1.2.2.2 IL-4Rα-mediated signaling on Foxp3$^+$ Treg cells is required for maintenance/upregulation of suppressive markers……. 98
4.1.2.2.3 IL-4Rα-mediated signaling on Foxp3$^+$ Treg cells is required to control cytokines production…….. 100
4.1.2.3 IL-4Rα-mediated signaling on Foxp3$^+$ Treg cells is required for Treg cells maintenance/upregulation of suppressive markers to control T cell proliferation and effector function in the hLN during *S. mansoni* infection…….. 101
4.1.2.3.1 Deletion of IL-4Rα on Foxp3$^+$ Treg cells impairs their ability to maintain/upregulate the expression of Treg suppressive markers…….. 101
4.1.2.3.2 IL-4Rα-mediated signaling on Foxp3$^+$ Treg cells is required to control T cell proliferation and effector function……..... 103
4.1.2.4 IL-4Rα-mediated signaling on Foxp3$^+$ Treg cells is required for Treg accumulation in the gut during *S. mansoni* infection…….. 106
4.1.2.5 IL-4Rα-mediated signaling on Foxp3$^+$ Treg cells is required for the maintenance/upregulation of Foxp3 expression in Tregs and the control of T cell proliferation and effector function in the MLN during *S. mansoni* infection……..…… 107
4.1.2.5.1 Deletion of IL-4Rα on Foxp3$^+$ Treg cells impairs their ability to maintain Foxp3 expression …… 107
4.1.2.5.2 IL-4Rα-mediated signaling on Foxp3$^+$ Treg cells is required to control T cell proliferation and effector function……... 109
4.1.2.6 Deletion of IL-4Rα on Foxp3$^+$ Treg cells impairs their ability to control egg-driven fibrogranulomatous inflammation during *S. mansoni* infection…… 113

4.1.2.7 Humoral immune response in Foxp3^{cre} IL-4Rα$^{-/lox}$ mice *S. mansoni* infection…… 120
4.1.2.8 IL-4Rα-mediated signaling on Foxp3^{+} Treg cells is dispensable for host survival during *S. mansoni* infection…….. 121
4.1.3 IL-4Rα-mediated signaling on Foxp3^{+} Treg cells is required for Treg accumulation and control of inflammation in the lung during primary *Nippostrongylus brasiliensis* infection…… 123
4.1.3.1 Deletion of IL-4Rα on Foxp3^{+} Treg cells does not alter worm expulsion ability of the host……. 123
4.1.3.2 IL-4Rα-mediated signaling is required to maintain/enhance Foxp3 expression on Foxp3^{+} Treg cells in the MLN during primary *N. brasiliensis* infection……. 124
4.1.3.3 IL-4Rα-mediated signaling on Foxp3^{+} Treg is required for Treg accumulation and the control of worm-driven emphysematous inflammation in the lung during primary *N. brasiliensis* infection……... 126
4.2 Discussion……..…….. 129
4.2.1 Upregulation of IL-4Rα expression by Foxp3^{+} Treg cell *in vivo* under inflammatory conditions…….. 129
4.2.2 Foxp3^{+} Treg cells do require IL-4Rα signaling to control inflammatory immune responses in disease……... 130
4.2.2.1 IL-4Rα signaling on Foxp3^{+} Treg is crucial in maintaining/promoting their Foxp3 expression *in vivo*…….…….. 130
4.2.2.2 Differential regulation of Foxp3^{+} Treg population by IL-4Rα signaling……..…… 131
4.2.2.3 IL-4Rα signaling on Foxp3^{+} Treg is required to control hookworm-induced emphysematous lung pathology…….. 133
4.2.2.4 IL-4Rα signaling mediates Foxp3^{+} Treg cell accumulation within inflamed tissues...…….…… 134
4.2.3 Exaggerated immune response and tissue inflammation following deletion of IL-4Rα specifically on Foxp3^{+} Treg cells……...……. 136
4.2.4 Deletion of IL-4Rα specifically on Foxp3^{+} Treg cells does not induce Foxp3^{+} Treg cells transdifferentiation to ex-Foxp3-Th2…. 136

Concluding remarks……	138
References……	139

List of Abbreviations

APC	Antigen presenting cell
AST	Aspartate aminotransferase
Bcl6	B-cell lymphoma 6
BCR	B cell receptor
BSA	Bovine serum albumin
CAB	Chromotrope 2R and analine blue solution
cAMP	Cyclic adenosine monophosphate
CD	Cluster of differentiation
CD25	Interleukin IL-2 receptor α chain
CD39	Ectonucleoside triphosphate diphosphohydrolase-1
CD73	Ecto-5'-nucleotidase
cDNA	complementary DNA
CLP	Common lymphoid progenitor
CMP	Common myeloid progenitor
Cre	Cyclic recombinase
CTLA-4	Cytotoxic T lymphocyte-associated antigen-4
CXCR3	CXC chemokine receptor 3
DC	Dendritic cell
DN	Double negative
DP	Double positive
EDTA	Ethylenediaminetetraacetic acid
ELISA	Enzyme-linked immunosorbent assay
EPG	Eggs per gram feces
ES	Embryonic stem
Foxp3	Forkhead box P3
GATA3	GATA-binding protein 3
GITR	Glucocorticoid-induced TNF receptor family related gene/protein
γc	Common gamma-chain
GMFI	Geometric mean fluorescence intensity
GM-CSF	Granulocyte macrophage-colony stimulating factor
H & E	Hematoxylin and eosin

HPRT	Hypoxanthine-guanine phosphoribosyl-transferase
HSCs	Hematopoietic stem cells
HSV	herpes simplex virus
IBD	Inflammatory bowel disease
IDO	Indolamine 2, 3-dioxygenase
iFBS	inactivated fetal bovine serum
IFN-γ	Interferon gamma
IFN-γR	IFN-γ receptor
Ig	Immunoglobulin
IL	Interleukin
IL-4	Interleukin-4
IL-4Rα	Interleukin-4 receptor alpha
IL-13R	Interleukin 13 receptor
ILC	Innate lymphoid cells
IMDM	Iscove's Modified Dulbecco's Medium
IPEX	Immune dysregulation polyendocrinopathy enteropathy
IRES	Internal ribosome entry site
IRF4	Interferon regulatory factor 4
IRS	Insulin receptor substrate
ITIM	Immunoreceptor tyrosine-based inhibitory motif
JAK	Janus kinase
L	Larval stage
LAG3	lymphocyte-activation gene 3
LN	lymph nodes
LoxP	locus of X-over P1
MAP	mitogen-activated protein
MLI	Mean linear intercept method
MHC	Major histocompatibility complex
NK	Natural killer
NTx	Neonatal thymectomy
PBS	Phosphate buffered saline
OVA	Ovalbumin

PAS	Periodic acid-Schiff reagent
PCR	Polymerase chain reaction
PI3K	phosphatidylinositol 3-kinase
PMA	Phorbol myristate acetate
PPARγ	Peroxisome proliferator-activated receptor gamma
pTreg	peripherally-induced Treg cell
qRT-PCR	Real-time reverse transcription PCR
RBCs	Red blood cells
RORγt	Retinoic acid receptor-related orphan receptor-γt
RPMI	Roswell Park Memorial Institute
RT	Room temperature
SCID	Severe combined immunodeficient
SDS	Sodium dodecyl sulfate
SEA	Soluble egg antigens
SEB	staphylococcal enterotoxin B
SH2	Src Homology 2
SP	Single positive
STAT	Signal transducer and activator of transcription
ST2	IL-33 receptor
T-bet	T-box transcription factor
TCR	T cell receptor
T_{FH}	T follicular helper cells
TGF-β	Transforming growth factor beta
Th	T helper cells
TK	Thymidine kinase
TNF	Tumor necrosis factor
tTreg	Thymus-derived Treg
Treg	T regulatory
VAT-Treg	Visceral adipose tissue-resident Treg

List of Tables

Table No.	Description	Page No.
Table 2.1	Primers sequence used for genotyping of Foxp3^{cre} IL-4 R$\alpha^{-/lox}$ mice……..	52
Table 2.2	Primers sequence for evaluation of Foxp3 expression…….	62

List of Flowcharts

Flowchart No.	Description	Page No.
Flowchart 1	Generation of Foxp3Cre$^{-/+}$ IL-4Rα$^{-/lox}$ BALB/c mice using males Foxp3Cre$^{-/+}$ mice ……..	73
Flowchart 2	Generation of Foxp3Cre$^{-/+}$ IL-4Rα$^{-/lox}$ BALB/c mice using females Foxp3Cre$^{-/+}$ mice ……..	74

List of Figures

Figure No.	Description	Page No.
Figure 1	Schematic representation of mechanisms of Treg cell-mediated suppression……....	30
Figure 2	Schematic representation of the IL-4Rα signaling pathway…	36
Figure 3	The Schistosome Life cycle……..	39
Figure 4	Life cycle of *Nippostrongylus brasiliensis*……...	43
Figure 5	The controversial effect of IL-4Rα-mediated signaling on $Foxp3^+$ Treg cells……..	46
Figure 6	General strategy for gene-targeting in mice……..	51
Figure 7	$Foxp3^+$ Treg cells express IL-4Rα under steady-state……..	69
Figure 8	Generation of IL-4R$\alpha^{-/-}$ BALB/c mice……..	70
Figure 9	Generation of IL-4R$\alpha^{lox/lox}$ BALB/c mice. ……...	71
Figure 10	Generation of Foxp3-IRES-Cre BALB/c mice…….	72
Figure 11	Generation of Foxp3$Cre^{-/+}$ IL-4R$\alpha^{-/lox}$ BALB/c mice……	75
Figure 12	Genotypic characterization of Foxp3$Cre^{-/+}$ IL-4R$\alpha^{-/lox}$ mice….	76
Figure 13	Phenotypic characterization of Foxp3$Cre^{-/+}$ IL-4R$\alpha^{-/lox}$ mice…	77
Figure 14	Functional characterization of Foxp3$Cre^{-/+}$ IL-4R$\alpha^{-/lox}$ mice…	79
Figure 15	Deletion of IL-4Rα on $Foxp3^+$ Treg cells does not have a major effect on body weight, organs weight, nor organs cellularities in young mice……	80
Figure 16	Deletion of IL-4Rα on $Foxp3^+$ Treg cells does not alter T cell ontogeny……...	81
Figure 17	Deletion of IL-4Rα on $Foxp3^+$ Treg cells does not alter cells distribution in secondary lymphoid organs……..	82
Figure 18	Deletion of IL-4Rα on $Foxp3^+$ Treg cells does not alter cells distribution or frequency in peripheral tissues…….	83
Figure 19	Deletion of IL-4Rα on $Foxp3^+$ Treg cells does not result in a spontaneous inflammatory response in young mice…….	85
Figure 20	IL-4Rα signaling is dispensable for Foxp3 Treg conversion *in vitro*……..	86

Figure 21	IL-4Rα signaling promotes the survival and enhances Foxp3 expression in $CD4^+$ $CD25^+$ T cell…….	88
Figure 22	$Foxp3^+$ Treg cells upregulate IL-4Rα expression upon infection……...	95
Figure 23	Efficiency of IL-4Rα deletion on $Foxp3^+$ Treg cells in *S. mansoni* infected $Foxp3^{cre}$ IL-$4R\alpha^{-/lox}$ mice……..	96
Figure 24	IL-4Rα mediated signaling on $Foxp3^+$ Treg is required for Treg accumulation in the liver during *S. mansoni* infection….	98
Figure 25	$Foxp3^+$ Treg cell profile in the liver of *S. mansoni* infected IL-$4R\alpha^{-/Lox}$ and $Foxp3^{Cre}$ IL-$4R\alpha^{-/Lox}$ mice…….	99
Figure 26	Deletion of IL-4Rα on $Foxp3^+$ Treg cells results in heightened cytokine production in the liver during *S. mansoni* infection…	100
Figure 27	$Foxp3^+$ Treg cell profile in the hLN of *S. mansoni* infected IL-$4R\alpha^{-/Lox}$ and $Foxp3^{Cre}$ IL-$4R\alpha^{-/Lox}$ mice……	102
Figure 28	Gating strategies…….	104
Figure 29	IL-4Rα mediated signaling on $Foxp3^+$ Treg is required for controlling T cells proliferation and GATA3 expression in hLN during *S. mansoni* infection……..	105
Figure 30	Deletion of IL-4Rα on $Foxp3^+$ Treg cells results in heightened Th2 cytokine production by $CD4^+$ $GATA3^+$ but not $CD4^+$ $Foxp3^+$ T cells in the hLN during *S. mansoni* infection…….	105
Figure 31	IL-4Rα mediated signaling on $Foxp3^+$ Treg is required for Treg accumulation in the gut during *S. mansoni* infection……	106
Figure 32	$Foxp3^+$ Treg cell profile in the MLN of *S. mansoni* infected IL-$4R\alpha^{-/Lox}$ and $Foxp3^{Cre}$ IL-$4R\alpha^{-/Lox}$ mice……	108
Figure 33	IL-4Rα mediated signaling on $Foxp3^+$ Treg is required for controlling T cells proliferation and effector function in MLN during *S. mansoni* infection……..	111
Figure 34	Deletion of IL-4Rα on $Foxp3^+$ Treg cells results in heightened $CD4^+$ $GATA3^+$ T cells in the MLN during *S. mansoni* infection……...	112

Figure 35	Deletion of IL-4Rα on Foxp3^{+} Treg cells results in heightened Th2 cytokine production by CD4^{+} GATA3^{+} but not CD4^{+} Foxp3^{+} T cells in the MLN during *S. mansoni* infection……..	112
Figure 36	Deletion of IL-4Rα on Foxp3^{+} Treg cells impairs the control of fibro-granulomatous inflammation in the liver during experimental *S. mansoni* infection……	114
Figure 37	Cre expression does neither alter Foxp3^{+} Treg phenotype nor infection-driven immune responses during experimental schistosomiasis…….	117
Figure 38	Cre expression does not induce exaggerated fibrogranulomatous inflammation during experimental *S. mansoni* infection…….	119
Figure 39	Humoral immune response of 8 wk *S. mansoni* infected IL-4Rα$^{-/lox}$ and Foxp3^{Cre} IL-4Rα$^{-/Lox}$ mice……	120
Figure 40	Deletion of IL-4Rα on Foxp3^{+} Treg cells does not alter gross pathology during acute schistosomiasis……...	121
Figure 41	Intact IL-4Rα-mediated signaling on Foxp3^{+} Treg cells is not critical for mice survival during schistosomiasis……..	122
Figure 42	Deletion of IL-4Rα on Foxp3^{+} Treg cells does not alter worm expulsion capacity of the host……...	123
Figure 43	Deletion of IL-4Rα on Foxp3^{+} Treg cells does not alter gut pathology during primary *N. brasiliensis* infection……..	125
Figure 44	Deletion of IL-4Rα on Foxp3^{+} Treg cells impairs the control of emphysema during primary *N. brasiliensis* infection……...	127
Figure 45	IL-4Rα signaling on Foxp3^{+} Treg cells is required to control worm-driven lung inflammation during *N. brasiliensis* infection……...	128
Figure 46	IL-4Rα is required by Foxp3^{+} Treg cells to control inflammation in disease……	137

Abstract:

T regulatory (Treg) cells play a pivotal role in the maintenance of self-tolerance and immune homeostasis. Forkhead box P3 (Foxp3)$^{+}$ Treg function is controlled by environmental cues of which cytokine-mediated signaling is a dominant component. Recently, Interleukin (IL)-4 has been shown to play an important role in determining the fate of Foxp3^{+} Tregs. *In vivo,* IL-4-mediated signaling via Interleukin-4 receptor alpha (IL-4Rα) was convincingly shown to mediate Treg transdifferentiation into ex-Foxp3 Th2 or Th17 cells, suggesting a negative regulation of Foxp3^{+} Tregs by IL-4Rα-mediated signaling. Puzzlingly, however, IL-4-mediated signaling was also independently found to reinforce the Foxp3^{+} Tregs, counter-arguing for the positive regulation of Foxp3^{+} Tregs by IL-4Rα-mediated signaling. In the face of such a conundrum, the present work was set forth as an attempt to unambiguously and conclusively decipher the bases of the regulation of Foxp3^{+} Treg by IL-4Rα-mediated signaling using transgenic murine models.

It was first noted that Foxp3^{+} Treg cells do express IL-4Rα under steady-state. Furthermore, *in vitro*, purified CD25^{+} Tregs were prompted to higher Foxp3 expression and increased survival upon stimulation with IL-4 arguing for a potentiating role of IL-4Rα mediated signaling on Foxp3^{+} Treg cells. To better address the need for the host Foxp3^{+} Treg cells to express IL-4Rα as observed, we generated Foxp3-specific IL-4Rα deficient mice where IL-4Rα is specifically deleted from Foxp3^{+} T cells in the whole organism. Even though naïve Foxp3^{cre} IL-4Rα$^{-/lox}$ mice model at homeostasis did neither reveal any significant alteration of the cellular, tissular and phenotypic profile nor development of spontaneous inflammatory disorder when compared to wild-type mice, under *S. mansoni* infection impairment IL-4Rα-mediated signaling on Foxp3^{+} Tregs resulted in heightened activation marker expression and elevated T cell effector functions as indicated by increased cytokines production and greater T cell proliferation rate. This heightened immune responsiveness translated overall into an exacerbated parasitic egg-driven fibrogranulomatous inflammation in the liver and the gut of schistosomiasis-diseased Foxp3^{cre} IL-4Rα$^{-/lox}$ mice. Furthermore, in another model of helminth infection with the parasitic nematode, *Nippostrongylus brasiliensis*, Foxp3^{cre} IL-4Rα$^{-/lox}$ mice showed a higher level of mucus and exaggerated emphysematous pathology in the lungs. Interestingly, the impairment of IL-4Rα signaling within the Foxp3^{+} Treg population in Foxp3^{cre} IL-4Rα$^{-/lox}$ mice led to a reduced recruitment of Foxp3^{+} Tregs and a diminished expression of Foxp3, and other associated Treg suppressive markers (i.e. IRF4 and Helios) during the course of these helminth infections. Taken together, our findings supported a role for IL-4Rα signaling in the positive regulation of Foxp3^{+} Tregs function and thus, the suppression of inflammatory responses during helminth infections.

In conclusion, this work demonstrated a positive role for IL-4Rα mediated signaling in the biology of Foxp3^{+} Treg cells whereby the latter cells require IL-4Rα signaling to survive and maintain Foxp3 expression and suppressive functions so as to efficiently control tissue inflammatory responses during infection. The data presented do provide insights into the mechanisms of Foxp3^{+} Treg regulation that are highly relevant for the therapeutic control of inflammation during infectious diseases.

Chapter 1:
Background and Problematic

Chapter 1: Background and Problematic

1.1 The immune system

The mammalian immune system has evolved to protect the host against the pathogenic environment as well as to remove and/or inhibit potentially pathogenic self-reactive immune cells (Murphy et al., 2008). The immune system carries out its function through complex interactions between different types of immune cells. These cells are derived from pluripotent stem cells, present in the bone marrow, known as hematopoietic stem cells (HSCs). Through a series of stochastic events as well as the support of cytokine signals, HSCs can be differentiated into two main progenitors: common myeloid progenitor (CMP) and common lymphoid progenitor (CLP) (Socolovsky et al., 1998; Blom and Spits, 2006; Robb, 2007; Murphy et al., 2008). While CMP can differentiate into basophils, eosinophils, neutrophils, mast cells, granulocytes, monocytes/macrophage, and dendritic cells, CLP differentiates into natural killer (NK) cells, innate lymphoid cells (ILCs), B cell, and T cells (Kondo et al., 1997; Akashi et al., 2000; Murphy et al., 2008; Serafini et al., 2015). Based on the specificity and the timing at which these cells are activated in response to the invading pathogen/antigen, the cells can be grouped into two main arms; innate immune arm, which is less specific and considered to be the first line of defense, and adaptive immune arm, that is characterized by high level of specificity and is always shaped by the early innate immune signals. Innate immunity includes ILCs, basophils, eosinophils, neutrophils, mast cells, granulocytes, monocytes /macrophage, NK cells, NKT cells, and gamma-delta T cells, while adaptive immunity includes B cells and T cells (Murphy et al., 2008).

1.2 The regulation of the adaptive immune system

Adaptive immune response is one of the two main pillars of the immune system. Its broad diversity and specificity confer by somatic recombination of T cell receptor (TCR) and B cell receptor (BCR) enables the host protection from rapidly evolving pathogens. The ability of the adaptive immune system to distinguish between self and non-self is the key to prevent deleterious immune-damage to the host, autoimmune diseases, and to mount an effective immune response against invading pathogens, respectively (Sprent and Cho, 2008). In fact, the immune response is orchestrated so as to “achieve the best possible

protection against pathogens and the altered/pathogenic self while causing the least possible amount of damage to the host". Therefore, multiple check-points and different levels of cell-intrinsic and cell-extrinsic immune-regulations are in place. These immune-regulations can be summarized into 3 main levels; i) First Tier Control, ii) Second Tier Control, and iii) Third Tier Control. First Tier Control is aimed at the elimination of autoreactive immature lymphocytes in the primary lymphoid organs (the thymus for T cells and the bone marrow for B cells) through a process known as negative selection. In negative selection, immature lymphocytes whose receptors confer a strong affinity to self-molecules are programmed to either die by apoptosis or clonal deletion, to produce a new receptor through a process known as receptor editing, to be functionally inactive, anergic, to self-antigens, or to have the state of immunological ignorance (Starr et al., 2003) and hence, only functionally competent lymphocytes migrate from the primary lymphoid organs to the periphery. In the periphery, there is a Second Tier Control whereby T cells and B cells do require two distinct signals for their activation (Lenschow et al., 1996). For T cells, the first signal originates from the engagement of TCR with the peptide-major histocompatibility complex (MHC) complex (Murphy et al., 2008) and the second signal depends on the interaction of T cell costimulatory receptor cluster of differentiation (CD)28 with CD80 and CD86 which are expressed on the surface of activated antigen-presenting cells (APC) (Lenschow et al., 1996). Although these two tiers of controls are very powerful, they are insufficient to counter the threat of immune-mediated pathology. Third Tier Control is therefore in place, mediated by a specialized T cell subset, known as regulatory T (Treg) cells, that possess immune suppression capability to keep in check the activation and expansion of aberrant or over-reactive T cells (Sakaguchi et al., 2008; Josefowicz et al., 2012).

1.3 T cell-mediated immune regulation

Initial discovery of thymus-derived T cell subset that can dampen the immune response and prevent autoimmunity, Treg cells, has been made 40 years ago thanks to neonatal and adult thymectomy experiments (Nishizuka and Sakakura, 1969; Penhale et al., 1973; Sakaguchi et al., 1982; Penhale et al., 1990; Fowell and Mason, 1993; Bonomo et al., 1995; Asano et al., 1996) as well as transplantation tolerance studies of chicken-quail chimera (Ohki et al., 1987) and mice chimera (Salaun et al., 1990). It has been shown by Nishizuka,

Sakaguchi, and others that neonatal thymectomy (NTx) of normal mice performed at a critical period (between 2 and 4 days after birth) leads to T cell-mediated inflammation of various organs and appearance of tissues specific auto-antibodies in the circulation (Nishizuka and Sakakura, 1969; Sakaguchi et al., 1982; Bonomo et al., 1995; Asano et al., 1996). In support, adult thymectomy of normal rats followed by four rounds of sublethal X-irradiation results in auto-immune thyroiditis as well as type 1 diabetes (Penhale et al., 1973; Penhale et al., 1990; Fowell and Mason, 1993). In all cases, development of T-cell mediated tissue damage was prevented upon reconstitution of depleted cells with normal T cells from adult syngenic animals. In the second set of experimentation, studies of chicken-quail chimera and mice chimera demonstrated that grafted thymic epithelium cells are responsible for xenograft tolerance (Ohki et al., 1987; Salaun et al., 1990). In these set of experiments, induction of tolerance to allogeneic tissue graft was mainly mediated by thymus-derived T cell subset that was capable of suppressing alloreactive T cells. Altogether, results of these experiments indicated the presence of a specialized T cell subset with the ability to prevent and control auto-immunity (Shevach, 2000; Sakaguchi et al., 2008; Benoist and Mathis, 2012; Josefowicz et al., 2012).

To distinguish this specialized T cell subset with immunoregulatory features from other T cells, several attempts were made to identify a specific cell marker for Treg cells. Although using $CD5^{high}$, $CD45RC^{low}$, $RT6.1^{high}$, or $CD45RB^{low}$ markers had helped in the better understanding of Treg cell biology (Sakaguchi et al., 1985; Sugihara et al., 1988; McKeever et al., 1990; Powrie and Mason, 1990; Morrissey et al., 1993; Powrie et al., 1993; Asano et al., 1996), the expression of these markers by other cells (Josefowicz et al., 2012), did not dismiss the pressing need for a more definitive phenotypic marker that would specifically identify Treg cells. In 1995, Sakaguchi and colleagues identified the interleukin (IL)-2 receptor α chain (CD25) as a candidate marker for Treg cell subsets, particularly under steady-state condition (Sakaguchi et al., 1995). Adoptive transfer of $CD4^+$ $CD25^+$ T cell subset to NTx mice and other different auto-immune models resulted in inhibition of auto-immunity. Although using CD25 as a marker for Treg cells further advanced our understanding of Treg cell biology *in vivo* under steady-state, showing that Treg cells are differentiated in the thymus, and *in vitro*, to study their suppressive function ability, the utility of that marker *in vivo* under inflammatory condition for more mechanistic insights was limited due to the upregulation of CD25 expression in all activated T cells (reviewed in Shevach, 2000; Sakaguchi et al., 2008; Benoist and Mathis, 2012; Josefowicz et al.,

2012). Intensive studies in the last decade have now identified the transcription factor forkhead box P3 (Foxp3) as a marker specific for Treg cells (Fontenot et al., 2003; Hori et al., 2003; Khattri et al., 2003).

1.4 Foxp3 is the master regulator of Treg cells development and function

Foxp3 is an X-linked suppressor gene that belongs to the forkhead/winged-helix family of transcription factors. Role of Foxp3 in Treg cells was appreciated after the identification and study of mutations in Scurfy mice and human IPEX (immune dysregulation, polyendocrinopathy, enteropathy, X-linked syndrome) patients (Chatila et al., 2000; Bennett et al., 2001; Brunkow et al., 2001; Wildin et al., 2001; Fontenot et al., 2003; Gambineri et al., 2003; Hori et al., 2003; Ochs et al., 2005). Scurfy is an X-linked recessive mutant that results from a loss-of-function mutation in *foxp3* encoding gene. Scurfy mice are characterized by hyperactivation of $CD4^+$ T cells and exacerbation of pro-inflammatory cytokines production (Brunkow et al., 2001). Similarly, human IPEX patients, the human counterpart of Scurfy mice, develop fatal autoimmunity in multiple endocrine organs, inflammatory bowel disease (IBD), diabetes, hemolytic anemia, and eczema due to multiple mutations in human *foxp3* homolog (reviewed in Gambineri et al., 2003; Ochs et al., 2005). In most cases, loss-of-function mutations in *foxp3* encoding gene affect hemizygous males but not heterozygous females due to random inactivation of the X-chromosome (Godfrey et al., 1994). Random inactivation of the X-chromosome happens as a result of the maternally derived X or the paternally derived X-chromosome randomly inactivated in the mammalian females (Lyon, 1961; Lyon, 1972). Hence, T cells that express a wild-type *foxp3* allele keep in check pathogenic Treg cells that express a mutant *foxp3* allele (Fontenot et al., 2005b; Gavin et al., 2007). Nevertheless, skewed X inactivation, that could allow for the expression of *foxp3* mutant allele, as well as leaky X inactivation at the *foxp3* locus can lead to disease manifestation in heterozygous females (Wildin and Freitas, 2005; Medema and Burgering, 2007; Zuo et al., 2007).

Similarities in autoimmune disease noticed in Scurfy mice and human IPEX patients prompted three different laboratories to investigate the possible role of Foxp3 in $CD25^+$ $CD4^+$ Treg cells development and function (Fontenot et al., 2003; Hori et al., 2003; Khattri et al., 2003). A culmination of these studies came in 2003 revealing that Foxp3 is highly

and stably expressed in peripheral $CD25^+$ $CD4^+$ T cells and thymus-derived $CD25^+$ $CD4^+$ $CD8^-$ T cells but not in activated $CD4^+$ T cells (Fontenot et al., 2003; Hori et al., 2003; Khattri et al., 2003). Furthermore, retroviral transduction of ectopic Foxp3 expression in activated peripheral $CD25^-$ $CD4^+$ T cells confers Treg-like suppressor function, dampening T cell proliferation *in vitro* and inhibiting the development of autoimmune disease *in vivo,* as well as cell surface phenotypic markers, i.e upregulation of CD25, glucocorticoid-induced tumor necrosis factor (TNF) receptor family related gene/protein (GITR), and cytotoxic T lymphocyte-associated antigen-4 (CTLA-4) expression on the surface of those cells (Fontenot et al., 2003; Hori et al., 2003). Also, expression of the *foxp3* transgene in mice was shown to confer suppressor activity to $CD25^-$ $CD4^+$ and $CD8^+$ $CD4^-$ T cells (Khattri et al., 2003). Indeed, the importance of Foxp3 in the differentiation of Treg cells came from the analysis of $CD25^+$ $CD4^+$ T cells in the thymus and secondary lymphoid organs of mixed bone marrow chimera experiments whereby a mixture of bone marrow cells from wildtype and *foxp3*-deficient mice were transferred into T cell-deficient mice. Only *foxp3*-sufficient but not *foxp3*-deficient precursors were able to give rise to $CD25^+$ $CD4^+$ Treg cells (Fontenot et al., 2003). In as much as, Foxp3 is not only crucial for the development, differentiation, and function of Treg cell, it's continuous expression in Treg cells is required to maintain the transcriptional and functional programs defining mature Treg cells (Fontenot et al., 2003; Hori et al., 2003; Khattri et al., 2003; Wan and Flavell, 2007; Williams and Rudensky, 2007). Cyclic recombinase (Cre)-induced ablation of the *foxp3* allele in mature Treg cells results in loss of their developmentally established suppressive capacity potentials with subsequent re-programming towards effector T helper (Th) cells (Williams and Rudensky, 2007). Quite notably, Foxp3 expression level within the $Foxp3^+$ Treg cells has also been considered to be a quality control indicator of Foxp3 suppressive function (Wan and Flavell, 2007; Williams and Rudensky, 2007). Although the frequency of $Foxp3^+$ Treg compartment could be possibly comparable, reduction in Foxp3 expression within Treg cells can cause immune diseases under steady-state and failure to control immune responses under inflammatory conditions (Wan and Flavell, 2007; Kitoh et al., 2009; Wohlfert et al., 2011). Altogether, these studies clearly indicated that Foxp3 is the master regulator of Treg cells development and suppressive function.

1.5 Mechanisms of Treg-mediated suppression

Treg cells are equipped with potent suppressive mechanisms to maintain immune-homeostasis under steady-state and to protect the host from immune-mediated collateral damage under inflammatory conditions. Treg-mediated suppression can be categorized, based on the location of the molecule/weapon used for suppression, into two main modes of action; transmembrane molecules-mediated suppression and secreted molecules-mediated suppression (Fig. 1) (Sakaguchi et al., 2008; Vignali et al., 2008; Campbell and Koch, 2011; Josefowicz et al., 2012).

1.5.1 Immune suppression by transmembrane molecules

Transmembrane molecule such as CD25, CTLA-4, lymphocyte-activation gene 3 (LAG3), ectonucleoside triphosphate diphosphohydrolase-1 (CD39), and ecto-5'-nucleotidase (CD73) are crucial mediators of Treg cells-mediated suppression (Reviewed in (Sakaguchi et al., 2008; Vignali et al., 2008; Campbell and Koch, 2011; Josefowicz et al., 2012)). Role of CD25 in the suppressor function of Treg cells had been a long-standing debate. While one school of thought was suggesting an indispensable role for CD25 in Treg cell suppressor function by depriving activated T cells from IL-2 that is required for their survival and hence, facilitates the death of activated T cells (Thornton et al., 2004; Barthlott et al., 2005; Pandiyan et al., 2007; Busse et al., 2010), another school of thought was suggesting a dispensable role of CD25 expression (Fontenot et al., 2005a; Tang et al., 2008). In fact, using recently available genetic tools, Rudensky and colleagues were successful to unambiguously interrogate the role of IL-2R in Treg cells suppressive function (Chinen et al., 2016). Rudensky and colleagues showed that IL-2R is dispensable for the suppression of activated $CD4^+$ T cells but indispensable for dampening $CD8^+$ T cell responses (Chinen et al., 2016).

In addition to the ability of Treg cells to directly control T cells function, Treg cells can indirectly control T cells via regulating the maturation, the activation, and/or the function of dendritic cells (DCs). CTLA-4, a homolog of CD28, is centrally implicated in Treg-mediated suppression of DCs. Constitutive expression of CLTA-4 on the surface of Treg cells empowers them with the ability to down-modulate the activity of DCs by reducing the expression of co-stimulatory ligands CD80 and CD86 on the surface of the

activated DCs (Wing et al., 2008). Furthermore, CTLA-4 can induce DCs to produce indolamine 2, 3-dioxygenase (IDO) that can catabolize the essential amino acid tryptophan to kynurenine which is toxic to T cells (Fallarino et al., 2003; Oldenhove et al., 2009). Selective deletion of CTLA-4 within $Foxp3^+$ $CD4^+$ Treg cells leads to aggressive lymphoproliferative autoimmune disorder (Wing et al., 2008). Similarly, Treg cells use another important molecule known as LAG3 to control T cell-mediated immune response through modulating DC maturation and function. LAG3 is a CD4 homolog that binds MHC class II molecules with high affinity. Interaction of MHC class II molecules, expressed on the surface of immature DCs, with LAG3 leads to inhibition of DCs maturation (Huang et al., 2004; Liang et al., 2008). Other transmembrane molecules that have been recently shown to play a role in Treg-mediated suppression are the two ectoenzymes; CD39 and CD73. CD39 and CD73 induce the generation of pericellular adenosine from the extracellular nucleotides. Pericellular adenosine can inhibit DCs function as well as T cell proliferation (Kobie et al., 2006; Borsellino et al., 2007; Deaglio et al., 2007).

1.5.2 Immune suppression by secreted molecules

In addition to the transmembrane molecules, Treg cells can also secrete functionally important proteins (such as IL-10, IL-35, transforming growth factor beta (TGF-β), cyclic adenosine mono-phosphate (cAMP), granzyme A, granzyme B, and perforin) that play an instrumental role in Treg-mediated suppression. IL-10 is an immunoregulatory cytokine that plays an essential role in the maintenance of immune-homeostasis and the prevention of excessive inflammation (Iyer and Cheng, 2012). Selective deletion of IL-10 in $Foxp3^+$ Treg cells demonstrated that IL-10 production by $Foxp3^+$ Treg cells is essential to keep in check the immune response at environmental interfaces such as colon and lungs (Rubtsov et al., 2008). Another immunoregulatory cytokine that has an important role in Treg-mediated suppression is IL-35. Vignali and colleagues showed that deletion of IL-35 specifically in $Foxp3^+$ Treg cells has a negative impact on Treg cells suppressive capacity *in vitro* and inability to suppress the development of IBD *in vivo*, upon adoptive transfer into the lymphopenic host (Collison et al., 2007). In support, a recently published report highlighted the presence of a distinct effector IL-35-Treg cell subset that produces IL-35 and localizes to the T cell zone of secondary lymphoid organs in order to target auto-reactive T cells (Wei et al., 2017). Similar to IL-35, TGF-β production by $Foxp3^+$ Treg cells

is required to inhibit IBD in particular as well as Th1 immune responses in general (Li et al., 2007). Treg cells can also generate second messenger cyclic adenosine monophosphate (cAMP) that traverses through gap junctions to self-reactive or activated T cells to inhibit their proliferation and IL-2 synthesis (Bopp et al., 2007). Moreover, Treg cells can directly kill the responder T cell or APCs in granzyme or perforin-dependent manner (Gondek et al., 2005; Zhao et al., 2006; Cao et al., 2007; Gondek et al., 2008; Velaga et al., 2015). How Treg cells orchestrate these different mechanisms and/or what determine which tool(s) will Treg use in lymphoid and non-lymphoid organs under steady-state and different sets of inflammatory conditions to maintain immune-homeostasis is still incompletely understood.

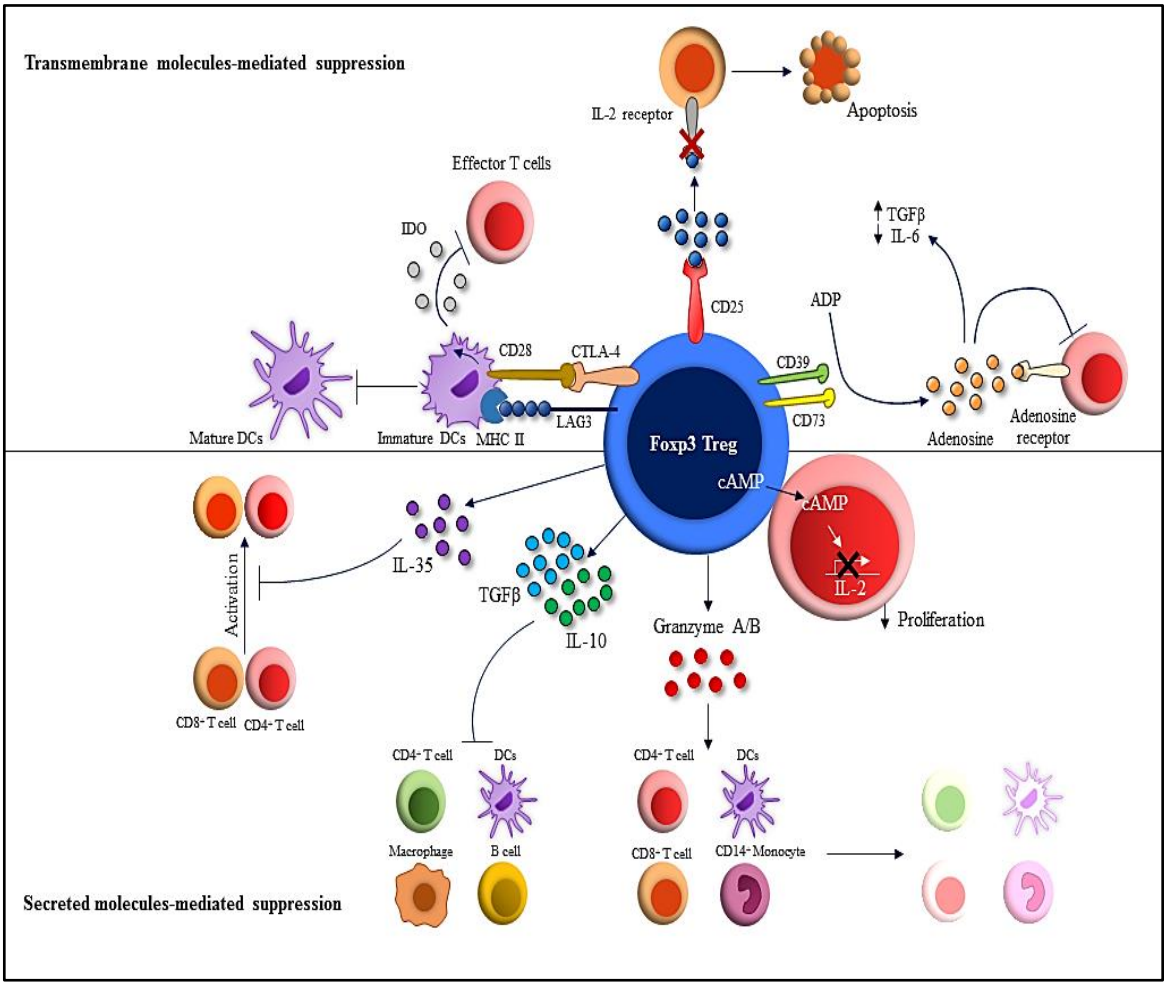

Figure 1. Schematic representation of mechanisms of Treg cell-mediated suppression. Treg cell-mediated suppression mechanisms can be grouped under two main modes of action; i) transmembrane molecules-mediated suppression and ii) secreted molecules-mediated suppression. The figure is adapted from (Vignali et al., 2008; Campbell and Koch, 2011; Meng et al., 2016).

1.6 Treg-mediated control of distinct immune responses

Adaptive immune responses are tailored to combat different types of pathogens. Based on the nature of the pathogen encountered and subsequently the cytokines available in the milieu, naïve $CD4^+$ T cells will be shaped to differentiate into a functionally distinct subset of effector Th cells (Th1, Th2, Th9, or Th17; Rothenberg, 2014). The functional specialization of these Th cell subsets is due to the expression of key transcription factors, namely T-box transcription factor (T-bet) for Th1 (Szabo et al., 2000), GATA-binding protein 3 (GATA3) for Th2 (Sauer, 1998), PU.1 for Th9 (Chang et al., 2010), and retinoic acid receptor-related orphan receptor-γt (RORγt) for Th17 (Ivanov et al., 2006), which activate the expression of a distinct set of genes that control their phenotypic and functional characteristics (Zhu et al., 2010). Tight regulation of these polarized immune responses is crucial to prevent unwanted immune-mediated pathology and tissues destruction. Hence, several groups suggested that subsets of $Foxp3^+$ Treg cells express canonical Th cell-associated transcription factors to initiate modular programs of suppression tailored to inhibit the polarized Th1, Th2, and Th17 cell-driven immune responses (Campbell and Koch, 2011; Josefowicz et al., 2012). For instance, T-bet expression by a subset of $Foxp3^+$ Treg cells was shown to be required to maintain Treg cell homeostasis and function under Th1 cell-mediated inflammation (Koch et al., 2009; Levine et al., 2017). T-bet expression in $Foxp3^+$ Treg cells promotes the expression of CXC chemokine receptor 3 (CXCR3) that facilitates migration, proliferation, and accumulation of these specialized Treg cell subset at the sites of Th1 immune responses (Koch et al., 2009). Conditional deletion of *Tbx21* (gene-encoding T-bet) in $Foxp3^+$ Treg cells results in failure in the regulation of Th1 cell-mediated immune responses, but not Th2 or Th17 cell-mediated immune responses (Koch et al., 2009; Levine et al., 2017).

Similarly, expression of interferon regulatory factor 4 (IRF4), a transcription factor involved in Th2 cell differentiation (Lohoff et al., 2002; Rengarajan et al., 2002), by a subset of $Foxp3^+$ Treg cells empowers them with the molecular machinery required to control Th2 cell-mediated immune responses (Zheng et al., 2009). Selective ablation of *irf4* in $Foxp3^+$ Treg cells results in selective dysregulation in the frequency and the number of IL-4- and IL-5- producing $CD4^+$ T cells, dramatic elevation in IL-4-dependent immunoglobulin (Ig)G1 and IgE production, and ubiquitous plasma cells infiltration in the spleen (Zheng et al., 2009). Under the same logic, deletion of signal transducer and

activator of transcription 3 (*stat3*), a transcription factor crucial for the generation of Th17 (Yang et al., 2007), specifically in Foxp3$^+$ Treg cells leads to the development of fatal intestinal inflammation driven by uncontrolled Th17 immune responses (Chaudhry et al., 2009). Furthermore, it has been shown that Foxp3$^+$ Treg cells do require B-cell lymphoma 6 (Bcl6) expression, a transcription factor directing T follicular helper cells (T_{FH}) differentiation (Nurieva et al., 2009; Yu et al., 2009), to control germinal center reactions (Chung et al., 2011; Linterman et al., 2011).

Treg cell subsets can also co-opt the expression of cell-/tissue-specific transcription factors in an attempt to endow themselves with particular molecular machinery to maintain homeostasis at a particular location/cell/or tissue-type. For instance, visceral adipose tissue-resident Treg cells, VAT-Treg cells, needs the expression of peroxisome proliferator-activated receptor gamma (PPARγ), a transcription factor necessary for adipocyte development and differentiation (Barak et al., 1999; Imai et al., 2004), to control obesity-associated inflammation and maintain insulin sensitivity (Feuerer et al., 2009; Feuerer et al., 2010; Cipolletta et al., 2012). Hence, the ability of Treg cells to co-opt the expression of certain transcription factors is crucial to drive the development of phenotypically and functionally specialized Treg cell subsets that can control distinct classes of immune response.

1.7 Cytokine-mediated regulation of Foxp3$^+$ Treg cells

The ability of Treg cells to sense changes in the micro-environment, the environmental cues, is crucial and mandatory for their development, differentiation, and expansion (Mellor and Munn, 2011). The most defining environmental cue in the context of the host immune system is cytokines. Binding of the cytokines, available in the milieu, to their specific receptors, trigger signaling pathways that promote cell development, differentiation, expansion, and/or cell death. Indeed, cytokines play an indispensable role in Treg cells development. It has been shown that in addition to TCR signals, development and differentiation of Treg cells in the thymus are critically dependent on the availability of IL-2 and, to lesser extent, IL-7 and IL-15, common gamma-chain (γc) receptor-dependent cytokines (Burchill et al., 2007; Vang et al., 2008). Whereas deletion of IL-2 or CD25 in mice leads to a two-fold reduction in the proportion and the absolute number of

Foxp3$^+$ Treg cells, deletion of either IL-7 or IL-15 does not disrupt Foxp3$^+$ Treg cells generation (Vang et al., 2008; Josefowicz et al., 2012). Interestingly, however, mice with combined deletion of IL-2, IL-7, and IL-15 are completely devoid of Treg cells (Fontenot et al., 2005a; Burchill et al., 2007; Malek, 2008; Vang et al., 2008). IL-2 also plays an important role in controlling Treg cells development. Recently, Robey and colleagues (2015) demonstrated that Treg cells within the thymus environment inhibit *de novo* generation of thymus (t)-derived Treg (tTreg) cells by limiting the supply of the available IL-2 and hence, providing a negative feedback loop to maintain a balanced production of Treg cells in the thymus (Weist et al., 2015; Kitagawa and Sakaguchi, 2017).

In addition to the γc receptor-dependent cytokines, TGF-β plays a critical role in the development of Treg cells in the thymus. It has been shown that thymocyte apoptosis drives the production of TGF-β intrathymically from thymic epithelial cells, macrophages, and DCs. This TGF-β induces Treg cells generation in the thymus via enhancing Foxp3 expression (Konkel et al., 2014; Hoeppli et al., 2015). TGF-β can also induce the generation of the peripherally-induced Treg cell (pTreg) in the presence of strong TCR signals. Moreover, TGF-β signaling pathway is crucial for Treg cells to maintain their homeostasis, regulatory functions and Foxp3 expression (Chen et al., 2003; Zheng et al., 2004; Marie et al., 2005; Selvaraj and Geiger, 2007).

The differentiation of Treg cells into specialized Treg cell subsets to control distinct immune responses is also regulated by cytokines. For instance, interferon gamma (IFN-γ)-mediated activation of STAT1 via IFN-γ receptor (IFN-γR) expressed on the surface of Foxp3$^+$ Treg cells drives the expression of T-bet by a subset of Treg cells (Koch et al., 2009). T-bet expression, as discussed earlier, plays a key role in controlling the migration, homeostasis, and immunoregulatory functions of those Treg cells during Type1 inflammatory responses (Koch et al., 2009). Similarly, it has been shown recently that IL-33 signaling through IL-33 receptor (ST2) is necessary and sufficient for VAT-Treg cells development, proliferation, as well as maintenance of transcriptional signature. Mice lacking either IL-33 or ST2 are completely devoid of VAT-Treg cells (Vasanthakumar et al., 2015). Nevertheless, the modulation of phenotypic and functional characteristics of Treg cells mediated by many other cytokines are not yet clear. For instance, the effect of interleukin-4 (IL-4)/IL-4 receptor alpha (IL4Rα)-mediated signaling on Foxp3$^+$ Treg cells

development, maintenance, and regulatory functions under steady-state and inflammatory conditions remain controversial.

1.8 Interleukin-4 and Interleukin-4 receptor alpha-mediated signaling

1.8.1 Interleukin-4

IL-4 is an anti-inflammatory cytokine that plays a crucial role in the induction and maintenance of type 2 immune response (Seder and Paul, 1994). Murine *il-4* encoding gene locates on chromosome 11, on close proximity to *il-5*, *il-13*, and granulocyte macrophage-colony stimulating factor (GM-CSF) encoding genes, and consists of 4 exons and 3 introns spanning over 6 kb (Lee et al., 1986; Otsuka et al., 1987; Paul, 1991). Murine IL-4 is a glycosylated protein with a molecular weight of 14-19 kDa based on the cellular source producing it (Ohara et al., 1985; Grabstein et al., 1986; Paul, 1991). IL-4 is produced by several immune cells including ILC2 (Noval Rivas et al., 2016; Pelly et al., 2016), basophils (Min et al., 2004), eosinophils (Sabin et al., 1996), mast cells (Plaut et al., 1989), gamma-delta T cells (Ferrick et al., 1995), $NK1.1^{+}$ T cells (Yoshimoto and Paul, 1994), and conventional T cells (Launois et al., 1995; Noben-Trauth et al., 2000).

IL-4 has pleiotropic actions on a variety of immune cells (Paul, 1991; Seder and Paul, 1994). For instance, IL-4 plays a key role in the induction, the establishment, and the regulation of Th2 cells (Paul, 1991; Seder and Paul, 1994). IL-4-mediated signaling on B cells enhances their expression of MHC class II (Noelle et al., 1984), Fc epsilon receptor (CD23) (Defrance et al., 1987), and co-stimulatory molecules (CD80 and CD86) (Stack et al., 1994), as well as it induces their class switching in order to produce type 2 antibody isotypes (IgE and IgG1) (Vitetta et al., 1985; Coffman et al., 1986). Moreover, it has been suggested recently that IL-4-mediated signaling on B cells helps in directing Th cells differentiation towards Th2 cells under inflammatory conditions (Hurdayal et al., 2017). IL-4 can also induce the generation of alternatively activated macrophages (Stein et al., 1992). In combination with TNF-α, IL-4 can alter the expression pattern of adhesion molecules in order to enhance endothelial cells adhesion and hence, facilitates the recruitment of T cells and eosinophils to the site of inflammation (Thornhill et al., 1991; Bennett et al., 1997; Nelms et al., 1999).

1.8.2 Interleukin-4 receptor alpha

IL-4 exerts its function(s) by binding to its specific receptors expressed on the surface of the target cells. There are two distinct heterodimeric IL-4R complexes (Fig. 2); Type I receptor complex (consists of IL-4R-alpha (IL-4Rα) and the γc chain) (Russell et al., 1993), and Type II receptor complex (consists of IL-4Rα and IL-13Rα1) (Obiri et al., 1995; Hilton et al., 1996). IL-4Rα is a common component in the two heterodimeric IL-4R complexes. Murine *il-4rα* encoding gene locates on chromosome 7 and consists of 12 exons of which 9 exons are encoding for IL-4Rα chain. IL-4Rα chain has an approximate molecular weight of 140 kDa and belongs to hematopoietic receptor superfamily (Bazan, 1990; Nelms et al., 1999). The structure of the receptor consists of three main parts; i) extracellular region that consists of a tandem of type III fibronectin domain as well as the WSXWS box that together form the classical "cytokine binding homology region" which binds to the IL-4, ii) transmembrane domain, and iii) a very long cytoplasmic tail, with more than 500 amino acid residues, that is constitutively associated with Janus kinase 1 (JAK1) which plays an indispensable role in the IL-4Rα-mediated signaling pathway (Fig. 2) (Mosley et al., 1989; Bazan, 1990).

IL-4Rα is expressed on the surface of hematopoietic cells (such as T cells, B cells, mast cells, and macrophages) as well as non-hematopoietic cells (such as hepatocytes, keratinocytes, fibroblast, epithelial cells, endothelial cells, brain tissues, stromal cells, and smooth muscles) (Ohara et al., 1985; Lowenthal et al., 1988). IL-4Rα chain is usually expressed in a range from 100 to 5000 receptors per cell (Ohara et al., 1985). IL-4 binds with a very high affinity to IL-4Rα chain with a dissociation constant ranging from 20 to 300 pM (Ohara et al., 1985; Park et al., 1987; Mosley et al., 1989). T cells do only express the Type I receptor complex (Graber et al., 1998), which will be our main focus.

1.8.3 Interleukin-4 receptor alpha-mediated signaling pathway

Binding of IL-4 to IL-4Rα chain induces its heterodimerization with the γc chain, which is usually coupled to JAK3 (Russell et al., 1993; Russell et al., 1994; Musso et al., 1995). Conformational changes induced by the IL-4 binding result in tyrosine phosphorylation of JAK1 and JAK3 that in turn phosphorylate tyrosine residues on the cytoplasmic tail of IL-4Rα chain (Smerz-Bertling and Duschl, 1995). The phospho-tyrosine

residues in IL-4Rα chain create docking sites for the Src Homology 2 (SH2) domain of STAT6 as well as insulin receptor substrate 1 and 2 (IRS-1 and IRS-2) which are subsequently phosphorylated by the JAKs (Darnell, 1997). Phosphorylated-STAT6 disengages from the receptor and forms homodimers (Fig. 2). STAT6 homodimers translocate into the nucleus whereby they bind to specific DNA sequence(s) on the promoter elements to switch on the expression of IL-4 responsive genes (Nelms et al., 1999). Tyrosine phosphorylation of IRS-1 and IRS-2 leads to activation of phosphatidylinositol 3-kinase (PI3K) and mitogen-activated protein (MAP) pathways which are of importance for cell cycle activation, cell survival, and proliferation (Fig. 2) (Wang et al., 1993; Sun et al., 1995; Izuhara et al., 1996; Wills-Karp and Finkelman, 2008).

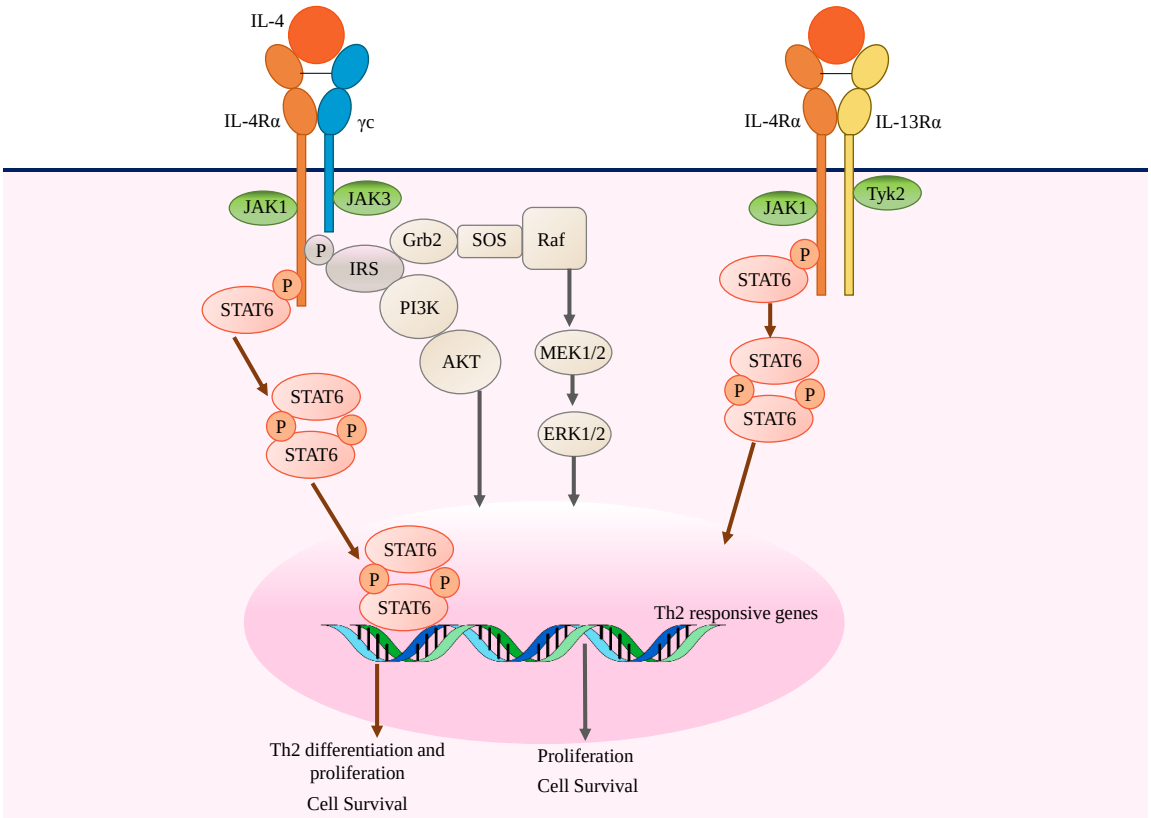

Figure 2. Schematic representation of the IL-4Rα signaling pathway. Two types of IL-4R can mediate the signaling pathway of IL-4. While type I receptor consists of IL-4Rα and γc, type II receptor consists of IL-4Rα and IL-13Rα. Only type I receptor is expressed on T cells. Binding of IL-4 to its receptor results in receptor dimerization and subsequent activation of JAKs associated with cytoplasmic tails of the receptor. Tyrosine residues, on the IL-4Rα cytoplasmic tail, phosphorylated by activated JAKs act as docking sites for STAT6 and IRS. Phosphorylation of STAT6 results in its dimerization, translocation into the nucleus, and activation of Th2-responsive genes required for Th2 differentiation and proliferation. Phosphorylation of IRS activates its signaling pathway that is linked to cell activation, proliferation, and cell survival. The figure is adapted from (Wills-Karp and Finkelman, 2008; Walker and McKenzie, 2018).

1.9 Th2 disease models

IL-4/IL-4Rα-mediated signaling has an indispensable role in conferring protection to the host against helminths infection. Indeed, abrogation of IL-4/IL-4Rα-mediated signaling results in host susceptibility to infection comes from seminal studies on the highly tractable murine models of experimental infection with the hookworm *Nippostrongylus brasiliensis* (*N. brasiliensis*) (Barner et al., 1998; Urban et al., 1998; Nono et al., 2017b), and the blood fluke *Schistosoma mansoni* (*S. mansoni*) (Jankovic et al., 1999; Fallon et al., 2000; Herbert et al., 2004; Nono et al., 2017a), principally.

1.9.1 Schistosomiasis

Schistosomiasis is also called bilharzia having been first described by Theodor Bilharz in 1851, in Cairo, Egypt. Schistosomiasis is the second most socio-economically devastating parasitic disease in the world after malaria. It is endemic in 74 African, Asian and Latin American countries and infects an estimated 240 million people with 280,000 deaths annually in sub-Saharan Africa and approximately 800 million at risk of infection (Chitsulo et al., 2000; Colley et al., 2014; Inobaya et al., 2014; Skelly et al., 2014). Schistosomiasis is caused by several blood-dwelling trematode species (flukes) of the genus *Schistosoma*, including *Schistosoma mansoni*, *S. japonicum*, *S. intercalatum* and *S. mekongi* that cause hepatic-intestinal schistosomiasis and *S. haematobium* that induces urinary disease (Barsoum et al., 2013; Elbaz and Esmat, 2013).

1.9.1.1 Schistosome life cycle

Schistosoma eggs are introduced to freshwater environment through urine or feces of the infected host where they hatch and release the free-living and ciliated miracidium (Fig. 3). The ciliated miracidium swims towards their specific intermediate snail host, penetrates it, loses its cilia, develops into sporocyst and then undergoes asexual reproduction until it becomes cercariae. Upon exposure to light, hundreds of free swimming, fork-tailed cercariae break out of snail tissue into freshwater where they swim actively until they come into contact with the skin of human or animal, the definitive host. Cercariae invade the skin

via secretion of excretory-secretory products (ESP), including proteolytic enzymes and immunogenic glycans (Hokke and Yazdanbakhsh, 2005; Knudsen et al., 2005; Hansell et al., 2008), undergo massive biochemical changes followed by their maturation into schistosomula (Walker, 2006; Collins et al., 2011). Schistosomes differ in their migratory pattern through skin layers; *S. mansoni and S. haematobium* are slower in their migration rate when compared to *S. japonicum.* For *S. japonicum* schistosomula, only two hours after exposure are enough for them to be found in the dermis and even some are already in the blood vessels, while *S. mansoni and S. haematobium* somula take 48 hours to reach the dermis and 72 hours to be found in the dermal blood vessels (McKerrow and Salter, 2002; Curwen and Wilson, 2003; He et al., 2005; Walker, 2011; Gryseels, 2012). Once in the blood capillaries, schistosomules migrate towards right heart ventricles and then to the lungs. Depending on the species, they reside in the pulmonary capillaries from 3-16 days which is consistent with their size and host spectra (Rheinberg et al., 1998; He et al., 2005). Schistosomules then make their way to the liver where they start feeding on blood and growing by active cell division. They become mature 28-35 days post-infection and start pairing and laying of eggs. The paired adults then travel to the place where they will finally reside; *S. mansoni* and *S. japonicum* reside in the portal and mesenteric vessels while *S. haematobium* resides in the pelvic venous plexus and veins around the bladder (Fig. 3). Massive numbers of eggs are laid daily; 300 eggs for *S. mansoni and S. haematobium* and 3000 eggs for *S. japonicum.* About half the number of eggs produced is excreted with the feces or urine while the rest of eggs are swept with the blood to the liver where they cause granulomatous inflammation (Elbaz and Esmat, 2013; Inobaya et al., 2014; Othman and El Ridi, 2014).

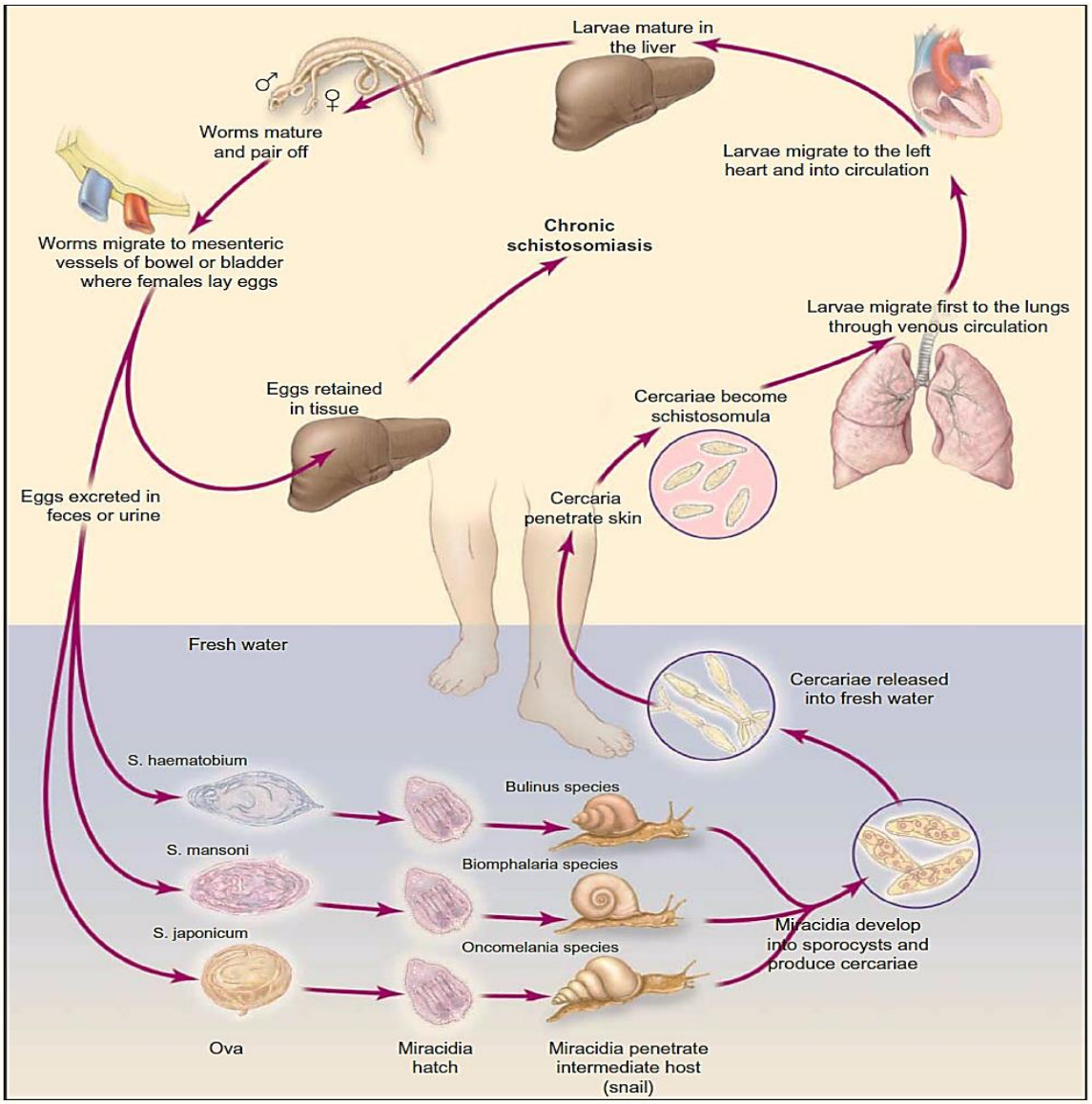

Figure 3. The Schistosome Life cycle. The figure is adapted from (Ross et al., 2002; Inobaya et al., 2014; Weerakoon et al., 2015).

1.9.1.2 Immunobiology of schistosomiasis

During *Schistosoma* journey from the invasion until the establishment of infection (Fig. 3), the host immune response progresses through 4 different immune phases; i) early pre-patent immune response phase, ii) late pre-patent immune response phase, iii) acute phase, and iv) chronic phase (Pearce and MacDonald, 2002; Abdel Aziz et al., 2016). Early pre-patent immune response phase is the first phase that starts from day 0 up to 3 weeks post-infection. Early pre-patent immune response phase is characterized by the production of type 1, type 2, and type 17 cytokines from epidermal, lymph node, and lung cells (Abdel

Aziz et al., 2016). Initiation of the three different arms of the immune response was suggested to be a possible evasion mechanism, in C57BL/6 mice, as these immunological signals can counteract and antagonize each other, helping in creating an immunological chaos and hence, the establishment of infection (Abdel Aziz et al., 2016). In support, during this period, humoral immune responses to parasite antigens remain negligible and preponderantly of IgM isotype well until patency (El Ridi et al., 2006a; El Ridi et al., 2006b; Tallima et al., 2009). Late pre-patent immune response phase takes place during 3-5 weeks post-infection whereby the host immune system skews towards type 1 immunity in response to migrating immature parasites (Pearce and MacDonald, 2002). Parasite maturation, copulation, and production of eggs (5-6 weeks post-infection) result in the initiation of the acute phase of schistosomiasis that usually peaks between 6 to 8 weeks post-infection. Schistosome egg antigens induce a drastic reduction in type 1 immune response in concurrence with a significant shift towards type 2 immune response (i.e. IL-4 and IL-13) which drives fibro-granulomatous inflammation around the eggs trapped within the tissue. It has been demonstrated that hegemony of type 2 immune response during acute schistosomiasis plays an indispensable role in host protection and survival (Pearce and MacDonald, 2002). For instance, infection of IL-4 deficient (IL-$4^{-/-}$) C57BL/6 mice with *S. mansoni* cercariae results in severe and rapid cachexia and eventually the mice succumbed pre-maturely to the infection when compared to their littermate controls (Bennett et al., 1997). Similarly, IL-4R$\alpha^{-/-}$ mice are highly susceptible to *S. mansoni* infection. *S. mansoni*-infected IL-4R$\alpha^{-/-}$ mice succumb to the infection by 8 weeks due to impaired ability of egg expulsion, abrogation of granuloma formation, and severe gut inflammation that results in leakage of lipopolysaccharides in the bloodstream causing septic shock (Herbert et al., 2004). Interrogation of IL-4Rα-responsive cells that play a key role in conferring protection or susceptibility to *S. mansoni* infection has been feasible by using Cre-locus of X-over P1(*loxP*) technology. For example, it has been suggested that IL-4Rα-responsive macrophages (using $LysM^{cre}$ IL-4R$\alpha^{-/lox}$) (Herbert et al., 2004), non $CD4^{+}$ T cells (using $iLCK^{cre}$ IL-4R$\alpha^{-/lox}$) (Dewals et al., 2009), and smooth muscle cells (using SM-MHC^{cre} IL-4R$\alpha^{-/lox}$) (Marillier et al., 2010) are critical in conferring protection to the host against acute schistosomiasis. The contribution of IL-4Rα-responsive $Foxp3^{+}$ Treg cells towards host susceptibility or protection during acute schistosomiasis is yet to be interrogated.

Ten weeks post-infection, the host immune system starts to down-modulate the type 2 immune response, probably by the induction of IL-10 production and expansion of Treg

cells (Bosshardt et al., 1997; Hoffmann et al., 2000; Fairfax et al., 2012), preparing the host for the final stage of infection which is chronic schistosomiasis. Chronic schistosomiasis (≥ 12 weeks post-infection) results in a clinically patent tissue fibroproliferative pathology during which granulomas-formed around the newly deposited eggs are smaller in size with a significantly higher collagen deposition and hence, higher level of fibrosis when compared to granulomas formed during the acute stage (Fallon, 2000; Pearce and MacDonald, 2002). The persistence of granulomatous inflammation and fibrosis during the chronic stage, in most cases, result in portal hypertension, ascites, hepatosplenomegaly, hypersplenism, varices, variceal bleeding and ultimately death (Burke et al., 2009; Elbaz and Esmat, 2013; Inobaya et al., 2014).

1.9.1.3 Foxp3$^+$ Treg cells in schistosomiasis

Unlike other helminths that induce activation and expansion of Foxp3$^+$ Treg cells during the first week of infection, i.e. filariasis (Gillan and Devaney, 2005; McSorley et al., 2008; Taylor et al., 2009) and intestinal nematodes infection (Finney et al., 2007; Blankenhaus et al., 2011; Redpath et al., 2013), in order to dampen the host effector immune mechanisms and hence, facilitates the establishment of infection, *Schistosoma*-infection does neither induce Foxp3$^+$ Treg cells expansion nor activation during the early pre-patent immune response phase (0-3 weeks post-infection) (Redpath et al., 2015). It has been demonstrated by Maizels and colleagues (2015) that C57BL/6 mice infection with *S. mansoni* does not induce Foxp3$^+$ Treg cells expansion in either skin-draining lymph nodes (LN), lungs, lung-draining LN, or spleen during the first 3 weeks of infection when compared to naïve mice (Redpath et al., 2015). Moreover, after infection, the expression levels of Foxp3$^+$ Treg cells activation markers (CD25, Foxp3, and Helios) are similar to naïve mice (Redpath et al., 2015). In support, Singh and colleagues (2005) showed that Foxp3 expression of splenocytes 8 weeks post-infection is similar to that of naïve mice (Singh et al., 2005). Nevertheless, upregulation of Foxp3 expression in the spleen 16 weeks post-infection was reported (Singh et al., 2005). In contrast to the spleen, liver of *S. mansoni*-infected mice showed 10 and 30 fold increase in Foxp3 gene expression level 8 and 16 weeks, respectively, post-infection (Singh et al., 2005), indicating that Foxp3$^+$ Treg cells might play a key role in the regulation of fibrogranulomatous inflammation in the liver. In fact, it was demonstrated that during acute egg-induced schistosomiasis, Foxp3$^+$

Treg cells do not play a major role in the regulation of effector T cell clonal expansion but rather they do control egg-induced effector Th2 cytokine production in an IL-10 independent manner (Baumgart et al., 2006). The precise mechanism(s) via which $Foxp3^+$ Treg cells control fibrogranulomatous inflammation is yet to be interrogated.

1.9.2 *Nippostrongylus brasiliensis*

N. brasiliensis is one of the most important gastrointestinal nematodes which physiologically and biochemically resemble the human hookworms (e.g. *Ancylostoma duodenale* and *Necator americanus*) (Finkelman et al., 1997; Gause et al., 2003) that represent a major part of neglected tropical disease as they do affect more than one billion people worldwide and cause severe morbidity and mortality especially in school-aged children (Hotez et al., 2008; Bouchery et al., 2017). *N. brasiliensis* is naturally a nematode parasite of rats, but it has been adapted to infect mice in order to understand how the host immune system can control the infection with these parasites and hence, identifies the factors that play a key role in conferring protection to the host (Bouchery et al., 2017).

1.9.2.1 *Nippostrongylus brasiliensis* life cycle

In the murine model, *N. brasiliensis* infection starts with administering the third larval stage (L3) subcutaneously, mimicking the natural infection. During the first 24-48 hours, the larvae exit the blood vessels and then enter the lungs where they moult into the fourth larval stage (L4). The parasites then migrate from the lungs and breach the alveolar spaces whereby they are coughed up and swallowed into the intestine. In the gut, the L4 parasites start to develop to the final mature stage (L5) (5-6 days post-infection), copulate and start to release eggs from day 6. The released eggs hatch in the soil within 24 hours and give rise to L1 stage that undergoes further differentiation to moult into L3 stage, the infectious stage (Fig. 4). *N. brasiliensis* infection is a naturally acute infection as the host can expel the worms from the intestinal lumen in less than 2 weeks (Finkelman et al., 1997; Gause et al., 2003; Bouchery et al., 2017).

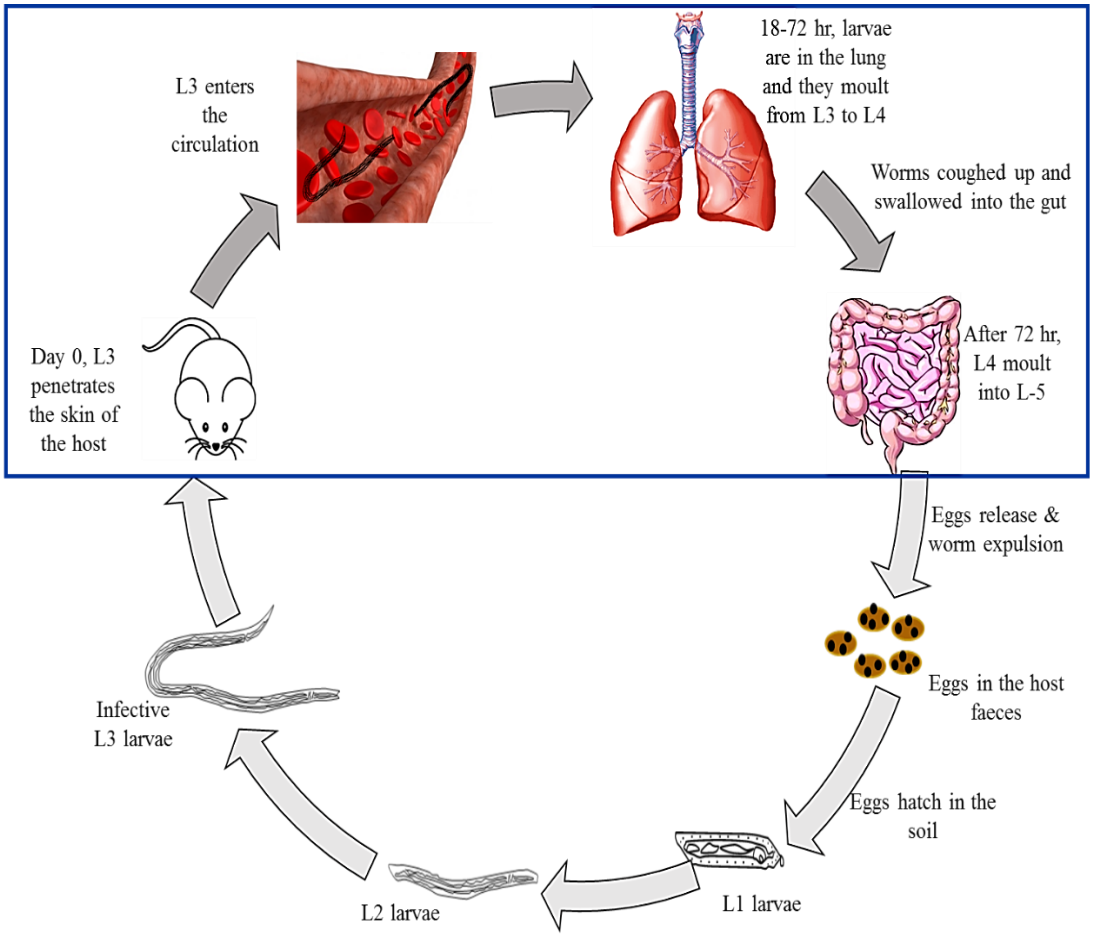

Figure 4. Life cycle of *Nippostrongylus brasiliensis*.

1.9.2.2 Immunobiology of *Nippostrongylus brasiliensis*

Mice infection with *N. brasiliensis* triggers a highly polarized type 2 immune response that is characterized by elevated production of type 2 cytokines (e.g. IL-4, IL-5, and IL-13) (Barner et al., 1998; Urban et al., 1998), eosinophilia, mastocytosis, as well as significant increase in serum antigen-specific type 2 antibody isotypes (IgG1 and IgE) (Finkelman et al., 1997; Gause et al., 2003). Furthermore, *N. brasiliensis* infection induces goblet cells hyperplasia and mucus secretion which are required to prevent the worms from either adhering to the intestinal lamina propria or feeding properly, facilitating the expulsion of the worms from the lumen (Koninkx et al., 1988). IL-4 was suggested to have a redundant protective role against *N. brasiliensis* infection as IL-$4^{-/-}$ mice can expel *N. brasiliensis* in time frame similar to immunocompetent mice, whereas treatment of severe combined immunodeficient (SCID) mice with exogenous IL-4 was sufficient to confer protection

against that parasite (Urban et al., 1995; Lawrence et al., 1996). In contrast, IL-13$^{-/-}$, IL-4$^{-/-}$/IL-13$^{-/-}$, STAT6$^{-/-}$, or IL-4Rα$^{-/-}$ mice fail to expel *N. brasiliensis* worms, pointing towards an instrumental role of IL-13 and IL-4Rα-mediated signaling in conferring protection to the host against *N. brasiliensis* infection (Finkelman et al., 1997; Barner et al., 1998). Conditional ablation of IL-4Rα from smooth muscle cells results in delayed goblet cells differentiation, reduced mucus production and hence, delayed worm expulsion (Horsnell et al., 2007; Zhao et al., 2008). The exact role of other IL-4Rα-responsive non-hematopoietic as well as IL-4Rα-responsive hematopoietic cells in mediating host protection or susceptibility against *N. brasiliensis* infection is yet to be interrogated.

1.9.2.3 Foxp3^{+} Treg cells in *N. brasiliensis* infection

It has been shown that CTLA-4, a transmembrane molecule implicated in Treg-mediated suppression, plays an important role in limiting Th2 immune response during *N. brasiliensis* infection (McCoy et al., 1997). Blockade of CTLA-4 during *N. brasiliensis* infection results in heightened Th2 cytokine production that drives accelerated worm expulsion (McCoy et al., 1997). Interestingly, it was reported that *N. brasiliensis* infection induces an increase in Foxp3^{+} Treg infiltration into the lung (Liu et al., 2008). These Foxp3^{+} Treg cells produce a high level of IL-10 (Liu et al., 2008), that was demonstrated to play a crucial role in controlling lung inflammation and down-modulating IL-17 expression (Chen et al., 2012). Treg depletion by using anti-CD25 results in heightened IL-17 production that drives severe lung inflammation during *N. brasiliensis* infection (Liu et al., 2008). The kinetics of Foxp3^{+} Treg cells during *N. brasiliensis* infection as well as their regulatory role from invasion until expulsion of worms is to be fully explored.

1.10 The controversial effect of IL-4Rα-mediated signaling on Foxp3$^+$ Treg cells

The role of IL-4Rα-mediated signaling on Foxp3$^+$ Treg cells has been a long-standing debate. It has been shown that oral sensitization of *il4ra*^{F709} mice, mice whose IL-4Rα chain has a single-amino-acid substitution of tyrosine (Y) to phenylalanine (F) at position 709 that leads to abrogation of immunoreceptor tyrosine-based inhibitory motif (ITIM) function and hence, augmentation of IL-4Rα-STAT6 signaling pathway (Tachdjian et al., 2010), with ovalbumin (OVA) in combination with staphylococcal enterotoxin B (SEB) results in impaired generation of allergen-specific Treg cells (Noval Rivas et al., 2016). In this study, it was demonstrated that selective augmentation of IL-4Rα-mediated signaling on Foxp3$^+$ Treg cells induces the transdifferentiation of Foxp3$^+$ Treg cells to Th2-like cells, termed ex-Foxp3 Th2 cells. In that case, ex-Foxp3 Th2 cells were producing IL-4 while maintaining Foxp3 expression (Noval Rivas et al., 2016; Noval Rivas and Chatila, 2016). Similarly, house dust mite sensitization of *il4ra*^{R576} mice, mice with a single-amino-acid substitution of glutamine (Q) to arginine (R) at position 576 of the IL-4Rα chain, results in transdifferentiation of pTreg cells to Th17-like cells, termed ex-Foxp3 Th17 cells, in an IL-4 dependent manner. Ex-Foxp3 Th17 cells started to produce IL-6 and IL-17 and to express RORγt, the canonical transcription factor of Th17 (Massoud et al., 2016). Using fate-reporter system, Wilson and colleagues (2017) suggested that chronic helminth infection such as *H. polygyrus* induces transdifferentiation of a significant proportion of Foxp3$^+$ Treg cells to become ex-Foxp3 Th2 cells in IL-4/IL-4Rα-dependent manner whereby Foxp3$^+$ Treg cells start to lose Foxp3 expression and to produce type 2 cytokines (Pelly et al., 2017). A strong case was therefore made for the negative regulation of Foxp3$^+$ Treg cells by IL-4Rα-mediated signaling.

Intriguingly, an independent report rather made mention of a supporting role of IL-4Rα-mediated signaling on Foxp3$^+$ Treg cells *in vitro* (Maerten et al., 2005). In that report, it was shown that CD4$^+$ CD25$^+$ Treg cells cultured in the presence of IL-4 have a better survival capacity and an enhanced Foxp3 expression (Maerten et al., 2005). This resulted into a higher potency of CD4$^+$ CD25$^+$ Treg cells to suppress CD4$^+$ T cell proliferation and cytokines production, when compared to CD4$^+$ CD25$^+$ Treg cells cultured in medium without IL-4 (Maerten et al., 2005).

Another study by Pillemer and colleagues (2009) reported on the controversial effect of IL-4/IL-4Rα-mediated signaling on Foxp3$^+$ Treg cells (Pillemer et al., 2009). The latter

study demonstrated *in vivo*, under allergic inflammation, and *in vitro*, that even though IL-4 maintains Foxp3 expression and enhances Treg proliferation, IL-4 signaling on Foxp3$^+$ Treg cells abrogates their suppressive functional capacity (Pillemer et al., 2009).

In conclusion, even though some studies are suggesting a positive influence of IL-4Rα-mediated signaling on Foxp3$^+$ Treg cells, these studies are conflicted with equally well-conducted studies indicating that IL-4Rα-mediated signaling on Foxp3$^+$ Treg cells might have a deleterious effect on the Treg cell functions, pointing overall a rather conflicting picture of the role of IL-4Rα signaling on Foxp3$^+$ Treg cells (Fig. 5).

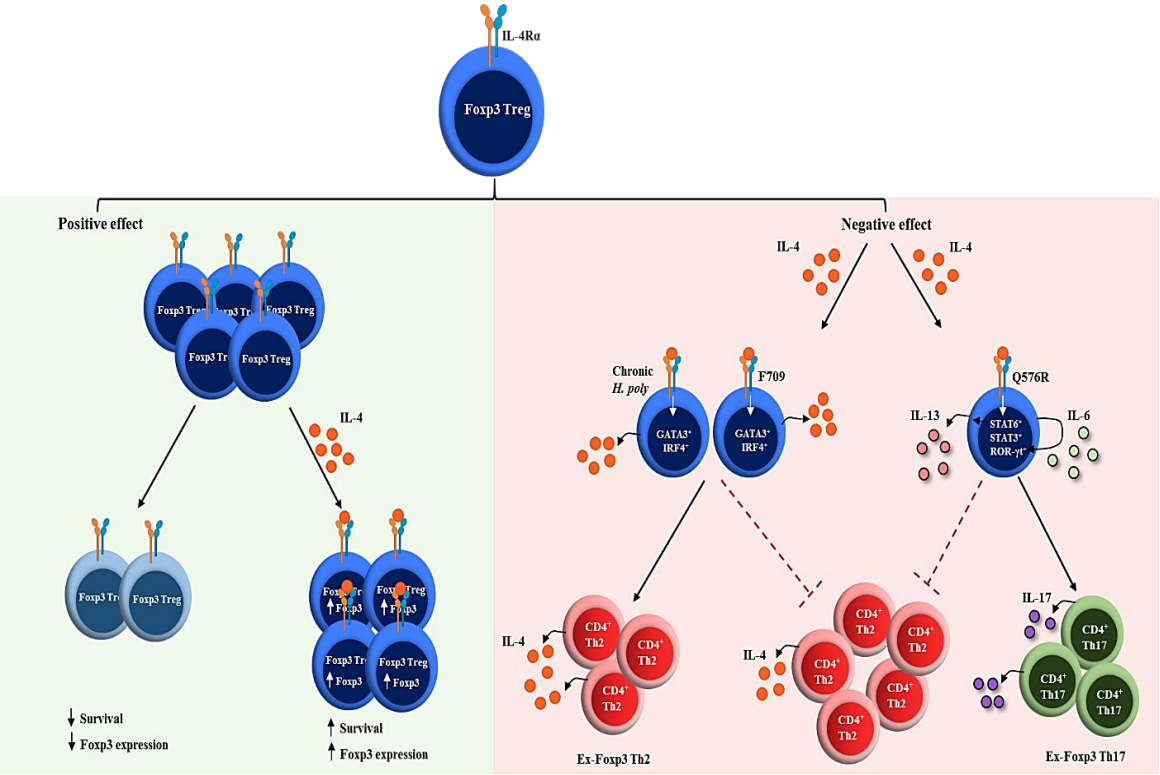

Figure 5. The controversial effect of IL-4Rα-mediated signaling on Foxp3$^+$ Treg cells. Schematic diagram showing the conundrum in the literature with regards to the role of IL-4Rα-mediated signaling on Foxp3$^+$ Treg cells. IL-4Rα signaling on Foxp3$^+$ Treg cells could have a supportive role (i.e. enhances their survival and enforces Foxp3 expression) or a detrimental role (i.e. induces Treg cells reprogramming towards Th2 or Th17). The figure is adapted from (Noval Rivas and Chatila, 2016).

1.11 Objectives

The present work was set forth as an attempt to unambiguously and conclusively decipher the bases of the regulation of Foxp3^{+} Treg by IL-4Rα-mediated signaling. To dissect this role of the IL-4Rα on Foxp3^{+} Treg cells, the present thesis sought to:

- generate a transgenic mouse model whereby IL-4Rα is specifically removed from Foxp3^{+} Treg cells (Foxp3^{cre} IL-4Rα$^{-/lox}$ mice).

- characterize, under steady-state, the cellular, tissular, and phenotypic profile as well as the inflammatory disorders in naïve Foxp3^{cre} IL-4Rα$^{-/lox}$ mice.

- characterize the overall fitness of Foxp3^{+} Treg cells in diseased Foxp3^{cre} IL-4Rα$^{-/lox}$ mice in controlling T cell proliferation, effector function, and tissue inflammation during infection

In combination, these objectives should help understand how IL-4Rα controls the Foxp3^{+} Treg cells under steady-state and inflammatory conditions.

Chapter 2:
Materials and Methods

Chapter 2: Materials and Methods

2.1 Mice generation and genotyping

IL-4Rα$^{-/-}$, IL-4Rα$^{-/lox}$, and Foxp3^{cre} IL-4Rα$^{-/lox}$ mice on BALB/c background were generated by using the Cre-*loxP* technology. Cre-*loxP* system is a site-specific recombination system that can be used to alter the genetic makeup of the host by mediating genetic deletion, insertion, inversion, and/or translocation (Sauer, 1987; Sauer and Henderson, 1988). The Cre-*loxP* system consists of two main components; the Cre-recombinase enzyme and it's recognition sequence which is known as *loxP* sites. Cre-recombinase enzyme is a bacteriophage P1 integrase protein with an approximate molecular weight of 38-kDa and two main domains; the amino-terminal domain (consists of five α-helices connected via short loops) and the carboxy-terminal domain (contains nine α-helices and small beta-sheet strand) (Abremski and Hoess, 1984; Guo et al., 1997; Guo et al., 1999). *loxP* site is 34-bp consensus sequence that consists of two sets of palindromic 13-bp sequence (ATAACTTCGTATA) with nonpalindromic 8-bp (GCATACAT or ATGTATGC) spacer in between (Abremski and Hoess, 1984; Nagy, 2000). Cre enzyme binds cooperatively to the *loxP* sites with sub-nanomolar affinity in order to catalyze the recombination reaction between the two sites and hence, deletion of a region of interest.

In brief, IL-4Rα$^{-/-}$ BALB/c mice were generated by constructing a gene-targeting vector containing an *Eco*RI-flanked fragment of the *il4ra* derived from BALB/c genomic clone spanning IL-4Rα exons 4–12 (Fig. 8) (Wrighton et al., 1992; Mohrs et al., 1999). *LoxP* sites flanking selection cassette (neomycin and the herpes simplex virus (HSV) thymidine kinase (tk)) at 5' of exon 7 as well as *LoxP* site at 5' of exon 10 were introduced (Fig. 8). The linear targeting construct was electroporated into BALB/c embryonic stem (ES) cells and the Geneticin (G418)-resistant ES cell colonies were isolated 9 days after the addition of selection medium. Clones with proper integration of the targeting vector were electroporated with a plasmid expressing the Cre-recombinase for the two-steps strategy (Mohrs et al., 1999). Two-steps strategy is a technique whereby Cre-recombinase enzyme used first to remove the selection cassette and then the intervening sequences between exon 6 and exon 10. Clones with a deletion of exons 7–9 were injected into C57BL/6 blastocysts. Chimeric male offspring were mated to BALB/c females, and progeny with the mutated allele were intercrossed to obtain mice homozygous for the gene disruption on BALB/c background. Mice were genotyped by doing PCR of tissue biopsies

(Mohrs et al., 1999). IL-4Rα$^{lox/lox}$ BALB/c mice were generated following the same exact strategy described for IL-4Rα$^{-/-}$ BALB/c mice generation except for inducing Cre-recombinase expression in a transient manner. Transient Cre-recombinase expression resulted in the deletion of the selection cassette and retention of the *LoxP* sites at 5' of exon 7 and exon 10, generating IL-4Rα$^{lox/lox}$ BALB/c mice (Fig. 9). IL-4Rα$^{lox/lox}$ BALB/c mice were intercrossed with IL-4Rα$^{-/-}$ BALB/c mice to generate IL-4Rα$^{-/lox}$ BALB/c mice (Herbert et al., 2004).

Generation of Foxp3^{cre} IL-4Rα$^{-/lox}$ mice required the intercrossing between three different mice strains; i) Foxp3-IRES-Cre BALB/c mice, ii) IL-4Rα$^{-/-}$ BALB/c mice and iii) IL-4Rα$^{lox/lox}$ BALB/c mice. Foxp3-IRES-Cre BALB/c mice were generated by following the standard gene-targeting strategy procedure (Fig. 6) whereby the gene-targeting vector was constructed to introduce *ires-cre* coding genes downstream *foxp3* gene stop codon (Fig. 10) (Wing et al., 2008). IRES is an internal ribosomal entry site that allows for the expression of several genes under the control of the same promoter through the generation of dicistronic fusion mRNA (Jang et al., 1988; Pelletier and Sonenberg, 1988; Mountford and Smith, 1995). Therefore, Cre-recombinase enzyme will be expressed under the control of *foxp3* gene promoter in Foxp3-IRES-Cre BALB/c mice. Transgenic Foxp3-IRES-Cre BALB/c mice were intercrossed for two generation with IL-4Rα$^{-/-}$ BALB/c mice (Mohrs et al., 1999). These mice were further intercrossed with homozygous IL-4Rα$^{lox/lox}$ BALB/c mice (Herbert et al., 2004) to generate hemizygous Foxp3^{cre} IL-4Rα$^{-/lox}$ BALB/c mice (Fig. 11, A-B and Flowcharts 1-2). Hemizygous littermates (IL-4Rα$^{-/lox}$) were used as wild-type controls in all experiments.

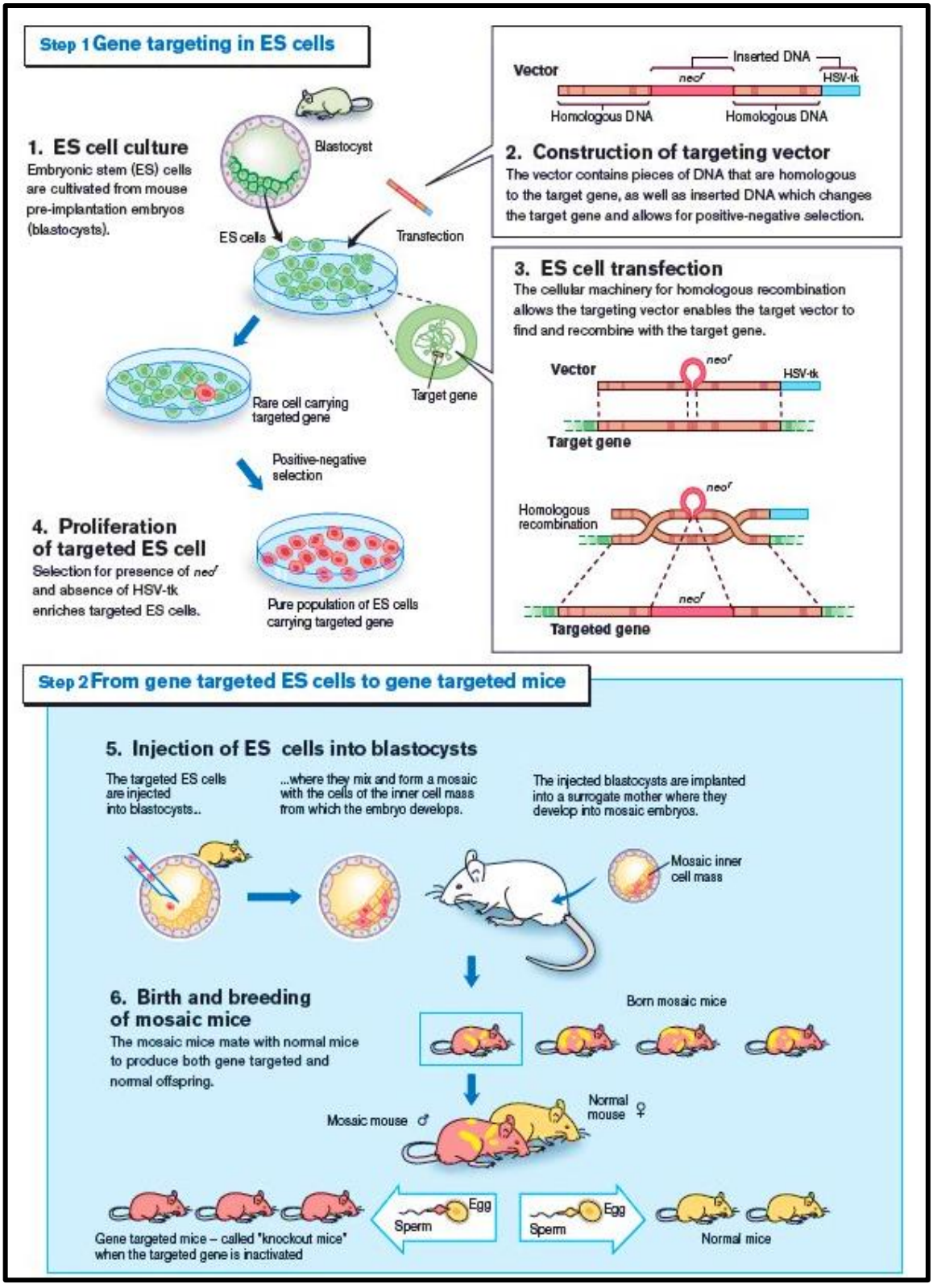

Figure 6. General strategy for gene-targeting in mice. Adapted from (Capecchi et al., 2007).

Mice were genotyped by extracting genomic DNA from the tail as previously described (Mohrs et al., 1999; Herbert et al., 2004). In brief, mouse tail was incubated overnight with 500 µl of lysis buffer (50 mM Tris-HCl (pH 8), 100 mM EDTA, 100 mM NaCl, and 1% (w/v) SDS) at 56ºC. The sample was spun down at 8000 x g for 10 mins at room temperature (RT) and the supernatant was transferred into a new tube. Equal volume of isopropanol was added to the supernatant, mixed gently by inversion, and then spun down at 8000 x g for 10 mins at RT. The supernatant was decanted and the pellet was washed twice with 70% ethanol. The tube was opened to allow for ethanol evaporation and the pellet was then resuspended in nuclease-free water. End-product polymerase chain reaction (PCR) was used for mice genotyping by using the following primer pairs:

Table 2.1. Primers sequence used for genotyping of Foxp3^{cre} IL-4 Rα$^{-/lox}$ mice

Gene target	Primer sequence
WT IL-4Rα-Forward	5’ TGACCTACAAGGAACCCAGGC 3’
WT IL-4Rα-Reverse	5’ CTCGGCGCACTGACCCATCT 3’
Deleted IL-4Rα-Forward	5’ GGCTGCTGACCTGGAATAACC 3’
Deleted IL-4Rα-Reverse	5’ CCTTTGAGAACTGCGGGCT 3’
LoxP-Forward	5’ GGCTGCTGACCTGGAATAACC 3’
LoxP -Reverse	5’ GTTTCCTCCTACCGCTGATT 3’
Cre-Forward	5’ CTGCTTCCTTCACGACATTCAAC 3’
Cre-Reverse	5’ TTCGCAAGAAGAGGAGCCAACG 3’

PCR conditions were 94ºC for 2 min, 94ºC for 30 seconds, 57ºC for 30 seconds, and 72ºC for 1 min for 40 cycles in T100™ Thermal Cycler (Bio-Rad, Hercules, California). PCR-products were then separated on a 1.5% agarose gel and stained with ethidium bromide.

2.2 Ethics statement

All mice were maintained in specific-pathogen-free barrier conditions in individually ventilated cages at the University of Cape Town biosafety level 2 animal facility. Experimental mice were sex and age-matched and used between 6-8 weeks of age. This study was performed in strict accordance with the recommendations of the South African national guidelines and University of Cape Town practice for laboratory animal procedures. All mouse experiments were conducted according to protocols approved by the Animal Research Ethics Committee of the Faculty of Health Science, University of Cape Town (ethics protocols number 014/003, 016/027, 016/024, and 017/002). All efforts were made to minimize animals suffering.

Prior to percutaneous infection with *S. mansoni* cercariae, animals were anaesthetized by intraperitoneal injection of a cocktail of Ketamine (100 mg/kg) and Xylazine (10 mg/kg) and monitored for 5 mins prior to confirming anaesthesia has been induced. Anaesthesia was confirmed by the absence of pedal reflex (toe pinch) and eyeblink reflex amid a regular respiratory rate. The anaesthesia duration was of a maximum of 30 min. During the anaesthesia phase, animals were exposed to an infra-red lamp (Philips, Amsterdam, Netherlands) to help them maintain their core body temperature. This procedure was performed and dully cared for by trained and authorized researchers. Post-infection, animals were monitored until regaining of consciousness and moistened food was added to the cage bedding. Upon reaching the study experimental endpoint and/or the protocol-defined humane endpoint, animals were euthanized via exposure to an excess of Halothane (4% in air) for 5 min. The fatal anaesthesia was confirmed by a total absence of pedal reflex (toe pinch) and eyeblink reflex as well as the total absence of a respiratory rate. Death was confirmed either by neck dislocation or exsanguination by cardiac puncture.

For survival study, the humane endpoint was determined by measuring the mice body weight and evaluating their physical performance. Mice that lost 20% of their initial body weight and/or showed aggravated weakness i.e. a grip scale of 3+ and/or persistent bloody diarrhoea (> 48 hr) apparent on the animal fur or combinatively, that displayed the simultaneous occurrence of 2 out of the 3 following symptoms i.e. “10-19 % weight loss”, “grip scale of +2” or “bloody diarrhoea for 24-48 hr”, were euthanized immediately as described before. The mice were then completely exsanguinated by cardiac puncture

followed by cervical dislocation. This set of procedures were carried out by researchers trained and South African Veterinary Council (SAVC) authorized.

2.3 Mice infection

2.3.1 *Schistosoma mansoni*

2.3.1.1 Life cycle maintenance

Biomphalaria glabrata snails (NMRI strain, NR-21962, provided by Biomedical Research Institute, Rockville, MD) were used as an intermediate host for the maintenance of *Schistosoma mansoni* (NMRI strain) life cycle as previously described (Tucker et al., 2013). In brief, *B. glabrata* snails were kept in clean tanks containing conditioned water (4.48 mM $CaCl_2.2H_2O$, 9.97 mM $MgSO_4$, 0.23 mM K_2SO_4, 4.99 mM $NaHCO_3$, and 0.5 ml of 0.03% $FeCl_3.6H_2O$ (Merck, Kenilworth, New Jersey)), aerated for 1 to 2 days before usage. The tanks were maintained at 24ºC with regulated light/dark cycle. For snails' infection, livers of 8 weeks *S. mansoni* infected mice were collected in saline (0.9% NaCl, Merck), chopped into small pieces, and homogenized at a maximum speed for 30 seconds. Eggs were then isolated by passing the liver homogenate thorough series of decreasing size sieves. The filtrate was diluted 40-times in conditioned water and then placed in volumetric flask partially covered with tin foil. The un-foiled area of the flask was exposed to an infra-red light for 20 min, for concentrating the photo-tactic miracidia at the neck region of the flask. Juvenile snails placed in conditioned water were individually infected overnight with 5-8 miracidia before placing them back into their respective tank.

Shedding of the cercariae from the infected *B. glabrata* snails were done 5-8 weeks post-infection whereby the infected snails were kept in dark for 48 hr, placed in 100 ml beaker containing conditioned water (at a density of one snail per 2 ml water), and then exposed to strong light for 30 min. Cercariae yield was then determined by using iodine (Merck), to kill and stain the cercariae, and dissecting microscope (SMZ800N Stereo Microscope, Nikon, Minato, Tokyo) prior to mice infection.

2.3.1.2 Mice infection and egg count

Mice were shaved ventrally and anaesthetized via intraperitoneal injection of 10 mg/kg Xylazine and 100 mg/kg Ketamine cocktail, as mentioned above. Mice were infected percutaneously via the abdomen, using stainless-steel rings, with 80 or 100 viable cercariae of NMRI strain of *S. mansoni* obtained from the infected *Biomphalaria glabrata* snails as described. For egg load in the infected animals, liver and ileum were digested in 5 ml of 5% KOH (Merck) overnight at 37^{o}C and the eggs were counted at 40× magnification as described previously (Cheever, 1970).

2.3.2 *Nippostrongylus brasiliensis*

2.3.2.1 Life cycle maintenance

Nippostrongylus brasiliensis life cycle was maintained by passage through Wistar rats as previously described (Camberis et al., 2003). In brief, rats were anaesthetized by exposure to Isoflurane for 3-5 min and then subcutaneously injected with 5000 L3 larvae/500 µl phosphate buffered saline (PBS, 136.9 mM NaCl, 2.68 mM KCl, 10.14 mM Na_2HPO_4, 1.76 mM KH_2PO_4, all from Merck)/rat by using a 18-G needle (Braun, Melsungen, Germany). From day 5 post-infection, rats were kept in wire-bottomed cages with a try beneath covered with a well-dampened paper for faeces collection. Rats' faecal pellets were collected on day 6, 7, and 8 whereby the faecal pellets were softened by incubating them for an hour with 5 µg/ml fungizone. The paste was then prepared, by mixing the soften pellets with activated charcoal (Sigma-Aldrich, St. Louis, Missouri, catalogue no. 242241), distributed on moistened filter paper placed in sterile Petri-dishes, and finally incubated in dark at 26^{o}C in order to facilitate egg hatching and development of L3 larvae. After 7-days, L3 larvae were harvested to be used for future infections.

2.3.2.2 Mice infection and worm count

L3 larvae were washed off the filter paper in saline (0.9% NaCl), counted under a dissecting microscope, and resuspended at a concentration of 2500 L3 larvae/ml. Mice were injected subcutaneously with 500 *N. brasiliensis* L3 larvae in 200 µl 0.9% NaCl using a

21-G needle. Mice were euthanized 9 days post-infection, worms were counted and tissue samples were collected for further analyses.

For worm count, the small intestine was removed from the infected animals, opened longitudinally to expose the lumen, cut into small pieces, and then incubated in saline in shaking incubator at 37ºC for 4 hr. After the incubation period, the gut suspension was poured out into a large graded Petri-dish and the total number of adult worms/intestine/mouse was determined by using a dissecting microscope (SMZ800N Stereo Microscope).

2.3.2.3 *Nippostrongylus brasiliensis* antigens preparation

L3 larvae were sediment by centrifugation at 315 x g (Heraeus™ Megafuge™ 40, Thermo Scientific, Waltham, Massachusetts) for 10 min at RT, resuspended in 2 ml PBS, and then homogenized at maximum speed for 30 seconds. The homogenate was filtered through 0.45 µm filter, and the protein content was measured by using Pierce BCA Protein Assay Kit (Thermo Fisher Scientific, catalogue no. 23225) as per manufacturer's instruction.

2.4 Cells isolation

2.4.1 Thymus, mesenteric lymph nodes, and hepatic lymph nodes

Thymus, mesenteric lymph nodes (MLN), and hepatic lymph node (hLN) were collected in 1 ml of filter-sterilized Iscove's Modified Dulbecco's Medium (IMDM) (Gibco, Waltham, Massachusetts) supplemented with 10% inactivated fetal bovine serum (iFBS, Gibco), and 100 U/ml penicillin-streptomycin (Gibco). Single-cell suspensions were achieved by mechanical squeezing, using plunger top part of 2 ml sterile syringe, through 70 µM cell strainer (Falcon, Corning, MA), followed by sieving through 40 µM cell strainer (Falcon), to get rid of any cell clumps and/or debris. The cell suspension was spun down at 315 x g for 10 min at 4ºC. The supernatant was decanted and the cell pellet was resuspended in 5 ml IMDM medium for checking cell viability and cell count by using trypan blue (Lonza, Walkersville, Maryland). After the cell number had been estimated, the cells were

sediment by centrifugation at 315 x g for 10 min at 4°C and then resuspended at a concentration of 10 million cells/ml.

2.4.2 Spleen

Spleen was collected in 1 ml of filter-sterilized IMDM Medium. Single-cell suspension was obtained by mechanical squeezing, using plunger top part of sterile syringe, through 100 µM cell strainer (Falcon), followed by sieving through 70 µM cell strainer, and then centrifugation at 315 x g for 10 min at 4°C. To get rid of red blood cells, the cell pellet was incubated for 10 min at RT with 5 ml of pre-warmed red blood cells (RBCs) lysis buffer (156 mM NH_4Cl, 0.127 mM EDTA, and 11.9 mM $NaHCO_3$, all from Merck). IMDM medium was then added up to 10 ml, to neutralize the effect of RBCs lysis buffer, and the cell suspension was spun down at 315 x g for 10 min at 4°C. The supernatant was decanted, the cell pellet was resuspended in 5 ml IMDM medium, and then sieved thorough 40 µM cell strainer. Trypan blue was used for checking cell viability and determining cell count. Then, the cells were sediment by centrifugation at 315 x g for 10 min at 4°C and finally resuspended at a concentration of 10 million cells/ml.

2.4.3 Lung

Lungs were chopped into 10 mm^3 pieces and then incubated in shaking incubator for 30 min at 37°C with digestion buffer (IMDM supplemented with 220 U/mg Collagenase I (Sigma, catalogue no. C9891), 13 U/mg DNase I (Sigma, catalogue no. DN25), and 5% iFBS). The resulting suspension was mechanically squeezed through 70 µM cell strainer, followed by sieving through 40 µM cell strainer. The cell suspension was spun down, treated with RBCs lysis buffer, and then resuspended in IMDM medium. Cell's viability, count and resuspension were done as mentioned before.

2.4.4 Liver and small intestine

Liver and gut lymphomyeloid cells were isolated following a modified version of the method of Gossen et al and Hardy et al (Goossens et al., 1990; Hardy et al., 1997). Briefly, luminal content of the small intestine was flushed out and then small intestine and liver tissues of individual animals were chopped, separately, into 10 mm^3 pieces. Liver and small intestine samples were incubated in shaking incubator for 30-45 min at 37ºC with either liver digestion buffer (IMDM medium supplemented with 110 U/mg Collagenase I, 110 U/mg Collagenase II (Sigma, catalogue no. C6885), 13 U/mg DNase I, and 5% iFBS) or small intestine digestion buffer (IMDM medium supplemented with 220 U/mg Collagenase I, 13 U/mg DNase I, and 5% iFBS), respectively. The resulting suspension was mechanically squeezed through 100 µM sterile cell strainer, followed by sieving through 70 µM sterile cell strainer and then centrifugation at 315 x g for 10 min at 4ºC. Supernatant was discarded, the cells were resuspended in 3 ml PBS containing 3% iFBS and then mixed with 1.7 ml Percoll (Sigma, catalogue no. P1644), giving a final concentration of 36% isotonic Percoll. The suspension was mixed thoroughly and the separation was performed at 500 x *g*, without breaks, for 10 min at 4ºC. Liver cells were treated with RBCs lysis buffer as described earlier. Cells were then washed, resuspended in IMDM medium, sieved through 40 µM cell strainer, counted by trypan blue staining, and finally resuspended at a concentration of 10 million cells/ml.

2.5 Flow cytometry

2.5.1 Antibodies

Antibodies used for flow cytometry analyses were as follows: CD3ε (BD Biosciences, Franklin Lakes, New Jersey, clone: 500A2), CD4 (BD, clone: RM4-5), CD8α (BD, clone: 53-6.7), CD25 (BD, clone: 7D4), CD19 (BD, clone: 1D3), Lineage (BD), CD124 (BD, clone: mIL4R-M1), Foxp3 (eBioscience, Waltham, Massachusetts, clone: FJK-16s), GATA3 (BD, clone: L50-823), T-bet (eBioscience, clone: eBio4B10), Bcl-6 (BD, clone: K112-91), RoRγt (BD, clone: Q31-378), Helios (BD, clone: 22F6), IRF4 (Biolegend, San Diego, California, clone: irf4.3e4), Ki67 (BD, clone: B56), IFN-γ (BD, clone: XMG1.2), IL-4 (BD, clone: 11B11), IL-10 (eBioscience, clone: JES5-16E3), IL-13 (eBioscience, clone: eBio13A), F4/80 (eBioscience, clone: BM8), Ly6G (eBioscience, clone: RB6-8C5),

CD11c (BD, clone: HL3), MHCII (eBioscience, clone: M5/114.15.2), SiglecF (BD, clone: E50-2440), T1/ST2 (BD, clone: DJ8), ICOS (BD, clone: MIH4), and CD11b (BD, clone: WT.5).

For staining of cell surface markers, cells were plated, at a density of 1 x 10^6 cells, in 96 well V-bottom plates (Thermo Fisher Scientific) and then sedimented by centrifugation at 315 x g for 10 min at 10ºC. Cells were stained with 50 µl antibody mix containing 2 % inactivated rat serum and 1 % unlabelled anti-CD32/CD16 antibody, to avoid non-specific binding, for 30 min at 4ºC in dark. Unbound antibodies were washed off by centrifugation at 315 x g for 10 min at 10ºC, and the cells were resuspended in FACS buffer (PBS containing 1% bovine serum albumin (BSA) (Roche, Switzerland) and 0.1% NaN_3 (Merck)) for acquisition.

2.5.2 Intracellular cytokine staining

For detection of intracellular cytokines, MLN or hLN cells were seeded at a density of 2 x 10^6 cells/well in complete IMDM culture medium and stimulated with 50 ng/ml phorbol myristate acetate (PMA), 250 ng/ml ionomycin, and 200 µM monensin (all from Sigma) for 8-12 hr at 37ºC in a humidified atmosphere containing 5% CO_2. After the incubation period, cells were harvested, washed with FACS buffer, stained with extracellular markers for 30 min, and then fixed with 2% (w/v) paraformaldehyde for 1 hr at 4ºC in dark. The cells were washed with ice-cold PBS and then permeabilized with 0.5% saponin buffer (PBS containing 1.58 mM saponin, 1 mM $CaCl_2$, 1.034 $MgSO_4$, 7.69 mM NaN_3, 1 g/l BSA, 10 mM HEPES, with pH adjusted to 7.4) for 1 hr at 4ºC in dark. The cells were sediment by centrifugation at 315 x g for 10 min at 10ºC and then stained for 1 hr with cytokines antibodies (IFN-γ, IL-4, IL-10, IL-13). Cells were washed with saponin buffer and then resuspended in FACS buffer for acquisition.

2.5.3 Intranuclear staining

For detection of transcription factors, BD Pharmingen™ Transcription Factor Buffer Set (BD Biosciences, catalogue no. 562574) was used as per manufacturer's instruction.

Briefly, single-cell suspensions (1 x 10^6 cells) were stained for cell surface markers for 30 min, washed with 1x Perm/Wash buffer, and then incubated in 1x Fix/Perm buffer for 1 hr at 4°C in dark, for fixation and permeabilization. The cells were washed with 1x Perm/Wash buffer and then stained with transcription factors antibodies and proliferation markers for 1 hr at 4°C in dark. Cells were washed with the 1x Perm/Wash buffer and then resuspended in FACS buffer.

In all staining settings, staining specificity was verified by appropriate isotype-matched antibody controls. All the incubation periods were done at 4°C in dark. Acquisition was performed using BD LSRFortessa™ (BD Biosciences) and data were analysed using FlowJo software (Treestar, Ashland, Oregon).

2.6 Real-time polymerase chain reaction

2.6.1 Genotypic evaluation of efficiency and specificity of IL-4Rα deletion

Genomic DNA was isolated, as described above, from $CD3^+$ $CD4^+$ $Foxp3^-$, $CD3^+$ $CD4^+$ $Foxp3^+$ T cells and $CD19^+$ B cells sorted using BD FACSAria™ III cell sorter (BD Biosciences). While cell purity was determined by flow cytometer and it was at least 99%, NanoDrop (ND-1000 Spectrophotometer, Thermo Fischer Scientific) was used for measuring DNA concentration and purity. Efficiency of *il-4rα* gene deletion was quantified by real-time PCR (qPCR) on LightCycler® 480 Instrument II (Roche) using the following primers; exon 5: forward 5' AACCTGGGAAGTTGTG 3' and reverse 5' CACAGTTCCATCTGGTAT 3', exon 8: forward 5' GTACAGCGCACATTGTTTTT 3' and reverse 5' CTCGGCACTGACCCATCT 3'. PCR conditions were 94°C for 2 min, 94°C for 20 seconds, 45°C for 30 seconds, and 72°C for 20 seconds for 55 cycles.

2.6.2 Transcriptional evaluation of Foxp3 expression by qRT-PCR

2.6.2.1 RNA extraction

Liver tissues from $Foxp3^{cre}$ IL-4R$\alpha^{-/lox}$ mice and their littermate controls were collected in QIAzol Lysis Reagent (Qiagen, Hilden, Germany) and RNA was extracted by using RNeasy Mini Kit (Qiagen) following manufacturer's instructions. In brief, Liver tissues

were homogenized in Qiazol on ice and then one-fifth volume of chloroform (Merck) was added to each sample. The homogenate and the chloroform were shaken vigorously, incubated at RT for 3 mins, shaken again, and then spun down by centrifugation at 8000 x g for 15 mins at 4^{o}C. Afterwards, the tubes had three different layers, the upper aqueous layer was transferred into a new tube, an equal volume of 70% ethanol was added, and the tubes were shaken for mixing. The mixture, up to 700 µl, was then transferred into the RNeasy spin column placed in a 2 ml collection tubes, incubated for 1 min, and then spun down at 8000 x g for 15 seconds at 4^{o}C. Flow-through was discarded, the RW1 buffer was added to the spin column, incubated for 1 min, and then spun down at 8000 x g for 15 seconds at 4^{o}C. To get rid of DNA contamination, samples were treated with DNase I for 15 mins at RT and then washed with RW1 buffer. RBE buffer was added to the spin column, incubated for 1 min, and then spun down at 8000 x g for 15 seconds at 4^{o}C. The previous step was repeated and then the spin column was placed into a new collection tube to get rid of any residual solution by centrifugation for 1 min at full speed. RNA was eluted in a new tube by using RNase-free water. RNA concentration was determined by using NanoDrop.

2.6.2.2 Complementary DNA synthesis

RNA was converted into a complementary DNA (cDNA) by using Transcriptor First Strand cDNA Synthesis Kit (Roche catalogue no. 04 379 012 001) following manufacturer's instructions. Briefly, RNA, with a concentration of at least 0.5 µg/ml, was mixed with the primer mix (2.5 µM anchored-oligo(dT)$_{18}$ primer, 60 µM random hexamer primer, and PCR-grade water up to 13 µl), incubated for 10 mins at 65^{o}C in T100™ Thermal Cycler (Bio-Rad), and then chilled on ice immediately. The master mix (transcriptor reverse transcriptase reaction buffer containing 8 mM $MgCl_2$, 20 U RNase inhibitor, 1 mM deoxy-nucleotide mix, and 10 U transcriptor reverse transcriptase) was added to the template-primer mix and then incubated in T100™ Thermal Cycler (with heated lid) for 10 mins at 25^{o}C, 60 mins at 50^{o}C, followed by 5 mins at 85^{o}C. The tube was placed on ice for 5 mins to stop the reaction and then aliquots of cDNA were prepared for PCR amplification later on.

2.6.2.3 RT-PCR amplification

Foxp3 and HPRT transcripts were quantified by qPCR on LightCycler® 480 Instrument II (Roche) using primer pairs in Table 2.2. PCR conditions were 95°C for 5 min, 95°C for 10 seconds, 62°C for 15 seconds, 72°C for 20 seconds, and 76°C for 5 seconds for 45 cycles. Foxp3 expression was normalized to the expression level of HPRT.

Table 2.2. Primers sequence for evaluation of Foxp3 expression

Gene target	Primer sequence
Foxp3-Forward	5' GTGCACGTACACACATGCAG 3'
Foxp3-Reverse	5' TAGGCATGGATTGGGGCTTG 3'
HPRT-Forward	5' GTT GGA TAT GCC CTT GAC 3'
HPRT-Reverse	5' AGG ACT AGA ACA CCT GCT 3'

2.7 Cell culture

2.7.1 Cytokine stimulation

Spleen and MLN cells from naïve Foxp3^{cre} IL-4Rα$^{-/lox}$ mice and their littermate controls were cultured at 5 x 10^6 cells/ml in Roswell Park Memorial Institute (RPMI) medium (Lonza) containing 10% iFBS and 100 U/ml penicillin-streptomycin (RPMI culture medium) with 0 or 1 ng/ml recombinant (r)IL-4 (BD Biosciences) for 40 hr at 37°C in a humidified atmosphere containing 5% CO_2. After the incubation period, cells were harvested, washed in FACS buffer and then stained for IL-4Rα (BD, clone: mIL4R-M1) in the presence of inactivated rat serum and unlabelled anti-CD32/CD16 antibody (2.4G2). IL-4Rα expression was detected by flow cytometry (BD LSRFortessa). In other settings, sorted CD4$^+$ CD25$^+$ T cells from naïve Foxp3^{cre} IL-4Rα$^{-/lox}$ mice and their littermate control were cultured at a density of 1 x 10^6 cells/ml in RPMI culture medium with 0 or 10 ng/ml

rIL-4 for 18 or 36 hr, at 37°C in a humidified atmosphere containing 5% CO_2. Cell survival and Foxp3 expression were assessed by flow cytometry.

2.7.2 Ex-vivo restimulation of MLN cells

Single cell suspensions from MLN cells were prepared as described above. The cells were cultured at a density of 1 x 10^7 cells/ml in 96 well flat-bottom plates (Thermo Fisher Scientific) either coated with α-CD3 (20 µg/ml) or supplemented with soluble egg antigens (SEA, 20 µg/ml, Theodor Bilharz Research Institute, Giza, Egypt). Cells were incubated at 37°C in a humidified atmosphere containing 5% CO2, supernatants were collected after 72-96 hr, and cytokines were measured by enzyme-linked immunosorbent assay (ELISA) (Herbert et al., 2004).

2.8 *In vitro* Treg assays

2.8.1 $CD4^+$ T cell enrichment

From naïve mice, lymph nodes (LNs) and spleen were collected in sterile RPMI culture medium. Single cell suspension preparation and cells counts were done as described before. Cells were resuspended in Easy Sep buffer (PBS containing 2% iFBS, and 1 mM EDTA (Merck)) at a concentration of 1 x 10^8 cells/ml for $CD4^+$ T cell enrichment by using EasySep™ Mouse T Cell Isolation Kit (Stemcell Technologies, Vancouver, Canada, Catalogue no.19852A) as per manufacturer's instruction. In brief, cells were mixed with rat serum (50 µl/ml of sample), transferred to polystyrene round-bottom tube (BD), mixed with antibody isolation cocktail (50 µl/ml of sample), and then incubated for 10 min at RT. RapidSpheres™ (75 µl/ml of sample) was added to the sample, mixed, incubated for 2.5 min, and then the tube (without lid) was placed into the magnet for 2.5 min at RT. The magnet was picked up and in one continuous motion, the magnet and the tube were inverted to pour the enriched cell suspension into a new tube. Enriched $CD4^+$ T cells were washed in FACS buffer and counted by using trypan blue for further sorting steps.

2.8.2 Cell sorting

Enriched $CD4^+$ T cells were surface stained with antibodies for CD4 and CD25, and 7-aminoactinomycin D (7AAD, Sigma, catalogue no. SML1633) as mentioned above. Cells were then washed and resuspended in 3 ml FACS buffer for sorting $CD4^+$ $CD25^-$ (for Treg conversion assay) and $CD4^+$ $CD25^+$ (to be cultured with 0 or 10 ng/ml rIL-4) cells using BD FACSAria™ III cell sorter (BD Biosciences).

2.8.3 Treg conversion assay

Sorted $CD4^+$ $CD25^-$ cells (2.5 x 10^6 cells/ml) were cultured with plate-bound anti-CD3 (10 µg/ml) in the presence of soluble anti-CD28 (2 µg/ml, eBioscience, clone: 37.51) and different concentration of transforming growth factor beta (TGF-β, BD Pharmingen) (0, 1, or 2, ng/ml) in 96 well, flat-bottomed plates in triplicates. After 3 days incubation at 37^{o}C in a humidified atmosphere containing 5% CO2, the induced Treg (iTreg) cells were harvested, washed in FACS buffer, and then stained for analysing CD25 and Foxp3 expression by flow cytometry.

2.9 Serum analyses

2.9.1 Serum collection and measurement of immunological parameters

Cardiac puncture was used to collect blood in serum separator tubes (BD Biosciences). Blood in serum separator tubes was then spun down at 8000 x *g* for 10 min at 4°C to separate the serum. Aliquots of sera, 50 µl each, were stored at -80°C on an individual basis to measure liver enzymes, serum cytokines (IL-4 and TNF-α) and antibody isotypes titer.

2.9.2 Liver enzymes

Hepatocellular damage was assessed by measuring the serum level of aspartate aminotransferase (AST) at the National Health Laboratory Service of South Africa (Cape Town).

2.10 Immunological analyses

2.10.1 Cytokine measurement by sandwich ELISA

The release of IFN-γ, IL-4, IL-5, IL-10, IL-13, and IL-17 (BD Pharmingen) was measured as follows. The Nunc™ MicroWell™ 96-Well Microplates (Thermo Fischer Scientific) were coated with 1 µg/ml capture antibody in coating buffer (PBS) and incubated overnight in a humidified chamber at 4°C. Plates were washed 3 times with washing buffer (13.4 mM KCL, 5.8 mM KH_2PO_4, 684.4 mM NaCl, and 0.25% Tween 20 (all from Merck)), blocked with 200 µl of 2% (w/v) milk powder in PBS for 2 hr at 37°C, washed 3 times, and then the samples were loaded and incubated overnight at 4°C. The plates were washed 3 times, (0.5 µg/ml) biotin-labelled antibody was added, incubated for 2 hr at 37°C, and then washed 3 times by washing buffer. Avidin-horseradish peroxidase or avidin-alkaline phosphatase (KPL, Gaithersburg, Maryland) was added and incubated for 1 hr at 37°C. Plates were washed 6 times, then developed by adding either TMB Microwell Peroxidase Substrate (KPL) or 1 mg/ml *p*-nitrophenyl phosphate disodium salt hexahydrate (Sigma, catalogue no. N2765), and finally The absorbance was read at 450 or 405 nm, respectively, using VersaMax™ microplate spectrophotometer (Molecular Devices, Sunnyvale, California).

2.10.2 Antibody isotype

S. mansoni soluble egg antigens specific serum antibody isotypes and total IgE titer from naïve/infected mice were measured by coating The Nunc™ MicroWell™ 96-Well Microplates (Thermo Fisher Scientific) with either 20 µg/ml SEA or 1 µg/ml of IgE capture antibody, respectively. Plates were sealed and incubated overnight at 4°C and then washed 3 times with washing buffer. Nonspecific sites were blocked with 200 µl of 2% (w/v) milk powder in PBS for 2 hr at 37°C, and then plates were washed 3 times. While sera were diluted 1:10, 1:100, 1:1000, and 1:1000 for detecting antibody isotypes (IgG1, IgG2a, and IgG2b) titers, 50 µl of undiluted sera was used to detect the total IgE. The serum samples were incubated overnight at 4°C. Alkaline phosphatase-labelled secondary antibody (0.5 µg/ml) was added, incubated for 3 hr at 37°C, and then plates were washed 6 times. Plates were developed by the addition of 1 mg/ml *p*-nitrophenyl phosphate disodium salt

hexahydrate (Sigma). The absorbance was read at 405 nm using VersaMax™ microplate spectrophotometer (Molecular Devices).

2.11 Histology

2.11.1 *S. mansoni* infection

Liver and gut tissues were fixed in 4% (v/v) formaldehyde in PBS, embedded in wax, processed, and 5–7 μm sections stained with hematoxylin and eosin (H & E). Micrographs of liver granuloma were captured using Nikon Eclipse 90i (Nikon). Granuloma diameter of 20-50 granulomas per animal was determined using Nikon NIS-Elements imaging software (Nikon Corporation). For fibrosis assessment, tissue sections were stained with chromotrope 2R and analine blue solution (CAB) and counterstained with Wegert's hematoxylin for collagen staining.

2.11.2 *N. brasiliensis* infection

Lung tissues were fixed in 4% (v/v) formaldehyde in PBS, embedded in wax, processed, and 5 μm sections were stained with periodic acid-Schiff reagent (PAS) to visualize mucus-producing goblet cells (Johannes and Klessen, 1984). Micrographs of lung sections were captured using Nikon Eclipse 90i.

2.12 Tissue homogenate for cytokine analyses

From naïve and infected animals, tissues were collected and homogenized in protein extraction buffer (PBS (pH 7.1) containing 0.1% Tween 20 (Merck), and 1% protease inhibitor cocktail (Sigma-Aldrich, catalogue no. P8340)). Cytokines were measured in the protein extracts by sandwich ELISA as described previously. Cytokine values were normalized according to the protein content measured by Pierce BCA Protein Assay Kit (Thermo Fisher Scientific) as per manufacturer’s instructions.

2.13 Hydroxyproline quantifications

Hydroxyproline content as a measure of collagen production was quantified using modified protocol (Bergman and Loxley, 1963). In brief, weighed liver samples were hydrolyzed overnight at 110^{o}C in 6 M HCl (Sigma) and then filtered through Whatman® filter papers. Filtrate was neutralized with 1% phenolphthalein and titrated against 10 M NaOH (Merck). An aliquot was mixed with isopropanol (Merck) and added to a chloramine-T/citrate buffer solution (pH 6.0) (Sigma). Ehrlich's reagent solution (25 g *p*-dimethyl-amino-benzaldehyde, 37.5 ml 60% perchloric acid (Merck)) was added and the absorbance was then measured at 570 nm using VersaMax™ microplate spectrophotometer (Molecular Devices). Hydroxyproline levels were calculated by using 4-hydroxy-L-proline (Calbiochem, San Diego, California) as a standard, and results were expressed as µg hydroxyproline per weight of liver tissue that contained 10^4 eggs.

2.14 Statistics

Statistical analysis was conducted using GraphPad Prism 4 software (http://www.prism-software.com). Data were calculated as mean ± SD. Statistical significance was determined using the unpaired Student's *t*-test or One-Way ANOVA with Bonferroni's post-test, defining differences to IL-4Rα$^{-/lox}$ mice ($p>0.05$; ns, *, $p\leq0.05$; **, $p\leq0.01$; ***, $p\leq0.001$).

Chapter 3:

The Role of IL-4Rα-mediated Signaling on Foxp3^{+} Treg Cells under Steady-State

Chapter 3: The role of IL-4Rα-mediated signaling on Foxp3$^+$ Treg cells under steady-state

3.1 Results

3.1.1 Foxp3$^+$ Treg cells express IL-4Rα under steady-state

IL-4Rα-mediated signaling and associated factors critically mediating the function of Th2 cells were recently shown to play an important role in controlling Foxp3$^+$ Treg cells function (Maerten et al., 2005; Pace et al., 2005; Pillemer et al., 2009; Kelada et al., 2013; Noval Rivas et al., 2015; Massoud et al., 2016; Pelly et al., 2017). However, whether IL-4Rα-mediated signaling on Foxp3$^+$ Treg cells promotes (Maerten et al., 2005; Kelada et al., 2013) or inhibits (Noval Rivas et al., 2015; Massoud et al., 2016; Pelly et al., 2017) their suppressive function(s) remains unclear. To address this, the surface protein expression pattern of IL-4Rα on Foxp3$^+$ Treg cells was examined in spleen and MLN of naïve BALB/c mice. Interestingly, the present study found that CD4$^+$ Foxp3$^+$ Treg cells did express IL-4Rα under steady-state condition (Fig. 7, A-C). This result suggests that IL-4Rα-mediated signaling might be needed by Foxp3$^+$ Treg cells to maintain immune-homeostasis under steady-state.

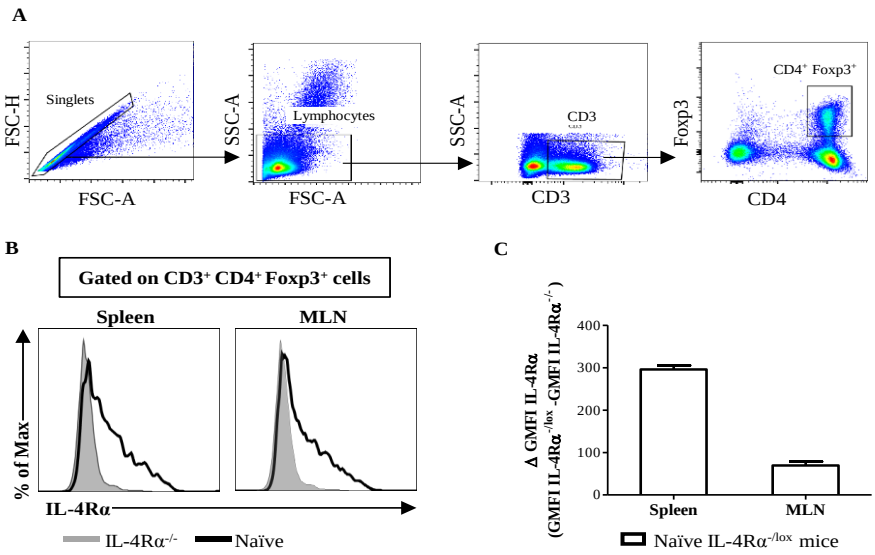

Figure 7. Foxp3$^+$ Treg cells express IL-4Rα under steady-state.

(A) Gating strategy for identifying CD4$^+$ Foxp3$^+$ Treg cell population. **(B)** Representative histograms of IL-4Rα expression by Foxp3$^+$ Treg cells in spleen and MLN of IL-4Rα$^{-/-}$ (gray tinted) mice and naïve (solid line) IL-4Rα$^{-/lox}$ mice with the mean of Δ GMFI IL-4Rα (GMFI IL-4Rα$^{-/lox}$-GMFI IL-4Rα$^{-/-}$) ± S.E.M summarized in **(C)**. Data are from two independent experiments.

3.1.2 Generation and characterization of Foxp3^{cre} IL-4Rα$^{-/lox}$ BALB/c mice

3.1.2.1 Generation of Foxp3^{cre} IL-4Rα$^{-/lox}$ BALB/c mice

To better dissect the role of IL-4Rα-mediated signaling on Foxp3^{+} Treg cells, a murine model, termed Foxp3^{cre} IL-4Rα$^{-/lox}$, with a specific cyclic recombinase (Cre)-mediated deletion of the *il-4rα* gene in Foxp3-expressing cells was generated. IL-4Rα$^{-/-}$ BALB/c mice, IL-4Rα$^{lox/lox}$ BALB/c mice, and Foxp3-IRES-Cre BALB/c mice were required for the generation of Foxp3^{cre} IL-4Rα$^{-/lox}$ mice. IL-4Rα$^{-/-}$ BALB/c mice were generated by gene-targeting strategy using an isogenic target vector (derived from BALB/c genomic clone) and the two-steps Cre-mediated site-specific recombination strategy in BALB/c ES cells (Fig. 8, Mohrs et al., 1999). Cre-recombinase enzyme-enabled the removal of the selection cassette first and then the intervening sequences (exon 7-9) between the remaining two *LoxP* sites, generating a non-functional allele of *il4ra* gene in BALB/c ES cells (Fig. 8, Mohrs et al., 1999).

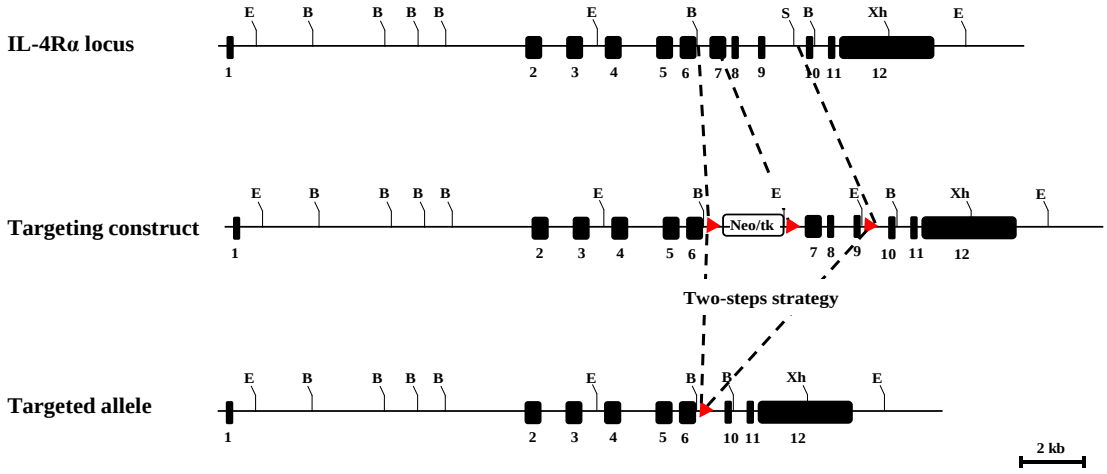

Figure 8. Generation of IL-4Rα$^{-/-}$ BALB/c mice.

Schematic representation of the targeted *il4ra* gene locus. Homologous recombination between the *il4ra* gene locus and the targeting vector, whereby *LoxP* sites flanking selection cassette at 5' of exon 7 as well as *LoxP* site at 5' of exon 10 were introduced, and the two-steps Cre-mediated recombination had resulted in the deletion of exon 7-9 and the generation of non-functional allele of *il4ra* gene in BALB/c embryonic stem cells. Numbers indicate the position of exons of *il4ra* gene. B, *BamHI;* E, *EcoRI*; S, *SmaI*; Xh, *XhoI*. Adapted from (Mohrs et al., 1999).

For IL-4Rα$^{lox/lox}$ BALB/c mice generation, transient expression of Cre-recombinase enzyme in successfully targeted ES cells, using an isogenic target vector, resulted in deletion of the selection cassette and maintenance of *LoxP* sites at the 5' of exon 7 and exon 10, generating a floxed allele of *il4ra* gene in BALB/c ES cells (Fig. 9, Herbert et al., 2004).

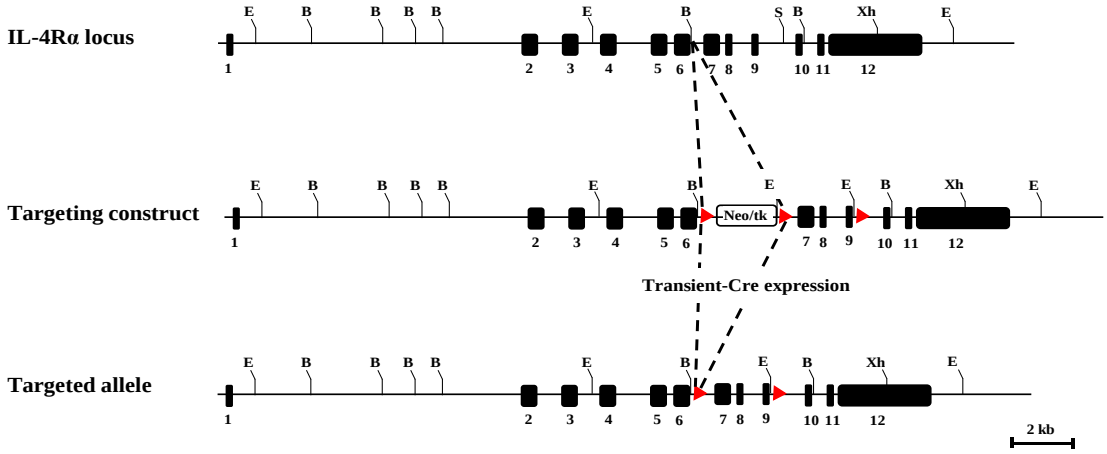

Figure 9. Generation of IL-4Rα$^{lox/lox}$ BALB/c mice.

Schematic representation of the targeted *il4ra* gene locus. Homologous recombination between the *il4ra* gene locus and the targeting vector, whereby *LoxP* sites flanking selection cassette at 5' of exon 7 as well as *LoxP* site at 5' of exon 10 were introduced, and transient Cre-mediated recombination had resulted in the generation of the conditional floxed (*LoxP* sites flanking exons 7 and 10) allele of *il4ra* gene in BALB/c embryonic stem cells. Numbers indicate the positions of exons of *il4ra* gene. B, *BamHI;* E, *EcoRI*; S, *SmaI*; Xh, *XhoI*. Adapted from (Herbert et al., 2004).

Standard gene-targeting strategy procedure and IRES technique were used for the selective expression of *Cre*-recombinase enzymes in Foxp3^{+} Treg cells in Foxp3-IRES-Cre BALB/c mice (Wing et al., 2008). The *ires-cre* construct was introduced downstream the *foxp3* gene stop codon to enable the expression of Cre-recombinase enzyme under the control of *foxp3* gene promoter (Fig. 10).

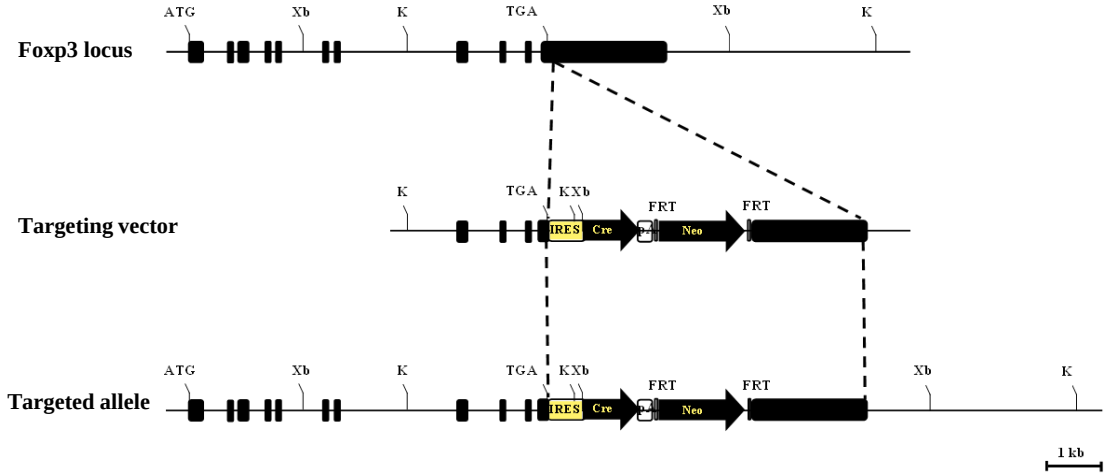

Figure 10. Generation of Foxp3-IRES-Cre BALB/c mice.

Schematic representation of the targeted *foxp3* gene locus. Homologous recombination between the *foxp3* gene locus and the targeting vector, whereby the *ires* and *cre*-coding genes were inserted downstream the *foxp3* gene stop codon, had resulted in the generation of the *foxp3-ires-cre* construct in BALB/c embryonic stem cells. K, *KpnI;* Xb, *XbaI*. Adapted from (Wing et al., 2008).

Foxp3^{cre} IL-4Rα$^{-/lox}$ mice were generated by intercrossing BALB/c mice expressing Cre under the control of *foxp3* gene promoter (Wing et al., 2008) with global knock-out (IL-4Rα$^{-/-}$) BALB/c mice (Mohrs et al., 1999), for two generations, to generate a Foxp3^{cre} IL-4Rα$^{-/-}$ BALB/c mice (Flow chart 1-2 and Fig. 11 A-B). These mice were further intercrossed with homozygous floxed IL-4Rα (IL-4Rα$^{lox/lox}$) BALB/c mice (exon 7 to 9 flanked by *LoxP* sites) (Herbert et al., 2004) to generate a Foxp3-specific IL-4Rα deficient mouse on BALB/c background (Foxp3^{cre} IL-4Rα$^{-/lox}$ BALB/c mice, Flow chart 1-2 and Fig. 11 A-B).

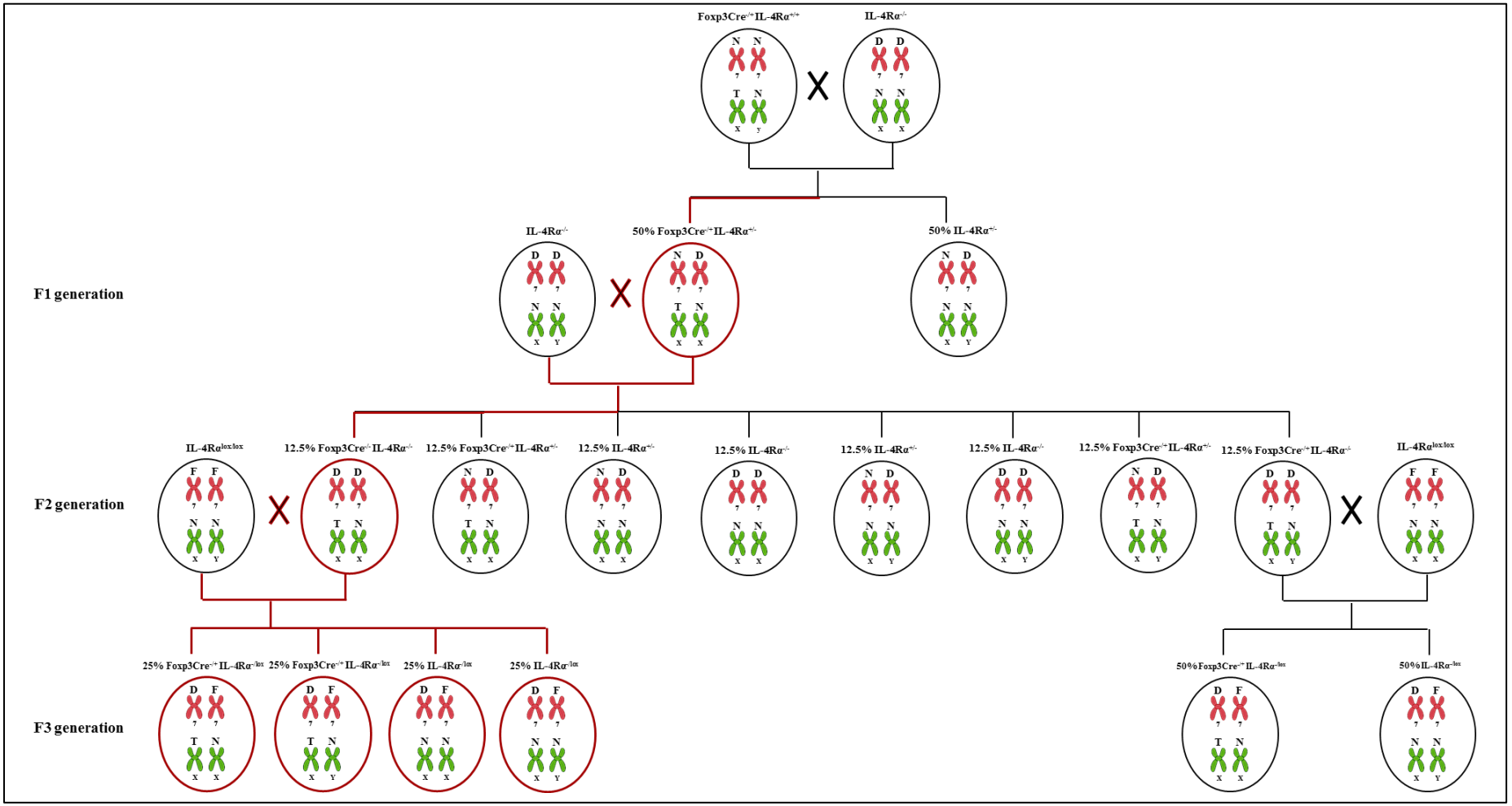

Flowchart 1: Generation of Foxp3Cre$^{-/+}$ IL-4Rα$^{-/lox}$ BALB/c mice using males Foxp3Cre$^{-/+}$ mice to start the generation of males and females Foxp3Cre$^{-/+}$ IL-4Rα$^{-/lox}$ mice and their littermate controls. The gene genotype is indicated above the drawn chromosome, while the number of the chromosome is indicated below. N, no modifications (wildtype); D, deleted; F, floxed; T, transgenic (Cre gene).

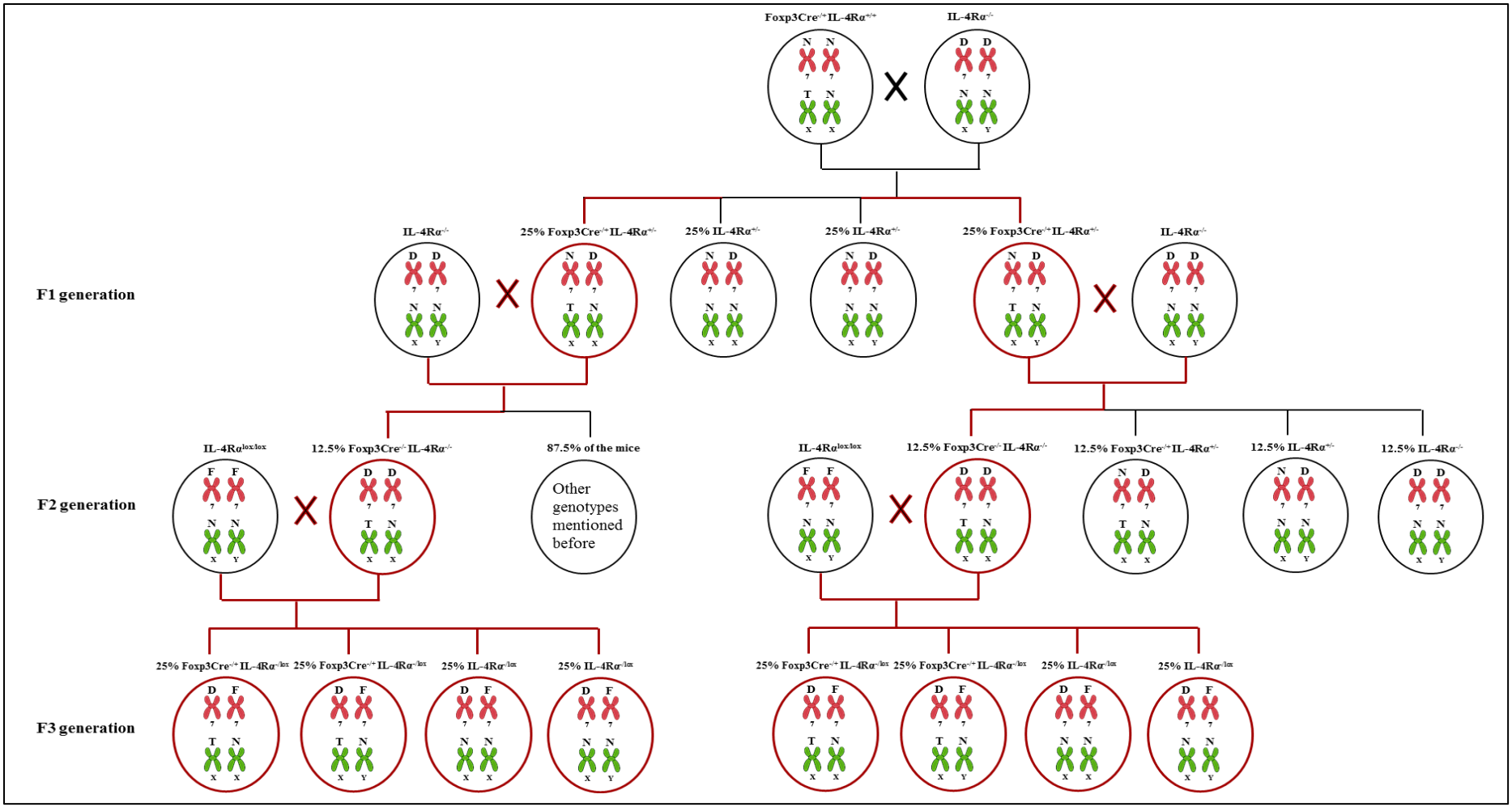

Flowchart 2: Generation of Foxp3Cre$^{-/+}$ IL-4Rα$^{-/lox}$ BALB/c mice using females Foxp3Cre$^{-/+}$ mice to start the generation of males and females Foxp3Cre$^{-/+}$ IL-4Rα$^{-/lox}$ mice and their littermate controls. The gene genotype is indicated above the drawn chromosome, while the number of the chromosome is indicated below. N, no modifications (wildtype); D, deleted; F, floxed; T, transgenic (Cre gene).

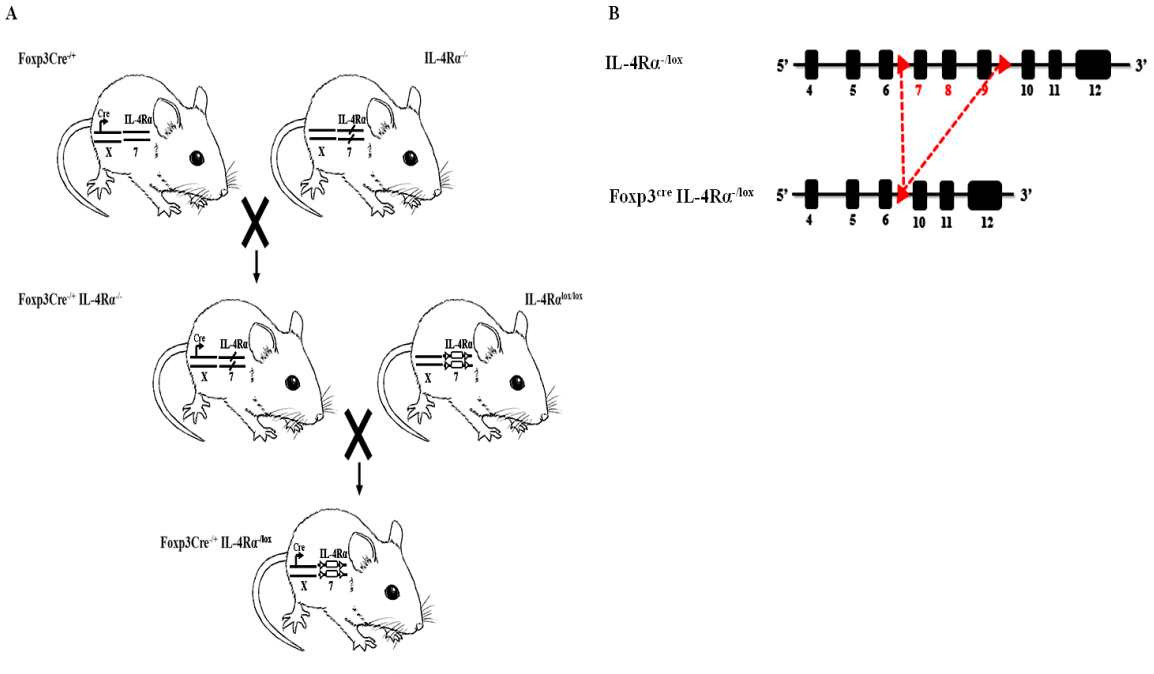

Figure 11. Generation of Foxp3Cre$^{-/+}$ IL-4Rα$^{-/lox}$ BALB/c mice.

(A) Mouse breeding strategy. IL-4Rα$^{-/-}$ BALB/c mice were intercrossed for two generations with transgenic BALB/c mice expressing Cre-recombinase under the control of *foxp3* gene promoter. The Foxp3Cre$^{-/+}$ IL-4Rα$^{-/-}$ progeny were further intercrossed with IL-4Rα$^{lox/lox}$ BALB/c mice to generate Foxp3Cre$^{-/+}$ IL-4Rα$^{-/lox}$ mice and their littermate controls on BALB/c background. **(B)** Schematic diagram showing the structure of *il4ra* gene loci in IL-4Rα$^{-/lox}$ and Foxp3^{cre} IL-4Rα$^{-/lox}$ mice.

3.1.2.2 Genotypic evaluation of IL-4Rα deletion on Foxp3^{+} Treg cells

Foxp3^{cre} IL-4Rα$^{-/lox}$ mice were identified by PCR genotyping (Fig. 12 A). The cellular specificity of Cre-mediated IL-4Rα deletion was assessed at the genomic level by performing quantitative real-time PCR. Genomic DNA was extracted from CD19^{+}, CD4^{+} Foxp3^{-}, and CD4^{+} Foxp3^{+} sorted cells from pooled spleen and MLN cells of naïve Foxp3^{cre} IL-4Rα$^{-/lox}$, their littermate control (IL-4Rα$^{-/lox}$), and global knock-out (IL-4Rα$^{-/-}$) mice (Fig. 12 B), and *il-4rα* exon 8 (absent in IL-4Rα-deficient cells) was quantified by qPCR and normalized to *il-4rα* exon 5 (present in all cells). As expected, only CD4^{+} Foxp3^{+} T cells, but not CD19^{+} nor CD4^{+} Foxp3^{-} cells, from Foxp3^{cre} IL-4Rα$^{-/lox}$ mice had a lower exon8/exon5 ratio, when compared to their littermate control (Fig. 12 C). Together, these data indicate a knock down, rather than knock-out, of *il-4rα* specifically on CD4^{+} Foxp3^{+} Tregs in the Foxp3^{cre} IL-4Rα$^{-/lox}$ mice.

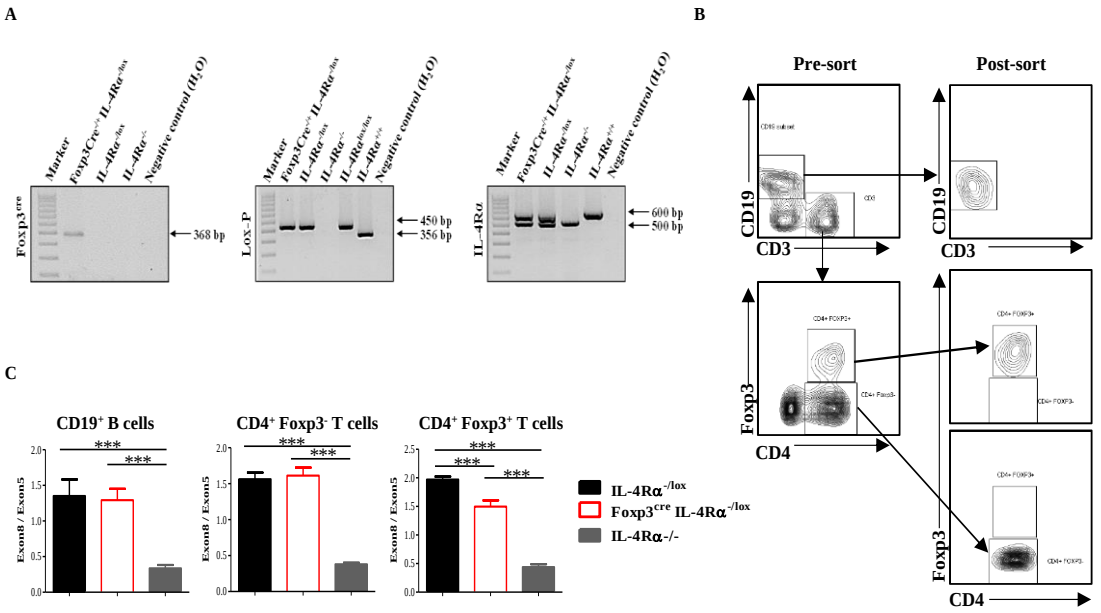

Figure 12. Genotypic characterization of Foxp3Cre$^{-/+}$ IL-4Rα$^{-/lox}$ mice.

(A) Genotyping of Foxp3Cre$^{-/+}$ IL-4Rα$^{-/lox}$ mice. DNA was extracted from the tail of naïve IL-4Rα$^{-/lox}$, Foxp3^{cre} IL-4Rα$^{-/lox}$, and IL-4Rα$^{-/-}$ mice and PCR was performed. The Cre specific amplicon is 368 bp, *loxP* is 450 bp (floxed) or 356 bp (wild-type), the wild-type IL4-Rα amplicon is 600 bp and the deleted IL-4Rα amplicon is 471 bp. **(B)** Representative flow cytometric analysis of the CD19^{+}, CD4^{+} Foxp3^{-}, and CD4^{+} Foxp3^{+} cell populations before and after FACS sorting of fixed-permeabilized cells from spleen and MLN of naïve IL-4Rα$^{-/lox}$, Foxp3^{cre} IL-4Rα$^{-/lox}$, and IL-4Rα$^{-/-}$ mice. **(C)** Efficiency of IL-4Rα deletion on sorted cells by quantitative real-time PCR. Genomic DNA was extracted from sorted CD19^{+} B cells, CD4^{+} Foxp3^{-} and CD4^{+} Foxp3^{+} T cell and *il-4ra* exon 8 (deleted in IL-4Rα

deficient cells) was quantified by qPCR and normalized to the quantity of exon 5 (present in all cells).

Results are representative of three independent experiments with 6-8 mice/group. Data are expressed as mean ± S.E.M. NS, not significant ($P > 0.05$); * $P < 0.05$, ** $P < 0.001$, *** $P < 0.0001$ by one-way ANOVA with Bonferroni post-test analysis.

3.1.2.3 Phenotypic evaluation of IL-4Rα deletion on Foxp3$^+$ Treg cells

Genotypic deletion of *il-4rα* within CD4$^+$ Foxp3$^+$ Treg cells in Foxp3^{cre} IL-4Rα$^{-/lox}$ mice was further confirmed at the protein level by flow cytometry analysis of IL-4Rα surface expression on spleen and MLN cells of naïve Foxp3^{cre} IL-4Rα$^{-/lox}$, their littermate control, and global knock-out mice. CD19$^+$ B cells and CD4$^+$ Foxp3$^-$ T cells from Foxp3^{cre} IL-4Rα$^{-/lox}$ mice and their littermate control had a comparable level of IL-4Rα expression in spleen (Fig. 13 A) and MLN (Fig. 13 B). In contrast, IL-4Rα was deleted specifically within CD4$^+$ Foxp3$^+$ Treg cell population in spleen (Fig. 13 A) and MLN (Fig. 13 B) of males and females Foxp3^{cre} IL-4Rα$^{-/lox}$ mice, when compared to their littermate controls. *il-4rα* gene deletion within the CD4$^+$ Foxp3$^+$ Treg cell population was more efficient in males (efficiency of deletion=90.48 ± 5.45%, Fig. 13, C and D) when compared to females (efficiency of deletion=39.74 ± 5.776%, Fig. 13, C and D), enabling via the present model an assessment of the effect of partial (female) versus quasi-complete (male) impairment of IL-4Rα-mediated signaling on CD4$^+$ Foxp3$^+$ Treg cell in Foxp3^{cre} IL-4Rα$^{-/lox}$ mice.

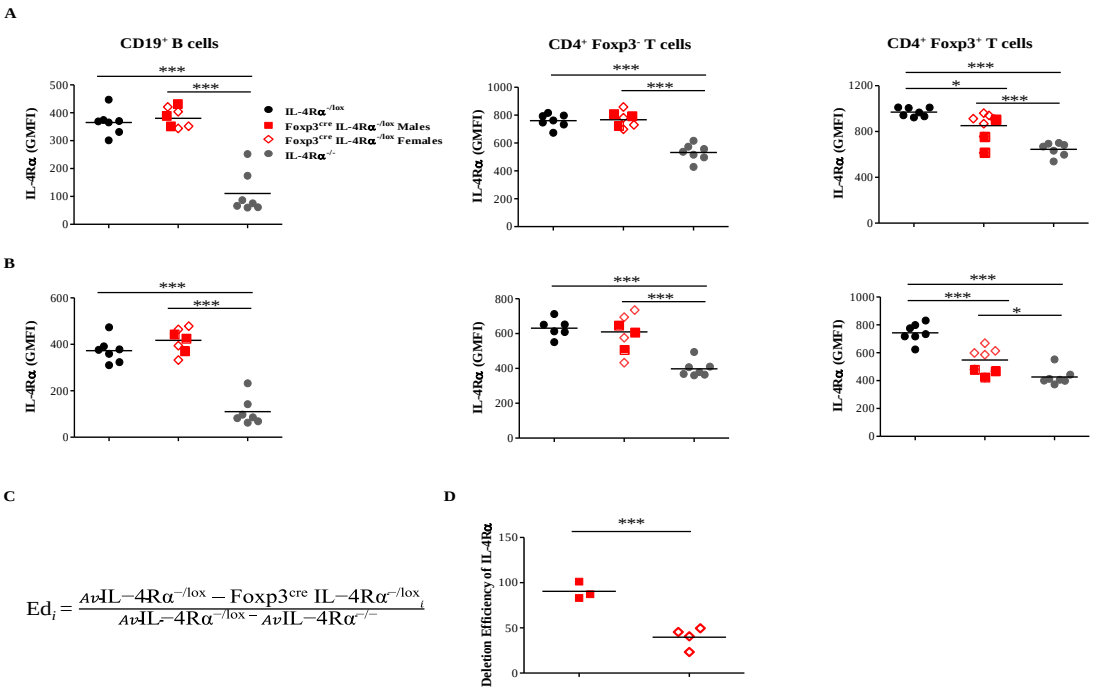

$$Ed_i = \frac{Av\,IL{-}4R\alpha^{-/lox} - Foxp3^{cre}\ IL{-}4R\alpha^{-/lox}{}_i}{Av\,IL{-}4R\alpha^{-/lox} - Av\,IL{-}4R\alpha^{-/-}}$$

Figure 13. Phenotypic characterization of Foxp3Cre$^{-/+}$ IL-4Rα$^{-/lox}$ mice.

(A) Flow cytometry analysis of IL-4Rα expression by CD19^{+} B cells, CD4^{+} Foxp3^{-} and CD4^{+} Foxp3^{+} T cell from the spleen of naïve IL-4Rα$^{-/lox}$, Foxp3^{cre} IL-4Rα$^{-/lox}$, and IL-4Rα$^{-/-}$ mice. **(B)** Flow cytometry analysis of IL-4Rα expression by CD19^{+} B cells, CD4^{+} Foxp3^{-} and CD4^{+} Foxp3^{+} T cell from the MLN of naïve mice. **(C)** Formula for calculating the efficiency of deletion of IL-4Rα. A level of 100% is defined here as the difference between the average IL-4Rα GMFI on cells from control mice (IL-4Rα$^{-/lox}$) and that of the average IL-4Rα GMFI on cells from IL-4Rα deficient mice (IL-4Rα$^{-/-}$). **(D)** Efficiency of IL-4Rα deletion in CD4^{+} Foxp3^{+} T cells in the MLN of naïve males and females Foxp3^{cre} IL-4Rα$^{-/lox}$ mice.

Results are representative of three independent experiments with 3-9 mice/group. Data are expressed as mean ± S.E.M. NS, not significant ($P > 0.05$); * $P < 0.05$, ** $P < 0.001$, *** $P < 0.0001$ by one-way ANOVA with Bonferroni post-test analysis and two-tailed unpaired Student's *t*-test.

3.1.2.4 Functional evaluation of IL-4Rα deletion on Foxp3^{+} Treg cells

To assess the functional impairment of IL-4Rα mediated-signaling on CD4^{+} Foxp3^{+} Treg cell, pooled spleen and MLN cells of naïve Foxp3^{cre} IL-4Rα$^{-/lox}$ mice and their littermate control were cultured with 0 or 1 ng rIL-4 for 40 hr and then IL-4Rα surface expression was measured by flow cytometry. CD19^{+} B cells and CD4^{+} Foxp3^{-} T cells from Foxp3^{cre} IL-4Rα$^{-/lox}$ mice and their littermate control had a comparable level of IL-4Rα expression after the addition of rIL-4 (Fig. 14 A). In contrast, a proportion of rIL-4 stimulated CD4^{+} Foxp3^{+} Treg cells derived from Foxp3^{cre} IL-4Rα$^{-/lox}$ mice were significantly impaired in their ability to upregulate IL-4Rα expression in response to IL-4 stimulation when compared to IL-4Rα expression by CD4^{+} Foxp3^{+} Treg cells derived from their littermate control (Fig. 14 A). This observation was substantiated by quantitative measurement of the increment of IL-4Rα expression in presence and absence of IL-4. CD19^{+} B cells and CD4^{+} Foxp3^{-} T cells in Foxp3^{cre} IL-4Rα$^{-/lox}$ mice and their littermate had a comparable level of IL-4Rα expression (Figure 14 B). In contrast, the increment of IL-4Rα expression by CD4^{+} Foxp3^{+} Treg cells derived from Foxp3^{cre} IL-4Rα$^{-/lox}$ mice was significantly lower than that of their littermate control (Figure 14 B).

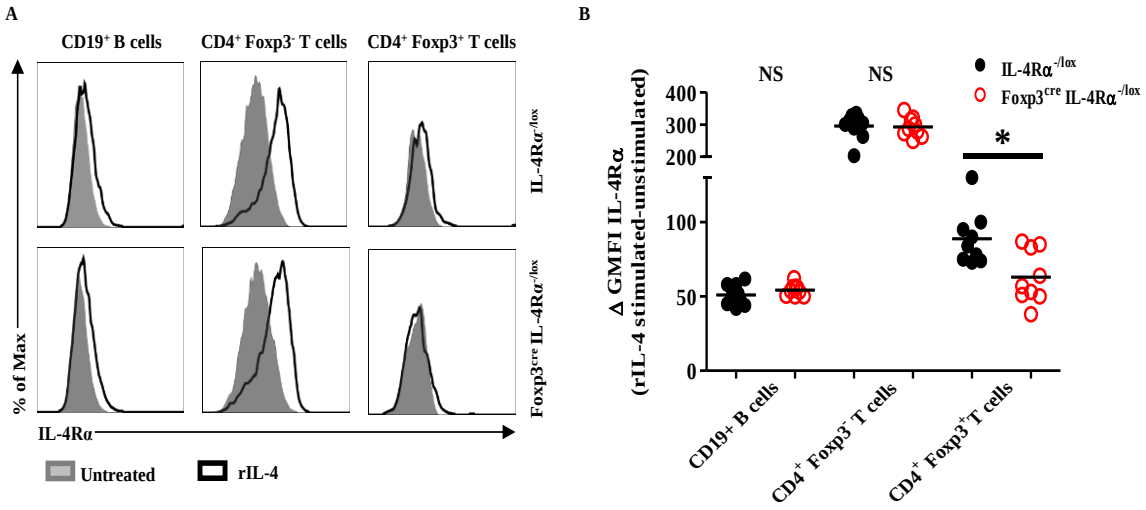

Figure 14. Functional characterization of Foxp3Cre$^{-/+}$ IL-4Rα$^{-/lox}$ mice.

(A) Representative histograms of IL-4Rα expression before and after rIL-4 stimulation. Cells pooled from spleen and MLN from naïve IL-4Rα$^{-/lox}$ and Foxp3^{cre} IL-4Rα$^{-/lox}$ mice were cultured for 40 hr in medium with 0 or 1 ng/ml of rIL-4. **(B)** Flow cytometry analysis of IL-4Rα expression from **(A)**.

Results are representative of three independent experiments with 6-8 mice/group. Data are expressed as mean ± S.E.M. NS, not significant ($P > 0.05$); * $P < 0.05$ by two-tailed unpaired Student's *t*-test.

Collectively, our results reveal that IL-4Rα is specifically deleted on Foxp3^{+} Treg cells in Foxp3^{cre} IL-4Rα$^{-/lox}$ mice either partially (~40% in females) or quasi completely (~90% in males), resulting - in both cases - in a significant impairment of IL-4Rα-mediated signaling on the Foxp3^{+} Treg cell population.

3.1.3 The role of IL-4Rα signaling on Foxp3^{+} Treg cells under steady-state *in vivo*

3.1.3.1 Deletion of IL-4Rα specifically within Foxp3^{+} Treg population does neither alter body weight, organs weight, nor tissue cellularities

Equipped with the aforementioned murine model, the present thesis first interrogated the need for Foxp3^{+} Treg cells to express IL-4Rα expression under steady state. Naïve Foxp3^{cre} IL-4Rα$^{-/lox}$ mice and littermate control, sex and age-matched, were examined for the alteration of overall tissue pathologies and tissue cellularities. No aberrant changes in body weight (Fig. 15 A), vital organs weight (Fig. 15 B), and organs cellularities (Fig. 15 C) were noted in young mice (8-10 weeks old). In-depth analyses were further conducted to assess the effect of deletion of IL-4Rα specifically on Foxp3^{+} Treg population on lymphocytes distribution in primary lymphoid organs, secondary lymphoid organs and peripheral tissues under steady-state.

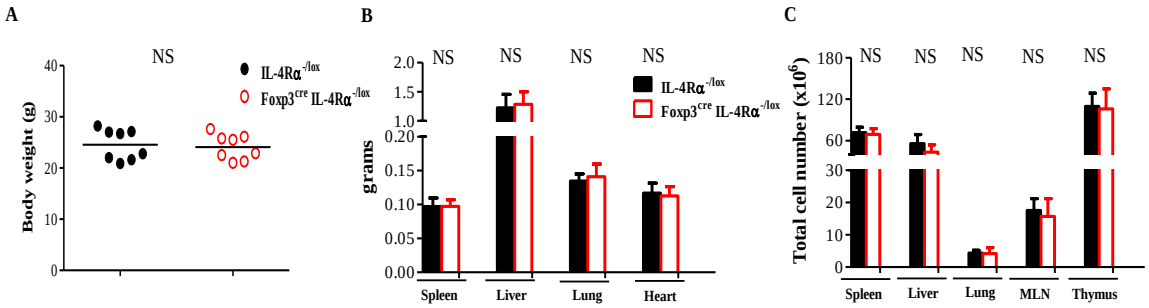

Figure 15. Deletion of IL-4Rα on Foxp3^{+} Treg cells does not have a major effect on body weight, organs weight, nor organs cellularities in young mice.

(A) Body weight of naïve IL-4Rα$^{-/lox}$ and Foxp3^{cre} IL-4Rα$^{-/lox}$ males and females mice. **(B)** Organs weight of naïve mice. **(C)** Total cell number of spleen, liver, lung, MLN, and thymus of naïve mice.

Results are representative of two independent experiments with 7-9 mice/group. Data are expressed as mean ± S.E.M. NS, not significant ($P > 0.05$) by two-tailed unpaired Student's *t*-test.

3.1.3.2 Deletion of IL-4Rα specifically on Foxp3$^+$ Treg population does not alter Tregs or other lymphocyte-compartments in primary lymphoid organ

To interrogate the effect of deletion of IL-4Rα specifically on Foxp3$^+$ Treg population on Treg cells compartment and T cell ontogeny in the primary lymphoid organ, thymus from naïve Foxp3^{cre} IL-4Rα$^{-/lox}$ mice and their littermate control was collected and checked for the Foxp3$^+$ Treg compartment as well as the other T cell subsets by flow cytometry. Similar to littermate control, Foxp3^{cre} IL-4Rα$^{-/lox}$ mice displayed normal Foxp3$^+$ Treg compartment (Fig. 16, A and B) and normal distribution of double negative (DN), double positive (DP), single positive 4 (SP4), and SP8 (Fig. 16, C-E) cells in the thymus. These data suggest that deletion of IL-4Rα specifically on Foxp3$^+$ Treg population does not affect Treg compartment or T cell ontogeny in the thymus.

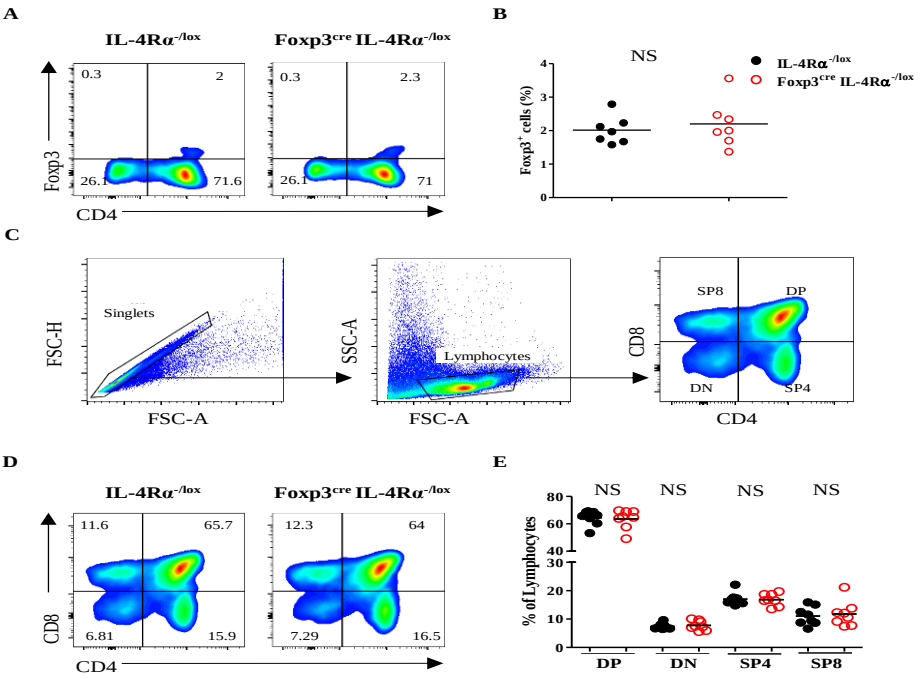

Figure 16. Deletion of IL-4Rα on Foxp3$^+$ Treg cells does not alter T cell ontogeny.

(A) Representative flow cytometry analysis of CD4$^+$ Foxp3$^+$ cells among CD3$^+$ cells from the thymus of naïve IL-4Rα$^{-/lox}$ and Foxp3^{cre} IL-4Rα$^{-/lox}$ males and females mice. **(B)** Frequency of CD4$^+$ Foxp3$^+$ T cells from **(A)**. **(C)** Gating strategy for identifying DN, DP, SP4, and SP8 populations in the thymus. **(D)** Representative flow cytometry analysis of DN, DP, SP4, and SP8 populations in the thymus of naïve mice. **(E)** Frequency of cell populations from **(D)**. Results are representative of two independent experiments with 7-9 mice/group. Data are expressed as mean ± S.E.M. NS, not significant ($P > 0.05$) by two-tailed unpaired Student's *t*-test.

3.1.3.3 Deletion of IL-4Rα specifically on Foxp3$^+$ Treg population does not alter Tregs or other lymphocyte-compartments in secondary lymphoid organs

To dissect the effect of deletion of IL-4Rα specifically on CD4$^+$ Foxp3$^+$ Treg population on Treg cells compartment and other T cell subsets in the secondary lymphoid organs, spleen and MLN from naïve Foxp3^{cre} IL-4Rα$^{-/lox}$ mice and their littermate control were collected and checked for Foxp3$^+$ Treg compartment, CD3$^+$, CD4$^+$, as well as CD8$^+$ T cells by flow cytometry. Similar to littermate control, Foxp3^{cre} IL-4Rα$^{-/lox}$ mice displayed normal Foxp3$^+$ Treg compartment (Fig. 17, A and B) and normal distribution of CD3$^+$ (Fig. 17, C and D), CD4$^+$ (Fig. 17, C and E), and CD8$^+$ (Fig. 17, C and F) T cells in spleen and MLN, suggesting that deletion of IL-4Rα specifically on Foxp3$^+$ Treg population does not affect either Treg compartment or other T-cell subsets in secondary lymphoid organs.

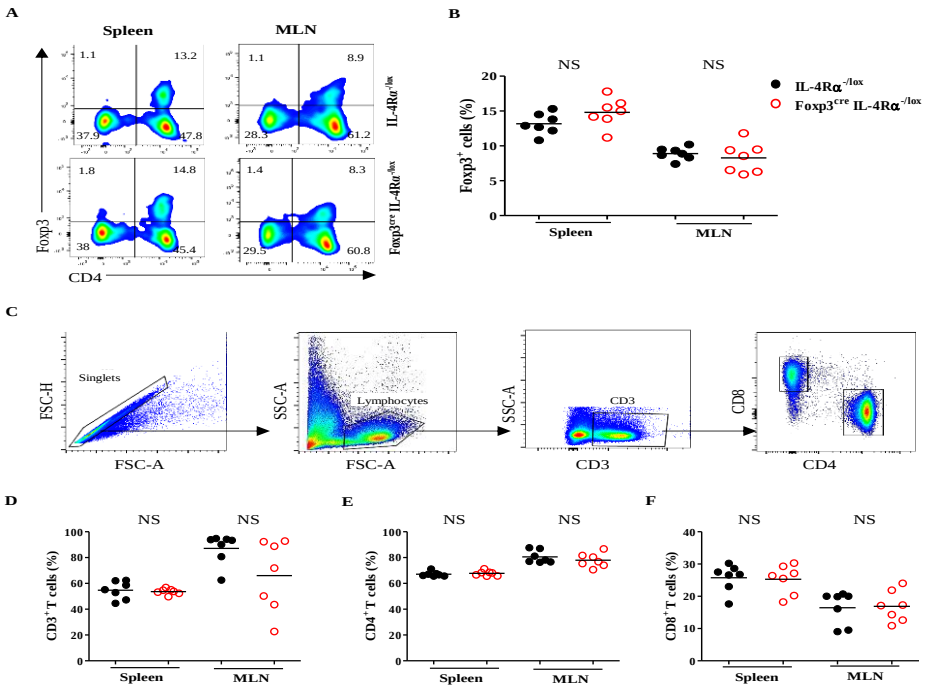

Figure 17. Deletion of IL-4Rα on Foxp3$^+$ Treg cells does not alter cells distribution in secondary lymphoid organs.

(A) Representative flow cytometry analysis of CD4$^+$ Foxp3$^+$ cells among CD3$^+$ cells from spleen and MLN of naïve IL-4Rα$^{-/lox}$ and Foxp3^{cre} IL-4Rα$^{-/lox}$ males and females mice. **(B)** Frequency of CD4$^+$ Foxp3$^+$ T cells from **(A)**. **(C)** Gating strategy for identifying CD3, CD4, and CD8 populations in spleen and MLN. **(D)** Frequency of CD3$^+$, **(E)** CD3$^+$ CD4$^+$, and **(F)** CD3$^+$ CD8$^+$ cells from organs of mice as in **(A)**. Results are representative of two independent experiments with 7-9 mice/group. Data are expressed as mean ± S.E.M. NS, not significant ($P > 0.05$) by two-tailed unpaired Student's *t*-test.

3.1.3.4 Deletion of IL-4Rα specifically on Foxp3$^+$ Treg population does not alter Tregs or other lymphocyte-compartments in peripheral tissues

Next, the present work sought to interrogate the effect of deletion of IL-4Rα on Foxp3$^+$ Treg population on Treg cells compartment and other T cell subsets in peripheral tissues. To do so, lung and liver from naïve Foxp3^{cre} IL-4Rα$^{-/lox}$ mice and their littermate control were collected and checked for Foxp3$^+$ Treg compartment, CD3$^+$, CD4$^+$, as well as CD8$^+$ T cells by flow cytometry. Similar to littermate control, Foxp3^{cre} IL-4Rα$^{-/lox}$ mice displayed normal Foxp3$^+$ Treg compartment (Fig. 18, A and B) and normal distribution of CD3$^+$ (Fig. 18 C), CD4$^+$ (Fig. 18 D), and CD8$^+$ (Fig. 18 E) T cells in lung and liver, suggesting that deletion of IL-4Rα specifically on Foxp3$^+$ Treg population does not affect either Treg compartment or other T-cell subsets in peripheral tissues.

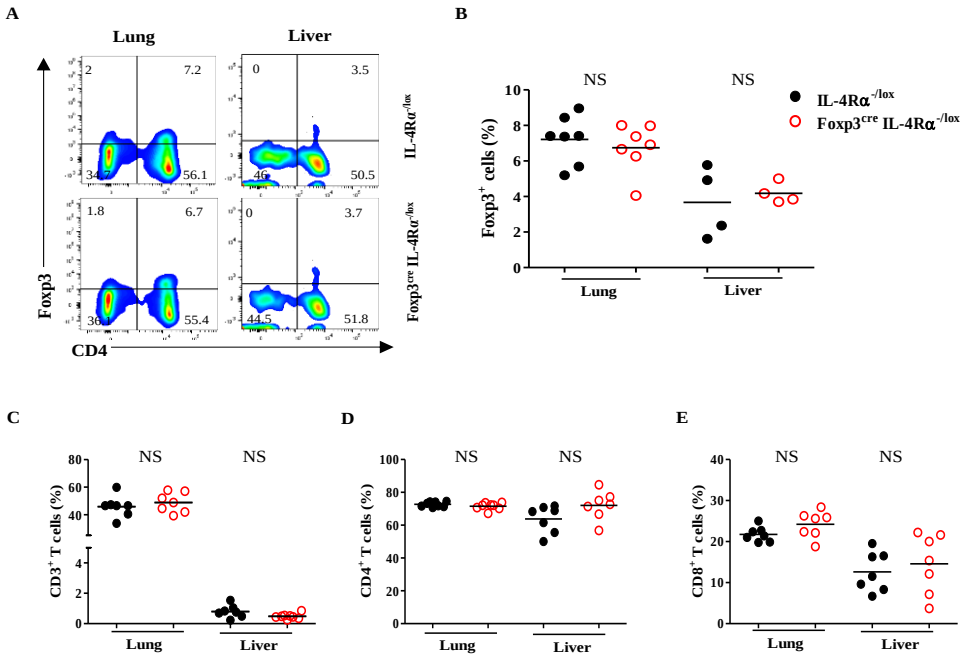

Figure 18. Deletion of IL-4Rα on Foxp3$^+$ Treg cells does not alter cells distribution or frequency in peripheral tissues.

(A) Representative flow cytometry analysis of CD4$^+$ Foxp3$^+$ cells among CD3$^+$ cells from lung and liver lymphocytes of naïve IL-4Rα$^{-/lox}$ and Foxp3^{cre} IL-4Rα$^{-/lox}$ males and females mice. **(B)** Frequency of CD4$^+$ Foxp3$^+$ T cells from **(A)**. **(C)** Frequency of CD3$^+$, **(D)** CD3$^+$ CD4$^+$, and **(E)** CD3$^+$ CD8$^+$ cells from organs of mice as in **(A)**.

Results are representative of two independent experiments with 7-9 mice/group. Data are expressed as mean ± S.E.M. NS, not significant ($P > 0.05$) by two-tailed unpaired Student's *t*-test.

3.1.3.5 Deletion of IL-4Rα specifically on Foxp3$^+$ Treg population does not lead to spontaneous inflammatory disorder in young mice

Mice with a Treg cell-specific deletion of GATA3, a transcription factor closely associated with IL-4Rα mediated signaling (Zheng and Flavell, 1997), have been shown to develop, at old age, a spontaneous inflammatory disorder with an increased release of inflammatory soluble mediators (Wang et al., 2011). To address whether the deletion of IL-4Rα on Foxp3$^+$ Tregs would also instruct a spontaneous and perhaps more subtle inflammatory response in Foxp3^{cre} IL-4Rα$^{-/lox}$ mice, serum levels of soluble inflammatory mediators, serum enzymes, cytokine production in liver and gut as well as cytokine production by CD4$^+$ T cells were analysed. Serum levels of interleukin IL-4, TNF-α, Immunoglobulin E (IgE) (Fig. 19 A), and liver enzyme aspartate transaminase (AST) (Fig. 19 B) in Foxp3^{cre} IL-4Rα$^{-/lox}$ mice were similar to those of littermate controls. Furthermore, naïve young Foxp3^{cre} IL-4Rα$^{-/lox}$ mice had a comparable level of type 1 (IFNγ), type 2 (IL-4, IL-5, IL-10, IL-13), and type 17 (IL-17) cytokine production in the liver (Fig. 19 C) and the gut (Fig. 19 D), when compared to their littermate controls. All CD4$^+$ T cell-derived cytokines tested (IFN-γ, IL-4, IL-10, and IL-13) were also similar between Foxp3^{cre} IL-4Rα$^{-/lox}$ mice and littermate controls (Fig. 19, E and F).

Together, our findings suggest that no major physical alteration are consequent to the impairment of IL-4Rα-mediated signaling within the Foxp3$^+$ T cell compartment in our Foxp3^{cre} IL-4Rα$^{-/lox}$ mouse model under steady-state. Moreover, impairment of IL-4Rα-mediated signaling within the Foxp3$^+$ T cell compartment does neither alter Foxp3$^+$ Treg tissue compartments nor result in spontaneous inflammatory disorder in young (6-8 weeks old) Foxp3^{cre} IL-4Rα$^{-/lox}$ mice.

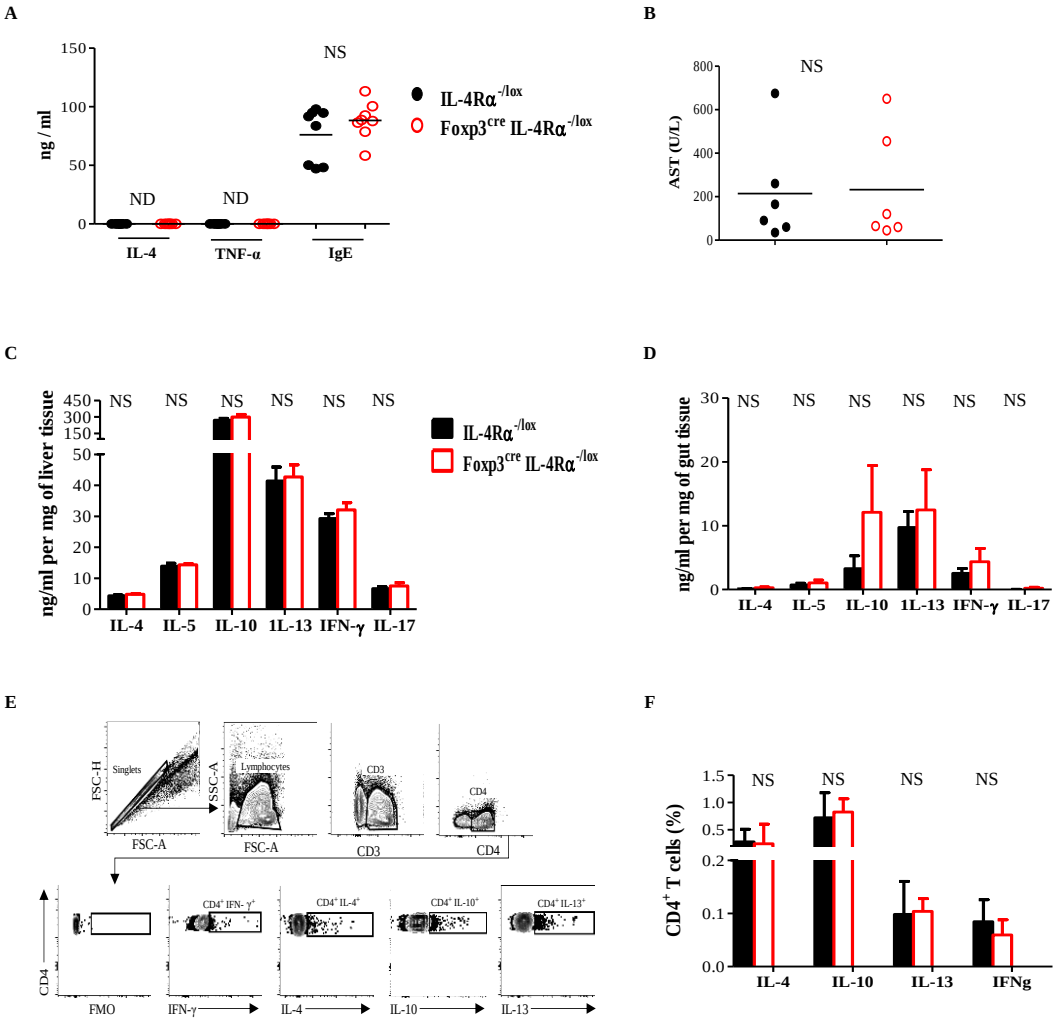

Figure 19. Deletion of IL-4Rα on Foxp3$^+$ Treg cells does not result in a spontaneous inflammatory response in young mice.

(A) Serum analysis of naïve IL-4Rα$^{-/lox}$ and Foxp3^{cre} IL-4Rα$^{-/lox}$ mice. **(B)** Analysis of liver function in naïve mice. **(C)** Liver cytokine production in naïve males and females mice. Livers from naïve mice were homogenized and the levels of the indicated cytokines were detected by ELISA and normalized to mg of liver tissue. **(D)** Gut cytokine production in naïve mice. Small intestines from naïve mice were homogenized and the levels of the indicated cytokines were detected by ELISA and normalized to mg of small intestine tissue. **(E)** Gating strategy for identifying cytokine-producing CD4$^+$ T cells. **(F)** Frequency of IFN-γ, IL-4, IL-10, and IL-13-expressing CD4$^+$ T cells. MLN cells from naïve mice were restimulated with PMA/Ionomycin in the presence of Monensin, after which CD4$^+$ T cells stained intracellularly for indicated cytokines.

Results are representative of two independent experiments with 7-9 mice/group. Data are expressed as mean ± S.E.M. NS, not significant ($P > 0.05$) by two-tailed unpaired Student's *t*-test.

3.1.4 The role of IL-4Rα signaling on Foxp3^{+} Treg cells *in vitro*

To further address the molecular basis of Foxp3^{+} Tregs need to express IL-4Rα signaling, the present study assessed the *in vitro* Foxp3 Treg conversion and/or expansion capacity of CD4^{+} CD25^{-}/CD4^{+} CD25^{+} cells from Foxp3^{cre} IL-4Rα$^{-/lox}$ mice, respectively, in comparison with CD4^{+} CD25^{-}/CD4^{+} CD25^{+} cells from IL-4Rα$^{-/lox}$ littermate controls.

3.1.4.1 IL-4Rα signaling inhibits Treg conversion *in vitro*

CD4^{+} CD25^{-} T cells were sorted with 99.8 % purity (Fig. 20 A) from naïve Foxp3^{cre}IL-4Rα$^{-/lox}$ mice and their IL-4Rα$^{-/lox}$ littermate controls. Sorted cells were cultured in the presence of gradient concentration (0, 1, and 2 ng) of TGF-β1 in combination with T cell receptor stimulation using anti-CD3 and anti-CD28 for 72 hr (Fig. 20, B and C), which are known to induce conversion from CD25 negative to CD25 positive CD4^{+} T cells (Fantini et al., 2007). As expected and in line with the previously published reports (Noval Rivas et al., 2015; Massoud et al., 2016), CD4^{+} CD25^{-} T cells converted to CD4^{+} CD25^{+} Foxp3^{+} T cells (iTreg cells) with the highest rate of conversion recorded from CD4^{+} CD25^{-} T cell cultures derived from Foxp3^{cre} IL-4Rα$^{-/lox}$ mice (Fig. 20, B and C). This suggests that IL-4Rα signaling in CD4^{+} CD25^{-} T cells might interfere with their ability to convert but is clearly not needed to promote their differentiation into Foxp3^{+} Treg cell *in vitro*.

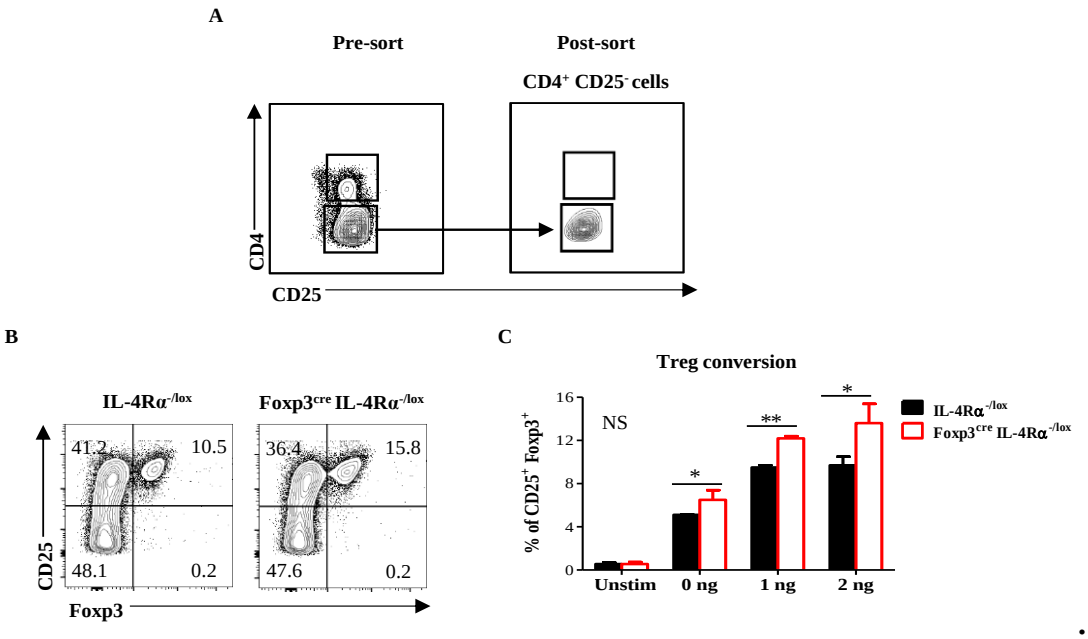

Figure 20. IL-4Rα signaling is dispensable for Foxp3 Treg conversion *in vitro*.

(A) Representative flow cytometry analysis of the $CD4^+$ $CD25^-$ cell populations before and after FACS sorting of pooled cells from spleen and MLN of naïve IL-4Rα$^{-/lox}$ and $Foxp3^{cre}$ IL-4Rα$^{-/lox}$ mice. (B) Representative flow cytometry of converted $CD4^+$ $CD25^+$ $Foxp3^+$ Treg cells from $CD4^+$ $CD25^-$ T cells cultured with gradient concentration of TGFβ for 72 hr. (C) Frequency of iTreg generated *in vitro* from (B).

Results are representative of four independent experiments with 5-7 mice/group. Data are expressed as mean ± S.E.M. NS, not significant ($P > 0.05$); * $P < 0.05$, ** $P < 0.001$ by two-tailed unpaired Student's *t*-test.

3.1.4.2 IL-4Rα signaling promotes the survival of $CD4^+$ $CD25^+$ Tregs and enhances their Foxp3 expression

Next, the effect of IL-4 stimulation on Tregs was evaluated. To do so, $CD4^+$ $CD25^+$ T cells, sorted from naïve $Foxp3^{cre}$ IL-4Rα$^{-/lox}$ mice and their littermate control (Fig. 21 A), were cultured in the presence or absence of rIL-4 for 18 or 36 hr. IL-4 treatment enhanced the survival of $CD4^+$ $CD25^+$ T cells from control mice, whereas the survival of $CD4^+$ $CD25^+$ T cells from $Foxp3^{cre}$ IL-4Rα$^{-/lox}$ mice remained unaltered (Fig. 21 B). These results suggest that IL-4/IL-4Rα signaling promotes $CD25^+$ Treg survival *in vitro*. Furthermore, IL-4 treatment of $CD4^+$ $CD25^+$ Treg cells derived from IL-4Rα$^{-/lox}$ mice considerably expanded $Foxp3^+$ Treg cells frequency (Fig. 21 C) and Foxp3 expression level (Fig. 21, D and E) in response to *in vitro* stimulation with rIL-4 whereas IL-4 treated $CD4^+$ $CD25^+$ Treg cells derived from $Foxp3^{cre}$ IL-4Rα$^{-/lox}$ mice failed to do so.

Taken together, these data indicate that even though IL-4Rα-mediated signaling negatively influences the ability of naive $CD4^+$ $CD25^-$ $Foxp3^-$ T cells to convert into $Foxp3^+$ Tregs, this receptor, later on, promotes the survival and enhances the Foxp3 expression of $CD4^+$ $CD25^+$ Treg cells *in vitro*.

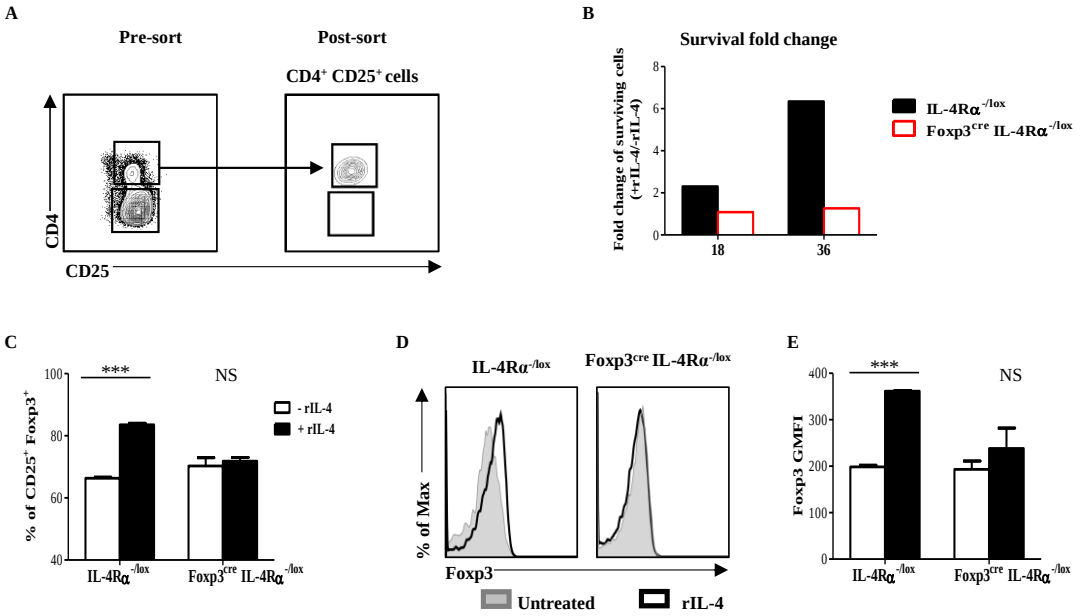

Figure 21. IL-4Rα signaling promotes the survival and enhances Foxp3 expression in CD4$^+$ CD25$^+$ T cell.

(A) Representative flow cytometry analysis of the CD4$^+$ CD25$^+$ cell populations before and after FACS sorting of pooled cells from spleen and MLN of naïve IL-4Rα$^{-/lox}$ and Foxp3^{cre} IL-4Rα$^{-/lox}$ mice. **(B)** CD4$^+$ CD25$^+$ T cells survival in presence and absence or rIL-4. Sorted CD4$^+$ CD25$^+$ T cells from naïve IL-4Rα$^{-/lox}$ and Foxp3^{Cre} IL-4Rα$^{-/lox}$ mice were cultured for 18 or 36 hr with 0 or 10 ng/ml rIL-4. **(C)** Frequency of CD25$^+$ Foxp3$^+$ T cells and **(D)** representative histograms of Foxp3 expression by CD25$^+$ Foxp3$^+$ T cells 36 hr post rIL-4 stimulation with the mean GMFI values summarized in **(E).**

Results are representative of four independent experiments with 5-7 mice/group. Data are expressed as mean ± S.E.M. NS, not significant ($P > 0.05$), *** $P < 0.0001$ by two-tailed unpaired Student's *t*-test.

3.2 Discussion

By using a newly generated mouse model, termed Foxp3^{cre} IL-4Rα$^{-/lox}$ mice, various levels of knockdown of IL-4Rα specifically on Foxp3^{+} Tregs were achieved by using Cre-*loxP* technology. The present thesis showed that partial or quasi-complete deletion of IL-4Rα specifically on Foxp3^{+} Treg cells does neither alter Foxp3 compartment nor break tolerance under steady-state in young mice (8-12 weeks old). Moreover, deletion of IL-4Rα specifically on Foxp3^{+} Tregs did not affect, but rather enhance, the ability of CD4^{+} CD25^{-} cells to convert into CD4^{+} CD25^{+} Treg cells *in vitro*. Interestingly, however, under *in vitro* polarized conditions, i.e. IL-4 conditioned environment, IL-4Rα-mediated signaling on Foxp3^{+} Tregs had a crucial role in enhancing the survival, expanding the Foxp3^{+} Treg population, and potentiating the expression of Treg suppressive marker, Foxp3, in CD4^{+} CD25^{+} Treg cells.

3.2.1 Foxp3^{+} Treg cells might need IL-4Rα signaling to potentiate their suppressive function

Micro-environmental cues play a crucial role in determining the fate of Treg cells. Foxp3^{+} Tregs pay close attention to the immune environment and alter their phenotype, migration, and function in response to specific cues that they encounter in the periphery. In this context, cytokines have been shown to have both phenotypical and functional influences on Foxp3^{+} Tregs (Campbell and Koch, 2011). Even though IL-4 is an important anti-inflammatory cytokine, the influence of IL-4/IL-4Rα-mediated signaling on Foxp3^{+} Treg cells suppressive activity is not yet clearly understood. Recently published reports have shown that augmentation of IL-4Rα-mediated signaling on Foxp3^{+} Treg cells leads to an impaired suppressive activity of those Treg cells with subsequent re-programming into ex-Foxp3 Th2 or Th17 cells (Noval Rivas et al., 2015; Massoud et al., 2016; Pelly et al., 2017). An elegant study by Noval Rivas and colleagues (2016) showed that gain of function mutation in IL4Rα^{F709}, single amino acid substitution of tyrosine (Y)709-to-phenylalanine (F) in the ITIM motif (Tachdjian et al., 2010), leads to significant reduction and impaired suppressive function of allergen-specific Foxp3^{+} Treg population as a result of their re-programming, in IL4Rα-dependent manner, towards Th2 cells (ex-Foxp3 Th2 cell) (Noval Rivas et al., 2015). Another study from the same group showed that another polymorphism

in IL4Rα, single amino acid substitution of glutamine (Q)507-to-arginine (R), known as IL4Rα^{Q507R}, augments allergic airway inflammation by a mechanism involving the IL-4-induced conversion of Foxp3$^+$ Treg cells into ex-Foxp3 Th17 cell (Massoud et al., 2016). In support, Pelly et al. (2017) has reported recently that chronic *Heligmosomoides polygyrus* infection leads to transdifferentiation of Foxp3$^+$ Treg cells to ex-Foxp3 Th2 effector cells, in IL-4/IL-4Rα-dependent manner, as an attempt to contribute to the overall anti-parasitic Th2 response (Pelly et al., 2017). Although these observations would suggest that IL-4Rα signaling might not favour Treg activity, our present analyses revealed that Foxp3$^+$ Treg cells have a basal expression level of IL-4Rα under steady-state, pointing at a possible requirement for this receptor in Treg biology. Our assumption is in accordance with other investigators that have reported the potency of IL-4 to prevent spontaneous apoptosis and reduction of Foxp3 expression in the cultures of isolated Tregs (Maerten et al., 2005). In fact, IL-4 stimulation of isolated cultures of CD4$^+$ CD25$^+$ Tregs in our study recapitulated such a need for IL-4Rα mediated signaling to prevent cell death and to maintain/enhance Foxp3 expression indicating a hitherto unappreciated need for IL-4Rα mediated signaling in Treg biology and arguing for a positive impact of IL-4/IL-4Rα-mediating signaling on Foxp3$^+$ Treg cells. Such a case is not uncommon as it has been shown that many cytokines can have both positive and negative impact on Treg suppressive capacity based on the magnitude of the immune response and the context in which the signal is perceived (Campbell and Koch, 2011). For instance, whereas IFN-γ, the principle effector cytokine produced by Th1 cells to control intracellular pathogens, can inhibit the generation of peripheral Foxp3$^+$ Treg cells from naïve CD4$^+$ T cells (Murphy et al., 1999; Caretto et al., 2010), under certain conditions, IFN-γ mediated signaling can induce as well the expression of T-bet, through STAT1 activation, within Foxp3$^+$ Treg compartment to generate/expand a functionally specialized Treg cells subset, T-bet$^+$ Foxp3$^+$ Treg cells, that is responsible for efficient control of Th1 cells (Koch et al., 2009; Levine et al., 2017). Another example is IL-6. Although IL-6 can induce the expression of STAT3 within Foxp3$^+$ Treg cells to endow them with molecular machineries to regulate Th17 immune response (Chaudhry et al., 2009; Campbell and Koch, 2011), IL-6 can as well inhibit TGFβ-mediated development of peripherally-induced Treg cells (Bettelli et al., 2006; Xu et al., 2007; Zheng et al., 2008). In addition to IFN-γ and IL-6, many other cytokines, i.e type I IFN, TNF, and IL-1, do have double-edged sword type of effect on Treg cells development and activity (Reviewed in Campbell and Koch, 2011). Hence, IL-4Rα-mediated signaling could also have a positive and a negative impact on Treg suppressive function.

3.2.2 IL-4Rα-mediated signaling on Foxp3$^+$ Treg cells is dispensable in young mice to maintain immune homeostasis

IL-4Rα removal specifically from Foxp3 Treg was achieved by intercrossing well-established BALB/c murine models; IL-4Rα$^{-/-}$ (Mohrs et al., 1999), IL-4Rα$^{-/lox}$ (Herbert et al., 2004), and Foxp3-IRES-Cre (Wing et al., 2008) mice. A murine model, Foxp3^{cre} IL-4Rα$^{-/lox}$, was obtained where IL-4Rα was deleted specifically within the Foxp3$^+$ Treg compartment in a dosage-dependent manner whereby IL-4Rα was partially deleted in females and quasi completely deleted in males. The more efficient Cre-mediated IL-4Rα deletion achieved in male when compared with female Foxp3^{cre} IL-4Rα$^{-/lox}$ mice strongly fits the phenomenon of random inactivation of the X-chromosome that can take place in females (Lyon, 1961). Random inactivation of the X-chromosome is a phenomenon whereby the maternally derived X or the paternally derived X-chromosome is randomly inactive in the mammalian females (Lyon, 1961; Lyon, 1972). The presence of *foxp3* gene on the X chromosome and the hemizygosity of *Cre* gene in our mouse model can, therefore, explain the differential efficiency of Cre-mediated *il4ra* deletion in males and females. Of importance, our approach herein described could, therefore, set a precedent for the generation of transgenic mouse models with various levels of knockdown of a target gene. Of note, minimal difference in the efficiency of Cre-mediated IL-4Rα deletion between different organs (i.e. more efficiency in MLN compared to spleen, Fig. 8) was observed. Although Cre-*loxP* system is one of the most powerful tools and one of the most widely used genetic approaches to generate genetically engineered mice, Cre-mediated *loxP* deletion efficiency is always a major concern in conditional knock-out mice (Schmidt-Supprian and Rajewsky, 2007; Sharma and Zhu, 2014). Previous reports have extensively demonstrated the differences in recombination efficiency among tissue types (Schmidt-Supprian and Rajewsky, 2007; Heffner et al., 2012; Liu et al., 2013; Nono et al., 2017b). Nevertheless, in our mouse model Foxp3^{cre} IL-4Rα$^{-/lox}$, a high degree of fidelity was achieved in the Cre-mediated targeting of IL-4Rα on Foxp3$^+$ Tregs specifically, as neither IL-4Rα expression on B-cells nor that of Foxp3$^-$ T cells was affected in our Foxp3^{cre} IL-4Rα$^{-/lox}$ model.

Partial or quasi-complete deletion of IL-4Rα from the Foxp3$^+$ Treg population did neither affect the Foxp3$^+$ Treg compartment ontogeny in the primary lymphoid organ, thymus, nor their recruitment/distribution/maintenance in either the secondary lymphoid

organs, MLN and spleen, or the peripheral tissues, lung and liver, under steady state. Furthermore, all the T cell subsets, $CD3^+$, $CD4^+$, and $CD8^+$ T cell compartments, were not affected in primary and secondary lymphoid organs as well as peripheral tissues, as the naïve $Foxp3^{cre}$ IL-4R$\alpha^{-/lox}$ mice and their littermate controls had a similar frequency of the indicated T cell populations. Analyses of serum immune response, liver homogenate, gut homogenate and cytokines production by $CD4^+$ T cells showed that either partial or quasi-complete removal of IL-4Rα specifically from $Foxp3^+$ Treg population did not result in spontaneous inflammatory disorder in $Foxp3^{cre}$ IL-4R$\alpha^{-/lox}$ young mice (8-10 weeks old) under steady state. A possible explanation could be that the remnant IL-4Rα^+ Foxp3 Tregs in our $Foxp3^{cre}$ IL-4R$\alpha^{-/lox}$ model is sufficient to preserve the Foxp3 Treg compartment and thus tolerance during steady state. This is consistent with previous studies that have attempted to define the physiological importance of factors expressed by $Foxp3^+$ Treg cells. Foxp3 specific GATA3 or T-bet deficient mice were clinically indistinguishable from their littermate controls and showed no defect in the function of $Foxp3^+$ Treg under steady-state in young mice (Koch et al., 2009; Wohlfert et al., 2011; Yu et al., 2015). In older mice (6 months upwards), however, the targeting of GATA3 within the $Foxp3^+$ Treg population led to spontaneous autoimmunity (Wang et al., 2011). It is therefore feasible that specific deletion of IL-4Rα from the $Foxp3^+$ Treg compartment would also lead to apparent physiological defects only in old mice but this is still to be addressed experimentally.

3.2.3 IL-4Rα-mediated signaling on Treg cells *in vitro*

In vitro, it was noted that the ability of $CD4^+$ $CD25^-$ T cells to convert into $CD4^+$ $CD25^+$ Treg cells was enhanced in the absence of IL-4Rα-mediated signaling on $Foxp3^+$ Treg cells. Our observation is in full accordance with previously published reports as it has been shown that gain of function mutation specifically on $Foxp3^+$ Treg cells results in decreased iTreg conversion capacity *in vivo* and *in vitro* (Noval Rivas et al., 2015; Massoud et al., 2016). In contrast, consistent with the literature (Maerten et al., 2005), isolated cultures of $CD25^+$ Tregs tightly depend on IL-4Rα-mediated signaling for survival, expansion of $Foxp3^+$ Treg population and maintenance/enhancement of Foxp3 expression. Altogether, our *in vitro* data indicated clearly that even though IL-4Rα-mediated signaling negatively influences the ability of naive $CD4^+$ $CD25^-$ $Foxp3^-$ T cells to convert into $Foxp3^+$ Tregs, this receptor,

later on, promotes the survival and enhances the Foxp3 expression of $CD4^+$ $CD25^+$ Treg cells.

In conclusion, the present study demonstrated that under steady-state IL-4Rα-mediated signaling on $Foxp3^+$ Treg cells might not be necessary for Treg compartment ontogeny/maintenance/distribution or maintenance of immune homeostasis *in vivo* or in inducible Treg conversion *in vitro* but definitely crucial under more polarized condition (i.e. IL-4 rich environment) for preventing spontaneous apoptosis of $CD4^+$ $CD25^+$ Treg cells and promoting their Foxp3 expression *in vitro*.

Chapter 4:

The Role of IL-4Rα-mediated Signaling on Foxp3^{+} Treg Cells under Inflammatory Conditions

Chapter 4: The role of IL-4Rα-mediated signaling on Foxp3$^+$ Treg cells under inflammatory conditions

4.1 Results

4.1.1 Foxp3$^+$ Treg cells upregulate IL-4Rα expression upon *S. mansoni* infection

The inability to unveil the role of a biological molecule (i.e. receptor or transcription factor) on Foxp3$^+$ Treg cells under steady state is not uncommon. It has been shown that conditional ablation of either *Tbx21* (gene-encoding T-bet) or *gata3* specifically from Foxp3$^+$ Treg cells does not result in any apparent defects in those mice under steady state (Koch et al., 2009; Wohlfert et al., 2011; Yu et al., 2015). Interestingly, however, the strategy of probing subtle immune impairments, non-apparent during steady state, through more inflammatory settings has previously proven to be efficient in unveiling hidden immune defects (Koch et al., 2009; Yu et al., 2015). Analysis of IL-4Rα expression on Foxp3$^+$ Treg cells in spleen and MLN of 8 weeks (8 wk) *Schistosoma mansoni* (*S. mansoni*) infected BALB/c mice demonstrated that CD4$^+$ Foxp3$^+$ Treg cells upregulated their IL-4Rα expression upon *S. mansoni* infection when compared to naïve mice (Fig. 22, A-C). The strikingly higher expression of IL-4Rα by Foxp3$^+$ Treg cells observed during infection warranted us to further address the possible higher need for this receptor by Foxp3$^+$ Tregs during inflammatory disease conditions.

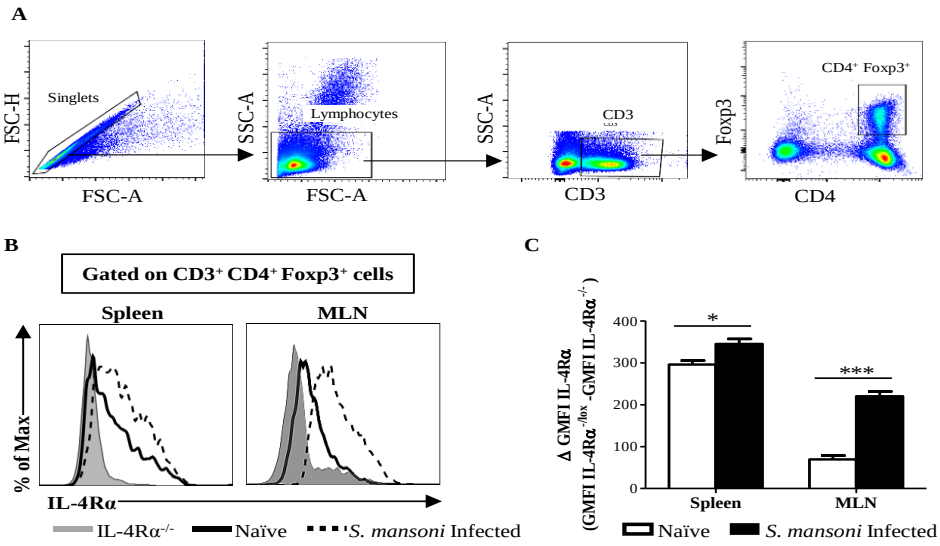

Figure 22. Foxp3$^+$ Treg cells upregulate IL-4Rα expression upon infection.

(A) Gating strategy for identifying CD4$^+$ Foxp3$^+$ Treg cell population. **(B)** Representative histograms of IL-4Rα expression by Foxp3$^+$ Treg cells in spleen and MLN of IL-4Rα$^{-/-}$

(gray tinted) mice, naïve (solid line), and *S. mansoni* infected (dashed line) IL-4Rα$^{-/lox}$ mice with the mean of Δ GMFI IL-4Rα (GMFI IL-4Rα$^{-/lox}$-GMFI IL-4Rα$^{-/-}$) ± S.E.M summarized in **(C)**. Data are from two independent experiments. n= 6-8 mice/group. * $P <$ 0.05, *** $P < 0.0001$ by two-tailed unpaired Student's *t*-test.

4.1.2 IL-4Rα-mediated signaling on Foxp3^{+} Treg cells is required to control egg-driven fibrogranulomatous inflammation during schistosomiasis

Since, adult *S. mansoni* worms reside in the portal and mesenteric vasculatures, where they copulate and the females start to release eggs that subsequently trapped within the hepatic sinusoids and the mesenteric vasculature (Pearce and MacDonald, 2002; Elbaz and Esmat, 2013), liver and small intestine of *S. mansoni* infected Foxp3^{cre} IL-4Rα$^{-/lox}$ and IL-4Rα$^{-/lox}$ were investigated in depth in order to dissect the role of IL-4Rα-mediated signaling on Foxp3^{+} Treg cells under highly polarized, Th2-dominated, condition.

4.1.2.1 Evaluation of efficiency and specificity of IL-4Rα deletion

Initially, the present study sought to confirm that IL-4Rα-mediated signaling on Foxp3^{+} Treg cells was impaired during the infection, deletion of IL-4Rα in *S. mansoni* infected (*Sm*-infected) Foxp3^{cre} IL-4Rα$^{-/lox}$ mice, at the genomic level and at the protein level, was evaluated in comparison to their littermate controls, *Sm*-infected IL-4Rα$^{-/lox}$, and *Sm*-infected IL-4Rα$^{-/-}$mice. Partial deletion of *il-4rα* within the Foxp3^{+} Treg cell population in *Sm*-infected Foxp3^{cre} IL-4Rα$^{-/lox}$ mice was confirmed at the genomic level by qPCR (Fig. 23 A), and at the protein level by flow cytometry (Fig. 23 C), where specific deletion of IL-4Rα on Foxp3^{+} Treg cells, more efficient in males when compared to females (Fig. 23 C), but not on CD19^{+} B cells (Fig. 23 B), was observed.

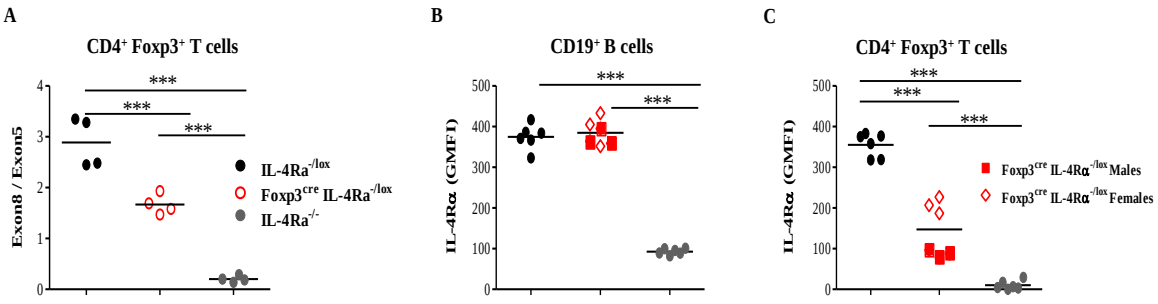

Figure 23. Efficiency of IL-4Rα deletion on Foxp3^{+} Treg cells in *S. mansoni* infected Foxp3^{cre} IL-4Rα$^{-/lox}$ mice.

IL-4Rα$^{-/lox}$, Foxp3^{cre} IL-4Rα$^{-/lox}$, and IL-4Rα$^{-/-}$ mice were infected with *S. mansoni* cercariae and euthanized 8 wk post-infection. **(A)** Efficiency of IL-4Rα deletion by quantitative real-time PCR. CD4^{+} Foxp3^{+} T cells were sorted 8 wk post-infection from pooled cells of spleen and MLN, genomic DNA was extracted, and the ratio of Exon8/Exon 5 was calculated. **(B)** Flow cytometry analysis of IL-4Rα expression by CD19^{+} B cell and **(C)** CD4^{+} Foxp3^{+} T cell in pooled cells from spleen and MLN 8 wk post-infection.

Results are representative of two independent experiments with 4-10 mice/group. Data are expressed as mean ± S.E.M. NS, not significant ($P > 0.05$), *** $P < 0.0001$ by one-way ANOVA with Bonferroni post-test analysis.

4.1.2.2 IL-4Rα-mediated signaling on Foxp3^{+} Treg cells is required for Treg cells accumulation and maintenance/upregulation of suppressive markers to suppress overshooting inflammation in the liver during *S. mansoni* infection

4.1.2.2.1 IL-4Rα-mediated signaling on Foxp3^{+} Treg cells is crucial for Treg accumulation

Next, the present work sought to investigate the effect of IL-4Rα deletion on Foxp3^{+} Treg cells accumulation in the liver of *S. mansoni* infected mice. To do so, Foxp3^{cre} IL-4Rα$^{-/lox}$ and IL-4Rα$^{-/lox}$ mice were infected with 100 *S. mansoni* cercariae, euthanized 8 wk post-infection, and Treg cells accumulation in the liver was assessed. At the transcriptional level, the Foxp3 expression level by real-time reverse transcription-PCR (qRT-PCR) relative to the expression level of hypoxanthine-guanine phosphoribosyl-transferase (HPRT, housekeeping gene) was quantified. The livers of *Sm*-infected Foxp3^{cre} IL-4Rα$^{-/lox}$ mice showed a significant reduction in Foxp3 expression level relative to HPRT when compared to the expression level of Foxp3 in the livers of *Sm*-infected IL-4Rα$^{-/lox}$ mice (Fig. 24 A). In support, at the translational level, flow cytometry analysis showed a drastic reduction in Foxp3^{+} Treg cell population in the liver of *Sm*-infected Foxp3^{cre} IL-4Rα$^{-/lox}$ mice (Fig. 24, B and C), indicating that Foxp3^{+} Treg cells do require IL-4Rα-mediated signaling to infiltrate liver tissue during *S. mansoni* infection.

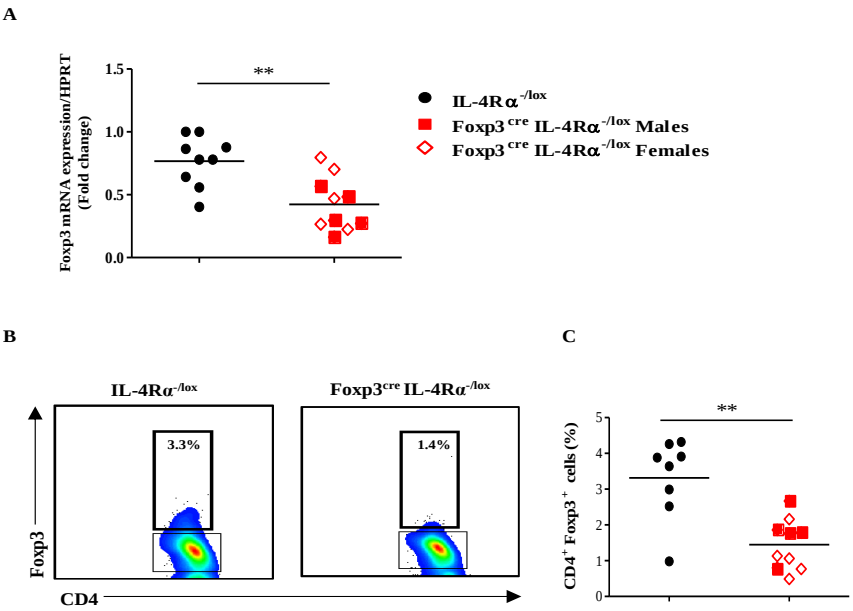

Figure 24. IL-4Rα mediated signaling on Foxp3$^+$ Treg is required for Treg accumulation in the liver during *S. mansoni* infection.

(A) qRT-PCR analysis of relative expression of Foxp3 to HPRT in the liver of 8 wk *S. mansoni* infected IL-4Rα$^{-/lox}$ and Foxp3^{Cre} IL-4Rα$^{-/lox}$ mice. **(B)** Representative flow cytometry of CD4$^+$ Foxp3$^+$ T cells from the liver of 8 wk *S. mansoni* infected mice. **(C)** Frequency of CD4$^+$ Foxp3$^+$ T cells from **(B)**.

Results are representative of two independent experiments with 8-10 mice/group. Data are expressed as mean ± S.E.M. ** $P < 0.001$ by two-tailed unpaired Student's *t*-test.

4.1.2.2.2 IL-4Rα-mediated signaling on Foxp3$^+$ Treg cells is required for maintenance/upregulation of suppressive markers

The present thesis next investigated the role of IL-4Rα-mediate signaling on Foxp3$^+$ Treg cell proliferation and expression of suppressive markers in the liver during *S. mansoni* infection. Rigorous analyses of Treg cells profile by flow cytometry demonstrated that Foxp3$^+$ Treg cells in the liver of *Sm*-infected Foxp3^{cre} IL-4Rα$^{-/lox}$ mice had a significant reduction in the expression levels of Foxp3 (Fig. 25, A and B), IRF4 (Fig. 25, C and D), Helios (Fig. 25, E and F), as well as GATA3 (Fig. 25, G and H) on a per cell basis, when compared to their infected littermate controls. In contrast, the expression level of CD25 (Fig. 25, I and J) as well as the proliferation capacity, as indicated by Ki-67 expression level, (Fig. 25, K and L) of Foxp3$^+$ Treg cells in the liver were comparable between *Sm*-infected Foxp3^{cre} IL-4Rα$^{-/lox}$ mice and *Sm*-infected IL-4Rα$^{-/lox}$ mice. These data suggest that

IL-4Rα-mediated signaling seems to be necessary for the Foxp3^{+} Treg cells to maintain and/or upregulate the expression of certain Treg suppressive markers (such as IRF4, Helios, and GATA3), but not CD25 expression nor Treg proliferation, *in vivo* during inflammation.

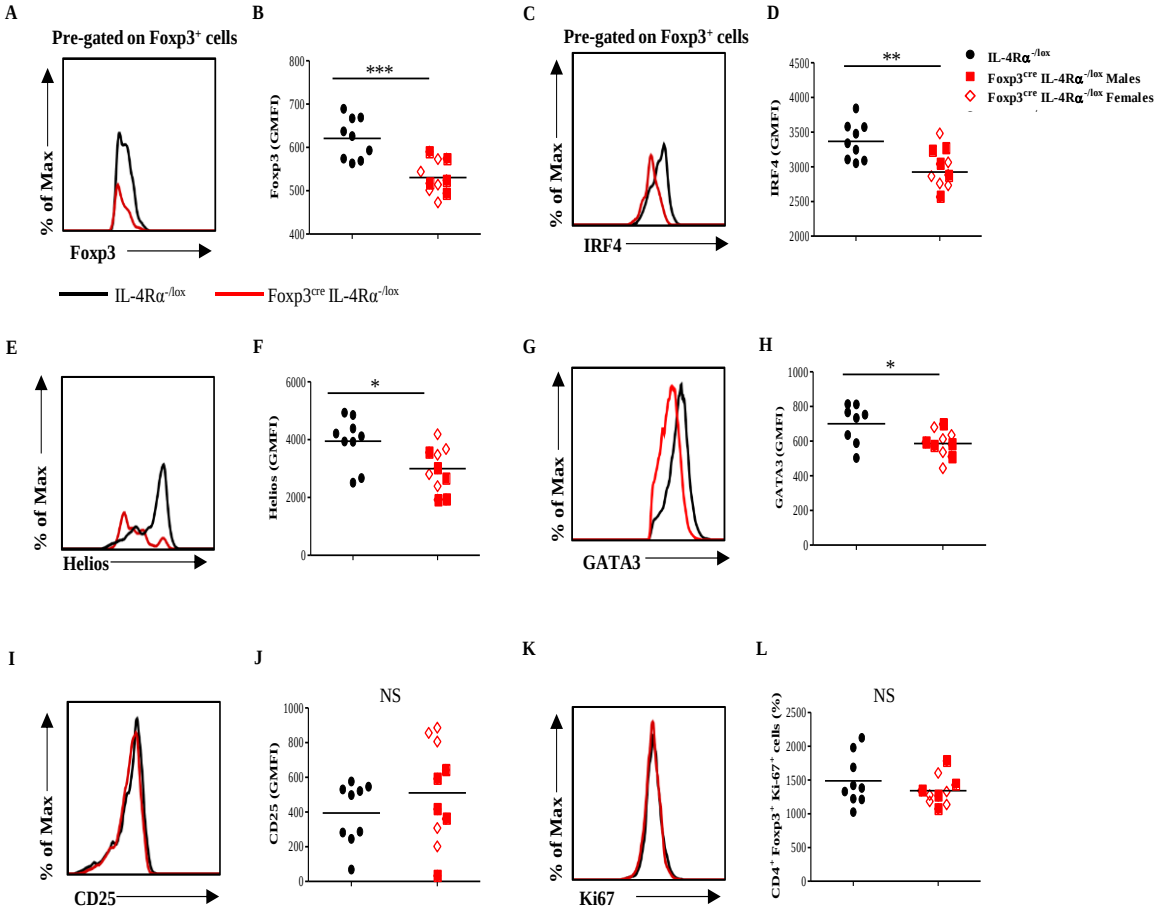

Figure 25. Foxp3^{+} Treg cell profile in the liver of *S. mansoni* infected IL-4Rα$^{-/Lox}$ and Foxp3^{Cre} IL-4Rα$^{-/Lox}$ mice.

Foxp3^{+} Treg cells from the liver of IL-4Rα$^{-/lox}$ and Foxp3^{Cre} IL-4Rα$^{-/lox}$ mice were analyzed 8 wk post *S. mansoni* infection for the expression of Treg suppresive and proliferation markers. **(A)** Representative histogram of Foxp3 expression by CD4^{+} Foxp3^{+} T cells. **(B)** Foxp3 GMFI in CD4^{+} Foxp3^{+} T cells from **(A)**. **(C)** Representative histogram of IRF4 expression by CD4^{+} Foxp3^{+} T cells. **(D)** IRF4 GMFI in CD4^{+} Foxp3^{+} T cells from **(C). (E)** Representative histogram of Helios expression by CD4^{+} Foxp3^{+} T cells. **(F)** Helios GMFI in CD4^{+} Foxp3^{+} T cells from **(E). (G)** Representative histogram of GATA3 expression by CD4^{+} Foxp3^{+} T cells. **(H)** GATA3 GMFI in CD4^{+} Foxp3^{+} T cells from **(G). (I)** Representative histogram of CD25 expression by CD4^{+} Foxp3^{+} T cells. **(J)** CD25 GMFI in CD4^{+} Foxp3^{+} T cells from **(I). (K)** Representative histogram of Ki-67 expression by CD4^{+} Foxp3^{+} T cells. **(L)** Ki-67 GMFI in CD4^{+} Foxp3^{+} T cells from **(K)**.

Results are representative of two independent experiments with 8-10 mice/group. Data are expressed as mean ± S.E.M. NS, not significant ($P > 0.05$); * $P < 0.05$, ** $P < 0.001$, *** $P < 0.0001$ by two-tailed unpaired Student's *t*-test.

4.1.2.2.3 IL-4Rα-mediated signaling on Foxp3^{+} Treg cells is required to control cytokines production

Given the drastic reduction in the Foxp3^{+} Treg population and the significant drop in their expression level of certain Treg suppressive markers, in the liver of *Sm*-infected Foxp3^{cre} IL-4Rα$^{-/lox}$ mice, we, therefore, asked whether such effect will have a consequence on the cytokines production in the *Sm*-diseased livers. To address that, livers of *Sm*-infected Foxp3^{cre} IL-4Rα$^{-/lox}$ mice and their littermate controls were collected 8 wk post-infection, homogenized, and level of cytokines was evaluated by ELISA. Deletion of IL-4Rα on Foxp3^{+} Treg cells resulted in a cytokine storm, including Type 1 (IFNγ), Type 17 (IL-17), and Type 2 (IL-4, IL-5, IL-10, IL-13) cytokines, in the liver of both male and female of *Sm*-infected Foxp3^{cre} IL-4Rα$^{-/lox}$ mice (Fig. 26), when compared to their littermate control. Of note, cytokine production was more pronounced in the females *Sm*-infected Foxp3^{cre} IL-4Rα$^{-/lox}$ mice than the males. Altogether, these data indicate that Foxp3^{+} Treg cells do require IL-4/IL-4Rα-mediated signaling to accumulate in the liver tissue and to maintain/enhance their suppressive marker in order to suppress overshooting cytokines-mediated inflammation during *S. mansoni* infection.

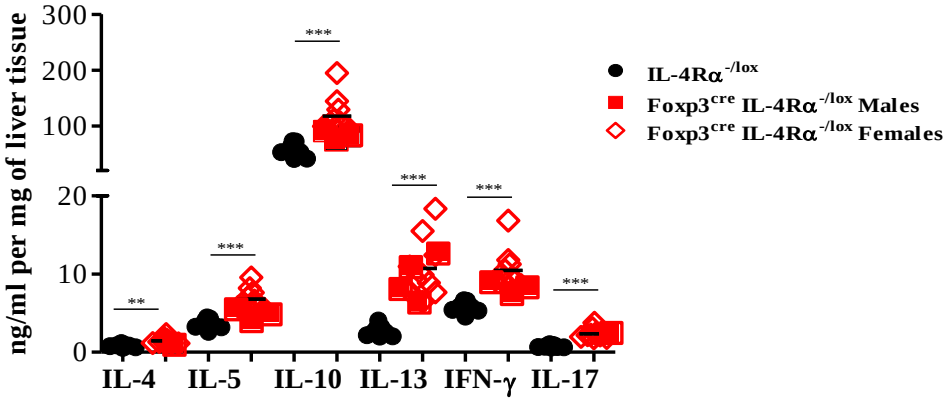

Figure 26. Deletion of IL-4Rα on Foxp3^{+} Treg cells results in heightened cytokine production in the liver during *S. mansoni* infection.

Liver cytokine production 8 wk post-infection of IL-4Rα$^{-/lox}$ and Foxp3^{Cre} IL-4Rα$^{-/lox}$ mice. Livers from infected mice were homogenized and the levels of the indicated cytokines were detected by ELISA and normalized to mg of liver tissue.

Results are representative of two independent experiments with 8-10 mice/group. Data are expressed as mean ± S.E.M. ** $P < 0.001$, *** $P < 0.0001$ by two-tailed unpaired Student's *t*-test.

4.1.2.3 IL-4Rα-mediated signaling on Foxp3$^+$ Treg cells is required for Treg cells maintenance/upregulation of suppressive markers to control T cell proliferation and effector functions in the hLN during *S. mansoni* infection

4.1.2.3.1 Deletion of IL-4Rα on Foxp3$^+$ Treg cells impairs their ability to maintain/upregulate the expression of Treg suppressive markers

The analyses of the hepatic lymph nodes (hLN) supported our observations in the liver. Even though, the frequency of Foxp3$^+$ Treg cells (Fig. 27, A and B) within the hLN of 8 wk *Sm*-infected Foxp3^{cre} IL-4Rα$^{-/lox}$ mice were slightly declined compared to the littermate controls, Foxp3 (Fig. 27, C and D) and IRF4 (Fig. 27, E and F) expression level on a per-cell basis were however dramatically reduced in Foxp3$^+$ Treg cells in the hLN of *Sm*-infected Foxp3^{cre} IL-4Rα$^{-/lox}$ mice, when compared to infected littermate controls. Foxp3$^+$ Treg cells in the hLN of *Sm*-infected Foxp3^{cre} IL-4Rα$^{-/lox}$ and IL-4Rα$^{-/lox}$ mice had similar expression level of Helios (Fig. 27, G and H) and GATA3 (Fig. 27, I and J). Deletion of IL-4Rα on Foxp3$^+$ Treg cells resulted in a modest reduction in their proliferation in the hLN during *S. mansoni* infection (Fig. 27, K and L). Together, these findings suggest that Foxp3$^+$ Treg cells do require IL-4Rα signaling to potentiate the expression of suppressive factors, in particular, Foxp3 and IRF4, but neither Helios expression nor GATA3 expression, as well as to enhance their proliferation capacity in the hLN during *S. mansoni* infection.

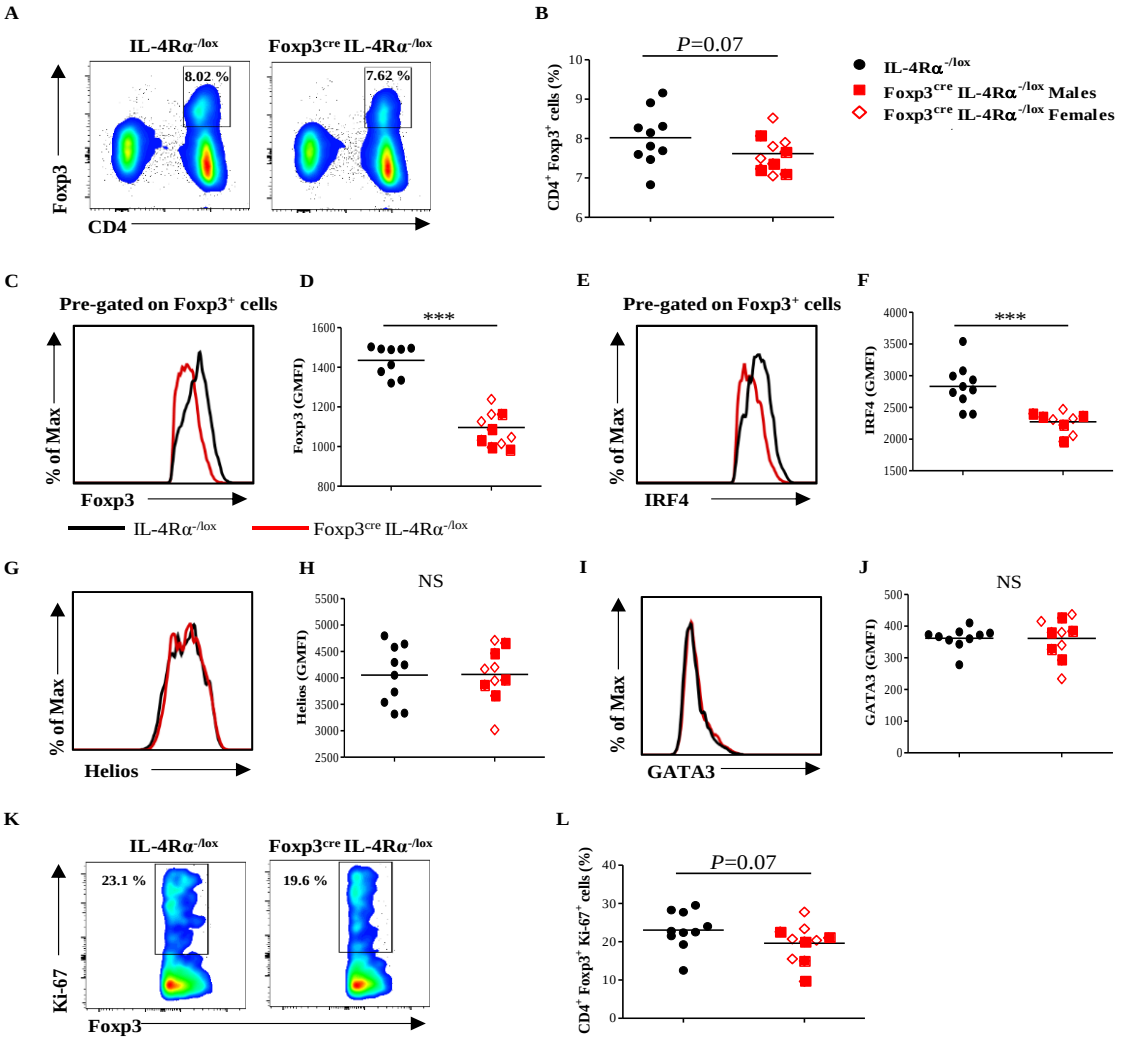

Figure 27. Foxp3^{+} Treg cell profile in the hLN of *S. mansoni* infected IL-4Rα$^{-/Lox}$ and Foxp3^{Cre} IL-4Rα$^{-/Lox}$ mice.

Foxp3^{+} Treg cells from the hLN of IL-4Rα$^{-/lox}$ and Foxp3^{Cre} IL-4Rα$^{-/lox}$ mice were analyzed 8 wk post *S. mansoni* infection for the expression of Treg suppressive and proliferation markers. (A) Representative flow cytometry of CD4^{+} Foxp3^{+} T cells. (B) Frequency of CD4^{+} Foxp3^{+} T cells from (A). (C) Representative histogram of Foxp3 expression by CD4^{+} Foxp3^{+} T cells. (D) Foxp3 GMFI in CD4^{+} Foxp3^{+} T cells from (C). (E) Representative histogram of IRF4 expression by CD4^{+} Foxp3^{+} T cells. (F) IRF4 GMFI in CD4^{+} Foxp3^{+} T cells from (E). (G) Representative histogram of Helios expression by CD4^{+} Foxp3^{+} T cells. (H) Helios GMFI in CD4^{+} Foxp3^{+} T cells from (G). (I) Representative histogram of GATA3 expression by CD4^{+} Foxp3^{+} T cells. (J) GATA3 GMFI in CD4^{+} Foxp3^{+} T cells from (I). (K) Representative flow cytometry of Ki-67 expression by CD4^{+} Foxp3^{+} T cells. (L) Frequency of CD4^{+} Foxp3^{-} Ki-67^{+} T cells from (K).

Results are representative of two independent experiments with 8-10 mice/group. Data are expressed as mean ± S.E.M. NS, not significant ($P > 0.05$); * $P < 0.05$, ** $P < 0.001$, *** $P < 0.0001$ by two-tailed unpaired Student's *t*-test.

4.1.2.3.2 IL-4Rα-mediated signaling on Foxp3$^+$ Treg cells is required to control T cell proliferation and effector function

Since it has been shown that Foxp3 expression within the Foxp3$^+$ Treg compartment can be used as one of the quality control indictors of Foxp3$^+$ Treg cell suppressive capacity potential and hence, its attenuation might abolish their ability to control the immune response (Wan and Flavell, 2007; Williams and Rudensky, 2007), the present study investigated the effect of the reduction of Foxp3 expression on Foxp3$^+$ Treg compartment, upon IL-4Rα deletion, on the CD4$^+$ Foxp3$^-$ T cell proliferation in the hLN during *S. mansoni* infection. It was noted that CD4$^+$ Foxp3$^-$ T cell in *Sm*-infected Foxp3^{cre} IL-4Rα$^{-/lox}$ mice had a higher proliferation capacity when compared to CD4$^+$ Foxp3$^-$ T cell proliferation in *Sm*-infected IL-4Rα$^{-/lox}$ mice (Fig. 29, A and B). This data arguing that Foxp3$^+$ Treg cells do require IL-4Rα signaling to control T cell proliferation *in vivo* under inflammatory condition.

Because schistosomiasis is a Th2-dominated disease (Pearce and MacDonald, 2002) and deletion of IL-4Rα specifically on Foxp3$^+$ Treg compartment led to a significant reduction in the expression level of IRF4, the transcription factor essential for the development of Th2 (Lohoff et al., 2002; Rengarajan et al., 2002) and crucial for Foxp3$^+$ Treg cells to endow themselves with the molecular machinery required to control Th2 immune response (Zheng et al., 2009), the present study therefore questioned whether the reduction of IRF4 expression on Foxp3$^+$ Treg compartment in the hLN of *Sm*-infected Foxp3^{cre} IL-4Rα$^{-/lox}$ mice will lead to heightened Th2 immune response. To address this, the present study investigated the expression level of GATA3 by CD4$^+$ T cells and the type 2 cytokines (IL-4 and IL-13) production by CD4$^+$ GATA3$^+$ T cells (Fig. 28). Consistently, a significant increase in the CD4$^+$ GATA3$^+$ T cells was noted in the hLN of *Sm*-infected Foxp3^{cre} IL-4Rα$^{-/lox}$ mice, when compared to *Sm*-infected IL-4Rα$^{-/lox}$ mice (Fig. 29, C and D). In line with that, CD4$^+$ GATA3$^+$ T cells in the hLN of *Sm*-infected Foxp3^{cre} IL-4Rα$^{-/lox}$ mice showed a significant increase in intracellular type 2 cytokines (IL-4 and IL-13, Fig. 30 A).

To further appraise the likelihood of cytokine production by newly formed ex-Foxp3$^+$ T cells dually expressing GATA3, Foxp3, and releasing cytokines following deletion of IL-4Rα (Noval Rivas et al., 2015; Massoud et al., 2016; Pelly et al., 2017), the source of the produced cytokines during *S. mansoni* infection was traced back by co-staining of

intracellular cytokines and Foxp3 in $CD4^+$ T cells. It was noted that $CD4^+$ $Foxp3^+$ T cells did not produce more cytokines in the hLN of *Sm*-infected $Foxp3^{cre}$ IL-$4R\alpha^{-/lox}$ mice (Fig. 30, B), ruling out their role in the heightened cytokine production observed in *Sm*-infected $Foxp3^{cre}$ IL-$4R\alpha^{-/lox}$ mice, but in contrast $CD4^+$ $GATA3^+$ T cells were the major producers of the upregulated cytokines observed in the hLN of *Sm*-infected $Foxp3^{cre}$ IL-$4R\alpha^{-/lox}$ mice (Fig. 30, A and B). Collectively, the present study concludes that the heightened immune response observed due to impairment of IL-4Rα-mediated signaling within the $Foxp3^+$ T cell compartment in *Sm*-infected $Foxp3^{cre}$ IL-$4R\alpha^{-/lox}$ mice is driven, at least in part, by $CD4^+$ $GATA3^+$ $Foxp3^-$ but not $Foxp3^+$ T-cells.

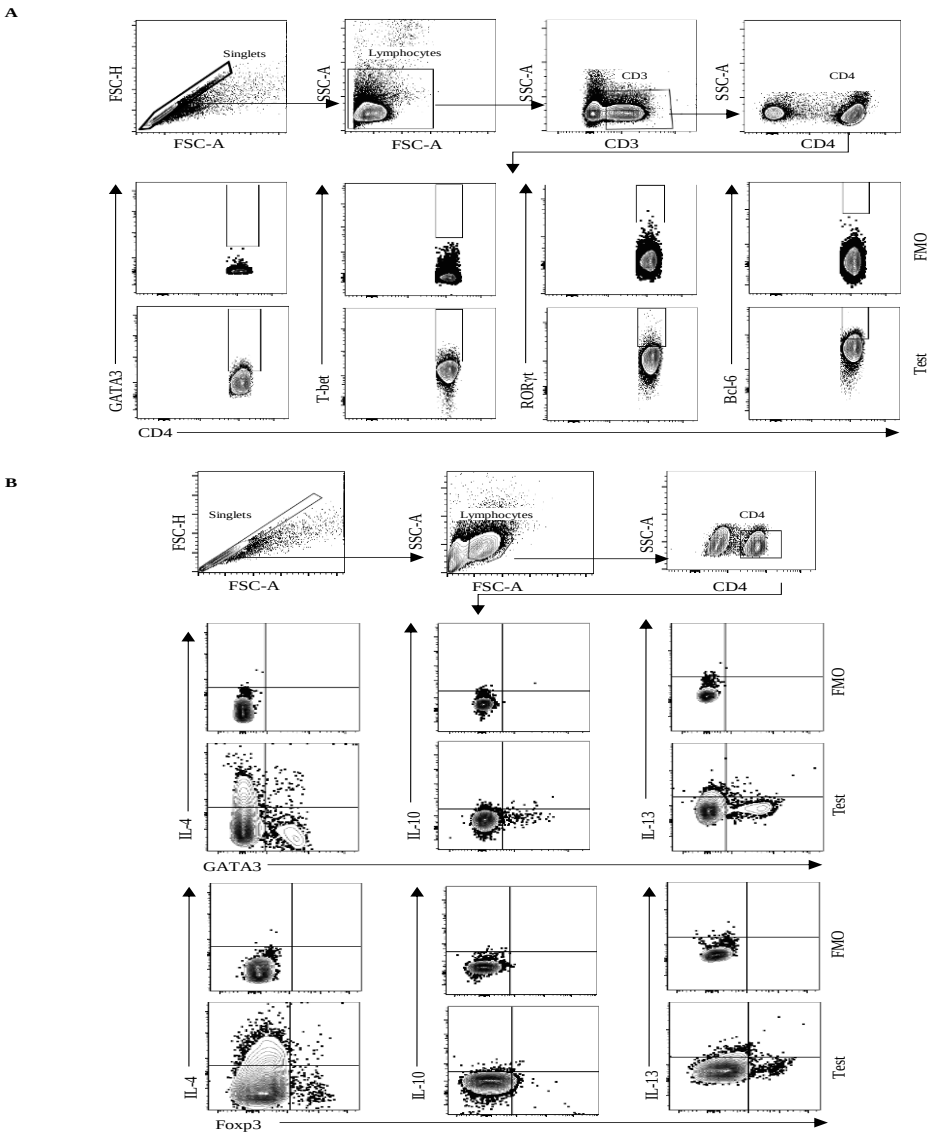

Figure 28. Gating strategies.

(A) Transcription factors-expressing $CD4^+$ T cells. **(B)** Cytokine-producing $CD4^+$ $GATA3^+$ and $CD4^+$ $Foxp3^+$ T cells.

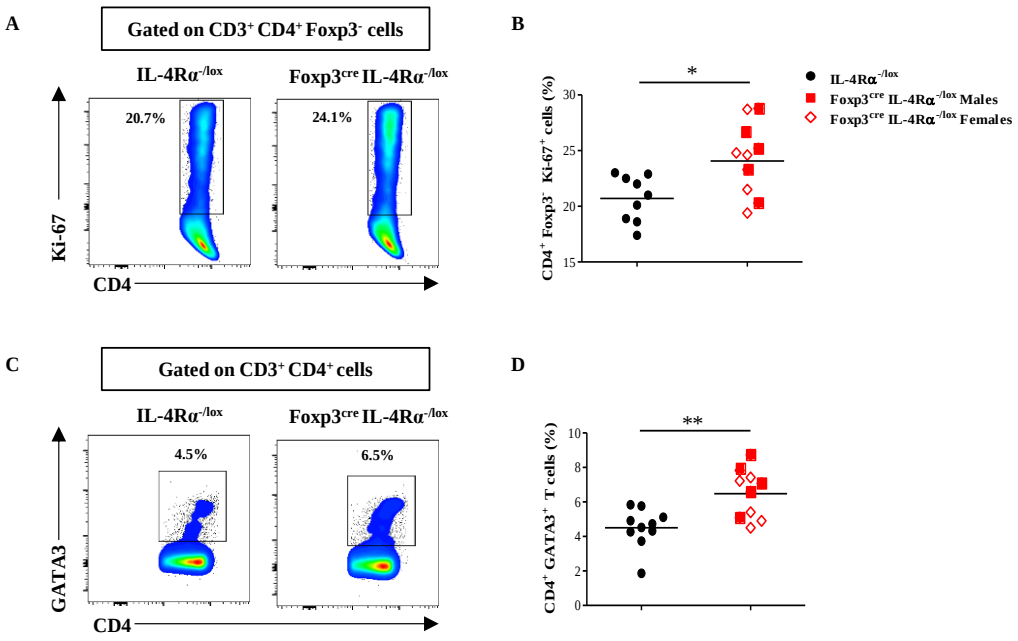

Figure 29. IL-4Rα mediated signaling on Foxp3$^+$ Treg is required for controlling T cell proliferation and GATA3 expression in hLN during *S. mansoni* infection.

(A) Representative flow cytometry of CD4$^+$ Ki-67$^+$ cells within CD4$^+$ Foxp3$^-$ T cell population in hLN of 8 wk *S. mansoni* infected IL-4Rα$^{-/lox}$ and Foxp3^{Cre} IL-4Rα$^{-/lox}$ mice. **(B)** Frequency of CD4$^+$ Foxp3$^-$ Ki-67$^+$ cells from **(A)**. **(C)** Representative flow cytometry of CD4$^+$ GATA3$^+$ T cells within CD4$^+$ T cell population in hLN 8 wk post-infection. **(D)** Frequency of CD4$^+$ GATA3$^+$ T cells from **(C)**. Results are representative of two independent experiments with 8-10 mice/group. Data are expressed as mean ± S.E.M. * $P < 0.05$, ** $P < 0.001$ by two-tailed unpaired Student's *t*-test.

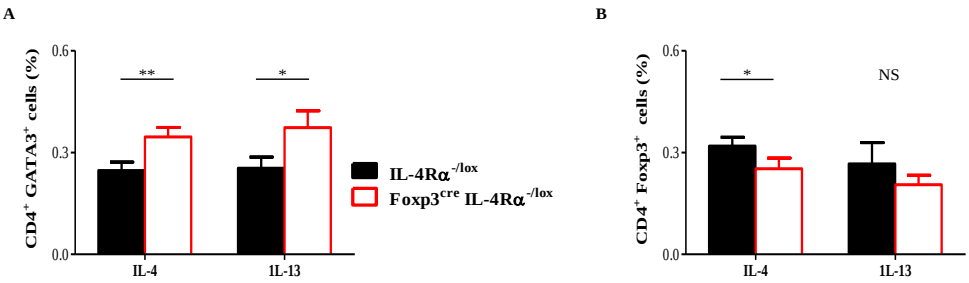

Figure 30. Deletion of IL-4Rα on Foxp3$^+$ Treg cells results in heightened Th2 cytokine production by CD4$^+$ GATA3$^+$ but not CD4$^+$ Foxp3$^+$ T cells in the hLN during *S. mansoni* infection.

hLN of 8 wk *S. mansoni* infected IL-4Rα$^{-/lox}$ and Foxp3^{Cre} IL-4Rα$^{-/lox}$ mice were stimulated with PMA/Ionomycin in the presence of Monensin and intracellular cytokines were measured by flow cytometry. (A) Frequency of cytokine-producing CD4$^+$ GATA3$^+$ T cells. (B) Frequency of cytokine-producing CD4$^+$ Foxp3$^+$ T cells. Results are representative of two independent experiments with 8-10 mice/group. Data are expressed as mean ± S.E.M. NS, not significant ($P > 0.05$); * $P < 0.05$, ** $P < 0.001$ by two-tailed unpaired Student's *t*-test.

4.1.2.4 IL-4Rα-mediated signaling on Foxp3$^+$ Treg cells is required for Treg accumulation in the gut during *S. mansoni* infection

Since the second major site of parasitism during *S. mansoni* infection is the mesenteric vasculature (Pearce and MacDonald, 2002; Elbaz and Esmat, 2013), the present study sought to address the effect of IL-4Rα deletion on Foxp3$^+$ Treg cells recruitment in the small intestine during *S. mansoni* infection. To do so, Foxp3$^+$ Treg population in the small intestine of 8 wk *Sm*-infected Foxp3^{cre} IL-4Rα$^{-/lox}$ and IL-4Rα$^{-/lox}$ mice was examined. Deletion of IL-4Rα specifically on Foxp3$^+$ Treg cells impaired their infiltration to the gut during *S. mansoni* infection (Fig. 31, A and B). Thus, and consistent with the liver data, IL-4Rα-mediated signaling on Foxp3$^+$ Treg cells is crucial for their infiltration in the inflamed tissues during *S. mansoni* infection.

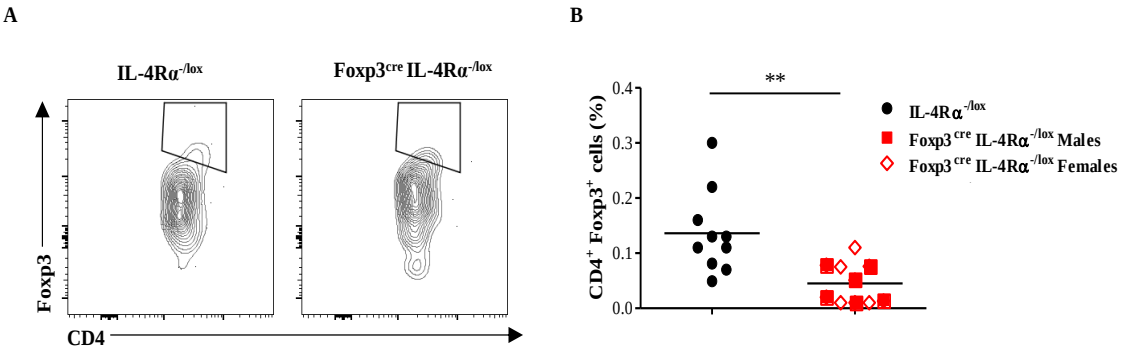

Figure 31. IL-4Rα mediated signaling on Foxp3$^+$ Treg is required for Treg accumulation in the gut during *S. mansoni* infection.

(A) Representative flow cytometry of CD4$^+$ Foxp3$^+$ T cells from the gut of 8 wk *S. mansoni* infected IL-4Rα$^{-/lox}$ and Foxp3^{Cre} IL-4Rα$^{-/lox}$ mice. **(B)** Frequency of CD4$^+$ Foxp3$^+$ T cells from **(A)**.

Results are representative of two independent experiments with 8-10 mice/group. Data are expressed as mean ± S.E.M. ** $P < 0.001$ by two-tailed unpaired Student's *t*-test.

4.1.2.5 IL-4Rα-mediated signaling on Foxp3$^+$ Treg cells is required for the maintenance/upregulation of Foxp3 expression in Tregs and the control of T cell proliferation and effector function in the MLN during *S. mansoni* infection

4.1.2.5.1 Deletion of IL-4Rα on Foxp3$^+$ Treg cells impairs their ability to maintain Foxp3 expression

Next, the present thesis sought to dissect the effect of IL-4Rα deletion on Foxp3$^+$ Treg cells on the expression level of suppressive markers and the proliferation capacity in the MLN during *S. mansoni* infection. To address this, MLN of 8 wk *Sm*-infected Foxp3^{cre} IL-4Rα$^{-/lox}$ and IL-4Rα$^{-/lox}$ mice were collected and Foxp3$^+$ Treg cells profile was investigated by flow cytometry. Although, the frequency of Foxp3$^+$ Treg cells (Fig. 32, A and B) within the MLN of *Sm*-infected Foxp3^{cre} IL-4Rα$^{-/lox}$ mice were similar to the littermate controls, Foxp3 expression level on a per-cell basis (Fig. 32, C and D) were however drastically reduced in Foxp3$^+$ Treg cells in the MLN of *Sm*-infected Foxp3^{cre} IL-4Rα$^{-/lox}$ mice, when compared to the infected littermate controls. In contrast, the expression level of IRF4 (32, E and F), Helios (Fig. 32, G and H), GATA3 (Fig. 32, I and J), and CD25 (Fig. 32, K and L) of Foxp3$^+$ Treg cells in the MLN of *Sm*-infected Foxp3^{cre} IL-4Rα$^{-/lox}$ controls were not affected, when compared to their infected littermate controls. Deletion of IL-4Rα on Foxp3$^+$ Treg cells resulted in a reduction in their proliferation in the MLN during *S. mansoni* infection (Fig. 32, M and N).

Together, these findings suggest that Foxp3$^+$ Treg cells do require IL-4Rα signaling to potentiate the expression of a suppressive factor, in particular, Foxp3, but neither IRF4 expression, Helios expression, GATA3 expression, nor CD25 expression, as well as to enhance their proliferation capacity, in the MLN during *S. mansoni* infection.

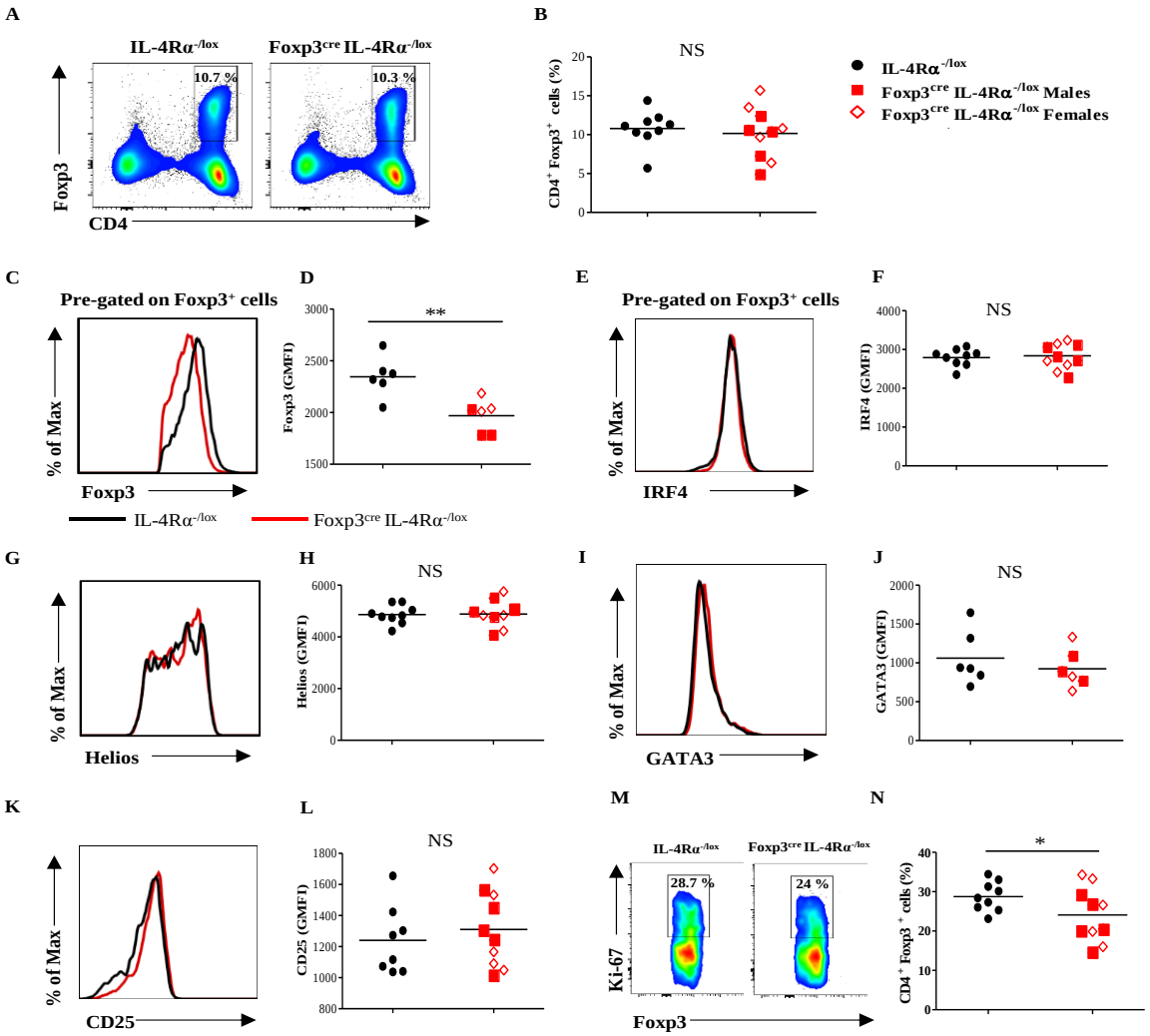

Figure 32. Foxp3^{+} Treg cell profile in the MLN of *S. mansoni* infected IL-4Rα$^{-/Lox}$ and Foxp3^{Cre} IL-4Rα$^{-/Lox}$ mice.

Foxp3^{+} Treg cells from the MLN of IL-4Rα$^{-/lox}$ and Foxp3^{Cre} IL-4Rα$^{-/lox}$ mice were analyzed 8 wk post *S. mansoni* infection for the expression of Treg suppresive and proliferation markers. **(A)** Representative flow cytometry of CD4^{+} Foxp3^{+} T cells. **(B)** Frequency of CD4^{+} Foxp3^{+} T cells from **(A)**. **(C)** Representative histogram of Foxp3 expression by CD4^{+} Foxp3^{+} T cells. **(D)** Foxp3 GMFI in CD4^{+} Foxp3^{+} T cells from **(C). (E)** Representative histogram of IRF4 expression by CD4^{+} Foxp3^{+} T cells. **(F)** IRF4 GMFI in CD4^{+} Foxp3^{+} T cells from **(E). (G)** Representative histogram of Helios expression by CD4^{+} Foxp3^{+} T cells. **(H)** Helios GMFI in CD4^{+} Foxp3^{+} T cells from **(G)**. **(I)** Representative histogram of GATA3 expression by CD4^{+} Foxp3^{+} T cells. **(J)** GATA3 GMFI in CD4^{+} Foxp3^{+} T cells from **(I)**. **(K)** Representative histogram of CD25 expression by CD4^{+} Foxp3^{+} T cells. **(L)** CD25 GMFI in CD4^{+} Foxp3^{-} Ki-67^{+} T cells from **(K)**. **(M)** Representative flow cytometry of Ki-67 expression by CD4^{+} Foxp3^{+} T cells. **(N)** Frequency of CD4^{+} Foxp3^{-} Ki-67^{+} T cells from **(M)**.

Results are representative of two independent experiments with 6-10 mice/group. Data are expressed as mean ± S.E.M. NS, not significant ($P > 0.05$); * $P < 0.05$, ** $P < 0.001$, *** $P < 0.0001$ by two-tailed unpaired Student's *t*-test.

4.1.2.5.2 IL-4Rα-mediated signaling on Foxp3$^+$ Treg cells is required to control T cell proliferation and effector function

The analyses within the MLN supported our previous observations in the hLN of *Sm*-infected Foxp3^{cre} IL-4Rα$^{-/lox}$ mice. Reduced suppressive capacity potential of Foxp3$^+$ Treg cells, as indicated by the significant reduction of Foxp3 expression (Fig. 31, C and D), was combined with increased frequency of proliferating (CD4$^+$ Foxp3$^-$ ki67$^+$; Fig. 33, A and B) and effector (CD4$^+$ CD44$^+$; Fig. 33, C and D) T cells within the MLN of *Sm*-infected Foxp3^{cre} IL-4Rα$^{-/lox}$ mice. To examine the effect of the uncontrolled T cell proliferation and effector function on cytokines production, cytokine production in the supernatant of SEA-stimulated MLN cells from *Sm*-infected Foxp3^{cre} IL-4Rα$^{-/lox}$ mice and their infected littermate controls was assessed by using ELISA. SEA-stimulated MLN cells from *Sm*-infected Foxp3^{cre} IL-4Rα$^{-/lox}$ mice showed a significant increase in IL-4, IL-5, and IL-10, amid a reduction of IFN-γ production (Fig. 33 E). In support, ex vivo stimulation of MLN cells with a cocktail of PMA/Ionomycin/Monensin and subsequent intracellular FACS analyses, induced a significant increase in IL-4, IL-10 and IL-13 production by CD4$^+$ T cells from *Sm*-infected Foxp3^{cre} IL-4Rα$^{-/lox}$ mice, when compared to infected littermate controls (Fig. 33 F). Together, these findings strongly suggest that the impairment of IL-4/IL-4Rα-mediated signaling within the Foxp3$^+$ T cell compartment impair Treg ability to upregulate suppressive factors, culminating into a heightened immune activation.

The present study next questioned the nature of the heightened immune response observed during inflammation in Foxp3^{cre} IL-4Rα$^{-/lox}$ mice. To do so, MLN cells from *Sm*-infected Foxp3^{cre} IL-4Rα$^{-/lox}$ mice and littermate controls were probed for CD4$^+$ T cell expressing GATA3, as a marker of Th2 responses (Zheng and Flavell, 1997), T-bet as a marker of Th1 responses (Szabo et al., 2000), RORγt, as a marker of Th17 responses (Ivanov et al., 2006), and Bcl-6 as a marker of T follicular responses (Nurieva et al., 2009; Yu et al., 2009). Consistent with the Th2 hegemony that is characteristic of *S. mansoni* infection (Pearce and MacDonald, 2002) and our hLN data, MLN CD4$^+$ T cells from *Sm*-infected Foxp3^{cre} IL-4Rα$^{-/lox}$ mice over-expressed GATA3 (Fig. 34), however, all other T cell polarization markers remained unaltered compared to littermate control (Fig. 34 and Fig. 28). Of importance, and consistently, CD4$^+$ GATA3$^+$ cells from *Sm*-infected Foxp3^{cre} IL-4Rα$^{-/lox}$ mice produced more IL-4, IL-10, and IL-13 compared to littermate controls (Fig. 35 A and Fig. 28). Together, these suggest that CD4$^+$ GATA3$^+$ responses likely drive the

heightened immune response and the cytokine storm observed in Foxp3^{cre} IL-4Rα$^{-/lox}$ mice during inflammation. Nevertheless, with the recent description of ex-Foxp3 T cells (Noval Rivas et al., 2015; Massoud et al., 2016; Pelly et al., 2017), this observation could be confounded by the likelihood of cytokine production by newly formed ex-Foxp3^{+} T cells dually expressing GATA3, Foxp3, and releasing cytokines following deletion of IL-4Rα. To examine that, the source of the produced cytokines during *S. mansoni* infection was traced back by co-staining of intracellular cytokines and Foxp3 in CD4^{+} T cells. It was observed that CD4^{+} Foxp3^{+} T cells did not produce more cytokines in the MLN of *Sm*-infected Foxp3^{cre} IL-4Rα$^{-/lox}$ mice (Fig. 35 B and; Fig. 28), ruling out a role for Foxp3^{+} T cells in the heightened cytokine production observed in *Sm*-infected Foxp3^{cre} IL-4Rα$^{-/lox}$ mice. Collectively, the present study concludes that the heightened immune response observed due to impairment of IL-4Rα-mediated signaling within the Foxp3^{+} T cell compartment in *Sm*-infected Foxp3^{cre} IL-4Rα$^{-/lox}$ mice is driven, at least in part, by CD4^{+} GATA3^{+} Foxp3^{-} but not Foxp3^{+} T-cells.

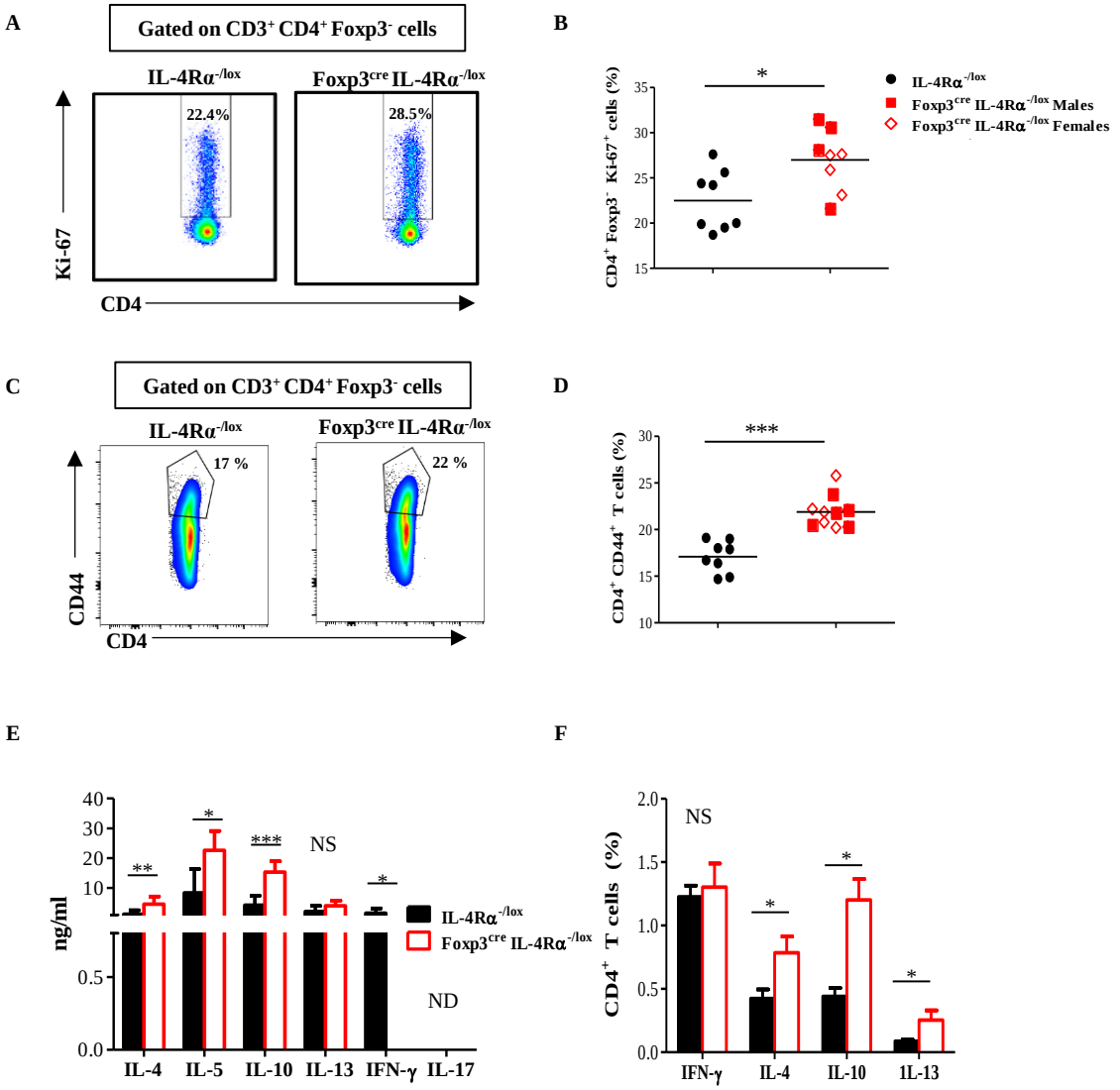

Figure 33. IL-4Rα mediated signaling on Foxp3$^+$ Treg is required for controlling T cell proliferation and effector function in MLN during *S. mansoni* infection.

(A) Representative flow cytometry of CD4$^+$ Ki-67$^+$ cells within CD4$^+$ Foxp3$^-$ T cell population in MLN of 8 wk *S. mansoni* infected IL-4Rα$^{-/lox}$ and Foxp3^{Cre} IL-4Rα$^{-/lox}$ mice. **(B)** Frequency of CD4$^+$ Foxp3$^-$ Ki-67$^+$ cells from **(A)**. **(C)** Representative flow cytometry of CD3$^+$ CD4$^+$ CD44$^+$ effector T cells within CD4$^+$ Foxp3$^-$ T cell population in MLN 8 wk post-infection. **(D)** Frequency of CD3$^+$ CD4$^+$ CD44$^+$ effector T cells from **(C)**. **(E)** Cytokine release detected by ELISA in the supernatant of SEA stimulated MLN cells of 8 wk *S. mansoni* infected IL-4Rα$^{-/lox}$ and Foxp3^{Cre} IL-4Rα$^{-/lox}$ mice. **(F)** Frequency of cytokine-producing CD3$^+$ CD4$^+$ T cells from MLN of 8 wk *S. mansoni* infected mice. MLN of infected mice was stimulated with PMA/Ionomycin in the presence of Monensin and intracellular cytokines were measured by flow cytometry.

Results are representative of two independent experiments with 8-10 mice/group. Data are expressed as mean ± S.E.M. * $P < 0.05$, *** $P < 0.0001$ by two-tailed unpaired Student's *t*-test.

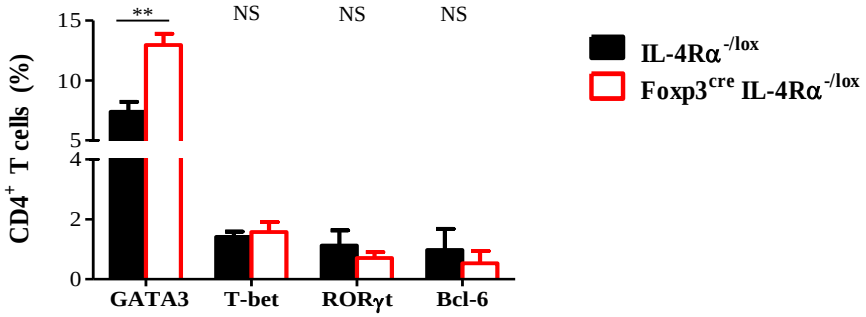

Figure 34. Deletion of IL-4Rα on Foxp3$^+$ Treg cells results in heightened CD4$^+$ GATA3$^+$ T cells in the MLN during *S. mansoni* infection.

Frequency of indicated transcription factors-expressing CD4$^+$ T cells in the MLN of 8 wk *S. mansoni* infected IL-4Rα$^{-/lox}$ and Foxp3^{Cre} IL-4Rα$^{-/lox}$ mice.

Results are representative of two independent experiments with 6-10 mice/group. Data are expressed as mean ± S.E.M. NS, not significant ($P > 0.05$); ** $P < 0.001$ by two-tailed unpaired Student's *t*-test.

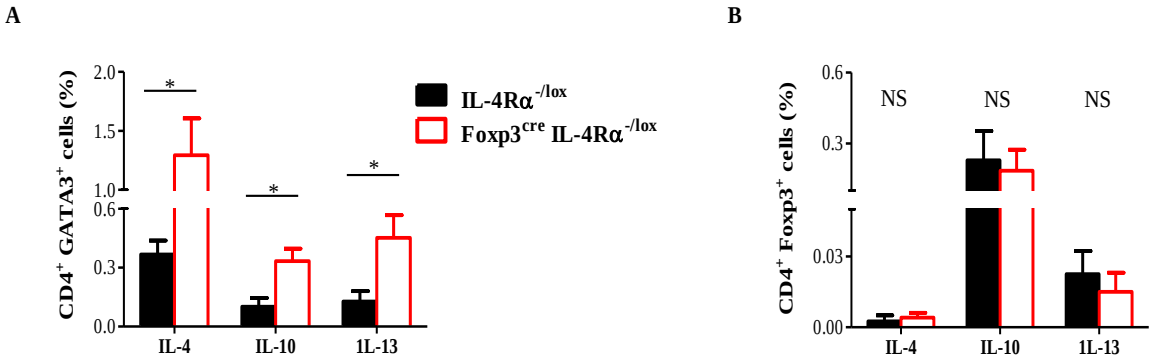

Figure 35. Deletion of IL-4Rα on Foxp3$^+$ Treg cells results in heightened Th2 cytokine production by CD4$^+$ GATA3$^+$ but not CD4$^+$ Foxp3$^+$ T cells in the MLN during *S. mansoni* infection.

MLN of 8 wk *S. mansoni* infected IL-4Rα$^{-/lox}$ and Foxp3^{Cre} IL-4Rα$^{-/lox}$ mice were stimulated with PMA/Ionomycin in the presence of Monensin and intracellular cytokines were measured by flow cytometry. (A) Frequency of cytokine-producing CD4$^+$ GATA3$^+$ T cells. (B) Frequency of cytokine-producing CD4$^+$ Foxp3$^+$ T cells.

Results are representative of two independent experiments with 8-10 mice/group. Data are expressed as mean ± S.E.M. NS, not significant ($P > 0.05$); * $P < 0.05$, ** $P < 0.001$ by two-tailed unpaired Student's *t*-test.

4.1.2.6 Deletion of IL-4Rα on Foxp3$^+$ Treg cells impairs their ability to control egg-driven fibrogranulomatous inflammation during *S. mansoni* infection

To further appraise the consequences of the heightened immune responses observed in diseased *Sm*-infected Foxp3^{cre} IL-4Rα$^{-/lox}$ mice, egg-driven fibro-granulomatous inflammation, as well as Foxp3$^+$ Treg cells infiltration in the liver of *Sm*-infected Foxp3^{cre} IL-4Rα$^{-/lox}$ mice, were microscopically assessed in comparison to that of *Sm*-infected littermate controls. It was noted that *S. mansoni* infection resulted in enlarged egg-driven granulomas in the liver of Foxp3^{cre} IL-4Rα$^{-/lox}$ mice when compared to granulomas in the liver of their littermate control (Fig. 36, A and B). In agreement with this observation, the average number of Foxp3$^+$ Treg cells within egg-driven granulomas in Foxp3^{cre} IL-4Rα$^{-/lox}$ mice was significantly reduced when compared with the amount of Foxp3$^+$ Tregs recruited to the liver of littermate controls (Fig. 36, C and D). Furthermore, collagen levels, attesting the degree of tissue fibrosis, were considerably higher in the livers of *Sm*-infected Foxp3^{cre} IL-4Rα$^{-/lox}$ mice when compared to the levels reported in *Sm*-infected littermate controls (Fig. 36 E). Indeed, colorimetric measurement of 4-hydroxyproline, a direct product of acid hydrolysis of collagen, confirmed our observed increased level of collagen in the liver of *Sm*-infected Foxp3^{cre} IL-4Rα$^{-/lox}$ mice (Fig. 36 F). In fact, with similar egg burdens in the guts and livers of Foxp3^{cre} IL-4Rα$^{-/lox}$ mice and their littermate control (Fig. 36 G), *Sm*-infected Foxp3^{cre} IL-4Rα$^{-/lox}$ mice still displayed much larger coalescing granulomas (Fig. 36 H) as indicated by hematoxylin and eosin (H&E) (Fig. 36 A) and chromotrope aniline blue (CAB) staining (Fig. 36 E). Similar to the liver, gut tissues of *Sm*-infected Foxp3^{cre} IL-4Rα$^{-/lox}$ mice revealed elevated levels of cellular recruitment around trapped parasite eggs (Fig. 36 I), that associated with a more pronounced deposition of collagen (Fig. 36 J), as confirmed by gut hydroxyproline content (Fig. 36 K) indicating a heightened fibro-granulomatous inflammation around *Sm*-trapped eggs in Foxp3^{cre} IL-4Rα$^{-/lox}$ mice when compared to littermate controls.

Taken together, these observations indicate that the impairment of IL-4Rα-mediated signaling within the Foxp3$^+$ Treg cells compartment during experimental schistosomiasis drives a poor accumulation of Foxp3$^+$ T cells in the inflamed tissues and consequently results in elevated host fibro-granulomatous responses around the trapped parasite eggs.

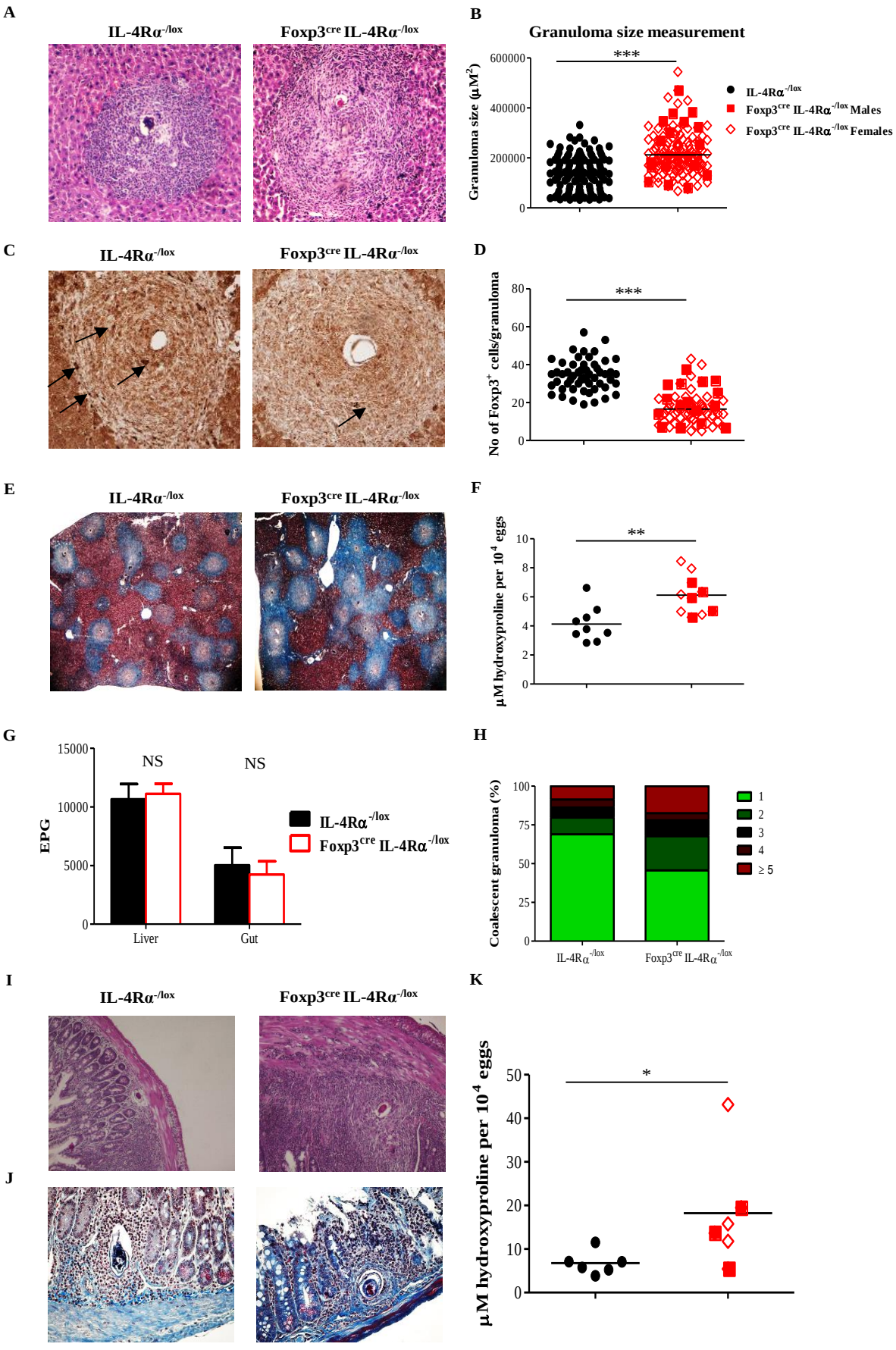
A
IL-4Rα-/lox
Foxp3cre IL-4Rα-/lox
B
Granuloma size measurement
***
Granuloma size (μM2)
600000
400000
200000
0
IL-4Rα-/lox
Foxp3cre IL-4Rα-/lox Males
Foxp3cre IL-4Rα-/lox Females
C
IL-4Rα-/lox
Foxp3cre IL-4Rα-/lox
D
***
No of Foxp3+ cells/granuloma
80
60
40
20
0
E
IL-4Rα-/lox
Foxp3cre IL-4Rα-/lox
F
**
μM hydroxyproline per 10^4 eggs
10
8
6
4
2
0
G
NS
NS
EPG
15000
10000
5000
0
Liver
Gut
IL-4Rα-/lox
Foxp3cre IL-4Rα-/lox
H
Coalescent granuloma (%)
100
75
50
25
0
IL-4Rα-/lox
Foxp3cre IL-4Rα-/lox
1
2
3
4
≥ 5
I
IL-4Rα-/lox
Foxp3cre IL-4Rα-/lox
J
K
*
μM hydroxyproline per 10^4 eggs
50
40
30
20
10
0

Figure 36. Deletion of IL-4Rα on Foxp3$^+$ Treg cells impairs the control of fibro-granulomatous inflammation in the liver during experimental *S. mansoni* infection. **(A)** Representative H&E staining of liver sections from 8 wk *S. mansoni* infected IL-4Rα$^{-/lox}$ and Foxp3^{Cre} IL-4Rα$^{-/lox}$ mice (original magnification 100X). **(B)** Liver granuloma size. Granuloma size was determined from **(A)** by using a computerized morphometric analysis program (NIS elements by NIKON) by measuring 100 granulomas/group. **(C)** Representative Foxp3 Tregs infiltration within liver granuloma 8 wk post *S. mansoni* infection (original magnification 100X) of IL-4Rα$^{-/lox}$ and Foxp3^{Cre} IL-4Rα$^{-/lox}$ mice. Thin arrows point to Foxp3$^+$ cells. **(D)** Quantification of the number of Foxp3$^+$ cells per each granuloma from **(C)**. **(E)** Representative CAB-stained liver sections from *S. mansoni* infected mice (original magnification 40X). **(F)** Liver hydroxyproline content measured by colorimetry 8 wk post-infection. **(G)** Liver and gut egg burden 8 wk post-infection. **(H)** Bar graphs showing the number of coalescent granulomas. **(I)** Representative H&E staining of gut sections from 8 wk *S. mansoni* infected mice (original magnification 100X). **(J)** Representative CAB-stained gut sections 8 wk post-infection (original magnification 200X). **(K)** Gut hydroxyproline content 8 wk post-infection.

Results are representative of two independent experiments with 8-10 mice/group. Data are expressed as mean ± S.E.M. NS, not significant ($P > 0.05$); * $P < 0.05$, ** $P < 0.001$, *** $P < 0.0001$ by two-tailed unpaired Student's *t*-test.

Because Cre expression can generate a phenotype of its own (Loonstra et al., 2001; Pomplun et al., 2007; Schmidt-Supprian and Rajewsky, 2007; Huh et al., 2010; Heffner et al., 2012; Qureshi et al., 2014; Carow et al., 2016), the present study sought to address whether the uncontrolled immune responses and the exaggerated fibrogranulomatous inflammation noted in the *S. mansoni*-infected Foxp3^{cre} IL-4Rα$^{-/lox}$ mice were due to the deletion of IL-4Rα specifically on the Foxp3$^+$ Treg cells or that was artefact effects from the Cre transgene alone. To test that, IL-4Rα$^{+/+}$ and Foxp3^{cre} IL-4Rα$^{+/+}$ mice were infected with 100 *S. mansoni* cercariae and then Foxp3$^+$ Treg compartments and fibrogranulomatous inflammation were investigated 8 wk post-infection. IL-4Rα expression on either CD19$^+$ B cells or Foxp3$^+$ Treg compartment (Fig. 37 A) in *Sm*-infected Foxp3^{cre} IL-4Rα$^{+/+}$ mice was similar to their littermate controls. Furthermore, in liver, frequency of Foxp3$^+$ Treg population (Fig. 37, B and C) and level of Foxp3 (Fig. 37, D and E) as well as GATA3 (Fig. 37, F and G) expression within the Foxp3$^+$ Treg compartment in *Sm*-infected Foxp3^{cre} IL-4Rα$^{+/+}$ mice were similar/slightly affected compared to their infected littermate controls. The similar frequency of Foxp3$^+$ Treg population (Fig. 37, H and I), as well as the comparable level of Foxp3 expression (Fig. 37, J and K) were also noted in the MLN of *Sm*-diseased mice. In fact, Cre transgene expression in Foxp3^{cre} IL-4Rα$^{+/+}$ mice did neither

lead to expansion of $CD4^+$ $GATA3^+$ T cell population (Fig. 37 L) nor uncontrolled Type 1 (IFNγ), Type 17 (IL-17), or Type 2 (IL-4, IL-5, IL-10, IL-13) cytokine production (Fig. 37 M). Thus, these data indicate that Cre-expression in our mouse model does not have any influences on either $Foxp3^+$ Treg compartment, their expression of the suppressive marker, or immune response-driven by the infection. In agreement of these observations, Cre expression did not affect either liver granuloma size (Fig. 38, A and B) or hepatic fibrosis as indicated by CAB staining (Fig. 38 C) and colourimetric measurement of 4-hydroxyproline (Fig. 38 D). Similar to the liver, gut tissues of *Sm*-infected $Foxp3^{cre}$ IL-$4R\alpha^{+/+}$ mice had a comparable granuloma size (Fig. 38 E), similar collagen deposition (Fig. 38 F), as well as similar level of 4-hydroxyproline content (Fig. 38 G), when compared to their infected littermate controls.

Taken together, Cre transgene, in our mouse model, does not have effects on either the immune response or tissue inflammation but rather the specific deletion of IL-4Rα on $Foxp3^+$ Treg cells is the main driver of the uncontrolled immune response.

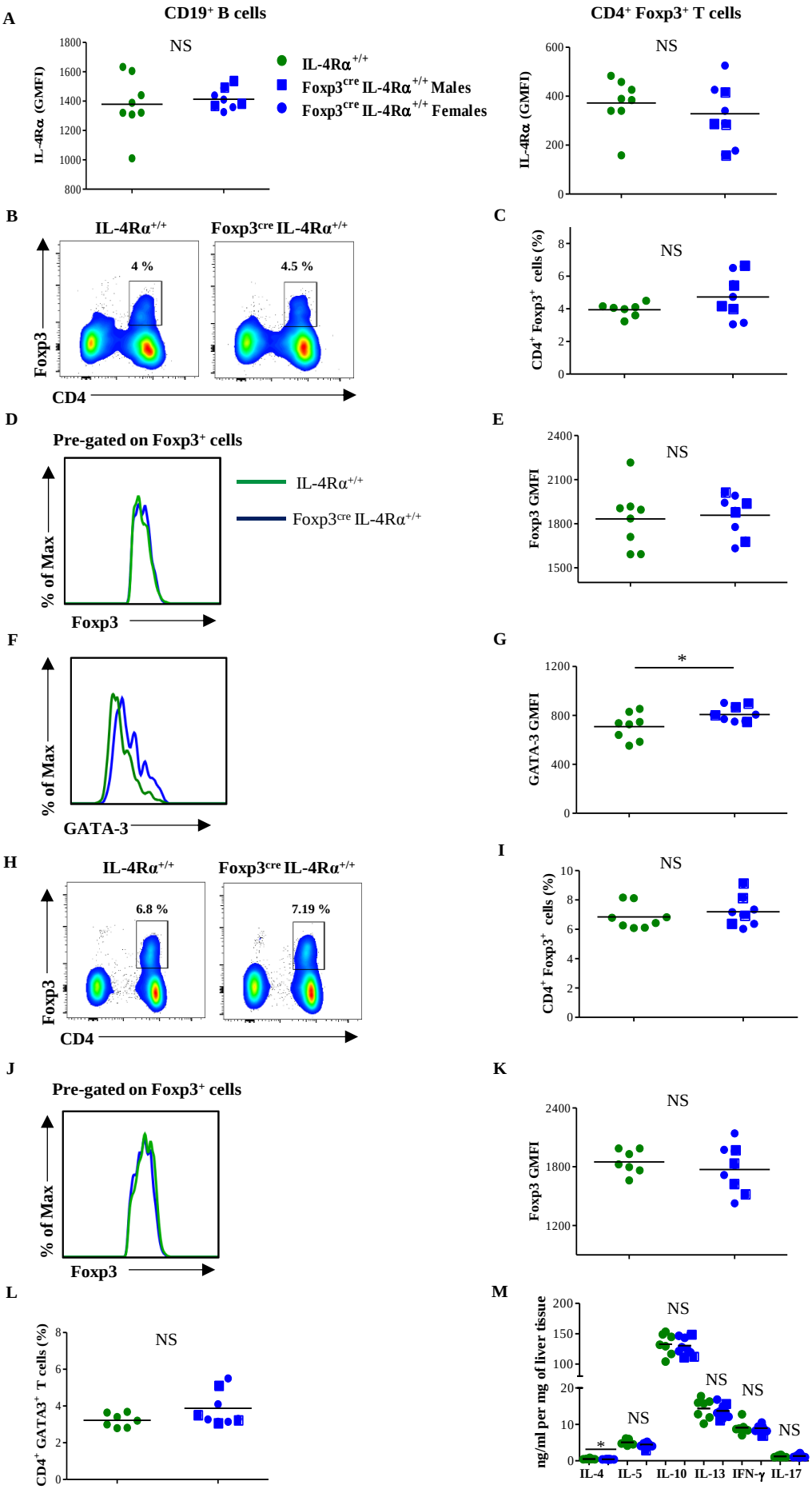
A
CD19⁺ B cells
CD4⁺ Foxp3⁺ T cells
NS
IL-4Rα (GMFI)
IL-4Rα+/+
Foxp3cre IL-4Rα+/+ Males
Foxp3cre IL-4Rα+/+ Females
B
IL-4Rα+/+
Foxp3cre IL-4Rα+/+
4 %
4.5 %
Foxp3
CD4
C
CD4⁺ Foxp3⁺ cells (%)
D
Pre-gated on Foxp3⁺ cells
% of Max
Foxp3
E
Foxp3 GMFI
F
GATA-3
G
GATA-3 GMFI
*
H
6.8 %
7.19 %
I
J
K
L
CD4⁺ GATA3⁺ T cells (%)
M
ng/ml per mg of liver tissue
IL-4
IL-5
IL-10
IL-13
IFN-γ
IL-17

Figure 37. Cre expression does neither alter Foxp3$^+$ Treg phenotype nor infection-driven immune responses during experimental schistosomiasis.

IL-4Rα$^{+/+}$ and Foxp3^{Cre} IL-4Rα$^{+/+}$ mice were infected with 100 *S. mansoni* cercariae, euthanized 8 weeks after, and Foxp3+ Treg compartment was analysed in liver and MLN. **(A)** Flow cytometry analysis of IL-4Rα expression by CD19$^+$ B cell and CD4$^+$ Foxp3$^+$ T cell in pooled spleen and MLN cells 8 wk post-infection. **(B)** Representative flow cytometry of CD4$^+$ Foxp3$^+$ T cells in the liver. **(C)** Frequency of CD4$^+$ Foxp3$^+$ T cells from **(A**). **(D)** Representative histogram of Foxp3 expression by CD4$^+$ Foxp3$^+$ T cells in the liver. **(E)** Foxp3 GMFI in CD4$^+$ Foxp3$^+$ T cells from **(D). (F)** Representative histogram of GATA-3 expression by CD4$^+$ Foxp3$^+$ T cells in the liver 8 wk post-infection with the mean values summarized in **(G)**. **(H)** Representative flow cytometry of CD4$^+$ Foxp3$^+$ T cells in the MLN. **(I)** Frequency of CD4$^+$ Foxp3$^+$ T cells from **(H). (J)** Representative histogram of Foxp3 expression by CD4$^+$ Foxp3$^+$ T cells in MLN. **(K)** Foxp3 GMFI in CD4$^+$ Foxp3$^+$ T cells from **(J)**. **(L)** Frequency of CD4$^+$ GATA3$^+$ T cells in MLN 8 wk post-infection. **(M)** Liver cytokine production 8 wk post-infection. Livers from infected mice were homogenized and the levels of the indicated cytokines were detected by ELISA and normalized to mg of liver tissue.

Results are representative of two independent experiments with 6-8 mice/group. Data are expressed as mean ± S.E.M. NS, not significant ($P > 0.05$); * $P < 0.05$, ** $P < 0.001$, *** $P < 0.0001$ by two-tailed unpaired Student's *t*-test.

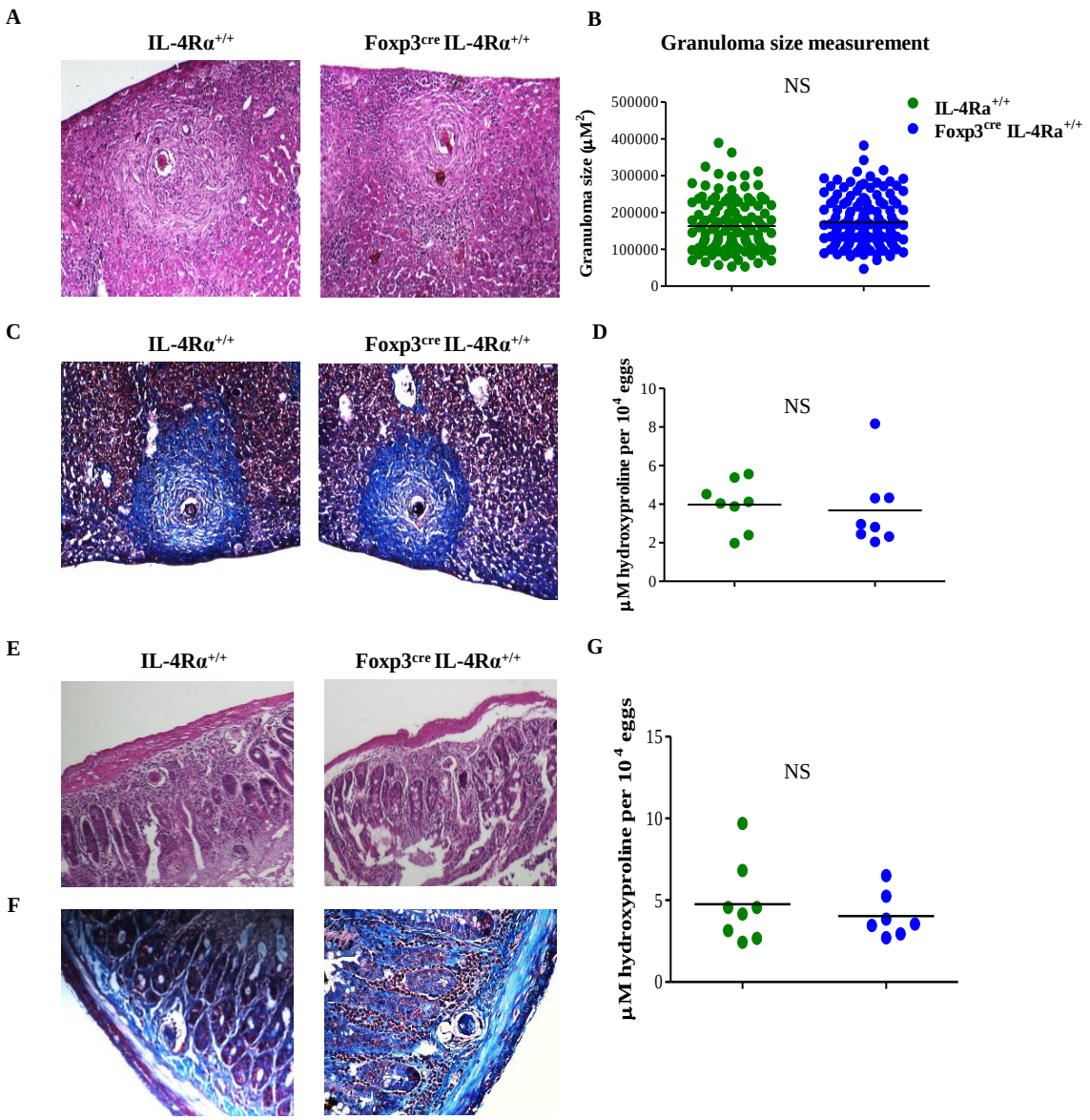

Figure 38. Cre expression does not induce exaggerated fibrogranulomatous inflammation during experimental *S. mansoni* infection.

A) Representative H&E staining of liver sections from 8 wk *S. mansoni* infected IL-4Rα$^{+/+}$ and Foxp3^{Cre} IL-4Rα$^{+/+}$ mice (original magnification 100X). **(B)** Liver granuloma size. Granuloma size was determined from **(A)** by using a computerized morphometric analysis program (NIS elements by NIKON) by measuring 100 granulomas/group. **(C)** Representative CAB-stained liver sections from *S. mansoni* infected mice (original magnification 100X). **(D)** Liver hydroxyproline content measured by colorimetry 8 wk post-infection. **(E)** Representative H&E staining of gut sections from 8 wk *S. mansoni* infected mice (original magnification 100X). **(F)** Representative CAB-stained gut sections 8 wk post-infection (original magnification 100X). **(G)** Gut hydroxyproline content 8 wk post-infection.

Results are representative of two independent experiments with 6-8 mice/group. Data are expressed as mean ± S.E.M. NS, not significant ($P > 0.05$); * $P < 0.05$, ** $P < 0.001$, *** $P < 0.0001$ by two-tailed unpaired Student's *t*-test.

4.1.2.7 Humoral immune response in Foxp3^{cre} IL-4Rα$^{-/lox}$ mice *S. mansoni* infection

Since it has been previously shown that Treg cells play a crucial role in the control of humoral immunity (Chung et al., 2011; Linterman et al., 2011; Wing and Sakaguchi, 2014), the present study questioned whether the deletion of IL-4Rα specifically on Foxp3^{+} Treg cells might have any impact on the humoral immune response during *S. mansoni* infection. To address that, blood from 8 wk *S. mansoni* infected Foxp3^{cre} IL-4Rα$^{-/lox}$ and IL-4Rα$^{-/lox}$ mice were collected, serum separated and, the humoral immune response was investigated. It was noted that despite a maintained level of total IgE (Fig. 39 A) and SEA-specific IgG2b (Fig. 39 D), a slight increase in SEA-specific IgG1 (Fig. 39 B) and a reduction in SEA-specific IgG2a (Fig. 39 C), were noted in the serum of *Sm*-infected Foxp3^{cre} IL-4Rα$^{-/lox}$ mice, when compared to their infected littermate controls, suggesting that IL-4Rα-mediated signaling on Foxp3^{+} Treg cells might play a minimal role, possibly indirect, in regulating the humoral immune response during *S. mansoni* infection.

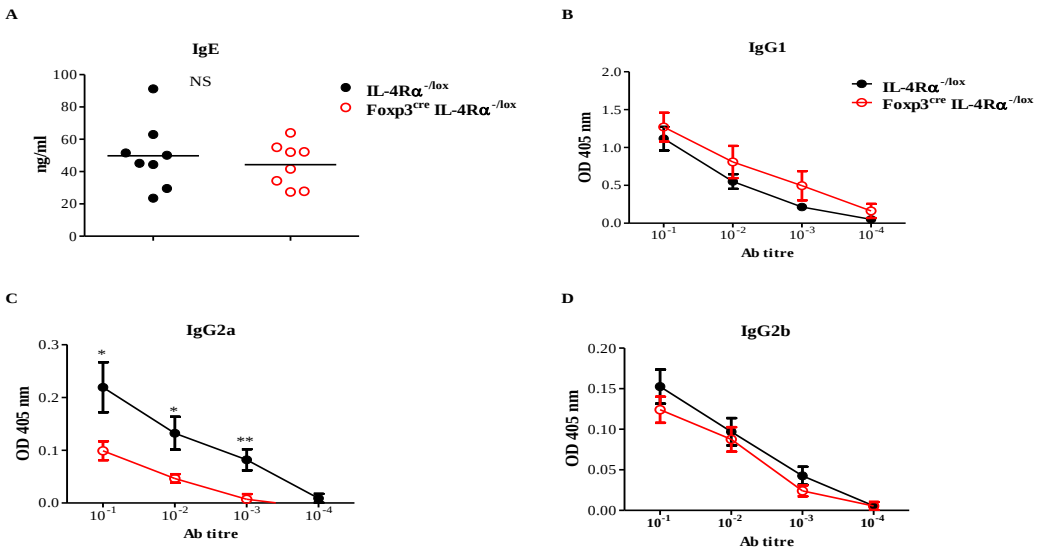

Figure 39. Humoral immune response of 8 wk *S. mansoni* infected IL-4Rα$^{-/lox}$ and Foxp3^{Cre} IL-4Rα$^{-/Lox}$ mice.

IL-4Rα$^{-/lox}$ and Foxp3^{cre} IL-4Rα$^{-/lox}$ mice were infected with 100 *S. mansoni* cercariae and euthanized 8 wk post-infection. Sera were collected and analysed by using ELISA for humoral immune response. (A) Total seric IgE in *S. mansoni* infected mice. (B) SEA-specific IgG1, (C) IgG2a, and (D) IgG2b isotype antibodies.

Results are representative of two independent experiments with 8-10 mice/group. Data are expressed as mean ± S.E.M. NS, not significant ($P > 0.05$); * $P < 0.05$, ** $P < 0.001$ by two-tailed unpaired Student's *t*-test.

4.1.2.8 IL-4Rα-mediated signaling on Foxp3^{+} Treg cells is dispensable for host survival during *S. mansoni* infection

Next, the present study asked whether the heightened immune activation observed in *Sm*-infected Foxp3^{cre} IL-4Rα$^{-/lox}$ mice might have any impact on gross pathology during schistosomiasis. To address that, the gross pathology of 8 wk *Sm*-infected Foxp3^{cre} IL-4Rα$^{-/lox}$ and IL-4Rα$^{-/lox}$ mice was investigated by evaluating body weight and organs (liver and spleen) weight as well as comparing autopsy images. No significant difference was noted between *Sm*-infected Foxp3^{cre} IL-4Rα$^{-/lox}$ mice and their littermate control in terms of final body weight (Fig. 40 A), livers weight (Fig. 40 B), spleens weight (Fig. 40 C), or autopsy images (Fig. 40 D). To further appraise the effect of deletion of IL-4Rα specifically within Foxp3^{+} Treg cells on the host susceptibility to *S. mansoni* infection, Foxp3^{cre} IL-4Rα$^{-/lox}$ mice and their littermate control were infected with a dose of 80 viable *S. mansoni* cercariae and monitored until the attainment of an pre-defined humane endpoint (persistent bloody diarrhoea, severe lethargy, and weight loss of 20% or more). No difference either in the pattern of the body weight changes (Fig. 41 A) or the survival rate (Fig. 41 B) was noted between *Sm*-infected Foxp3^{cre} IL-4Rα$^{-/lox}$ mice and their littermate controls. Together, these data suggest that IL-4Rα-mediated signaling on Foxp3^{+} Treg cells might be dispensable for gross pathology and host survival during *S. mansoni* infection.

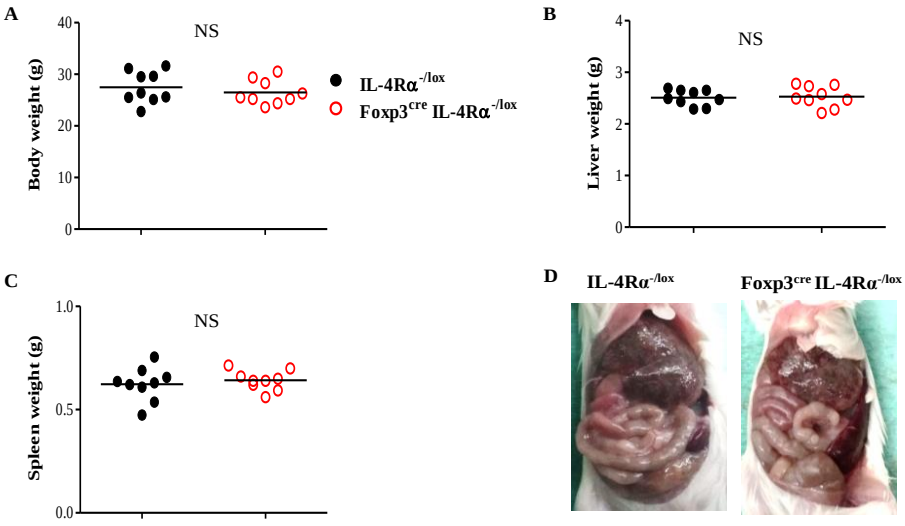

Figure 40. Deletion of IL-4Rα on Foxp3^{+} Treg cells does not alter gross pathology during acute schistosomiasis.

(A) Body weight of IL-4Rα$^{-/lox}$ and Foxp3^{cre} IL-4Rα$^{-/lox}$ mice 8 wk post *S. mansoni* infection. **(B)** Liver weight, **(C)** Spleen weight, and **(D)** Gross pathology of 8 wk *S. mansoni* infected mice.

Results are representative of two independent experiments with 8-10 mice/group. Data are expressed as mean ± S.E.M. NS, not significant ($P > 0.05$) by two-tailed unpaired Student's *t*-test.

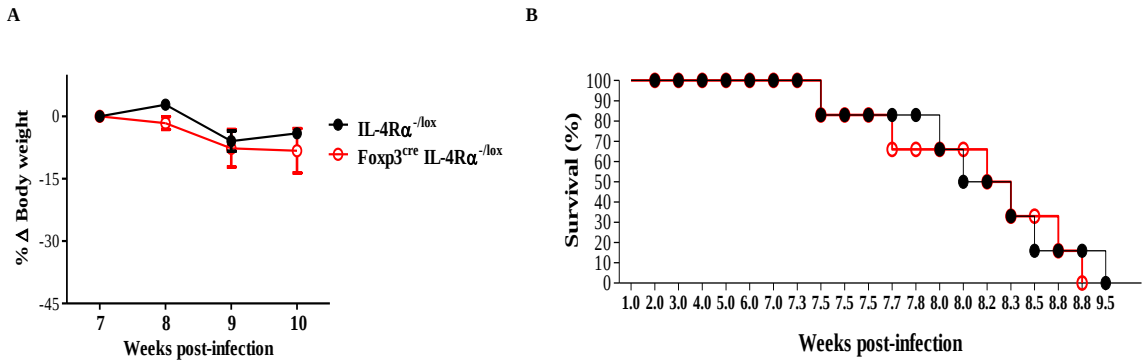

Figure 41. Intact IL-4Rα-mediated signaling on Foxp3^{+} Treg cells is not critical for mice survival during schistosomiasis.

IL-4Rα$^{-/lox}$ and Foxp3^{cre} IL-4Rα$^{-/lox}$ mice were infected with 80 *S. mansoni* cercariae and host survival was recorded. **(A)** Body weight measured weekly during the onset of infection. **(B)** Survival curve of *S. mansoni* infected IL-4Rα$^{-/lox}$ and Foxp3^{cre} IL-4Rα$^{-/lox}$ mice.

Results are representative of two independent experiments with 8-10 mice/group.

4.1.3 IL-4Rα-mediated signaling on Foxp3^{+} Treg cells is required for Treg accumulation and control of inflammation in the lung during primary *Nippostrongylus brasiliensis* infection

4.1.3.1 Deletion of IL-4Rα on Foxp3^{+} Treg cells does not alter worm expulsion ability of the host

The present study next aimed to appraise whether the heightened inflammatory response in *Sm*-infected Foxp3^{cre} IL-4Rα$^{-/lox}$ mice is specific to *S. mansoni* infection, sub-cutaneous infection of Foxp3^{cre} IL-4Rα$^{-/lox}$ and the littermate control mice was performed with 500 L3 *Nippostrongylus brasiliensis* larvae. Worm count, MLN immune response, gut pathology, and lung pathology were assessed 9 days post-infection. Similar to *Nb*-infected IL-4Rα$^{-/lox}$ mice, *Nb*-infected Foxp3^{cre} IL-4Rα$^{-/lox}$ were able to clear the worms by day 9 post-infection (Fig. 42, A and B), suggesting that IL-4Rα-mediated signaling on Foxp3^{+} Treg cells might not be necessary for worm expulsion during *N. brasiliensis* infection.

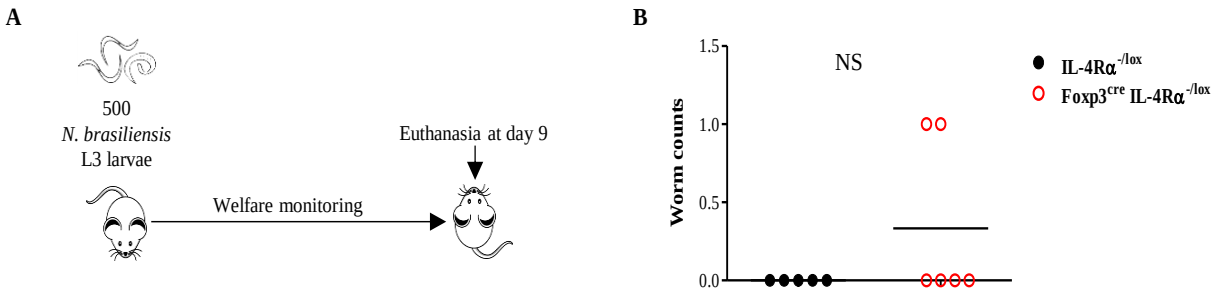

Figure 42. Deletion of IL-4Rα on Foxp3^{+} Treg cells does not alter worm expulsion capacity of the host.

(A) Experimental design. **(B)**Worm count. IL-4Rα$^{-/lox}$ and Foxp3^{cre} IL-4Rα$^{-/lox}$ mice were infected with 500 L3 larvae of *N. brasiliensis*, euthanized 9 days after, and worms in the gut were counted.

Results are representative of two independent experiments with 6 mice/group. Data are expressed as mean ± S.E.M. NS, not significant by two-tailed unpaired Student's *t*-test.

4.1.3.2 IL-4Rα-mediated signaling is required to maintain/enhance Foxp3 expression on Foxp3$^+$ Treg cells in the MLN during primary *N. brasiliensis* infection

To examine the effect of IL-4Rα deletion on Foxp3$^+$ Treg cells on the Foxp3$^+$ Treg cells and their expression level of the suppressive marker, Foxp3, in the MLN during *N. brasiliensis* infection, MLNs of *Nb*-infected Foxp3^{cre} IL-4Rα$^{-/lox}$ and IL-4Rα$^{-/lox}$ mice were collected 9 days post-infection and Foxp3$^+$ Treg cells profile was investigated by flow cytometry. Although, the frequency of Foxp3$^+$ Treg cells (Fig. 43, A and B) within the MLN of *Nb*-infected Foxp3^{cre} IL-4Rα$^{-/lox}$ mice was significantly higher compared to the littermate controls, Foxp3 expression level on a per-cell basis (Fig. 43, C and D) were however drastically reduced in Foxp3$^+$ Treg cells in the MLN of *Nb*-infected Foxp3^{cre} IL-4Rα$^{-/lox}$ mice, when compared to the infected littermate controls, suggesting that, consistently *in vitro* and *in vivo* under inflammatory conditions, Foxp3$^+$ Treg cells do require IL-4Rα-signaling to potentiate Foxp3 expression. Although, however, T cell polarization markers (Fig. 43 E), as well as cytokines production (IL-4, IL-10, IL-13, and IFN-γ) by CD4$^+$ T (Fig. 43 F) cells in the MLN of *Nb*-infected Foxp3^{cre} IL-4Rα$^{-/lox}$ mice, were similar to those of infected littermate control. In support, no significant difference in the number of mucus-producing goblet cells in the gut of *Nb*-infected Foxp3^{cre} IL-4Rα$^{-/lox}$ mice and their infected littermate controls was noted (Fig. 43, G and H).

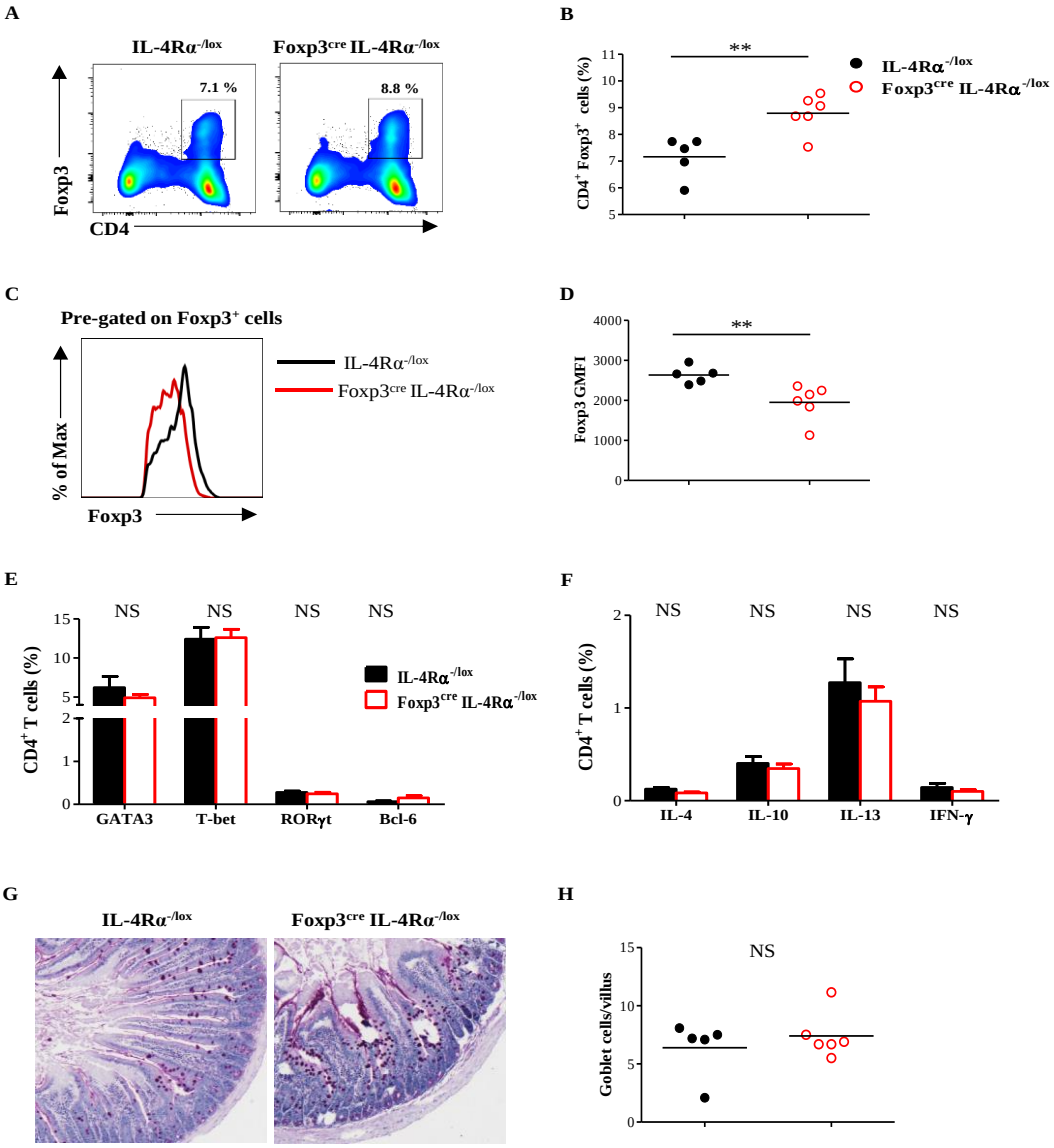

Figure 43. Deletion of IL-4Rα on Foxp3$^+$ Treg cells does not alter gut pathology during primary *N. brasiliensis* infection.

(A) Representative flow cytometry of CD4$^+$ Foxp3$^+$ T cells from the MLN of *N. brasiliensis* infected IL-4Rα$^{-/lox}$ and Foxp3^{Cre} IL-4Rα$^{-/lox}$ mice. **(B)** Frequency of CD4$^+$ Foxp3$^+$ T cells from **(A)**. **(C)** Representative histogram of Foxp3 expression by CD4$^+$ Foxp3$^+$ T cells in the MLN of *N. brasiliensis* infected mice. **(D)** Foxp3 GMFI in CD4$^+$ Foxp3$^+$ T cells from **(C)**. **(E)** Frequency of indicated transcription factors-expressing CD4$^+$ T cells in the MLN *N. brasiliensis* infected mice. (F) Frequency of cytokine-producing CD3$^+$ CD4$^+$ T cells from MLN of *N. brasiliensis* infected mice. MLN of infected mice was stimulated with PMA/Ionomycin in the presence of Monensin and intracellular cytokines were measured by flow cytometry. **(G)** Representative PAS staining of mucus-producing goblet cells (original magnification 100X) in the gut tissues 9-days post-infection. **(H)** Quantification of PAS$^+$ goblet cells/villus/mouse from **(G)**.

Results are representative of two independent experiments with 6 mice/group. Data are expressed as mean ± S.E.M. NS, not significant by two-tailed unpaired Student's *t*-test.

4.1.3.3 IL-4Rα-mediated signaling on Foxp3$^+$ Treg is required for Treg accumulation and the control of worm-driven emphysematous inflammation in the lung during primary *N. brasiliensis* infection

Since *N. brasiliensis* larvae migration through the lung to the bronchi causes a dilatation of distal airway spaces and a significant reduction in lung function, a phenomenon known as emphysema, and it was previously published that IL-4Rα signaling plays a crucial role in mediating acute wound healing (Chen et al., 2012), the present study asked whether IL-4Rα signaling, particularly on Foxp3$^+$ Treg cell, plays a role in the regulation of worm-driven lung emphysema. To address this hypothesis, emphysema in the lung of *Nb*-infected Foxp3^{cre} IL-4Rα$^{-/lox}$ and IL-4Rα$^{-/lox}$ mice was measured using mean linear intercept method (MLI) (Brandsma et al., 2008; Knudsen et al., 2010; Cremona et al., 2013; Bouchery et al., 2017) 9 days post-infection. Deletion of IL-4Rα specifically on Foxp3$^+$ Treg cell resulted in worsened emphysema in the lung of *Nb*-infected Foxp3^{cre} IL-4Rα$^{-/lox}$, when compared to infected littermate controls (Fig 44, A and B), indicating that IL-4Rα-mediated signaling on Foxp3$^+$ Treg cells is critical in controlling parasite-induced emphysema.

Moreover, the airways of *Nb*-infected Foxp3^{cre} IL-4Rα$^{-/lox}$ mice showed much heavier mucus production 9 days post-infection (Fig. 45, A and B). Furthermore, it was noted that Foxp3$^+$ Treg cells recruitment to the inner layer of the alveoli of the lungs of *Nb*-infected Foxp3^{cre} IL-4Rα$^{-/lox}$ mice (Fig. 45, C and D) was diminished, indicating that in this model as well the impairment of IL-4Rα-mediated signaling within the Foxp3$^+$ Treg cell compartment impair their ability to accumulate at the inflamed tissue and to control local tissue inflammation. Collectively, these results clearly suggest, in two different and major inflammatory helminth models that impairment of IL-4Rα-mediated signaling within the Foxp3$^+$ T cell compartment leads to uncontrolled immune responses and exacerbated tissue(s) inflammation, underscoring a hitherto unappreciated role of IL-4Rα mediated signaling on Foxp3$^+$ Treg cells to control inflammatory responses *in vivo*.

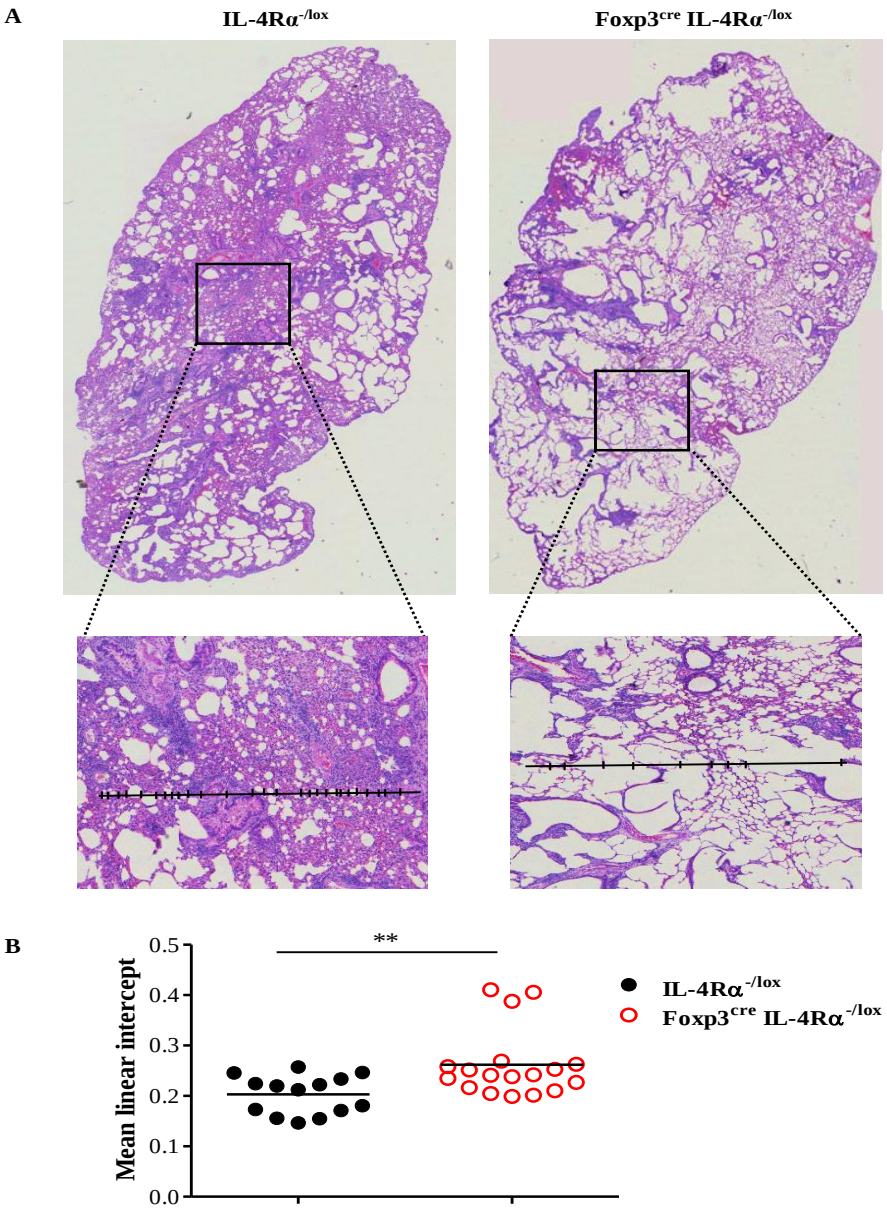

Figure 44. Deletion of IL-4Rα on Foxp3^{+} Treg cells impairs the control of emphysema during primary *N. brasiliensis* infection.

(A) Representative H&E staining of lung section (original magnification 4X) from *N. brasiliensis* infected IL-4Rα$^{-/lox}$ and Foxp3^{cre} IL-4Rα$^{-/lox}$ mice. H&E lung sections were used to measure emphysema by drawing horizontal lines across the section and then count the number of intercepts between the line and the lung septa to measure MLI. **(B)** Measurement of MLI from **(A)**.

Results are representative of two independent experiments with 6 mice/group. Data are expressed as mean ± S.E.M. NS, not significant by two-tailed unpaired Student's *t*-test.

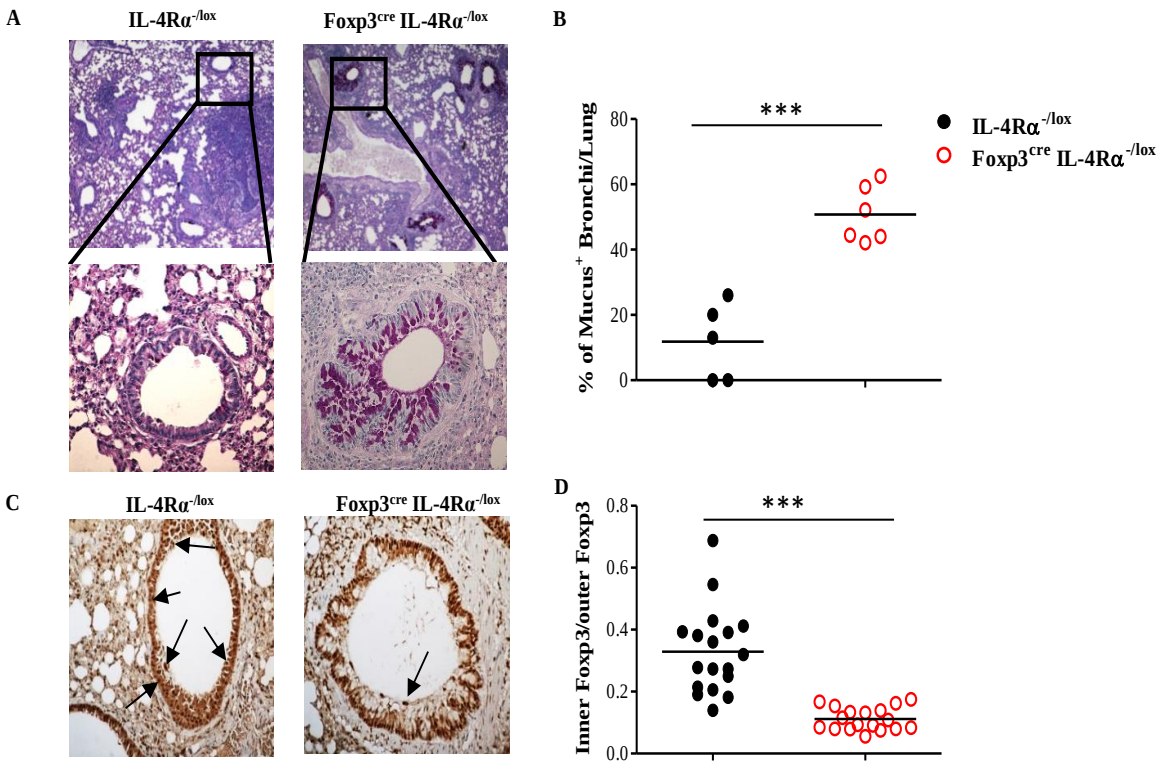

Figure 45. IL-4Rα signaling on Foxp3^{+} Treg cells is required to control worm-driven lung inflammation during *N. brasiliensis* infection.

(A) Representative PAS staining of mucus-producing goblet cells, with lower (20X, top) and higher (200X) magnifications, in the lung tissues 9-days post-infection of IL-4Rα$^{-/lox}$ and Foxp3^{cre} IL-4Rα$^{-/lox}$ mice with 500 L3 larvae of *N. brasiliensis*. **(B)** Quantification of PAS^{+} bronchi/lung/mouse. **(C)** Representative of Foxp3^{+} Treg cells infiltration within the lung alveoli 9-days post-*N. brasiliensis* infection (original magnification 200X). Thin arrows point to inner and outer Foxp3^{+} cells. **(D)** Ratio of inner to outer Foxp3^{+} Treg cells per alveoli from **(C)**.

Results are representative of two independent experiments with 6 mice/group. Data are expressed as mean ± S.E.M. NS, not significant ($P > 0.05$); * $P < 0.05$, ** $P < 0.001$, *** $P < 0.0001$ by two-tailed unpaired Student's *t-test*.

4.2 Discussion

Even though naïve Foxp3^{cre} IL-4Rα$^{-/lox}$ mice were indistinguishable from their littermate controls, by using two different models of tissue-dwelling helminth infections, *Schistosoma mansoni* and *Nippostrongylus brasiliensis*, the present thesis showed that Foxp3^{+} Treg cells do require an intact IL-4Rα signaling to maintain/potentiate Foxp3^{+} Tregs. The present thesis does show that Foxp3^{+} Treg cells require an intact IL-4Rα to maintain/upregulate Foxp3 expression, and other suppressive markers based on the anatomical location, to control T cell proliferation as well as effector functions, as evidenced by overshooting cytokine production and exacerbated parasite-driven tissue inflammation. Mechanistically, IL-4Rα-mediated signaling on Foxp3^{+} Treg cells is crucial for their infiltration /accumulation at the inflamed tissues. Our data reveal for the first time, the host requirement for an intact, rather than a threshold, level of expression of IL-4Rα mediated signaling on Foxp3^{+} Treg cells to optimally control inflammation during helminth infections, describing a positive regulation of Foxp3^{+} Tregs function by IL-4Rα *in vivo*.

4.2.1 Upregulation of IL-4Rα expression by Foxp3^{+} Treg cell *in vivo* under inflammatory conditions

Similar to mice with specific deletion of either GATA3 or T-bet on Foxp3^{+} Treg cells (Koch et al., 2009; Yu et al., 2015), deletion of IL-4Rα specifically on Foxp3^{+} Treg cells did not show any physical alteration or spontaneous inflammatory disorders under steady-state in naïve young mice and hence, induction of inflammatory conditions, i.e. by infecting the mice with tissue-dwelling helminth, was crucial in dissecting the role of IL-4Rα-mediated signaling on Foxp3^{+} Treg cells. It was first noted that Foxp3^{+} Treg cells do upregulate the expression of IL-4Rα during acute experimental schistosomiasis. The IL-4Rα upregulation on the Foxp3^{+} Treg compartment during acute experimental schistosomiasis led to two opposing but not mutually exclusive hypotheses; i) the first hypothesis is that IL-4Rα is a critical receptor in conferring to Foxp3^{+} Treg cells the necessary potency to control inflammatory immune responses in disease and/or ii) the second hypothesis is that the need for this IL-4Rα receptor to foster Foxp3^{+} Treg transdifferentiation into effector T cells.

4.2.2 Foxp3$^+$ Treg cells do require IL-4Rα signaling to control inflammatory immune responses in disease

4.2.2.1 IL-4Rα signaling on Foxp3$^+$ Treg is crucial in maintaining/promoting their Foxp3 expression *in vivo*

The first hypothesis does find support in our observations. Deletion of IL-4Rα specifically on Foxp3$^+$ Treg resulted in a significant reduction of Foxp3$^+$ Treg population in the liver and the gut during *S. mansoni* infection, arguing for the need of that receptor by Foxp3$^+$ Treg to maintain/enforce their pool in the infected tissues. In fact, and despite the effect of different anatomical locations on Foxp3$^+$ Treg cells phenotypical and functional characteristics, conditional ablation of IL-4Rα specifically on Foxp3$^+$ Treg cells led to a drastic reduction in Foxp3 expression in Foxp3$^+$ Treg population in the liver, hLN, and MLN of *S. mansoni* infected Foxp3^{cre} IL-4Rα$^{-/lox}$ mice. The pattern that was reproducible in another helminth infection, *N. brasiliensis*. Even though, the mechanism in *N. brasiliensis* might be slightly different as Foxp3$^+$ Treg population was higher in *N. brasiliensis* infected Foxp3^{cre} IL-4Rα$^{-/lox}$ mice compared to their littermate controls, Foxp3 expression on a per cell basis were significantly reduced in those Foxp3$^+$ Treg population in the *N. brasiliensis* infected Foxp3^{cre} IL-4Rα$^{-/lox}$ mice. One possible explanation could be that the host was trying to compensate for the reduction of Treg cells suppressive capacity, as indicated by the reduction of the Foxp3 expression, by increasing the number of the available Foxp3$^+$ Treg population. Foxp3 is the canonical transcription factor of Foxp3$^+$ Treg cells. Its expression is crucial in endowing Treg cells with their suppressive ability (Fontenot et al., 2003; Hori et al., 2003; Wan and Flavell, 2007; Williams and Rudensky, 2007). Most importantly, sustained and continuous expression of Foxp3 in Treg cells is required to maintain the transcriptional and functional programs in developmentally established Treg cells. Foxp3 expression level within the Foxp3$^+$ Treg population has been considered to be a quality control indicator for the Foxp3 suppressive functional capacity (Wan and Flavell, 2007; Williams and Rudensky, 2007). Although the frequency of Foxp3$^+$ Treg compartment could be possibly comparable, reduction in Foxp3 expression within Treg cells can cause auto-immune diseases under steady-state and failure to control immune responses under inflammatory conditions (Wan and Flavell, 2007; Kitoh et al., 2009; Wohlfert et al., 2011). Consequently, our observation of a reduced Foxp3 expression

during inflammation following IL-4Rα removal on Foxp3^{+} Treg cells define, rather remarkably, a need for this receptor in stabilizing/promoting Foxp3 expression by Foxp3^{+} Treg cells *in vivo* under inflammatory conditions.

4.2.2.2 Differential regulation of Foxp3^{+} Treg population by IL-4Rα signaling

Unlike the marked reduction in Foxp3 expression observed, the expression level of CD25, a consensus receptor expressed by Treg cells (Zemmour et al., 2018), on Foxp3^{+} Treg cells was not affected in the liver, hLN, and MLN of *S. mansoni* infected Foxp3^{cre} IL-4Rα$^{-/lox}$ mice, suggesting that IL-4Rα signaling on Foxp3^{+} Treg cells is dispensable for CD25 expression by Foxp3^{+} Treg cells. Of importance, differential regulation of IL-4Rα signaling on Foxp3^{+} Treg cells in different anatomical location was noted. Such a case is not uncommon. The Foxp3^{+} Treg population is one of the most heterogeneous T cell population. Its phenotypical heterogeneity reflects the diverse environment and the different cell types these cells do regulate (Zhou et al., 2015; Zemmour et al., 2018). With recently available high throughput technologies, i.e. single-cell RNA sequencing, it has been shown that transcriptional profile of lymphoid and non-lymphoid Treg cells are quite distinct (Zhou et al., 2015), which might partially explain why in our case the specific deletion of IL-4Rα on Foxp3^{+} Treg cells affected their proliferation only in the lymph nodes (MLN and hLN) but not in the tissue (the liver) during *S. mansoni* infection. Similarly, single-cell transcriptomic analyses showed that non-lymphoid Treg cells present in different non-lymphoid tissues/lymphoid Treg cells present in different LNs do have similar but not identical transcriptional profile, indicating Treg cells adaptation to support a particular tissue/LN specific function (Miragaia et al., unpublished data). Hence, it is not surprising that IL-4Rα signaling could present with different impacts on the expression level of different suppressive molecules by Foxp3^{+} Treg cells from different anatomical locations.

The reduction of Foxp3 expression by Foxp3^{+} Treg population noted in the MLN and hLN of *S. mansoni* infected male and female Foxp3^{cre} IL-4Rα$^{-/lox}$ mice can very well explain the uncontrolled T cell proliferation and effector function observed in both organs. Thus, the data are arguing for a need of Foxp3^{+} Treg to have an intact IL-4Rα signaling to potentiate their suppressive function. Even though IRF4 expression, the transcription factor

required by Treg cells to control Th2 immune response (Zheng et al., 2009), by Foxp3^{+} Treg compartments was differentially regulated in the MLN and hLN of *S. mansoni* infected Foxp3^{cre} IL-4Rα$^{-/lox}$ mice, the present study noted a consistent increase in CD4^{+} GATA3^{+} Th2 cell paralleled by an augmentation of type 2 cytokine production, suggesting that Treg cells in different lymphoid organs could use different suppressive mechanisms in order to maintain homeostasis. One likelihood could be that Foxp3^{+} Treg population in the MLN controls Th2 immune response in IRF4-independent manner. The uncontrolled T cell proliferation, T cell effector function and type 2 cytokines production in the MLN, as well as the reduction in Foxp3^{+} Treg population in the gut, observed in *S. mansoni* infected Foxp3^{cre} IL-4Rα$^{-/lox}$ mice can, therefore, explain the exacerbated egg-driven fibrogranulomatous inflammation in the gut accompanied by high level of fibrosis as indicated by histology and hydroxy-proline content.

In the liver, the present study noted that partial or quasi-complete deletion of IL-4Rα specifically on Foxp3^{+} Treg cells results in significant reduction in IRF4 and Helios expression by Foxp3^{+} Treg cells during *S. mansoni* infection, suggesting that IL-4Rα-mediated signaling on Foxp3^{+} Treg cells is crucial for maintaining/enhancing IRF4 and Helios expression by Foxp3^{+} Treg cells present in the liver. Helios and IRF4 expression by Foxp3^{+} Treg cells are crucial in maintaining and stabilizing Tregs suppressive capacity potential in the face of the inflammatory immune response (Zheng et al., 2009; Kim et al., 2015; Nakagawa et al., 2016). It has been shown that Foxp3^{+} Treg cells do require the expression of IRF4 to endow themselves with molecular machineries required to control Th2 immune response (Zheng et al., 2009). A study by Kim and colleagues (2015) showed that conditional ablation of *helios* specifically on Foxp3^{+} Treg cells results in a reduction in Foxp3 expression as well as uncontrolled cytokine production (Kim et al., 2015). In fact, a recently published report demonstrated that effector Treg cells, Treg cells that populate the non-lymphoid tissues (Smigiel et al., 2014), have a higher need for Helios expression to maintain their fitness (Sebastian et al., 2016). Therefore, the heterogeneous effect of IL-4Rα deletion specifically on Foxp3^{+} Treg cells on Helios expression by Foxp3 Treg population present in the liver and those present in the MLN and hLN of *S. mansoni* infected Foxp3^{cre} IL-4Rα$^{-/lox}$ mice could be that Helios expression by Foxp3^{+} Treg cells is independent of IL-4Rα signaling but once in the tissues where the peak of inflammation is present, IL-4Rα could be possibly playing a role in boosting Helios expression on Foxp3^{+}

Treg cells in order to stabilize Foxp3 expression and survival of Treg cells in the face of the heightened immune response.

Consequently, our observation of the marked reduction in the expression of Treg suppressive markers, Foxp3, Helios, and IRF4, in $Foxp3^+$ Treg cells in the *S. mansoni* infected $Foxp3^{cre}$ IL-4R$\alpha^{-/lox}$ mice could give an explanation for the significant increase in type 1 (IFN-γ), type 2 (IL-4, IL-5, IL-10, and IL-13), and type 17 (IL-17) cytokine production, exaggerated egg-driven fibro-granulomatous inflammation, and large coalescing granuloma, accompanied by dramatic increase in the level of tissue fibrosis. It is also important to point out that similarly heightened cytokine release and inflammation were noted in diseased female $Foxp3^{cre}$ IL-4R$\alpha^{-/lox}$ mice, where the less efficient deletion of IL-4Rα was observed when compared to *Sm*-infected male $Foxp3^{cre}$ IL-4R$\alpha^{-/lox}$ mice. Even though the effect of IL-4Rα deletion on $Foxp3^+$ Treg cell on *S. mansoni*-induced immunopathology at different time points is yet to be experimentally validated, the present study, as it stands, convincingly argues for a requirement of IL-4Rα in full, i.e. intact, on $Foxp3^+$ Tregs, rather than beyond a threshold level, to enable $Foxp3^+$ Treg-mediated control of inflammatory responses in diseases.

4.2.2.3 IL-4Rα signaling on $Foxp3^+$ Treg is required to control hookworm-induced emphysematous lung pathology

Deletion of IL-4Rα on $Foxp3^+$ Treg cells did not alter the host ability to expel the worms during *N. brasiliensis* infection. Even though this finding argues for a dispensable role of IL-4Rα signaling on $Foxp3^+$ Treg cell in the worm expulsion capacity of the host, it does not rule out the possibility that $Foxp3^{cre}$ IL-4R$\alpha^{-/lox}$ mice might have cleared the worms before IL-4R$\alpha^{-/lox}$ mice. Hence, checking worm counts, cytokines production, and gut pathology at earlier time points (i.e. 6-7 days) might help in dissecting the role of IL-4Rα signaling on $Foxp3^+$ Treg cell in gut pathology and worm clearance during primary *N. brasiliensis* infection. Interestingly, however, in the lung, the present study found that conditional ablation of IL-4Rα specifically within $Foxp3^+$ Treg cells results in higher mucus production and exacerbated emphysema. Emphysema is a devastating pathology, which can be replicated by *N. brasiliensis* infection and migration of the parasite through the lungs where a reduction in lung function and a difficulty in breathing arise. Emphysema

gets worse over time and continues even after the parasite has left the lung (Marsland et al., 2008; Heitmann et al., 2012; Bouchery et al., 2017). The mechanism(s) underlying the host protection or susceptibility to emphysema is (are) yet to be defined (Brandsma et al., 2008; Knudsen et al., 2010; Cremona et al., 2013; Bouchery et al., 2017). Previously published reports showed that IL-4Rα signaling plays a crucial in mediating acute wound healing in the lung during helminth infection (Chen et al., 2012) making it desirable to specifically pinpoint the IL-4Rα responsive cell type(s) involved in this repair process for a role was previously suggested for alternatively activated macrophages (Marsland et al., 2008). The present study now shows for the first time that IL-4Rα-mediated signaling on $Foxp3^+$ Treg cells, in particular, is crucial in protecting the host against helminth-induced lung emphysematous pathology.

4.2.2.4 IL-4Rα signaling mediates $Foxp3^+$ Treg cells accumulation within inflamed tissues

Partial or quasi-complete removal of IL-4Rα within the $Foxp3^+$ Treg compartment of $Foxp3^{cre}$ IL-$4R\alpha^{-/lox}$ diseased mice led to an impaired accumulation of Tregs to the site of inflammation. The impaired accumulation of $Foxp3^+$ Treg population was recorded in two different models; i) in the liver and the gut of *S. mansoni* diseased $Foxp3^{cre}$ IL-$4R\alpha^{-/lox}$ mice and ii) in the inner layer of the alveoli of the lungs during *N. brasiliensis* infection. In-depth investigations showed that $Foxp3^+$ Tregs that failed to accumulate in the liver of our *S. mansoni* diseased $Foxp3^{cre}$ IL-$4R\alpha^{-/lox}$ mice had a significant reduction in their expression levels of GATA3. In fact, this is consistent with previous report showing that GATA3 deficient $Foxp3^+$ Tregs fail to efficiently accumulate in inflamed tissues, that report can as well explain the comparable expression level of GATA3 by $Foxp3^+$ Treg cells in the MLN and hLN of *S. mansoni* diseased $Foxp3^{cre}$ IL-$4R\alpha^{-/lox}$ mice compared to their littermate controls (Wohlfert et al., 2011). Thus our data argue for the need of an intact IL-4Rα within the $Foxp3^+$ Treg compartment to maintain/enhance GATA3 expression for endowing $Foxp3^+$ Treg cells with the ability to accumulate at the inflamed tissues and to be able to protect the host against exacerbated tissue inflammation. Mechanistically, various processes can mediate such an impaired accumulation of $Foxp3^{cre}$ IL-$4R\alpha^{-/lox}$ Tregs observed in our infectious settings including

a) defects in extra-thymic Treg conversion,

b) reduced Treg proliferation, and/or

c) increased Treg apoptosis

With regard to the hypothesis a), it was noted that no obvious defect of $CD25^{-}$ $CD4^{+}$ cell precursors from $Foxp3^{cre}$ IL-4R$\alpha^{-/lox}$ mice in converting into $Foxp3^{+}$ Treg *in vitro* arguing against a defect in extra-thymic Treg conversion.

For b), *ex-vivo* analyses of $Foxp3^{+}$ Tregs from diseased $Foxp3^{cre}$ IL-4R$\alpha^{-/lox}$ mice showed no signs of impaired proliferation, as indicated by the comparable expression level of Ki-67 by $Foxp3^{+}$ Treg cells in the liver of *Sm*-infected $Foxp3^{cre}$ IL-4R$\alpha^{-/lox}$ and their littermate controls, dismissing $Foxp3^{+}$ Treg defective proliferation as a possible cause of the poor accumulation reported.

Interestingly, however, with regards to the option c), $CD25^{+}$ Tregs survival and stability (as judged by cell viability staining and Foxp3 expression) were compromised in the absence of IL-4 *in vitro* supporting $Foxp3^{+}$ Treg impaired survival and disturbed stability as likely mediating the poor accumulation of Tregs to inflamed sites shown in the diseased- $Foxp3^{cre}$ IL-4R$\alpha^{-/lox}$ mice.

It should be also noted that defective Treg migration to the inflamed tissues could further explain the observed reduction of Tregs in the livers of *S. mansoni*-infected or the lungs of *N. brasiliensis*-infected $Foxp3^{cre}$ IL-4R$\alpha^{-/lox}$ mice. In as much as our present study does not provide an experimental appraisal of this possibility, a follow-up approach would be to test for the frequencies of CCR7 low, CD44 high effector Tregs –usual tissue recruited Tregs- within the Foxp3 Treg compartment.

As of yet, however, our present data support an impaired survival and a disturbed stability of Foxp3 Tregs in our $Foxp3^{cre}$ IL-4R$\alpha^{-/lox}$ mice as likely the driving causes of the impaired accumulation observed.

4.2.3 Exaggerated immune response and tissue inflammation following deletion of IL-4Rα specifically on Foxp3$^+$ Treg cells

The reduction in Foxp3$^+$ Treg population, as well as Treg suppressive capacity that resulted in uncontrolled immune response and exaggerated tissue inflammation in diseased Foxp3^{cre} IL-4Rα$^{-/lox}$ mice, were due to the deletion of IL-4Rα specifically on Foxp3$^+$ Treg cells rather than a bystander effect from the Cre-expression. Plethora of reports have shown that Cre alone can produce a phenotype as they can excise genomic DNA sequences flanked by *loxP*-like sites or possibly because the expression level of Cre could be high to an extent that affects the physiology of the cells (Loonstra et al., 2001; Pomplun et al., 2007; Schmidt-Supprian and Rajewsky, 2007; Huh et al., 2010; Heffner et al., 2012; Qureshi et al., 2014; Carow et al., 2016). The similar Foxp3$^+$ Treg cell frequency, Foxp3 expression by Foxp3$^+$ Tregs, as well as the comparable level of fibrogranulomatous inflammation in the liver and the gut of *S. mansoni* infected IL-4Rα$^{+/+}$ and Foxp3^{cre} IL-4Rα$^{+/+}$ were sufficiently dismissive of the potential unspecific effects of Cre-expression and were further proving that our phenotype was specifically due to the deletion of IL-4Rα on Foxp3$^+$ Treg cells.

4.2.4 Deletion of IL-4Rα specifically on Foxp3$^+$ Treg cells does not induce Foxp3$^+$ Treg cells transdifferentiation to ex-Foxp3-Th2

The second hypothesis that Foxp3$^+$ Treg cells need IL-4Rα receptor to foster their transdifferentiation into effector T cells is less supported and even dismissed by some of our present observations: i) Should ex-Foxp3 Th2 effector cells be mounted during experimental acute schistosomiasis from IL-4Rα responsive Foxp3$^+$ Treg cells, the absence of these cells from the pool of the Th2 effector population – that is widely reported to ensure survival during acute schistosomiasis (Pelly et al., 2017) - did not affect the host survival, arguing either against the need for IL-4Rα to mount the pool of the required Foxp3-derived protective Th2 cells in our system or denotes a lack of ex-Foxp3 Th2 requirement by the host to survive acute schistosomiasis. Secondly, the present study noted that ii) the T-cells responsible for the increased cytokine production reported in Foxp3^{cre} IL-4Rα$^{-/lox}$ diseased mice did not express Foxp3 but rather GATA3 in both MLN and hLN, a profile inconsistent with recently reported ex-Foxp3 T cells during helminth infections (Pelly et al., 2017).

Even though a clear-cut can only be established by using FATE-mapping mice, our present data argue against Foxp3 Treg transdifferentiation into cytokine-producing effector T cells as mediating the heightened inflammation observed in diseased Foxp3^{cre} IL-4Rα$^{-/lox}$ mice.

Overall, our results support the idea that an intact, rather than a potentiated/diminished, IL-4Rα-mediated signaling is optimal to endow Foxp3^{+} Treg cells with their most efficient ability to control inflammation in disease as illustrated here in helminthiases. As per our current findings, such an optimal response is most likely achieved by preventing Foxp3^{+} Treg death and stabilizing the expression of canonical Treg suppressive and associated markers such as Foxp3, IRF4, GATA3, and Helios (Fig. 46).

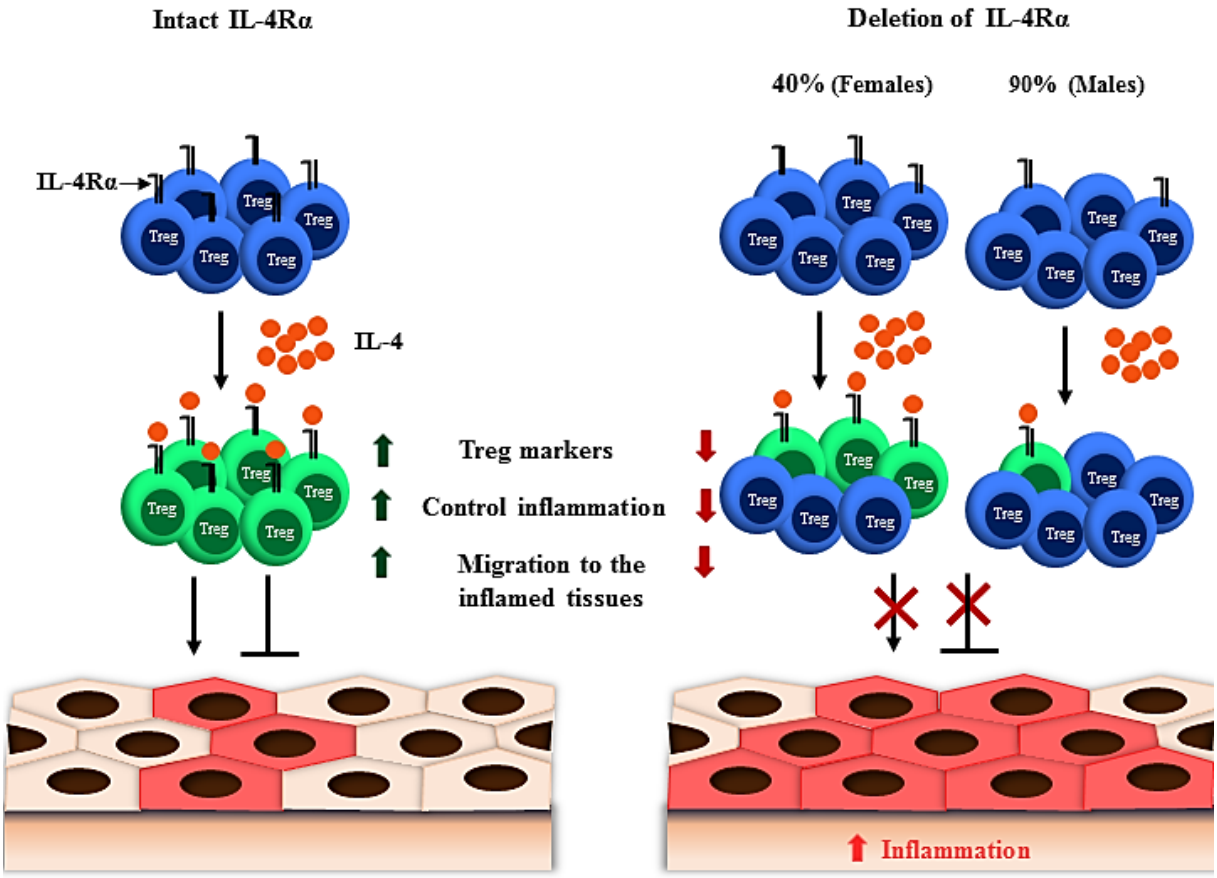

Figure 46. IL-4Rα is required by Foxp3^{+} Treg cells to control inflammation in disease. Schematic diagram showing that either partial or complete deletion of IL-4Rα from Foxp3^{+} Treg cells lead to aggravated pathology and uncontrolled inflammation, but rather Foxp3^{+} Treg cells do require intact IL-4Rα signaling to control inflammation in diseases.

Concluding remarks

This study further highlights the fact that a cytokine can have both a positive and negative effects on Treg cell activity and reinstates the notion that balance is key. Promoting or impairing IL-4Rα mediated signaling yielded a similar impairment of $Foxp3^+$ Treg cell, therefore, strongly arguing against the benefits of uninformedly modulating this cytokine receptor on $Foxp3^+$ Tregs to ameliorate/break tolerance, particularly in the current global context where helminthiases are rampant. This is, therefore, particularly important in the light of recent therapeutic advances against non-communicable diseases such as asthma or atopic dermatitis, where IL-4Rα targeting is being introduced and is attracting considerable interest and funding (Noval Rivas et al., 2015; Massoud et al., 2016). Although potentially disease-specific, thus not applicable to the above-mentioned diseases, the observations reported in the present work remain alarming and warrant more caution when proceeding with the clinical modulation of IL-4Rα signalling as a mean for therapy.

References

Abdel Aziz, N., H. Tallima, E.A. Hafez, and R. El Ridi. 2016. Papain-Based Vaccination Modulates *Schistosoma mansoni* Infection-Induced Cytokine Signals. *Scand J Immunol* 83:128-138.

Abremski, K., and R. Hoess. 1984. Bacteriophage P1 site-specific recombination. Purification and properties of the Cre recombinase protein. *J Biol Chem* 259:1509-1514.

Akashi, K., D. Traver, T. Miyamoto, and I.L. Weissman. 2000. A clonogenic common myeloid progenitor that gives rise to all myeloid lineages. *Nature* 404:193-197.

Asano, M., M. Toda, N. Sakaguchi, and S. Sakaguchi. 1996. Autoimmune disease as a consequence of developmental abnormality of a T cell subpopulation. *J Exp Med* 184:387-396.

Barak, Y., M.C. Nelson, E.S. Ong, Y.Z. Jones, P. Ruiz-Lozano, K.R. Chien, A. Koder, and R.M. Evans. 1999. PPAR gamma is required for placental, cardiac, and adipose tissue development. *Mol Cell* 4:585-595.

Barner, M., M. Mohrs, F. Brombacher, and M. Kopf. 1998. Differences between IL-4R alpha-deficient and IL-4-deficient mice reveal a role for IL-13 in the regulation of Th2 responses. *Curr Biol* 8:669-672.

Barsoum, R.S., G. Esmat, and T. El-Baz. 2013. Human schistosomiasis: clinical perspective: review. *J Adv Res* 4:433-444.

Barthlott, T., H. Moncrieffe, M. Veldhoen, C.J. Atkins, J. Christensen, A. O'Garra, and B. Stockinger. 2005. CD25+ CD4+ T cells compete with naive CD4+ T cells for IL-2 and exploit it for the induction of IL-10 production. *Int Immunol* 17:279-288.

Baumgart, M., F. Tompkins, J. Leng, and M. Hesse. 2006. Naturally occurring CD4+Foxp3+ regulatory T cells are an essential, IL-10-independent part of the immunoregulatory network in *Schistosoma mansoni* egg-induced inflammation. *J Immunol* 176:5374-5387.

Bazan, J.F. 1990. Structural design and molecular evolution of a cytokine receptor superfamily. *Proc Natl Acad Sci U S A* 87:6934-6938.

Bennett, B.L., R. Cruz, R.G. Lacson, and A.M. Manning. 1997. Interleukin-4 suppression of tumor necrosis factor alpha-stimulated E-selectin gene transcription is mediated by STAT6 antagonism of NF-kappaB. *J Biol Chem* 272:10212-10219.

Bennett, C.L., J. Christie, F. Ramsdell, M.E. Brunkow, P.J. Ferguson, L. Whitesell, T.E. Kelly, F.T. Saulsbury, P.F. Chance, and H.D. Ochs. 2001. The immune dysregulation, polyendocrinopathy, enteropathy, X-linked syndrome (IPEX) is caused by mutations of FOXP3. *Nat Genet* 27:20-21.

Benoist, C., and D. Mathis. 2012. Treg cells, life history, and diversity. *Cold Spring Harb Perspect Biol* 4:a007021.

Bergman, I., and R. Loxley. 1963. Two improved and simplified methods for the spectrophotometric determination of hydroxyproline. *Anal Chem* 35:1961–1965.

Bettelli, E., Y. Carrier, W. Gao, T. Korn, T.B. Strom, M. Oukka, H.L. Weiner, and V.K. Kuchroo. 2006. Reciprocal developmental pathways for the generation of pathogenic effector TH17 and regulatory T cells. *Nature* 441:235-238.

Blankenhaus, B., U. Klemm, M.L. Eschbach, T. Sparwasser, J. Huehn, A.A. Kuhl, C. Loddenkemper, T. Jacobs, and M. Breloer. 2011. *Strongyloides ratti* infection induces expansion of Foxp3+ regulatory T cells that interfere with immune response and parasite clearance in BALB/c mice. *J Immunol* 186:4295-4305.

Blom, B., and H. Spits. 2006. Development of human lymphoid cells. *Annu Rev Immunol* 24:287-320.

Bonomo, A., P.J. Kehn, E. Payer, L. Rizzo, A.W. Cheever, and E.M. Shevach. 1995. Pathogenesis of post-thymectomy autoimmunity. Role of syngeneic MLR-reactive T cells. *J Immunol* 154:6602-6611.

Bopp, T., C. Becker, M. Klein, S. Klein-Hessling, A. Palmetshofer, E. Serfling, V. Heib, M. Becker, J. Kubach, S. Schmitt, S. Stoll, H. Schild, M.S. Staege, M. Stassen, H. Jonuleit, and E. Schmitt. 2007. Cyclic adenosine monophosphate is a key component of regulatory T cell-mediated suppression. *J Exp Med* 204:1303-1310.

Borsellino, G., M. Kleinewietfeld, D. Di Mitri, A. Sternjak, A. Diamantini, R. Giometto, S. Hopner, D. Centonze, G. Bernardi, M.L. Dell'Acqua, P.M. Rossini, L. Battistini, O. Rotzschke, and K. Falk. 2007. Expression of ectonucleotidase CD39 by Foxp3+ Treg cells: hydrolysis of extracellular ATP and immune suppression. *Blood* 110:1225-1232.

Bosshardt, S.C., G.L. Freeman, Jr., W.E. Secor, and D.G. Colley. 1997. IL-10 deficit correlates with chronic, hypersplenomegaly syndrome in male CBA/J mice infected with *Schistosoma mansoni*. *Parasite Immunol* 19:347-353.

Bouchery, T., B. Volpe, K. Shah, L. Lebon, K. Filbey, G. LeGros, and N. Harris. 2017. The Study of Host Immune Responses Elicited by the Model Murine Hookworms *Nippostrongylus brasiliensis* and *Heligmosomoides polygyrus*. *Curr Protoc Mouse Biol* 7:236-286.

Brandsma, C.A., M.N. Hylkema, B.W. van der Strate, D.J. Slebos, M.A. Luinge, M. Geerlings, W. Timens, D.S. Postma, and H.A. Kerstjens. 2008. Heme oxygenase-1 prevents smoke induced B-cell infiltrates: a role for regulatory T cells? *Respir Res* 9:17.

Brunkow, M.E., E.W. Jeffery, K.A. Hjerrild, B. Paeper, L.B. Clark, S.A. Yasayko, J.E. Wilkinson, D. Galas, S.F. Ziegler, and F. Ramsdell. 2001. Disruption of a new forkhead/winged-helix protein, scurfin, results in the fatal lymphoproliferative disorder of the scurfy mouse. *Nat Genet* 27:68-73.

Burchill, M.A., J. Yang, C. Vogtenhuber, B.R. Blazar, and M.A. Farrar. 2007. IL-2 receptor beta-dependent STAT5 activation is required for the development of Foxp3+ regulatory T cells. *J Immunol* 178:280-290.

Burke, M.L., M.K. Jones, G.N. Gobert, Y.S. Li, M.K. Ellis, and D.P. McManus. 2009. Immunopathogenesis of human schistosomiasis. *Parasite Immunol* 31:163-176.

Busse, D., M. de la Rosa, K. Hobiger, K. Thurley, M. Flossdorf, A. Scheffold, and T. Hofer. 2010. Competing feedback loops shape IL-2 signaling between helper and regulatory T lymphocytes in cellular microenvironments. *Proc Natl Acad Sci U S A* 107:3058-3063.

Camberis, M., G. Le Gros, and J. Urban, Jr. 2003. Animal model of *Nippostrongylus brasiliensis* and *Heligmosomoides polygyrus*. *Curr Protoc Immunol* Chapter 19:Unit 19 12.

Campbell, D.J., and M.A. Koch. 2011. Phenotypical and functional specialization of FOXP3+ regulatory T cells. *Nat Rev Immunol* 11:119-130.

Cao, X., S.F. Cai, T.A. Fehniger, J. Song, L.I. Collins, D.R. Piwnica-Worms, and T.J. Ley. 2007. Granzyme B and perforin are important for regulatory T cell-mediated suppression of tumor clearance. *Immunity* 27:635-646.

Capecchi, M.R., M.J. Evans, and O. Smithies. 2007. The Nobel Prize in Physiology or Medicine 2007. In.

Caretto, D., S.D. Katzman, A.V. Villarino, E. Gallo, and A.K. Abbas. 2010. Cutting edge: the Th1 response inhibits the generation of peripheral regulatory T cells. *J Immunol* 184:30-34.

Carow, B., Y. Gao, J. Coquet, M. Reilly, and M.E. Rottenberg. 2016. *lck*-driven Cre expression alters T cell development in the thymus and the frequencies and functions of peripheral T cell subsets. *J Immunol* 197:2261-2268.

Chang, H.C., S. Sehra, R. Goswami, W. Yao, Q. Yu, G.L. Stritesky, R. Jabeen, C. McKinley, A.N. Ahyi, L. Han, E.T. Nguyen, M.J. Robertson, N.B. Perumal, R.S. Tepper, S.L. Nutt, and M.H. Kaplan. 2010. The transcription factor PU.1 is required for the development of IL-9-producing T cells and allergic inflammation. *Nat Immunol* 11:527-534.

Chatila, T.A., F. Blaeser, N. Ho, H.M. Lederman, C. Voulgaropoulos, C. Helms, and A.M. Bowcock. 2000. JM2, encoding a fork head-related protein, is mutated in X-linked autoimmunity-allergic disregulation syndrome. *J Clin Invest* 106:R75-81.

Chaudhry, A., D. Rudra, P. Treuting, R.M. Samstein, Y. Liang, A. Kas, and A.Y. Rudensky. 2009. CD4+ regulatory T cells control TH17 responses in a Stat3-dependent manner. *Science* 326:986-991.

Cheever, A.W. 1970. Relative resistance of the eggs of human schistosomes to digestion in potassium hydroxide. *Bulletin of the World Health Organization* 43:601-603.

Chen, F., Z. Liu, W. Wu, C. Rozo, S. Bowdridge, A. Millman, N. Van Rooijen, J.F. Urban, Jr., T.A. Wynn, and W.C. Gause. 2012. An essential role for TH2-type responses in limiting acute tissue damage during experimental helminth infection. *Nat Med* 18:260-266.

Chen, W., W. Jin, N. Hardegen, K.J. Lei, L. Li, N. Marinos, G. McGrady, and S.M. Wahl. 2003. Conversion of peripheral CD4+CD25- naive T cells to CD4+CD25+ regulatory T cells by TGF-beta induction of transcription factor Foxp3. *J Exp Med* 198:1875-1886.

Chinen, T., A.K. Kannan, A.G. Levine, X. Fan, U. Klein, Y. Zheng, G. Gasteiger, Y. Feng, J.D. Fontenot, and A.Y. Rudensky. 2016. An essential role for the IL-2 receptor in Treg cell function. *Nat Immunol* 17:1322-1333.

Chitsulo, L., D. Engels, A. Montresor, and L. Savioli. 2000. The global status of schistosomiasis and its control. *Acta Trop* 77:41-51.

Chung, Y., S. Tanaka, F. Chu, R.I. Nurieva, G.J. Martinez, S. Rawal, Y.H. Wang, H. Lim, J.M. Reynolds, X.H. Zhou, H.M. Fan, Z.M. Liu, S.S. Neelapu, and C. Dong. 2011. Follicular regulatory T cells expressing Foxp3 and Bcl-6 suppress germinal center reactions. *Nat Med* 17:983-988.

Cipolletta, D., M. Feuerer, A. Li, N. Kamei, J. Lee, S.E. Shoelson, C. Benoist, and D. Mathis. 2012. PPAR-gamma is a major driver of the accumulation and phenotype of adipose tissue Treg cells. *Nature* 486:549-553.

Coffman, R.L., J. Ohara, M.W. Bond, J. Carty, A. Zlotnik, and W.E. Paul. 1986. B cell stimulatory factor-1 enhances the IgE response of lipopolysaccharide-activated B cells. *J Immunol* 136:4538-4541.

Colley, D.G., A.L. Bustinduy, W.E. Secor, and C.H. King. 2014. Human schistosomiasis. *Lancet* 383:2253-2264.

Collins, J.J., 3rd, R.S. King, A. Cogswell, D.L. Williams, and P.A. Newmark. 2011. An atlas for Schistosoma mansoni organs and life-cycle stages using cell type-specific markers and confocal microscopy. *PLoS Negl Trop Dis* 5:e1009.

Collison, L.W., C.J. Workman, T.T. Kuo, K. Boyd, Y. Wang, K.M. Vignali, R. Cross, D. Sehy, R.S. Blumberg, and D.A. Vignali. 2007. The inhibitory cytokine IL-35 contributes to regulatory T-cell function. *Nature* 450:566-569.

Cremona, T.P., S.A. Tschanz, C. von Garnier, and C. Benarafa. 2013. SerpinB1 deficiency is not associated with increased susceptibility to pulmonary emphysema in mice. *Am J Physiol Lung Cell Mol Physiol* 305:L981-989.

Curwen, R.S., and R.A. Wilson. 2003. Invasion of skin by schistosome cercariae: some neglected facts. *Trends Parasitol* 19:63-66; discussion 66-68.

Darnell, J.E., Jr. 1997. STATs and gene regulation. *Science* 277:1630-1635.

Deaglio, S., K.M. Dwyer, W. Gao, D. Friedman, A. Usheva, A. Erat, J.F. Chen, K. Enjyoji, J. Linden, M. Oukka, V.K. Kuchroo, T.B. Strom, and S.C. Robson. 2007. Adenosine generation catalyzed by CD39 and CD73 expressed on regulatory T cells mediates immune suppression. *J Exp Med* 204:1257-1265.

Defrance, T., J.P. Aubry, F. Rousset, B. Vanbervliet, J.Y. Bonnefoy, N. Arai, Y. Takebe, T. Yokota, F. Lee, K. Arai, and et al. 1987. Human recombinant interleukin 4 induces Fc epsilon receptors (CD23) on normal human B lymphocytes. *J Exp Med* 165:1459-1467.

Dewals, B., J.C. Hoving, M. Leeto, R.G. Marillier, U. Govender, A.J. Cutler, W.G. Horsnell, and F. Brombacher. 2009. IL-4Ralpha responsiveness of non-CD4 T cells contributes to resistance in *Schistosoma mansoni* infection in pan-T cell-specific IL-4Ralpha-deficient mice. *Am J Pathol* 175:706-716.

El Ridi, R., A. Wagih, R. Salem, N. Mahana, M. El Demellawy, and H. Tallima. 2006a. Impact of interleukin-1 and interleukin-6 in murine primary schistosomiasis. *Int Immunopharmacol* 6:1100-1108.

El Ridi, R., A. Wagih, R. Salem, N. Mahana, M. El Demellawy, and H. Tallima. 2006b. Influence of interleukin-2 and interferon-gamma in murine schistosomiasis. *Cytokine* 33:281-288.

Elbaz, T., and G. Esmat. 2013. Hepatic and intestinal schistosomiasis: review. *J Adv Res* 4:445-452.

Fairfax, K.C., E. Amiel, I.L. King, T.C. Freitas, M. Mohrs, and E.J. Pearce. 2012. IL-10R blockade during chronic schistosomiasis mansoni results in the loss of B cells from the liver and the development of severe pulmonary disease. *PLoS Pathog* 8:e1002490.

Fallarino, F., U. Grohmann, K.W. Hwang, C. Orabona, C. Vacca, R. Bianchi, M.L. Belladonna, M.C. Fioretti, M.L. Alegre, and P. Puccetti. 2003. Modulation of tryptophan catabolism by regulatory T cells. *Nat Immunol* 4:1206-1212.

Fallon, P.G. 2000. Immunopathology of schistosomiasis: a cautionary tale of mice and men. *Immunol Today* 21:29-35.

Fallon, P.G., E.J. Richardson, G.J. McKenzie, and A.N. McKenzie. 2000. Schistosome infection of transgenic mice defines distinct and contrasting pathogenic roles for IL-4 and IL-13: IL-13 is a profibrotic agent. *J Immunol* 164:2585-2591.

Fantini, M.C., S. Dominitzki, A. Rizzo, M.F. Neurath, and C. Becker. 2007. In vitro generation of CD4+ CD25+ regulatory cells from murine naive T cells. *Nat Protoc* 2:1789-1794.

Ferrick, D.A., M.D. Schrenzel, T. Mulvania, B. Hsieh, W.G. Ferlin, and H. Lepper. 1995. Differential production of interferon-gamma and interleukin-4 in response to Th1- and Th2-stimulating pathogens by gamma delta T cells in vivo. *Nature* 373:255-257.

Feuerer, M., L. Herrero, D. Cipolletta, A. Naaz, J. Wong, A. Nayer, J. Lee, A.B. Goldfine, C. Benoist, S. Shoelson, and D. Mathis. 2009. Lean, but not obese, fat is enriched for a unique population of regulatory T cells that affect metabolic parameters. *Nat Med* 15:930-939.

Feuerer, M., J.A. Hill, K. Kretschmer, H. von Boehmer, D. Mathis, and C. Benoist. 2010. Genomic definition of multiple ex vivo regulatory T cell subphenotypes. *Proc Natl Acad Sci U S A* 107:5919-5924.

Finkelman, F.D., T. Shea-Donohue, J. Goldhill, C.A. Sullivan, S.C. Morris, K.B. Madden, W.C. Gause, and J.F. Urban, Jr. 1997. Cytokine regulation of host defense against parasitic gastrointestinal nematodes: lessons from studies with rodent models. *Annu Rev Immunol* 15:505-533.

Finney, C.A., M.D. Taylor, M.S. Wilson, and R.M. Maizels. 2007. Expansion and activation of CD4(+)CD25(+) regulatory T cells in *Heligmosomoides polygyrus* infection. *Eur J Immunol* 37:1874-1886.

Fontenot, J.D., M.A. Gavin, and A.Y. Rudensky. 2003. Foxp3 programs the development and function of CD4+CD25+ regulatory T cells. *Nat Immunol* 4:330-336.

Fontenot, J.D., J.P. Rasmussen, M.A. Gavin, and A.Y. Rudensky. 2005a. A function for interleukin 2 in Foxp3-expressing regulatory T cells. *Nat Immunol* 6:1142-1151.

Fontenot, J.D., J.P. Rasmussen, L.M. Williams, J.L. Dooley, A.G. Farr, and A.Y. Rudensky. 2005b. Regulatory T cell lineage specification by the forkhead transcription factor foxp3. *Immunity* 22:329-341.

Fowell, D., and D. Mason. 1993. Evidence that the T cell repertoire of normal rats contains cells with the potential to cause diabetes. Characterization of the CD4+ T cell subset that inhibits this autoimmune potential. *J Exp Med* 177:627-636.

Gambineri, E., T.R. Torgerson, and H.D. Ochs. 2003. Immune dysregulation, polyendocrinopathy, enteropathy, and X-linked inheritance (IPEX), a syndrome of systemic autoimmunity caused by mutations of FOXP3, a critical regulator of T-cell homeostasis. *Curr Opin Rheumatol* 15:430-435.

Gause, W.C., J.F. Urban, Jr., and M.J. Stadecker. 2003. The immune response to parasitic helminths: insights from murine models. *Trends Immunol* 24:269-277.

Gavin, M.A., J.P. Rasmussen, J.D. Fontenot, V. Vasta, V.C. Manganiello, J.A. Beavo, and A.Y. Rudensky. 2007. Foxp3-dependent programme of regulatory T-cell differentiation. *Nature* 445:771-775.

Gillan, V., and E. Devaney. 2005. Regulatory T cells modulate Th2 responses induced by *Brugia pahangi* third-stage larvae. *Infect Immun* 73:4034-4042.

Godfrey, V.L., B.T. Rouse, and J.E. Wilkinson. 1994. Transplantation of T cell-mediated, lymphoreticular disease from the scurfy (sf) mouse. *Am J Pathol* 145:281-286.

Gondek, D.C., V. Devries, E.C. Nowak, L.F. Lu, K.A. Bennett, Z.A. Scott, and R.J. Noelle. 2008. Transplantation survival is maintained by granzyme B+ regulatory cells and adaptive regulatory T cells. *J Immunol* 181:4752-4760.

Gondek, D.C., L.F. Lu, S.A. Quezada, S. Sakaguchi, and R.J. Noelle. 2005. Cutting edge: contact-mediated suppression by CD4+CD25+ regulatory cells involves a granzyme B-dependent, perforin-independent mechanism. *J Immunol* 174:1783-1786.

Goossens, P.L., H. Jouin, G. Marchal, and G. Milon. 1990. Isolation and flow cytometric analysis of the free lymphomyeloid cells present in murine liver. *J Immunol Methods* 132:137-144.

Graber, P., D. Gretener, S. Herren, J.P. Aubry, G. Elson, J. Poudrier, S. Lecoanet-Henchoz, S. Alouani, C. Losberger, J.Y. Bonnefoy, M.H. Kosco-Vilbois, and J.F. Gauchat. 1998. The distribution of IL-13 receptor alpha1 expression on B cells, T cells and monocytes and its regulation by IL-13 and IL-4. *Eur J Immunol* 28:4286-4298.

Grabstein, K., J. Eisenman, D. Mochizuki, K. Shanebeck, P. Conlon, T. Hopp, C. March, and S. Gillis. 1986. Purification to homogeneity of B cell stimulating factor. A molecule that stimulates proliferation of multiple lymphokine-dependent cell lines. *J Exp Med* 163:1405-1414.

Gryseels, B. 2012. Schistosomiasis. *Infect Dis Clin North Am* 26:383-397.

Guo, F., D.N. Gopaul, and G.D. van Duyne. 1997. Structure of Cre recombinase complexed with DNA in a site-specific recombination synapse. *Nature* 389:40-46.

Guo, F., D.N. Gopaul, and G.D. Van Duyne. 1999. Asymmetric DNA bending in the Cre-loxP site-specific recombination synapse. *Proc Natl Acad Sci U S A* 96:7143-7148.

Hansell, E., S. Braschi, K.F. Medzihradszky, M. Sajid, M. Debnath, J. Ingram, K.C. Lim, and J.H. McKerrow. 2008. Proteomic analysis of skin invasion by blood fluke larvae. *PLoS Negl Trop Dis* 2:e262.

Hardy, C.L., P.S. Bhathal, K.J. Snibson, and T.E. Adams. 1997. Comparison of intrahepatic lymphocytes from normal and growth hormone transgenic mice with chronic hepatitis and liver cancer. *Immunology* 90:412-420.

He, Y.X., B. Salafsky, and K. Ramaswamy. 2005. Comparison of skin invasion among three major species of *Schistosoma*. *Trends Parasitol* 21:201-203.

Heffner, C.S., C. Herbert Pratt, R.P. Babiuk, Y. Sharma, S.F. Rockwood, L.R. Donahue, J.T. Eppig, and S.A. Murray. 2012. Supporting conditional mouse mutagenesis with a comprehensive cre characterization resource. *Nat Commun* 3:1218.

Heitmann, L., R. Rani, L. Dawson, C. Perkins, Y. Yang, J. Downey, C. Holscher, and D.R. Herbert. 2012. TGF-beta-responsive myeloid cells suppress type 2 immunity and emphysematous pathology after hookworm infection. *Am J Pathol* 181:897-906.

Herbert, D.R., C. Holscher, M. Mohrs, B. Arendse, A. Schwegmann, M. Radwanska, M. Leeto, R. Kirsch, P. Hall, H. Mossmann, B. Claussen, I. Forster, and F. Brombacher. 2004. Alternative macrophage activation is essential for survival during schistosomiasis and downmodulates T helper 1 responses and immunopathology. *Immunity* 20:623-635.

Hilton, D.J., J.G. Zhang, D. Metcalf, W.S. Alexander, N.A. Nicola, and T.A. Willson. 1996. Cloning and characterization of a binding subunit of the interleukin 13 receptor that is also a component of the interleukin 4 receptor. *Proc Natl Acad Sci U S A* 93:497-501.

Hoeppli, R.E., D. Wu, L. Cook, and M.K. Levings. 2015. The environment of regulatory T cell biology: cytokines, metabolites, and the microbiome. *Front Immunol* 6:61.

Hoffmann, K.F., A.W. Cheever, and T.A. Wynn. 2000. IL-10 and the dangers of immune polarization: excessive type 1 and type 2 cytokine responses induce distinct forms of lethal immunopathology in murine schistosomiasis. *J Immunol* 164:6406-6416.

Hokke, C.H., and M. Yazdanbakhsh. 2005. Schistosome glycans and innate immunity. *Parasite Immunol* 27:257-264.

Hori, S., T. Nomura, and S. Sakaguchi. 2003. Control of regulatory T cell development by the transcription factor Foxp3. *Science* 299:1057-1061.

Horsnell, W.G., A.J. Cutler, J.C. Hoving, H. Mearns, E. Myburgh, B. Arendse, F.D. Finkelman, G.K. Owens, D. Erle, and F. Brombacher. 2007. Delayed goblet cell hyperplasia, acetylcholine receptor expression, and worm expulsion in SMC-specific IL-4Ralpha-deficient mice. *PLoS Pathog* 3:e1.

Hotez, P.J., P.J. Brindley, J.M. Bethony, C.H. King, E.J. Pearce, and J. Jacobson. 2008. Helminth infections: the great neglected tropical diseases. *J Clin Invest* 118:1311-1321.

Huang, C.T., C.J. Workman, D. Flies, X. Pan, A.L. Marson, G. Zhou, E.L. Hipkiss, S. Ravi, J. Kowalski, H.I. Levitsky, J.D. Powell, D.M. Pardoll, C.G. Drake, and D.A. Vignali. 2004. Role of LAG-3 in regulatory T cells. *Immunity* 21:503-513.

Huh, W.J., I.U. Mysorekar, and J.C. Mills. 2010. Inducible activation of Cre recombinase in adult mice causes gastric epithelial atrophy, metaplasia, and regenerative changes in the absence of "floxed" alleles. *Am J Physiol Gastrointest Liver Physiol* 299:G368-380.

Hurdayal, R., H.H. Ndlovu, M. Revaz-Breton, S.P. Parihar, J.K. Nono, M. Govender, and F. Brombacher. 2017. IL-4-producing B cells regulate T helper cell dichotomy in type 1- and type 2-controlled diseases. *Proc Natl Acad Sci U S A* 114:E8430-E8439.

Imai, T., R. Takakuwa, S. Marchand, E. Dentz, J.M. Bornert, N. Messaddeq, O. Wendling, M. Mark, B. Desvergne, W. Wahli, P. Chambon, and D. Metzger. 2004. Peroxisome proliferator-activated receptor gamma is required in mature white and brown adipocytes for their survival in the mouse. *Proc Natl Acad Sci U S A* 101:4543-4547.

Inobaya, M.T., R.M. Olveda, T.N. Chau, D.U. Olveda, and A.G. Ross. 2014. Prevention and control of schistosomiasis: a current perspective. *Res Rep Trop Med* 2014:65-75.

Ivanov, II, B.S. McKenzie, L. Zhou, C.E. Tadokoro, A. Lepelley, J.J. Lafaille, D.J. Cua, and D.R. Littman. 2006. The orphan nuclear receptor RORgammat directs the differentiation program of proinflammatory IL-17+ T helper cells. *Cell* 126:1121-1133.

Iyer, S.S., and G. Cheng. 2012. Role of interleukin 10 transcriptional regulation in inflammation and autoimmune disease. *Crit Rev Immunol* 32:23-63.

Izuhara, K., R.A. Feldman, P. Greer, and N. Harada. 1996. Interleukin-4 induces association of the c-fes proto-oncogene product with phosphatidylinositol-3 kinase. *Blood* 88:3910-3918.

Jang, S.K., H.G. Krausslich, M.J. Nicklin, G.M. Duke, A.C. Palmenberg, and E. Wimmer. 1988. A segment of the 5' nontranslated region of encephalomyocarditis virus RNA directs internal entry of ribosomes during in vitro translation. *J Virol* 62:2636-2643.

Jankovic, D., M.C. Kullberg, N. Noben-Trauth, P. Caspar, J.M. Ward, A.W. Cheever, W.E. Paul, and A. Sher. 1999. Schistosome-infected IL-4 receptor knockout (KO) mice, in contrast to IL-4 KO mice, fail to develop granulomatous pathology while maintaining the same lymphokine expression profile. *J Immunol* 163:337-342.

Johannes, M.L., and C. Klessen. 1984. Alcianblue/PAS or PAS/alcianblue? Remarks on a classical technic used in carbohydrate histochemistry. *Histochemistry* 80:129-132.

Josefowicz, S.Z., L.F. Lu, and A.Y. Rudensky. 2012. Regulatory T cells: mechanisms of differentiation and function. *Annu Rev Immunol* 30:531-564.

Khattri, R., T. Cox, S.A. Yasayko, and F. Ramsdell. 2003. An essential role for Scurfin in CD4+CD25+ T regulatory cells. *Nat Immunol* 4:337-342.

Kim, H.J., R.A. Barnitz, T. Kreslavsky, F.D. Brown, H. Moffett, M.E. Lemieux, Y. Kaygusuz, T. Meissner, T.A. Holderried, S. Chan, P. Kastner, W.N. Haining, and H. Cantor. 2015. Stable inhibitory activity of regulatory T cells requires the transcription factor Helios. *Science* 350:334-339.

Kitagawa, Y., and S. Sakaguchi. 2017. Molecular control of regulatory T cell development and function. *Curr Opin Immunol* 49:64-70.

Kitoh, A., M. Ono, Y. Naoe, N. Ohkura, T. Yamaguchi, H. Yaguchi, I. Kitabayashi, T. Tsukada, T. Nomura, Y. Miyachi, I. Taniuchi, and S. Sakaguchi. 2009. Indispensable role of the Runx1-Cbfbeta transcription complex for in vivo-suppressive function of FoxP3+ regulatory T cells. *Immunity* 31:609-620.

Knudsen, G.M., K.F. Medzihradszky, K.C. Lim, E. Hansell, and J.H. McKerrow. 2005. Proteomic analysis of *Schistosoma mansoni* cercarial secretions. *Mol Cell Proteomics* 4:1862-1875.

Knudsen, L., E.R. Weibel, H.J. Gundersen, F.V. Weinstein, and M. Ochs. 2010. Assessment of air space size characteristics by intercept (chord) measurement: an accurate and efficient stereological approach. *J Appl Physiol (1985)* 108:412-421.

Kobie, J.J., P.R. Shah, L. Yang, J.A. Rebhahn, D.J. Fowell, and T.R. Mosmann. 2006. T regulatory and primed uncommitted CD4 T cells express CD73, which suppresses

effector CD4 T cells by converting 5'-adenosine monophosphate to adenosine. *J Immunol* 177:6780-6786.

Koch, M.A., G. Tucker-Heard, N.R. Perdue, J.R. Killebrew, K.B. Urdahl, and D.J. Campbell. 2009. The transcription factor T-bet controls regulatory T cell homeostasis and function during type 1 inflammation. *Nat Immunol* 10:595-602.

Kondo, M., I.L. Weissman, and K. Akashi. 1997. Identification of clonogenic common lymphoid progenitors in mouse bone marrow. *Cell* 91:661-672.

Koninkx, J.F., M.H. Mirck, H.G. Hendriks, J.M. Mouwen, and J.E. van Dijk. 1988. *Nippostrongylus brasiliensis*: histochemical changes in the composition of mucins in goblet cells during infection in rats. *Exp Parasitol* 65:84-90.

Konkel, J.E., W. Jin, B. Abbatiello, J.R. Grainger, and W. Chen. 2014. Thymocyte apoptosis drives the intrathymic generation of regulatory T cells. *Proc Natl Acad Sci U S A* 111:E465-473.

Launois, P., T. Ohteki, K. Swihart, H.R. MacDonald, and J.A. Louis. 1995. In susceptible mice, *Leishmania major* induce very rapid interleukin-4 production by CD4+ T cells which are NK1.1. *Eur J Immunol* 25:3298-3307.

Lawrence, R.A., C.A. Gray, J. Osborne, and R.M. Maizels. 1996. *Nippostrongylus brasiliensis*: cytokine responses and nematode expulsion in normal and IL-4-deficient mice. *Exp Parasitol* 84:65-73.

Lee, F., T. Yokota, T. Otsuka, P. Meyerson, D. Villaret, R. Coffman, T. Mosmann, D. Rennick, N. Roehm, C. Smith, and et al. 1986. Isolation and characterization of a mouse interleukin cDNA clone that expresses B-cell stimulatory factor 1 activities and T-cell- and mast-cell-stimulating activities. *Proc Natl Acad Sci U S A* 83:2061-2065.

Lenschow, D.J., T.L. Walunas, and J.A. Bluestone. 1996. CD28/B7 system of T cell costimulation. *Annu Rev Immunol* 14:233-258.

Levine, A.G., A. Medoza, S. Hemmers, B. Moltedo, R.E. Niec, M. Schizas, B.E. Hoyos, E.V. Putintseva, A. Chaudhry, S. Dikiy, S. Fujisawa, D.M. Chudakov, P.M. Treuting, and A.Y. Rudensky. 2017. Stability and function of regulatory T cells expressing the transcription factor T-bet. *Nature*

Li, M.O., Y.Y. Wan, and R.A. Flavell. 2007. T cell-produced transforming growth factor-beta1 controls T cell tolerance and regulates Th1- and Th17-cell differentiation. *Immunity* 26:579-591.

Liang, B., C. Workman, J. Lee, C. Chew, B.M. Dale, L. Colonna, M. Flores, N. Li, E. Schweighoffer, S. Greenberg, V. Tybulewicz, D. Vignali, and R. Clynes. 2008.

Regulatory T cells inhibit dendritic cells by lymphocyte activation gene-3 engagement of MHC class II. *J Immunol* 180:5916-5926.

Linterman, M.A., W. Pierson, S.K. Lee, A. Kallies, S. Kawamoto, T.F. Rayner, M. Srivastava, D.P. Divekar, L. Beaton, J.J. Hogan, S. Fagarasan, A. Liston, K.G. Smith, and C.G. Vinuesa. 2011. Foxp3+ follicular regulatory T cells control the germinal center response. *Nat Med* 17:975-982.

Liu, J., S.G. Willet, E.D. Bankaitis, Y. Xu, C.V. Wright, and G. Gu. 2013. Non-parallel recombination limits Cre-LoxP-based reporters as precise indicators of conditional genetic manipulation. *Genesis* 51:436-442.

Liu, Z., H. Lin, Q. Liu, G. Mousavi, and W.C. Gause. 2008. The parasite *Nippostrongylus brasiliensis* induces multiple regulatory pathways that control increases of IL-17 expression and associated pathology in the lung. *FASEB J* 22:

Lohoff, M., H.W. Mittrucker, S. Prechtl, S. Bischof, F. Sommer, S. Kock, D.A. Ferrick, G.S. Duncan, A. Gessner, and T.W. Mak. 2002. Dysregulated T helper cell differentiation in the absence of interferon regulatory factor 4. *Proc Natl Acad Sci U S A* 99:11808-11812.

Loonstra, A., M. Vooijs, H.B. Beverloo, B.A. Allak, E. van Drunen, R. Kanaar, A. Berns, and J. Jonkers. 2001. Growth inhibition and DNA damage induced by Cre recombinase in mammalian cells. *Proc Natl Acad Sci U S A* 98:9209-9214.

Lowenthal, J.W., B.E. Castle, J. Christiansen, J. Schreurs, D. Rennick, N. Arai, P. Hoy, Y. Takebe, and M. Howard. 1988. Expression of high affinity receptors for murine interleukin 4 (BSF-1) on hemopoietic and nonhemopoietic cells. *J Immunol* 140:456-464.

Lyon, M.F. 1961. Gene action in the X-chromosome of the mouse (*Mus musculus* L.). *Nature* 190:372-373.

Lyon, M.F. 1972. X-chromosome inactivation and developmental patterns in mammals. *Biol Rev Camb Philos Soc* 47:1-35.

Maerten, P., C. Shen, D.M. Bullens, G. Van Assche, S. Van Gool, K. Geboes, P. Rutgeerts, and J.L. Ceuppens. 2005. Effects of interleukin 4 on CD25+CD4+ regulatory T cell function. *J Autoimmun* 25:112-120.

Malek, T.R. 2008. The biology of interleukin-2. *Annu Rev Immunol* 26:453-479.

Marie, J.C., J.J. Letterio, M. Gavin, and A.Y. Rudensky. 2005. TGF-beta1 maintains suppressor function and Foxp3 expression in CD4+CD25+ regulatory T cells. *J Exp Med* 201:1061-1067.

Marillier, R.G., T.M. Brombacher, B. Dewals, M. Leeto, M. Barkhuizen, D. Govender, L. Kellaway, W.G. Horsnell, and F. Brombacher. 2010. IL-4R{alpha}-responsive smooth muscle cells increase intestinal hypercontractility and contribute to resistance during acute Schistosomiasis. *Am J Physiol Gastrointest Liver Physiol* 298:G943-951.

Marsland, B.J., M. Kurrer, R. Reissmann, N.L. Harris, and M. Kopf. 2008. *Nippostrongylus brasiliensis* infection leads to the development of emphysema associated with the induction of alternatively activated macrophages. *Eur J Immunol* 38:479-488.

Massoud, A.H., L.M. Charbonnier, D. Lopez, M. Pellegrini, W. Phipatanakul, and T.A. Chatila. 2016. An asthma-associated IL4R variant exacerbates airway inflammation by promoting conversion of regulatory T cells to TH17-like cells. *Nat Med* 22:1013-1022.

McCoy, K., M. Camberis, and G.L. Gros. 1997. Protective immunity to nematode infection is induced by CTLA-4 blockade. *J Exp Med* 186:183-187.

McKeever, U., J.P. Mordes, D.L. Greiner, M.C. Appel, J. Rozing, E.S. Handler, and A.A. Rossini. 1990. Adoptive transfer of autoimmune diabetes and thyroiditis to athymic rats. *Proc Natl Acad Sci U S A* 87:7618-7622.

McKerrow, J.H., and J. Salter. 2002. Invasion of skin by Schistosoma cercariae. *Trends Parasitol* 18:193-195.

McSorley, H.J., Y.M. Harcus, J. Murray, M.D. Taylor, and R.M. Maizels. 2008. Expansion of Foxp3+ regulatory T cells in mice infected with the filarial parasite *Brugia malayi*. *J Immunol* 181:6456-6466.

Medema, R.H., and B.M. Burgering. 2007. The X factor: skewing X inactivation towards cancer. *Cell* 129:1253-1254.

Mellor, A.L., and D.H. Munn. 2011. Physiologic control of the functional status of Foxp3+ regulatory T cells. *J Immunol* 186:4535-4540.

Meng, X., J. Yang, M. Dong, K. Zhang, E. Tu, Q. Gao, W. Chen, C. Zhang, and Y. Zhang. 2016. Regulatory T cells in cardiovascular diseases. *Nat Rev Cardiol* 13:167-179.

Min, B., M. Prout, J. Hu-Li, J. Zhu, D. Jankovic, E.S. Morgan, J.F. Urban, Jr., A.M. Dvorak, F.D. Finkelman, G. LeGros, and W.E. Paul. 2004. Basophils produce IL-4 and accumulate in tissues after infection with a Th2-inducing parasite. *J Exp Med* 200:507-517.

Mohrs, M., B. Ledermann, G. Kohler, A. Dorfmuller, A. Gessner, and F. Brombacher. 1999. Differences between IL-4- and IL-4 receptor alpha-deficient mice in chronic

leishmaniasis reveal a protective role for IL-13 receptor signaling. *J Immunol* 162:7302-7308.

Morrissey, P.J., K. Charrier, S. Braddy, D. Liggitt, and J.D. Watson. 1993. CD4+ T cells that express high levels of CD45RB induce wasting disease when transferred into congenic severe combined immunodeficient mice. Disease development is prevented by cotransfer of purified CD4+ T cells. *J Exp Med* 178:237-244.

Mosley, B., M.P. Beckmann, C.J. March, R.L. Idzerda, S.D. Gimpel, T. VandenBos, D. Friend, A. Alpert, D. Anderson, J. Jackson, and et al. 1989. The murine interleukin-4 receptor: molecular cloning and characterization of secreted and membrane bound forms. *Cell* 59:335-348.

Mountford, P.S., and A.G. Smith. 1995. Internal ribosome entry sites and dicistronic RNAs in mammalian transgenesis. *Trends Genet* 11:179-184.

Murphy, K.M., W. Ouyang, S.J. Szabo, N.G. Jacobson, M.L. Guler, J.D. Gorham, U. Gubler, and T.L. Murphy. 1999. T helper differentiation proceeds through Stat1-dependent, Stat4-dependent and Stat4-independent phases. *Curr Top Microbiol Immunol* 238:13-26.

Murphy, K.P., P. Travers, M. Walport, and C. Janeway. 2008. Janeway's Immunobiology. Garland Science,

Musso, T., J.A. Johnston, D. Linnekin, L. Varesio, T.K. Rowe, J.J. O'Shea, and D.W. McVicar. 1995. Regulation of JAK3 expression in human monocytes: phosphorylation in response to interleukins 2, 4, and 7. *J Exp Med* 181:1425-1431.

Nagy, A. 2000. Cre recombinase: the universal reagent for genome tailoring. *Genesis* 26:99-109.

Nakagawa, H., J.M. Sido, E.E. Reyes, V. Kiers, H. Cantor, and H.J. Kim. 2016. Instability of Helios-deficient Tregs is associated with conversion to a T-effector phenotype and enhanced antitumor immunity. *Proc Natl Acad Sci U S A* 113:6248-6253.

Nelms, K., A.D. Keegan, J. Zamorano, J.J. Ryan, and W.E. Paul. 1999. The IL-4 receptor: signaling mechanisms and biologic functions. *Annu Rev Immunol* 17:701-738.

Nishizuka, Y., and T. Sakakura. 1969. Thymus and reproduction: sex-linked dysgenesia of the gonad after neonatal thymectomy in mice. *Science* 166:753-755.

Noben-Trauth, N., J. Hu-Li, and W.E. Paul. 2000. Conventional, naive CD4+ T cells provide an initial source of IL-4 during Th2 differentiation. *J Immunol* 165:3620-3625.

Noelle, R., P.H. Krammer, J. Ohara, J.W. Uhr, and E.S. Vitetta. 1984. Increased expression of Ia antigens on resting B cells: an additional role for B-cell growth factor. *Proc Natl Acad Sci U S A* 81:6149-6153.

Nono, J.K., H. Ndlovu, N. Abdel Aziz, T. Mpotje, L. Hlaka, and F. Brombacher. 2017a. Host regulation of liver fibroproliferative pathology during experimental schistosomiasis via interleukin-4 receptor alpha. *PLoS Negl Trop Dis* 11:e0005861.

Nono, J.K., H. Ndlovu, N. Abdel Aziz, T. Mpotje, L. Hlaka, and F. Brombacher. 2017b. Interleukin-4 receptor alpha is still required after Th2 polarization for the maintenance and the recall of protective immunity to Nematode infection. *PLoS Negl Trop Dis* 11:e0005675.

Noval Rivas, M., O.T. Burton, H.C. Oettgen, and T. Chatila. 2016. IL-4 production by group 2 innate lymphoid cells promotes food allergy by blocking regulatory T-cell function. *J Allergy Clin Immunol* 138:801-811 e809.

Noval Rivas, M., O.T. Burton, P. Wise, L.M. Charbonnier, P. Georgiev, H.C. Oettgen, R. Rachid, and T.A. Chatila. 2015. Regulatory T cell reprogramming toward a Th2-cell-like lineage impairs oral tolerance and promotes food allergy. *Immunity* 42:512-523.

Noval Rivas, M., and T.A. Chatila. 2016. Regulatory T cells in allergic diseases. *J Allergy Clin Immunol* 138:639-652.

Nurieva, R.I., Y. Chung, G.J. Martinez, X.O. Yang, S. Tanaka, T.D. Matskevitch, Y.H. Wang, and C. Dong. 2009. Bcl6 mediates the development of T follicular helper cells. *Science* 325:1001-1005.

Obiri, N.I., W. Debinski, W.J. Leonard, and R.K. Puri. 1995. Receptor for interleukin 13. Interaction with interleukin 4 by a mechanism that does not involve the common gamma chain shared by receptors for interleukins 2, 4, 7, 9, and 15. *J Biol Chem* 270:8797-8804.

Ochs, H.D., S.F. Ziegler, and T.R. Torgerson. 2005. FOXP3 acts as a rheostat of the immune response. *Immunol Rev* 203:156-164.

Ohara, J., S. Lahet, J. Inman, and W.E. Paul. 1985. Partial purification of murine B cell stimulatory factor (BSF)-1. *J Immunol* 135:2518-2523.

Ohki, H., C. Martin, C. Corbel, M. Coltey, and N.M. Le Douarin. 1987. Tolerance induced by thymic epithelial grafts in birds. *Science* 237:1032-1035.

Oldenhove, G., N. Bouladoux, E.A. Wohlfert, J.A. Hall, D. Chou, L. Dos Santos, S. O'Brien, R. Blank, E. Lamb, S. Natarajan, R. Kastenmayer, C. Hunter, M.E. Grigg, and Y. Belkaid. 2009. Decrease of Foxp3+ Treg cell number and acquisition of effector cell phenotype during lethal infection. *Immunity* 31:772-786.

Othman, A., and R. El Ridi. 2014. Schistosomiasis. In Helminth infections and their impact on global public health. F. Bruschi, editor Springer 49-92.

Otsuka, T., D. Villaret, T. Yokota, Y. Takebe, F. Lee, N. Arai, and K. Arai. 1987. Structural-analysis of the mouse chromosomal gene encoding Interleukin-4 which expresses B-cell, T-cell and mast-cell stimulating activities. *Nucleic Acids Res* 15:333-344.

Pandiyan, P., L. Zheng, S. Ishihara, J. Reed, and M.J. Lenardo. 2007. CD4+CD25+Foxp3+ regulatory T cells induce cytokine deprivation-mediated apoptosis of effector CD4+ T cells. *Nat Immunol* 8:1353-1362.

Park, L.S., D. Friend, K. Grabstein, and D.L. Urdal. 1987. Characterization of the high-affinity cell-surface receptor for murine B-cell-stimulating factor 1. *Proc Natl Acad Sci U S A* 84:1669-1673.

Paul, W.E. 1991. Interleukin-4: a prototypic immunoregulatory lymphokine. *Blood* 77:1859-1870.

Pearce, E.J., and A.S. MacDonald. 2002. The immunobiology of schistosomiasis. *Nat Rev Immunol* 2:499-511.

Pelletier, J., and N. Sonenberg. 1988. Internal initiation of translation of eukaryotic mRNA directed by a sequence derived from poliovirus RNA. *Nature* 334:320-325.

Pelly, V.S., S.M. Coomes, Y. Kannan, M. Gialitakis, L.J. Entwistle, J. Perez-Lloret, S. Czieso, I.S. Okoye, D. Ruckerl, J.E. Allen, F. Brombacher, and M.S. Wilson. 2017. Interleukin 4 promotes the development of ex-Foxp3 Th2 cells during immunity to intestinal helminths. *J Exp Med* 214:1809-1826.

Pelly, V.S., Y. Kannan, S.M. Coomes, L.J. Entwistle, D. Ruckerl, B. Seddon, A.S. MacDonald, A. McKenzie, and M.S. Wilson. 2016. IL-4-producing ILC2s are required for the differentiation of TH2 cells following *Heligmosomoides polygyrus* infection. *Mucosal Immunol* 9:1407-1417.

Penhale, W.J., A. Farmer, R.P. McKenna, and W.J. Irvine. 1973. Spontaneous thyroiditis in thymectomized and irradiated Wistar rats. *Clin Exp Immunol* 15:225-236.

Penhale, W.J., P.A. Stumbles, C.R. Huxtable, R.J. Sutherland, and D.W. Pethick. 1990. Induction of diabetes in PVG/c strain rats by manipulation of the immune system. *Autoimmunity* 7:169-179.

Pillemer, B.B., Z. Qi, B. Melgert, T.B. Oriss, P. Ray, and A. Ray. 2009. STAT6 activation confers upon T helper cells resistance to suppression by regulatory T cells. *J Immunol* 183:155-163.

Plaut, M., J.H. Pierce, C.J. Watson, J. Hanley-Hyde, R.P. Nordan, and W.E. Paul. 1989. Mast cell lines produce lymphokines in response to cross-linkage of Fc epsilon RI or to calcium ionophores. *Nature* 339:64-67.

Pomplun, D., S. Florian, T. Schulz, A.F. Pfeiffer, and M. Ristow. 2007. Alterations of pancreatic beta-cell mass and islet number due to Ins2-controlled expression of Cre recombinase: RIP-Cre revisited; part 2. *Horm Metab Res* 39:336-340.

Powrie, F., M.W. Leach, S. Mauze, L.B. Caddle, and R.L. Coffman. 1993. Phenotypically distinct subsets of CD4+ T cells induce or protect from chronic intestinal inflammation in C. B-17 scid mice. *Int Immunol* 5:1461-1471.

Powrie, F., and D. Mason. 1990. OX-22high CD4+ T cells induce wasting disease with multiple organ pathology: prevention by the OX-22low subset. *J Exp Med* 172:1701-1708.

Qureshi, W., C. Mittal, I. Patsias, K. Garikapati, A. Kuchipudi, G. Cheema, M. Elbatta, Z. Alirhayim, and F. Khalid. 2014. Restarting anticoagulation and outcomes after major gastrointestinal bleeding in atrial fibrillation. *Am J Cardiol* 113:662-668.

Redpath, S.A., N. van der Werf, A.M. Cervera, A.S. MacDonald, D. Gray, R.M. Maizels, and M.D. Taylor. 2013. ICOS controls Foxp3(+) regulatory T-cell expansion, maintenance and IL-10 production during helminth infection. *Eur J Immunol* 43:705-715.

Redpath, S.A., N. van der Werf, A.S. MacDonald, R.M. Maizels, and M.D. Taylor. 2015. *Schistosoma mansoni* larvae do not expand or activate Foxp3+ regulatory T cells during their migratory phase. *Infect Immun* 83:3881-3889.

Rengarajan, J., K.A. Mowen, K.D. McBride, E.D. Smith, H. Singh, and L.H. Glimcher. 2002. Interferon regulatory factor 4 (IRF4) interacts with NFATc2 to modulate interleukin 4 gene expression. *J Exp Med* 195:1003-1012.

Rheinberg, C.E., H. Mone, C.R. Caffrey, D. Imbert-Establet, J. Jourdane, and A. Ruppel. 1998. *Schistosoma haematobium*, *S. intercalatum*, *S. japonicum*, *S. mansoni*, and *S. rodhaini* in mice: relationship between patterns of lung migration by schistosomula and perfusion recovery of adult worms. *Parasitol Res* 84:338-342.

Robb, L. 2007. Cytokine receptors and hematopoietic differentiation. *Oncogene* 26:6715-6723.

Ross, A.G., P.B. Bartley, A.C. Sleigh, G.R. Olds, Y. Li, G.M. Williams, and D.P. McManus. 2002. Schistosomiasis. *N Engl J Med* 346:1212-1220.

Rothenberg, E.V. 2014. The chromatin landscape and transcription factors in T cell programming. *Trends Immunol* 35:195-204.

Rubtsov, Y.P., J.P. Rasmussen, E.Y. Chi, J. Fontenot, L. Castelli, X. Ye, P. Treuting, L. Siewe, A. Roers, W.R. Henderson, Jr., W. Muller, and A.Y. Rudensky. 2008. Regulatory T cell-derived interleukin-10 limits inflammation at environmental interfaces. *Immunity* 28:546-558.

Russell, S.M., J.A. Johnston, M. Noguchi, M. Kawamura, C.M. Bacon, M. Friedmann, M. Berg, D.W. McVicar, B.A. Witthuhn, O. Silvennoinen, and et al. 1994. Interaction of IL-2R beta and gamma c chains with Jak1 and Jak3: implications for XSCID and XCID. *Science* 266:1042-1045.

Russell, S.M., A.D. Keegan, N. Harada, Y. Nakamura, M. Noguchi, P. Leland, M.C. Friedmann, A. Miyajima, R.K. Puri, W.E. Paul, and et al. 1993. Interleukin-2 receptor gamma chain: a functional component of the interleukin-4 receptor. *Science* 262:1880-1883.

Sabin, E.A., M.A. Kopf, and E.J. Pearce. 1996. *Schistosoma mansoni* egg-induced early IL-4 production is dependent upon IL-5 and eosinophils. *J Exp Med* 184:1871-1878.

Sakaguchi, S., K. Fukuma, K. Kuribayashi, and T. Masuda. 1985. Organ-specific autoimmune diseases induced in mice by elimination of T cell subset. I. Evidence for the active participation of T cells in natural self-tolerance; deficit of a T cell subset as a possible cause of autoimmune disease. *J Exp Med* 161:72-87.

Sakaguchi, S., N. Sakaguchi, M. Asano, M. Itoh, and M. Toda. 1995. Immunologic self-tolerance maintained by activated T cells expressing IL-2 receptor alpha-chains (CD25). Breakdown of a single mechanism of self-tolerance causes various autoimmune diseases. *J Immunol* 155:1151-1164.

Sakaguchi, S., T. Takahashi, and Y. Nishizuka. 1982. Study on cellular events in postthymectomy autoimmune oophoritis in mice. I. Requirement of Lyt-1 effector cells for oocytes damage after adoptive transfer. *J Exp Med* 156:1565-1576.

Sakaguchi, S., T. Yamaguchi, T. Nomura, and M. Ono. 2008. Regulatory T cells and immune tolerance. *Cell* 133:775-787.

Salaun, J., A. Bandeira, I. Khazaal, F. Calman, M. Coltey, A. Coutinho, and N.M. Le Douarin. 1990. Thymic epithelium tolerizes for histocompatibility antigens. *Science* 247:1471-1474.

Sauer, B. 1987. Functional expression of the cre-lox site-specific recombination system in the yeast Saccharomyces cerevisiae. *Mol Cell Biol* 7:2087-2096.

Sauer, B. 1998. Inducible gene targeting in mice using the Cre/lox system. *Methods* 14:381-392.

Sauer, B., and N. Henderson. 1988. Site-specific DNA recombination in mammalian cells by the Cre recombinase of bacteriophage P1. *Proc Natl Acad Sci U S A* 85:5166-5170.

Schmidt-Supprian, M., and K. Rajewsky. 2007. Vagaries of conditional gene targeting. *Nat Immunol* 8:665-668.

Sebastian, M., M. Lopez-Ocasio, A. Metidji, S.A. Rieder, E.M. Shevach, and A.M. Thornton. 2016. Helios controls a limited subset of regulatory T cell functions. *J Immunol* 196:144-155.

Seder, R.A., and W.E. Paul. 1994. Acquisition of lymphokine-producing phenotype by CD4+ T cells. *Annu Rev Immunol* 12:635-673.

Selvaraj, R.K., and T.L. Geiger. 2007. A kinetic and dynamic analysis of Foxp3 induced in T cells by TGF- *J Immunol* 179:1390-1390.

Serafini, N., C.A. Vosshenrich, and J.P. Di Santo. 2015. Transcriptional regulation of innate lymphoid cell fate. *Nat Rev Immunol* 15:415-428.

Sharma, S., and J. Zhu. 2014. Immunologic applications of conditional gene modification technology in the mouse. *Curr Protoc Immunol* 105:10 34 11-13.

Shevach, E.M. 2000. Regulatory T cells in autoimmunity*. *Annu Rev Immunol* 18:423-449.

Singh, K.P., H.C. Gerard, A.P. Hudson, T.R. Reddy, and D.L. Boros. 2005. Retroviral Foxp3 gene transfer ameliorates liver granuloma pathology in *Schistosoma mansoni* infected mice. *Immunology* 114:410-417.

Skelly, P.J., A.A. Da'dara, X.H. Li, W. Castro-Borges, and R.A. Wilson. 2014. Schistosome feeding and regurgitation. *PLoS Pathog* 10:e1004246.

Smerz-Bertling, C., and A. Duschl. 1995. Both interleukin 4 and interleukin 13 induce tyrosine phosphorylation of the 140-kDa subunit of the interleukin 4 receptor. *J Biol Chem* 270:966-970.

Smigiel, K.S., E. Richards, S. Srivastava, K.R. Thomas, J.C. Dudda, K.D. Klonowski, and D.J. Campbell. 2014. CCR7 provides localized access to IL-2 and defines homeostatically distinct regulatory T cell subsets. *J Exp Med* 211:121-136.

Socolovsky, M., H.F. Lodish, and G.Q. Daley. 1998. Control of hematopoietic differentiation: lack of specificity in signaling by cytokine receptors. *Proc Natl Acad Sci U S A* 95:6573-6575.

Sprent, J., and J.H. Cho. 2008. Self/non-self discrimination and the problem of keeping T cells alive. *Immunol Cell Biol* 86:54-56.

Stack, R.M., D.J. Lenschow, G.S. Gray, J.A. Bluestone, and F.W. Fitch. 1994. IL-4 treatment of small splenic B cells induces costimulatory molecules B7-1 and B7-2. *J Immunol* 152:5723-5733.

Starr, T.K., S.C. Jameson, and K.A. Hogquist. 2003. Positive and negative selection of T cells. *Annu Rev Immunol* 21:139-176.

Stein, M., S. Keshav, N. Harris, and S. Gordon. 1992. Interleukin 4 potently enhances murine macrophage mannose receptor activity: a marker of alternative immunologic macrophage activation. *J Exp Med* 176:287-292.

Sugihara, S., Y. Izumi, T. Yoshioka, H. Yagi, T. Tsujimura, O. Tarutani, Y. Kohno, S. Murakami, T. Hamaoka, and H. Fujiwara. 1988. Autoimmune thyroiditis induced in mice depleted of particular T cell subsets. I. Requirement of Lyt-1 dull L3T4 bright normal T cells for the induction of thyroiditis. *J Immunol* 141:105-113.

Sun, X.J., L.M. Wang, Y. Zhang, L. Yenush, M.G. Myers, Jr., E. Glasheen, W.S. Lane, J.H. Pierce, and M.F. White. 1995. Role of IRS-2 in insulin and cytokine signalling. *Nature* 377:173-177.

Szabo, S.J., S.T. Kim, G.L. Costa, X. Zhang, C.G. Fathman, and L.H. Glimcher. 2000. A novel transcription factor, T-bet, directs Th1 lineage commitment. *Cell* 100:655-669.

Tachdjian, R., S. Al Khatib, A. Schwinglshackl, H.S. Kim, A. Chen, J. Blasioli, C. Mathias, H.Y. Kim, D.T. Umetsu, H.C. Oettgen, and T.A. Chatila. 2010. In vivo regulation of the allergic response by the IL-4 receptor alpha chain immunoreceptor tyrosine-based inhibitory motif. *J Allergy Clin Immunol* 125:1128-1136 e1128.

Tallima, H., M. Salah, F.R. Guirguis, and R. El Ridi. 2009. Transforming growth factor-beta and Th17 responses in resistance to primary murine *Schistosomiasis mansoni*. *Cytokine* 48:239-245.

Tang, Q., J.Y. Adams, C. Penaranda, K. Melli, E. Piaggio, E. Sgouroudis, C.A. Piccirillo, B.L. Salomon, and J.A. Bluestone. 2008. Central role of defective interleukin-2 production in the triggering of islet autoimmune destruction. *Immunity* 28:687-697.

Taylor, M.D., N. van der Werf, A. Harris, A.L. Graham, O. Bain, J.E. Allen, and R.M. Maizels. 2009. Early recruitment of natural CD4+ Foxp3+ Treg cells by infective larvae determines the outcome of filarial infection. *Eur J Immunol* 39:192-206.

Thornhill, M.H., S.M. Wellicome, D.L. Mahiouz, J.S. Lanchbury, U. Kyan-Aung, and D.O. Haskard. 1991. Tumor necrosis factor combines with IL-4 or IFN-gamma to

selectively enhance endothelial cell adhesiveness for T cells. The contribution of vascular cell adhesion molecule-1-dependent and -independent binding mechanisms. *J Immunol* 146:592-598.

Thornton, A.M., E.E. Donovan, C.A. Piccirillo, and E.M. Shevach. 2004. Cutting edge: IL-2 is critically required for the in vitro activation of CD4+CD25+ T cell suppressor function. *J Immunol* 172:6519-6523.

Tucker, M.S., L.B. Karunaratne, F.A. Lewis, T.C. Freitas, and Y.S. Liang. 2013. Schistosomiasis. *Curr Protoc Immunol* 103:Unit 19 11.

Urban, J.F., Jr., C.R. Maliszewski, K.B. Madden, I.M. Katona, and F.D. Finkelman. 1995. IL-4 treatment can cure established gastrointestinal nematode infections in immunocompetent and immunodeficient mice. *J Immunol* 154:4675-4684.

Urban, J.F., Jr., N. Noben-Trauth, D.D. Donaldson, K.B. Madden, S.C. Morris, M. Collins, and F.D. Finkelman. 1998. IL-13, IL-4Ralpha, and Stat6 are required for the expulsion of the gastrointestinal nematode parasite *Nippostrongylus brasiliensis*. *Immunity* 8:255-264.

Vang, K.B., J. Yang, S.A. Mahmud, M.A. Burchill, A.L. Vegoe, and M.A. Farrar. 2008. IL-2, -7, and -15, but not thymic stromal lymphopoeitin, redundantly govern CD4+Foxp3+ regulatory T cell development. *J Immunol* 181:3285-3290.

Vasanthakumar, A., K. Moro, A. Xin, Y. Liao, R. Gloury, S. Kawamoto, S. Fagarasan, L.A. Mielke, S. Afshar-Sterle, S.L. Masters, S. Nakae, H. Saito, J.M. Wentworth, P. Li, W. Liao, W.J. Leonard, G.K. Smyth, W. Shi, S.L. Nutt, S. Koyasu, and A. Kallies. 2015. The transcriptional regulators IRF4, BATF and IL-33 orchestrate development and maintenance of adipose tissue-resident regulatory T cells. *Nat Immunol* 16:276-285.

Velaga, S., S.N. Ukena, U. Dringenberg, C. Alter, J. Pardo, O. Kershaw, and A. Franzke. 2015. Granzyme A is required for regulatory T-cell mediated prevention of gastrointestinal graft-versus-host disease. *PLoS One* 10:e0124927.

Vignali, D.A., L.W. Collison, and C.J. Workman. 2008. How regulatory T cells work. *Nat Rev Immunol* 8:523-532.

Vitetta, E.S., J. Ohara, C.D. Myers, J.E. Layton, P.H. Krammer, and W.E. Paul. 1985. Serological, biochemical, and functional identity of B cell-stimulatory factor 1 and B cell differentiation factor for IgG1. *J Exp Med* 162:1726-1731.

Walker, A.J. 2006. Biology of schistosome life stages. *Parasit Vectors*.

Walker, A.J. 2011. Insights into the functional biology of schistosomes. *Parasit Vectors* 4:203.

Walker, J.A., and A.N.J. McKenzie. 2018. TH2 cell development and function. *Nat Rev Immunol* 18:121-133.

Wan, Y.Y., and R.A. Flavell. 2007. Regulatory T-cell functions are subverted and converted owing to attenuated Foxp3 expression. *Nature* 445:766-770.

Wang, L.M., M.G. Myers, Jr., X.J. Sun, S.A. Aaronson, M. White, and J.H. Pierce. 1993. IRS-1: essential for insulin- and IL-4-stimulated mitogenesis in hematopoietic cells. *Science* 261:1591-1594.

Wang, Y., M.A. Su, and Y.Y. Wan. 2011. An essential role of the transcription factor GATA-3 for the function of regulatory T cells. *Immunity* 35:337-348.

Weerakoon, K.G., G.N. Gobert, P. Cai, and D.P. McManus. 2015. Advances in the diagnosis of human schistosomiasis. *Clin Microbiol Rev* 28:939-967.

Wei, X., J. Zhang, Q. Gu, M. Huang, W. Zhang, J. Guo, and X. Zhou. 2017. Reciprocal expression of IL-35 and IL-10 defines two distinct effector Treg subsets that are required for maintenance of immune tolerance. *Cell Rep* 21:1853-1869.

Weist, B.M., N. Kurd, J. Boussier, S.W. Chan, and E.A. Robey. 2015. Thymic regulatory T cell niche size is dictated by limiting IL-2 from antigen-bearing dendritic cells and feedback competition. *Nat Immunol* 16:635-641.

Wildin, R.S., and A. Freitas. 2005. IPEX and FOXP3: clinical and research perspectives. *J Autoimmun* 25 Suppl:56-62.

Wildin, R.S., F. Ramsdell, J. Peake, F. Faravelli, J.L. Casanova, N. Buist, E. Levy-Lahad, M. Mazzella, O. Goulet, L. Perroni, F.D. Bricarelli, G. Byrne, M. McEuen, S. Proll, M. Appleby, and M.E. Brunkow. 2001. X-linked neonatal diabetes mellitus, enteropathy and endocrinopathy syndrome is the human equivalent of mouse scurfy. *Nat Genet* 27:18-20.

Williams, L.M., and A.Y. Rudensky. 2007. Maintenance of the Foxp3-dependent developmental program in mature regulatory T cells requires continued expression of Foxp3. *Nat Immunol* 8:277-284.

Wills-Karp, M., and F.D. Finkelman. 2008. Untangling the complex web of IL-4- and IL-13-mediated signaling pathways. *Sci Signal* 1:pe55.

Wing, J.B., and S. Sakaguchi. 2014. Foxp3(+) T(reg) cells in humoral immunity. *Int Immunol* 26:61-69.

Wing, K., Y. Onishi, P. Prieto-Martin, T. Yamaguchi, M. Miyara, Z. Fehervari, T. Nomura, and S. Sakaguchi. 2008. CTLA-4 control over Foxp3+ regulatory T cell function. *Science* 322:271-275.

Wohlfert, E.A., J.R. Grainger, N. Bouladoux, J.E. Konkel, G. Oldenhove, C.H. Ribeiro, J.A. Hall, R. Yagi, S. Naik, R. Bhairavabhotla, W.E. Paul, R. Bosselut, G. Wei, K. Zhao, M. Oukka, J. Zhu, and Y. Belkaid. 2011. GATA3 controls Foxp3(+) regulatory T cell fate during inflammation in mice. *J Clin Invest* 121:4503-4515.

Wrighton, N., L.A. Campbell, N. Harada, A. Miyajima, and F. Lee. 1992. The murine interleukin-4 receptor gene: genomic structure, expression and potential for alternative splicing. *Growth Factors* 6:103-118.

Xu, L.L., A. Kitani, I. Fuss, and W. Strober. 2007. Cutting edge: Regulatory T cells induce CD4(+)CD25(-)Foxp3(-) T cells or are self-induced to become Th17 cells in the absence of exogenous TGF-beta. *J Immunol* 178:6725-6729.

Yang, X.O., A.D. Panopoulos, R. Nurieva, S.H. Chang, D. Wang, S.S. Watowich, and C. Dong. 2007. STAT3 regulates cytokine-mediated generation of inflammatory helper T cells. *J Biol Chem* 282:9358-9363.

Yoshimoto, T., and W.E. Paul. 1994. CD4pos, NK1.1pos T cells promptly produce interleukin 4 in response to in vivo challenge with anti-CD3. *J Exp Med* 179:1285-1295.

Yu, D., S. Rao, L.M. Tsai, S.K. Lee, Y. He, E.L. Sutcliffe, M. Srivastava, M. Linterman, L. Zheng, N. Simpson, J.I. Ellyard, I.A. Parish, C.S. Ma, Q.J. Li, C.R. Parish, C.R. Mackay, and C.G. Vinuesa. 2009. The transcriptional repressor Bcl-6 directs T follicular helper cell lineage commitment. *Immunity* 31:457-468.

Yu, F., S. Sharma, J. Edwards, L. Feigenbaum, and J. Zhu. 2015. Dynamic expression of transcription factors T-bet and GATA-3 by regulatory T cells maintains immunotolerance. *Nat Immunol* 16:197-206.

Zemmour, D., R. Zilionis, E. Kiner, A.M. Klein, D. Mathis, and C. Benoist. 2018. Single-cell gene expression reveals a landscape of regulatory T cell phenotypes shaped by the TCR. *Nat Immunol* 19:291-301.

Zhao, A., J.F. Urban, Jr., R.M. Anthony, R. Sun, J. Stiltz, N. van Rooijen, T.A. Wynn, W.C. Gause, and T. Shea-Donohue. 2008. Th2 cytokine-induced alterations in intestinal smooth muscle function depend on alternatively activated macrophages. *Gastroenterology* 135:217-225 e211.

Zhao, D.M., A.M. Thornton, R.J. DiPaolo, and E.M. Shevach. 2006. Activated CD4+CD25+ T cells selectively kill B lymphocytes. *Blood* 107:3925-3932.

Zheng, S.G., J. Wang, and D.A. Horwitz. 2008. Cutting edge: Foxp3+CD4+CD25+ regulatory T cells induced by IL-2 and TGF-beta are resistant to Th17 conversion by IL-6. *J Immunol* 180:7112-7116.

Zheng, S.G., J.H. Wang, J.D. Gray, H. Soucier, and D.A. Horwitz. 2004. Natural and induced CD4+CD25+ cells educate CD4+CD25- cells to develop suppressive activity: the role of IL-2, TGF-beta, and IL-10. *J Immunol* 172:5213-5221.

Zheng, W., and R.A. Flavell. 1997. The transcription factor GATA-3 is necessary and sufficient for Th2 cytokine gene expression in CD4 T cells. *Cell* 89:587-596.

Zheng, Y., A. Chaudhry, A. Kas, P. deRoos, J.M. Kim, T.T. Chu, L. Corcoran, P. Treuting, U. Klein, and A.Y. Rudensky. 2009. Regulatory T-cell suppressor program co-opts transcription factor IRF4 to control T(H)2 responses. *Nature* 458:351-356.

Zhou, X., J. Tang, H. Cao, H. Fan, and B. Li. 2015. Tissue resident regulatory T cells: novel therapeutic targets for human disease. *Cell Mol Immunol* 12:543-552.

Zhu, J., H. Yamane, and W.E. Paul. 2010. Differentiation of effector CD4 T cell populations. *Annu Rev Immunol* 28:445-489.

Zuo, T., L. Wang, C. Morrison, X. Chang, H. Zhang, W. Li, Y. Liu, Y. Wang, X. Liu, M.W. Chan, J.Q. Liu, R. Love, C.G. Liu, V. Godfrey, R. Shen, T.H. Huang, T. Yang, B.K. Park, C.Y. Wang, P. Zheng, and Y. Liu. 2007. FOXP3 is an X-linked breast cancer suppressor gene and an important repressor of the HER-2/ErbB2 oncogene. *Cell* 129:1275-1286.